Online: http://dust.ess.uci.edu/facts Built: Wed 24th Oct, 2018, 13:34

Radiative Transfer in the Earth System

by Charlie Zender
University of California, Irvine

Department of Earth System Science
University of California
Irvine, CA 92697-3100

zender@uci.edu
Voice: (949) 891-2429
Fax: (949) 824-3256

Facts about FACTs: This document is part of the Freely Available Community Text (fact) project. facts are created, reviewed, and continuously maintained and updated by members of the international academic community communicating with eachother through a well-organized project website. facts are intended to standardize and disseminate our fundamental knowledge of Earth System Sciences in a flexible, adaptive, distributed framework which can evolve to fit the changing needs and technology of the geosciences community. Currently available facts and their urls are listed in Table 1. Because of its international

Table 1: Freely Available Community Texts

Format	URL Location
	Radiative Transfer in the Earth System
DVI	http://dust.ess.uci.edu/facts/rt/rt.dvi
PDF	http://dust.ess.uci.edu/facts/rt/rt.pdf
Postscript	http://dust.ess.uci.edu/facts/rt/rt.ps
	Particle Size Distributions: Theory and Application to Aerosols, Clouds, and Soils
DVI	http://dust.ess.uci.edu/facts/psd/psd.dvi
PDF	http://dust.ess.uci.edu/facts/psd/psd.pdf
Postscript	http://dust.ess.uci.edu/facts/psd/psd.ps
	Natural Aerosols in the Climate System
DVI	http://dust.ess.uci.edu/facts/aer/aer.dvi
PDF	http://dust.ess.uci.edu/facts/aer/aer.pdf
Postscript	http://dust.ess.uci.edu/facts/aer/aer.ps

scope and availability to students of all income levels, the fact project may impact more students, and to a greater depth, than imaginable to before the advent of the Internet. If you are interested in learning more about facts and how you might contribute to or benefit from the project please contact zender@uci.edu.

Notes for Students of ESS 223, Earth System Physics:

This monograph on Radiative Transfer provides some core and some supplementary reading material for ESS 223. We will discuss much of the material in the first twenty pages, and the figures at the end. The Index beginning on page 171 is also helpful.

Notes for Students of ESS 236, Radiative Transfer and Remote Sensing:

Yada yada yada.

Contents

List of Figures

List of Tables

1 Introduction

This document describes mathematical and computational considerations pertaining to radiative transfer processes and radiative transfer models of the Earth system. Our approach is to present a detailed derivation of the tools of radiative transfer needed to predict the radiative quantities (irradiance, mean intensity, and heating rates) which drive climate. In so doing we begin with discussion of the intensity field which is the quantity most often measured by satellite remote sensing instruments. Our approach owes much to Bohren and Huffman (1983) (particle scattering), Goody and Yung (1989) (band models), and Thomas and Stamnes (1999) (nomenclature, discrete ordinate methods, general approach). The nomenclature follows these authors where possible. These sections will evolve and differentiate from their original sources as the manuscript takes on the flavor of the researchers who contribute to it.

1.1 Planetary Radiative Equilibrium

The important role that radiation plays in the climate system is perhaps best illustrated by a simple example showing that without atmospheric radiative feedbacks (especially, ironically, the greenhouse effect), our planet's mean temperature would be well below the freezing point of water. Earth is surrounded by the near vacuum of space so the only way to transport energy to or from the planet is via radiative processes. If E is the thermal energy of the planet, and F^{ASR} and F^{OLR} are the absorbed solar radiation and emitted longwave radiation, respectively, then

$$\frac{\partial E}{\partial t} = F^{\text{ASR}} - F^{\text{OLR}} \tag{1}$$

On timescales longer than about a year the Earth as a whole is thought to be in planetary radiative equilibrium. That, is, the global annual mean planetary temperature is nearly constant because the absorbed solar energy is exactly compensated by thermal radiation lost to space over the course of a year. Thus

$$F^{\mathrm{ASR}} = F^{\mathrm{OLR}} \tag{2}$$

The total amount of solar energy available for the Earth to absorb is the incoming solar flux (or irradiance) at the top of Earth's atmosphere, $F_\odot$ (aka the solar constant), times the intercepting area of Earth's disk which is $\pi r_\oplus^2$. Since Earth rotates, the total mean incident flux $\pi r_\oplus^2 F_\odot$ is actually distributed over the entire surface area of the Earth. The surface area of a sphere is four times its cross-sectional area so the mean incident flux per unit surface area is $F_\odot/4$. The fraction of incident solar flux which is reflected back to space, and thus unable to heat the planet, is called the aplanetary albedo or spherical albedo, R. Satellite observations show that $R \approx 0.3$. Thus only $(1-R)$ of the mean incident solar flux contributes to warming the planet and we have

$$F^{\mathrm{ASR}} = (1-R)F_\odot/4 \tag{3}$$

Earth does not cool to space as a perfect blackbody (41a) of a single temperature and emissivity. Nevertheless the spectrum of thermal radiation F^{OLR} which escapes to space and thus cools Earth does resemble blackbody emission with a characteristic temperature. The effective temperature T_E of an object is the temperature of the blackbody which would produce the same irradiance. Inverting the Stefan-Boltzmann Law (73) yields

$$T_\mathrm{E} \equiv (F^{\mathrm{OLR}}/\sigma)^{1/4} \tag{4}$$

For a perfect blackbody, $T = T_\mathrm{E}$. For a planet, the difference between T_E and the mean surface temperature T_s is due to the radiative effects of the overlying atmosphere. The insulating behavior of the atmosphere is more commonly known as the greenhouse effect.

Substituting (3) and (4) into (2)

$$(1-R)F_\odot/4 = \sigma T_\mathrm{E}^4 \tag{5}$$

$$T_\mathrm{E} = \left(\frac{(1-R)F_\odot}{4\sigma}\right)^{1/4} \tag{6}$$

For Earth, $R \approx 0.3$ and $F_\odot \approx 1367\,\mathrm{W\,m^{-2}}$. Using these values in (6) yields $T_\mathrm{E} = 255\,\mathrm{K}$. Observations show the mean surface temperature $T_\mathrm{s} = 288\,\mathrm{K}$.

1.2 Fundamentals

The fundamental quantity describing the electromagnetic spectrum is frequency, ν. Frequency measures the oscillatory speed of a system, counting the number of oscillations (waves) per unit time. Usually ν is expressed in cycles-per-second, or Hertz. Units of Hertz may be abbreviated Hz, hz, cps, or, as we prefer, $\mathrm{s^{-1}}$. Frequency is intrinsic to the

oscillator and does not depend on the medium in which the waves are travelling. The energy carried by a photon is proportional to its frequency

$$E = \mathrm{h}\nu \tag{7}$$

where h is Planck's constant. Regrettably, almost no radiative transfer literature expresses quantities in frequency.

A related quantity, the angular frequency ω measures the rate of change of wave phase in radians per second. Wave phase proceeds through 2π radians in a complete cycle. Thus the frequency and angular frequency are simply related

$$\omega = 2\pi\nu \tag{8}$$

Since radians are considered dimensionless, the units of ω are s^{-1}. However, angular frequency is also rarely used in radiative transfer. Thus some authors use the symbol ω to denote the element of solid angle, as in $\mathrm{d}\omega$. The reader should be careful not to misconstrue the two meanings. In this text we use ω only infrequently.

Most radiative transfer literature use wavelength or wavenumber. Wavelength, λ (m), measures the distance between two adjacent peaks or troughs in the wavefield. The universal relation between wavelength and frequency is

$$\lambda\nu = \mathrm{c} \tag{9}$$

where c is the speed of light. Since c depends on the medium, λ also depends on the medium.

The wavenumber $\tilde{\nu}\,\mathrm{m}^{-1}$, is exactly the inverse of wavelength

$$\tilde{\nu} \equiv \frac{1}{\lambda} = \frac{\nu}{\mathrm{c}} \tag{10}$$

Thus $\tilde{\nu}$ measures the number of oscillations per unit distance, i.e., the number of wavecrests per meter. Using (9) in (10) we find $\tilde{\nu} = \nu/\mathrm{c}$ so wavenumber $\tilde{\nu}$ is indeed proportional to frequency (and thus to energy). Historically spectroscopists have favored $\tilde{\nu}$ rather than λ or ν. Because of this history, it is much more common in the literature to find $\tilde{\nu}$ expressed in CGS units of cm^{-1} than in SI units of m^{-1}. The CGS wavenumber is used analogously to frequency and to wavelength, i.e., to identify spectral regions. The energy of radiative transitions are commonly expressed in CGS wavenumber units. The relation between $\tilde{\nu}$ expressed in CGS wavenumber units (cm^{-1}) and energy in SI units (J) is obtained by using (10) in (7)

$$E = 100\mathrm{hc}\nu \tag{11}$$

There is another, distinct quantity also called wavenumber. This secondary usage of wavenumber in this text is the traditional measure of spatial wave propagation and is denoted by k.

$$\mathrm{k} \equiv 2\pi\tilde{\nu} \tag{12}$$

The wavenumber k is set in Roman typeface as an additional distinction between it and other symbols [1].

Table 2 summarizes the relationships between the fundamental parameters which describe wave-like phenomena.

[1] The script k is already used for Boltzmann's constant, absorption coefficients, and vibrational modes

Table 2: Wave Parameter Conversion Table[ab]

Variable	ν	λ	$\tilde{\nu}$	ω	k	τ
Units	s^{-1}	m	cm^{-1}	s^{-1}	m^{-1}	s
ν	–	$\frac{\mathrm{c}}{\nu}$	$\frac{\nu}{100\mathrm{c}}$	$2\pi\nu$	$\frac{2\pi\nu}{\mathrm{c}}$	$\frac{1}{\nu}$
λ	$\frac{\mathrm{c}}{\lambda}$	–	$\frac{1}{100\lambda}$	$\frac{2\pi\mathrm{c}}{\lambda}$	$\frac{2\pi}{\lambda}$	$\frac{\lambda}{\mathrm{c}}$
$\tilde{\nu}$	$100\mathrm{c}\tilde{\nu}$	$\frac{1}{100\tilde{\nu}}$	–	$\frac{\tilde{\nu}}{200\pi\mathrm{c}}$	$200\pi\tilde{\nu}$	$\frac{1}{100\mathrm{c}\tilde{\nu}}$
ω	$\frac{\omega}{2\pi}$	$\frac{2\pi\mathrm{c}}{\omega}$	$\frac{\omega}{200\pi\mathrm{c}}$	–	$\frac{\omega}{\mathrm{c}}$	$\frac{2\pi}{\omega}$
k	$\frac{\mathrm{kc}}{2\pi}$	$\frac{2\pi}{\mathrm{k}}$	$\frac{\mathrm{k}}{200\pi}$	ck	–	$\frac{2\pi}{\mathrm{ck}}$
τ	$\frac{1}{\tau}$	$\mathrm{c}\tau$	$\frac{1}{100\mathrm{c}\tau}$	$\frac{2\pi}{\tau}$	$\frac{2\pi}{\mathrm{c}\tau}$	–

[a]The speed of light is $\mathrm{c} = 2.99792458 \times 10^8\,\mathrm{m\,s^{-1}}$.
[b]Table entries express the column in terms of the row.

2 Radiative Transfer Equation

2.1 Definitions

2.1.1 Intensity

The fundamental quantity defining the radiation field is the specific intensity of radiation. Specific intensity, also known as radiance, measures the flux of radiant energy transported in a given direction per unit cross sectional area orthogonal to the beam per unit time per unit solid angle per unit frequency (or wavelength, or wavenumber). The units of I_λ are Joule meter^{-2} second^{-1} steradian^{-1} meter^{-1}. In SI dimensional notation, the units condense to $\mathrm{J\,m^{-2}\,s^{-1}\,sr^{-1}\,m^{-1}}$. The SI unit of power ($1\,\mathrm{Watt} \equiv 1\,\mathrm{Joule\ per\ second}$) is preferred, leading to units of $\mathrm{W\,m^{-2}\,sr^{-1}\,m^{-1}}$. Often the specific intensity is expressed in terms of spectral frequency I_ν with units $\mathrm{W\,m^{-2}\,sr^{-1}\,Hz^{-1}}$ or spectral wavenumber (also $I_{\tilde{\nu}}$) with units $\mathrm{W\,m^{-2}\,sr^{-1}\,(cm^{-1})^{-1}}$.

Consider light travelling in the direction $\hat{\mathbf{\Omega}}$ through the point $\mathbf{r}$. Construct an infinitesimal element of surface area $\mathrm{d}S$ intersecting $\mathbf{r}$ and orthogonal to $\hat{\mathbf{\Omega}}$. The radiant energy $\mathrm{d}E$ crossing $\mathrm{d}S$ in time $\mathrm{d}t$ in the solid angle $\mathrm{d}\Omega$ in the frequency range $[\nu, \nu + \mathrm{d}\nu]$ is related to $I_\nu(\mathbf{r}, \hat{\mathbf{\Omega}})$ by

$$\mathrm{d}E = I_\nu(\mathbf{r}, \hat{\mathbf{\Omega}}, t, \nu)\,\mathrm{d}S\,\mathrm{d}t\,\mathrm{d}\Omega\,\mathrm{d}\nu \tag{13}$$

It is not convenient to measure the radiant flux across surface orthogonal to $\hat{\mathbf{\Omega}}$, as in (13), when we consider properties of radiation fields with preferred directions. If instead, we

measure the intensity orthogonal to an arbitrarily oriented surface element $\mathrm{d}A$ with surface normal $\hat{\mathbf{n}}$, then we must alter (13) to account for projection of $\mathrm{d}S$ onto $\mathrm{d}A$. If the angle between $\hat{\mathbf{n}}$ and $\hat{\mathbf{\Omega}}$ is θ then

$$\cos\theta = \hat{\mathbf{n}} \cdot \hat{\mathbf{\Omega}} \tag{14}$$

and the projection of $\mathrm{d}S$ onto $\mathrm{d}A$ yields

$$\mathrm{d}A = \cos\theta \, \mathrm{d}S \tag{15}$$

so that

$$\mathrm{d}E = I_\nu(\mathbf{r}, \hat{\mathbf{\Omega}}, t, \nu) \cos\theta \, \mathrm{d}A \, \mathrm{d}t \, \mathrm{d}\Omega \, \mathrm{d}\nu \tag{16}$$

The conceptual advantage that (16) has over (13) is that (16) builds in the geometric factor required to convert to any preferred coordinate system defined by $\mathrm{d}A$ and its normal $\hat{\mathbf{n}}$. In practice $\mathrm{d}A$ is often chosen to be the local horizon.

The radiation field is a seven-dimensional quantity, depending upon three coordinates in space, one in time, two in angle, and one in frequency. We shall usually indicate the dependence of spectral radiance and irradiance on frequency by using ν as a subscript, as in I_ν, in favor of the more explicit, but lengthier, notation $I(\nu)$. Three of the dimensions are superfluous to climate models and will be discarded: The time dependence of I_ν is a function of the atmospheric state and solar zenith angle and will only be discussed further in those terms, so we shall drop the explicitly dependence on t. We reduce the number of spatial dimensions from three to one by assuming a stratified atmosphere which is horizontally homogeneous and in which physical quantities may vary only in the vertical dimension z. Thus we replace $\mathbf{r}$ by z. This approximation is also known as a plane-parallel atmosphere, and comes with at least two important caveats: The first is the neglect of horizontal photon transport which can be important in inhomogeneous cloud and surface environments. The second is the neglect of path length effects at large solar zenith angles which can dramatically affect the mean intensity of the radiation field, and thus the atmospheric photochemistry.

With these assumptions, the intensity is a function only of vertical position and of direction, $I_\nu(z, \hat{\mathbf{\Omega}})$. Often the optical depth τ (defined below), which increases monotonically with z, is used for the vertical coordinate instead of z. The angular direction of the radiation is specified in terms of the polar angle θ and the azithumal angle ϕ. The polar angle θ is the angle between $\hat{\mathbf{\Omega}}$ and the normal surface $\hat{\mathbf{n}}$ that defines the coordinate system. The specific intensity of radiation traveling at polar angle θ and azimuthal angle ϕ at optical depth level τ in a plane parallel atmosphere is denoted by $I_\nu(\tau, \theta, \phi)$. Specific intensity is also referred to as intensity.

Further simplification of the intensity field is possible if it meets certain criteria. If I_ν is not a function of position (τ), then the field is homogeneous. If I_ν is not a function of direction ($\hat{\mathbf{\Omega}}$), then the field is isotropic.

2.1.2 Mean Intensity

The mean intensity is an integrated measure of the radiation field at any point r. Mean intensity $\bar{I}_\nu$ is defined as the mean value of the intensity field integrated over all angles.

$$\bar{I}_\nu = \frac{\int_\Omega I_\nu \, \mathrm{d}\Omega}{\int_\Omega \mathrm{d}\Omega} \tag{17}$$

The solid angle subtended by Ω is the ratio of the area A enclosed by Ω on a spherical surface to the square of the radius of the sphere. Since the area of a sphere is $4\pi r^2$, there must be 4π steradians in a sphere. It is straightforward to demonstrate that the differential element of area in spherical polar coordinates is $r^2 \sin\theta \, \mathrm{d}\theta \, \mathrm{d}\phi$. Thus the element of solid angle is

$$\begin{aligned} \Omega &= A/r^2 \\ \mathrm{d}\Omega &= r^{-2} \, \mathrm{d}A \\ &= r^{-2} \, r^2 \sin\theta \, \mathrm{d}\theta \, \mathrm{d}\phi \\ &= \sin\theta \, \mathrm{d}\theta \, \mathrm{d}\phi \end{aligned} \tag{18}$$

The field of view of an instrument, e.g., a telescope, is most naturally measured by a solid angle.

The definition of $\bar{I}_\nu$ (17) demands the radiation field be integrated over all angles, i.e., over all 4π steradians. Evaluating the denominator demonstrates the properties of angular integrals. The denominator of (17) is

$$\begin{aligned} \int_\Omega \mathrm{d}\Omega &= \int_{\theta=0}^{\theta=\pi} \int_{\phi=0}^{\phi=2\pi} \sin\theta \, \mathrm{d}\theta \, \mathrm{d}\phi \\ &= [\phi]_0^{2\pi} \int_{\theta=0}^{\theta=\pi} \sin\theta \, \mathrm{d}\theta \\ &= 2\pi \int_{\theta=0}^{\theta=\pi} \sin\theta \, \mathrm{d}\theta \\ &= 2\pi \, [-\cos\theta]_0^\pi \\ &= 2\pi[-(-1) - (-1)] \\ &= 4\pi \end{aligned} \tag{19}$$

As expected, there are 4π steradians in a sphere, and 2π steradians in a hemisphere.

It is convenient to return briefly to the definition of isotropic radiation. Isotropic radiation is, by definition, equal intensity in all directions so that the total emitted radiation is simply 4π times the intensity of emission in any direction.

Applying (19) to (17) yields

$$\bar{I}_\nu = \frac{1}{4\pi} \int_\Omega I_\nu \, \mathrm{d}\Omega \tag{20}$$

$\bar{I}_\nu$ has units of radiance, $\mathrm{W\,m^{-2}\,sr^{-1}\,Hz^{-1}}$. If the radiation field is azimuthally independent (i.e., I_ν does not depend on ϕ), then

$$\bar{I}_\nu = \frac{1}{2} \int_0^\pi I_\nu \sin\theta \, \mathrm{d}\theta \tag{21}$$

Let us simplify (21) by introducing the change of variables

$$u = \cos\theta \tag{22}$$

$$\mathrm{d}u = -\sin\theta \, \mathrm{d}\theta \tag{23}$$

This maps $\theta \in [0, \boldsymbol{\pi}]$ into $u \in [1, -1]$ so that (21) becomes

$$\begin{aligned} \bar{I}_\nu &= -\frac{1}{2}\int_1^{-1} I_\nu \, \mathrm{d}u \\ \bar{I}_\nu &= \frac{1}{2}\int_{-1}^{1} I_\nu \, \mathrm{d}u \end{aligned} \tag{24}$$

The hemispheric intensities or half-range intensities are simply the up- and downwelling components of which the full intensity is composed

$$I_\nu(\tau, \hat{\boldsymbol{\Omega}}) = I_\nu(\tau, \theta, \phi) = \begin{cases} I_\nu^+(\tau, \theta, \phi) & : \quad 0 < \theta < \boldsymbol{\pi}/2 \\ I_\nu^-(\tau, \theta, \phi) & : \quad \boldsymbol{\pi}/2 < \theta < \boldsymbol{\pi} \end{cases} \tag{25a}$$

$$I_\nu(\tau, \hat{\boldsymbol{\Omega}}) = I_\nu(\tau, u, \phi) = \begin{cases} I_\nu^+(\tau, u, \phi) & : \quad 0 \leq u < 1 \\ I_\nu^-(\tau, u, \phi) & : \quad -1 < u < 0 \end{cases} \tag{25b}$$

$$I_\nu^+(\tau, \mu, \phi) = I_\nu(\tau, +\mu, \phi) = I_\nu(\tau, 0 < \theta < \boldsymbol{\pi}/2, \phi) = I_\nu(\tau, 0 < u < 1, \phi) \tag{26a}$$

$$I_\nu^-(\tau, \mu, \phi) = I_\nu(\tau, +\mu, \phi) = I_\nu(\tau, \boldsymbol{\pi}/2 < \theta < \boldsymbol{\pi}, \phi) = I_\nu(\tau, -1 < u < 0, \phi) \tag{26b}$$

2.1.3 Irradiance

The spectral irradiance F_ν measures the radiant energy flux transported through a given surface per unit area per unit time per unit wavelength. Although it is somewhat ambiguous, "flux" is used a synonym for irradiance, and has become deeply embedded in the literature (Madronich, 1987). Consider a surface orthogonal to the $\hat{\boldsymbol{\Omega}}'$ direction. All radiant energy travelling parallel to $\hat{\boldsymbol{\Omega}}'$ crosses this surface and thus contributes to the irradiance with 100% efficiency. Energy travelling orthogonal to $\hat{\boldsymbol{\Omega}}'$ (and thus parallel to the surface), however, never crosses the surface and does not contribute to the irradiance. In general, the intensity $I_\nu(\hat{\boldsymbol{\Omega}})$ projects onto the surface with an efficiency $\cos\Theta = \hat{\boldsymbol{\Omega}} \cdot \hat{\boldsymbol{\Omega}}'$, thus

$$\begin{aligned} F_\nu &= \int_\Omega I_\nu \cos\theta \, \mathrm{d}\Omega \\ &= \int_{\theta=0}^{\theta=\boldsymbol{\pi}} \int_{\phi=0}^{\phi=2\boldsymbol{\pi}} I_\nu \cos\theta \, \sin\theta \, \mathrm{d}\theta \, \mathrm{d}\phi \end{aligned} \tag{27}$$

In a plane-parallel medium, this defines the net specific irradiance passing through a given vertical level. Note the similarity between (20) and (27). The former contains the zeroth moment of the intensity with respect to the cosine of the polar angle, the latter contains the first moment. Also note that (27) integrates the cosine-weighted radiance over all angles. If I_ν is isotropic, i.e., $I_\nu = \mathrm{I}_\nu^0$, then $F_\nu = 0$ due to the symmetry of $\cos\theta$.

Let us simplify (27) by introducing the change of variables $u = \cos\theta$, $du = -\sin\theta \, \mathrm{d}\theta$. This maps $\theta \in [0, \boldsymbol{\pi}]$ into $u \in [1, -1]$:

$$\begin{aligned} F_\nu &= \int_{u=1}^{u=-1} \int_{\phi=0}^{\phi=2\boldsymbol{\pi}} I_\nu u \, (-\mathrm{d}u) \, \mathrm{d}\phi \\ &= \int_{u=-1}^{u=1} \int_{\phi=0}^{\phi=2\boldsymbol{\pi}} I_\nu u \, \mathrm{d}u \, \mathrm{d}\phi \end{aligned} \tag{28}$$

The irradiance per unit frequency, F_ν, is simply related to the irradiance per unit wavelength, F_λ. The total irradiance over any given frequency range, $[\nu, \nu + \mathrm{d}\nu]$, say, is $F_\nu \,\mathrm{d}\nu$. The irradiance over the same physical range when expressed in wavelength, $[\lambda, \lambda - \mathrm{d}\lambda]$, say, is $F_\lambda \,\mathrm{d}\lambda$. The negative sign is introduced since $-\mathrm{d}\lambda$ increases in the same direction as $+\mathrm{d}\nu$. Equating the total irradiance over the same region of frequency/wavelength, we obtain

$$\begin{aligned} F_\nu \,\mathrm{d}\nu &= -F_\lambda \,\mathrm{d}\lambda \\ F_\nu &= -F_\lambda \frac{\mathrm{d}\lambda}{\mathrm{d}\nu} \\ &= -F_\lambda \frac{d}{\mathrm{d}\nu}\left(\frac{\mathrm{c}}{\nu}\right) \\ &= -F_\lambda \left(-\frac{\mathrm{c}}{\nu^2}\right) \\ F_\nu &= \frac{\mathrm{c}}{\nu^2} F_\lambda = \frac{\lambda^2}{\mathrm{c}} F_\lambda \qquad (29) \\ F_\lambda &= \frac{\mathrm{c}}{\lambda^2} F_\nu = \frac{\nu^2}{\mathrm{c}} F_\nu \qquad (30) \end{aligned}$$

Thus F_ν and F_λ are always of the same sign.

2.1.4 Actinic Flux

A quantity of great importance in photochemistry is the total convergence of radiation at a point. This quantity, called the actinic flux, F^J, determines the availability of photons for photochemical reactions. By definition, the intensity passing through a point P in the direction $\hat{\mathbf{\Omega}}$ within the solid angle $\mathrm{d}\Omega$ is $I_\nu \,\mathrm{d}\Omega$. We have not multiplied by $\cos\theta$ since we are interested in the energy passing along $\hat{\mathbf{\Omega}}$ (i.e., $\theta = 0$). The energy from all directions passing through P is thus

$$\begin{aligned} F^J_\nu &= \int_{4\pi} I_\nu \,\mathrm{d}\Omega \\ &= 4\pi \bar{I}_\nu \qquad (31) \end{aligned}$$

Thus the actinic flux is simply 4π times the mean intensity $\bar{I}_\nu$ (20). F^J_ν has units of $\mathrm{W\,m^{-2}\,Hz^{-1}}$ which are identical to the units of irradiance F_ν (27). Although the nomenclature "actinic flux" is somewhat appropriate, it is also somewhat ambiguous. The "flux" measured by F^J_ν at a point P is the energy convergence (per unit time, frequency, and area) through the surface of the sphere containing P. This differs from the "flux" measured by F_ν, which is the net energy transport (per unit time, frequency, and area) through a defined horizontal surface. Thus it is safest to use the terms "actinic radiation field" for F^J_ν and "irradiance" for F_ν. Unfortunately the literature is permeated with the ambiguous terms "actinic flux" and "flux", respectively.

The usefulness of actinic flux F^J_ν becomes apparent only in conjunction with additional, species-dependent data describing the probability of photon absorption, or photo-absorption. Photo-absorption is the process of molecules absorbing photons. Each absorption removes energy (a photon) from the actinic radiation field. The amount of photo-absorption per

unit volume is proportional to the number concentration of the absorbing species N_A [m^{-3}], the actinic radiation field F_ν^J, and the efficiency with with each molecule absorbs photons. This efficiency is called the absorption cross-section, molecular cross section, or simply cross-section. The absorption cross-section is denoted by α and has units of [m^{-2}]. In the literature, however, values of α usually appear in CGS units [cm^{-2}]. To make explicit the frequency-dependence of α we write $\alpha(\nu)$. If α depends significantly on temperature, too (as is true for ozone), we must consider $\alpha(\nu, T)$.

The probability, per unit time, per unit frequency that a single molecule of species A will absorb a photon with frequency in $[\nu, \nu + d\nu]$ is proportional to $F_\nu^J(\nu)\alpha(\nu)$[2]. Thus $\alpha(\nu)$ is the effective cross-sectional area of a molecule for absorption. The absorption cross-section is the ratio between the number of photons (or total energy) absorbed by a molecule to the number (or total energy) per unit area convergent on the molecule. Let F_ν^α [$W\,m^{-3}$] be the energy absorbed per unit time, per unit frequency, per unit volume of air. Then

$$F_\nu^\alpha(\nu) \;=\; N_A F_\nu^J(\nu)\alpha(\nu) \tag{32}$$

where $N_A\,m^{-3}$ is the number concentration of A.

Photochemists are interested in the probability of absorbed radiation severing molecular bonds, and thus decomposing species AB into constituent species A and B. Notationally this process may be written in any of the equivalent forms

$$\begin{aligned} AB + h\nu &\longrightarrow A + B \\ AB + h\nu &\overset{\nu>\nu_0}{\longrightarrow} A + B \\ AB + h\nu &\overset{\lambda<\lambda_0}{\longrightarrow} A + B \end{aligned} \tag{33}$$

Both forms indicate that the efficiency with which reaction (33) proceeds is a function of photon energy $h\nu$. The second form makes explicit that the photodissociation reaction does not proceed unless $\nu < \nu_0$, where ν_0 is the photolysis cutoff frequency. In any case, photon energy is conventionally written $h\nu$, rather than the less convenient hc/λ.

The probability that a photon absorbed by AB will result in the photodissociation of AB, and the completion of (33), is called the quantum yield or quantum efficiency and is represented by ϕ. The probability ϕ is dimensionless[3]. In addition to its dependence on ν, ϕ depends on temperature T for some important atmospheric reactions (such as ozone photolysis). We explicitly annotate the T-dependence of ϕ only for pertinent reactions. Measurement of $\phi(\nu)$ for all conditions and reactions of atmospheric interest is an ongoing and important laboratory task.

The specific photolysis rate coefficient for the photodissociation of a species A is the number of photodissociations of A occuring per unit time, per unit volume of air, per unit frequency, per molecule of A. In accord with convention we denote the specific photolysis

[2]The proportionality constant is $(h\nu)^{-1}$, i.e., when the actinic radiation field $F_\nu^J(\nu)$ is converted from energy ($J\,m^{-2}\,s^{-1}\,Hz^{-1}$) to photons ($\#\,m^{-2}\,s^{-1}\,Hz^{-1}$) then $F_\nu^J(\nu)\alpha(\nu)$ is the probability of absorption per second per unit frequency

[3]Azimuthal angle and quantum yield are both dimensionless quantities denoted by ϕ. The meaning of ϕ should be clear from the context.

rate coefficient by J_ν. The units of J_ν are $\mathrm{s}^{-1}\,\mathrm{Hz}^{-1}$.

$$\begin{aligned} J_\nu &= \frac{F_\nu^J(\nu)\alpha(\nu)\phi(\nu)}{\mathrm{h}\nu} \\ &= \frac{4\pi\bar{I}_\nu(\nu)\alpha(\nu)\phi(\nu)}{\mathrm{h}\nu} \end{aligned} \tag{34}$$

The photon energy in the denominator converts the energy per unit area in F_ν^J to units of photons per unit area. The factor of α turns this photon flux into a photo-absorption rate per unit area. The final factor, ϕ, converts the photo-absorption rate into a photodissociation rate coefficient. Note that each factor in the numerator of (34) requires detailed spectral knowledge, either of the radiation field or of the photochemical behavior of the molecule in question. This complexity is a hallmark of atmospheric photochemistry.

The total photolysis rate coefficient J is obtained by integrating (34) over all frequencies that may contribute to photodissociation

$$\begin{aligned} J &= \int_{\nu>\nu_0} J_\nu(\nu)\,\mathrm{d}\nu \\ &= \int_{\nu>\nu_0} \frac{F_\nu^J(\nu)\alpha(\nu)\phi(\nu)}{\mathrm{h}\nu}\,\mathrm{d}\nu \\ &= \frac{4\pi}{\mathrm{h}}\int_{\nu>\nu_0} \frac{\bar{I}_\nu(\nu)\alpha(\nu)\phi(\nu)}{\nu}\,\mathrm{d}\nu \end{aligned} \tag{35}$$

As mentioned above, evaluation of (35) requires essentially a complete knowledge of the radiative and photochemical properties of the environment and species of interest.

J is notoriously sensitive to uncertainty in the input quantities. Integration errors due to the discretization of (35) are quite common. To compute J with high accuracy, regular grids must have resolution of $\sim$1 nm in the ultraviolet, (Madronich, 1989). Much of the difficulty is due to the steep but opposite gradients of F_ν^J and ϕ that occur in the ultraviolet. High frequency features in α worsen this problem for some molecules.

The utility of J has motivated researchers to overcome these computational difficulties by brute force techniques and by clever parameterizations and numerical techniques (Chang et al., 1987; Dahlback and Stamnes, 1991; Toon et al., 1989; Stamnes and Tsay, 1990; Petropavlovskikh, 1995; Landgraf and Crutzen, 1998; Wild et al., 2000). It is common to refer to photolysis rate coeffients as "J-rates", and to affix the name of the molecule to specify which individual reaction is pertinent. Another description for J is the first order rate coefficient in photochemical reactions. For example, $J_{\mathrm{NO_2}}$ is the first order rate coefficient for

$$\mathrm{NO_2} + \mathrm{h}\nu \overset{\lambda<420\,\mathrm{nm}}{\longrightarrow} \mathrm{NO} + \mathrm{O} \tag{36}$$

If $[\mathrm{NO_2}]$ denotes the number concentration of $\mathrm{NO_2}$ in a closed system where photolysis is the only sink of $\mathrm{NO_2}$, then

$$\frac{\mathrm{d}[\mathrm{NO_2}]}{\mathrm{d}t} = -J_{\mathrm{NO_2}}[\mathrm{NO_2}] + S_{\mathrm{NO_2}} \tag{37}$$

Table 3: Actinic Flux Enhancement by Scattering[a]

Description	F_ν^-	$\rho_\mathrm{L}(\nu)$	$I_\nu(\hat{\mathbf{\Omega}})$	F_ν^+	$\bar{I}_\nu$	F_ν^J
Collimated, non-reflecting	$F_\nu^\odot$	0	$F_\nu^\odot \delta(\hat{\mathbf{\Omega}} - \hat{\mathbf{\Omega}}_\odot)$	0	$\frac{F_\nu^\odot}{4\pi}$	$F_\nu^\odot$
Isotropic, non-reflecting	$F_\nu^\odot$	0	$I_\nu^- = F_\nu^\odot/\pi$ $I_\nu^+ = 0$	0	$\frac{F_\nu^\odot}{2\pi}$	$2F_\nu^\odot$
Collimated, reflecting	$F_\nu^\odot$	1	$I_\nu^- = F_\nu^\odot \delta(\hat{\mathbf{\Omega}} - \hat{\mathbf{\Omega}}_\odot)$ $I_\nu^+ = F_\nu^\odot/\pi$	$F_\nu^\odot$	$\frac{3F_\nu^\odot}{4\pi}$	$3F_\nu^\odot$
Isotropic, reflecting	$F_\nu^\odot$	1	$F_\nu^\odot/\pi$	$F_\nu^\odot$	$\frac{F_\nu^\odot}{\pi}$	$4F_\nu^\odot$

[a]Terminology: F_ν^- is downwelling irradiance of source, $\rho_\mathrm{L}(\nu)$ is Lambertian reflectance of surface (or cloud), $I_\nu(\hat{\mathbf{\Omega}})$ is resulting intensity field, F_ν^+ is upwelling irradiance, $\bar{I}_\nu$ is mean intensity, F_ν^J is actinic flux.

where S_{NO_2} represents all sources of NO_2. The terms in (37) all have dimensions of $\mathrm{m}^{-3}\,\mathrm{s}^{-1}$. The first term on the RHS is the photolysis rate of NO_2 in the system.

Figure 1 shows the spectral distribution of actinic flux in a clear mid-latitude summer atmosphere, and the absorption cross-section and quantum yield of NO_2.

Figure 2 shows the vertical distribution of $J_{\mathrm{NO}_2}\,[\mathrm{s}^{-1}]$ for the conditions shown in Figure (1).

In this section we have assumed the quantities F_ν^J, α, and ϕ are somehow known and therefore available to use to compute J. Typically, α and ϕ are considered known quantities since they usually do not vary with time or space. Models may store their values in lookup tables or precompute their contributions to (35). The essence of forward radiative problems is to determine $I_{\tilde{\nu}}$ so that quantities such as J_ν and F^α may be determined. In inverse radiative transfer problems, which are encountered in much of remote sensing, both J and the species concentration are initially unknown and must be determined. We shall continue describing the methods of forward radiative transfer until we have tools at our disposal to solve for J_ν. At that point we shall re-visit the inverse problem.

2.1.5 Actinic Flux Enhancement

The actinic flux F_ν^J (31) is sensitive to the angular distribution of radiance I_ν. Nearly all scattering processes diffuse the radiation field, i.e., convert collimated photons to more isotropic photons. Such diffusion causes actinic flux enhancement. It is instructive to examine how the relationship between downwelling flux and actinic flux changes in the presence of scattering. Four limiting cases may be identified and are summarized in Table 3. The scenarios differ in the isotropicity of the downwelling radiance (collimated or isotropic) and the reflectance $\rho_\mathrm{L}(\nu)$ (0 or 1) of the lower boundary, taken to be a Lambertian surface. All scenarios are driven by the same downwelling irradiance, taken to be the direct solar beam. The scenarios are arranged in order of increasing actinic flux F_ν^J, shown in the final column. F_ν^J increases with both the number and the brightness of reflecting surfaces. The reflectiv-

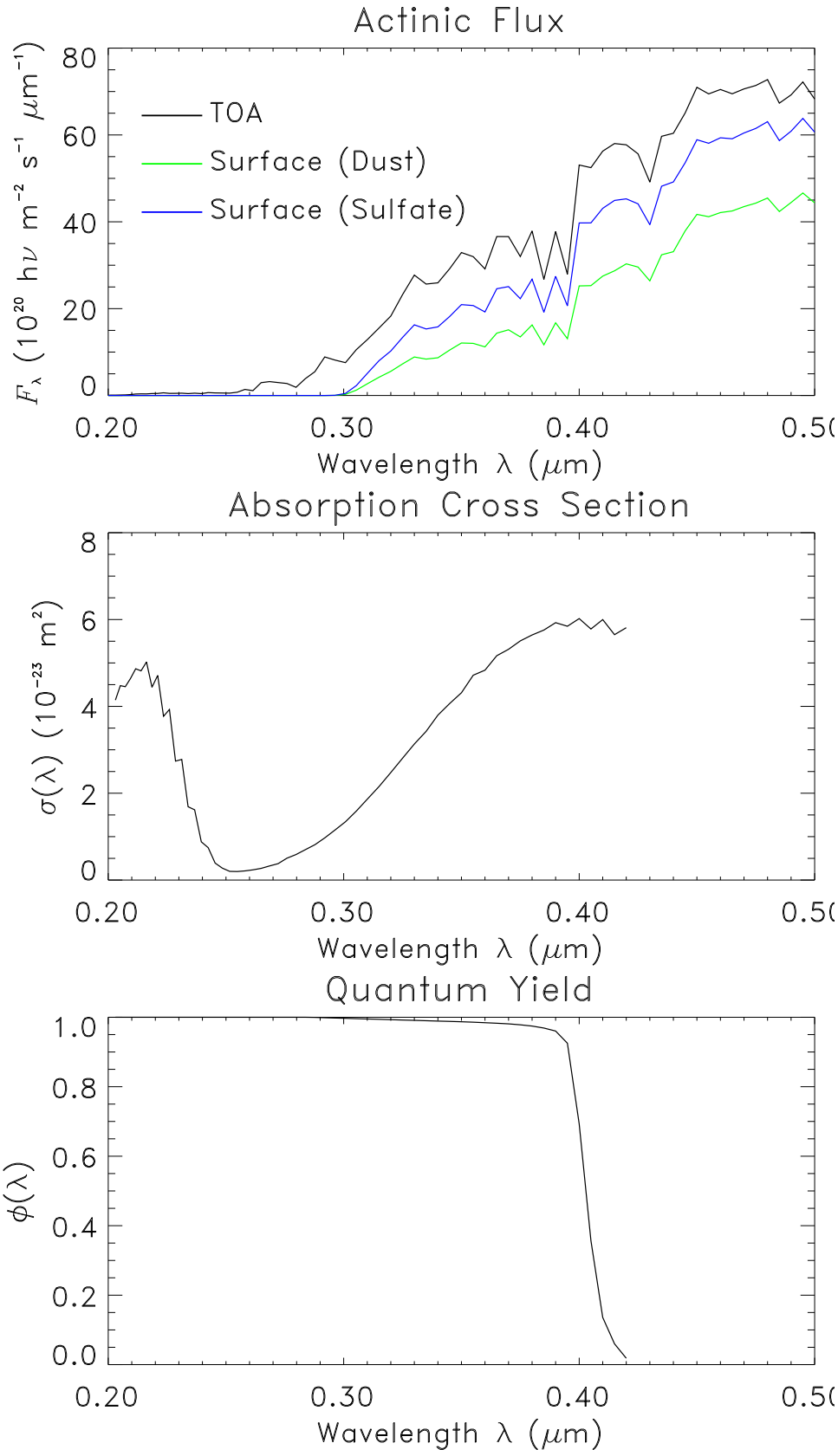

Figure 1: (a) Spectral distribution of actinic flux F^J [# m^{-2} s^{-1} µm^{-1}] at TOA and at the surface for a mid-latitude summer (MLS) atmosphere with a unit optical depth of dust or sulfate in the lowest kilometer. (b) Absorption cross section of NO_2, α_{NO_2} [m^2 molecule^{-1}]. (c) Quantum yield of NO_2, ϕ_{NO_2} (36).

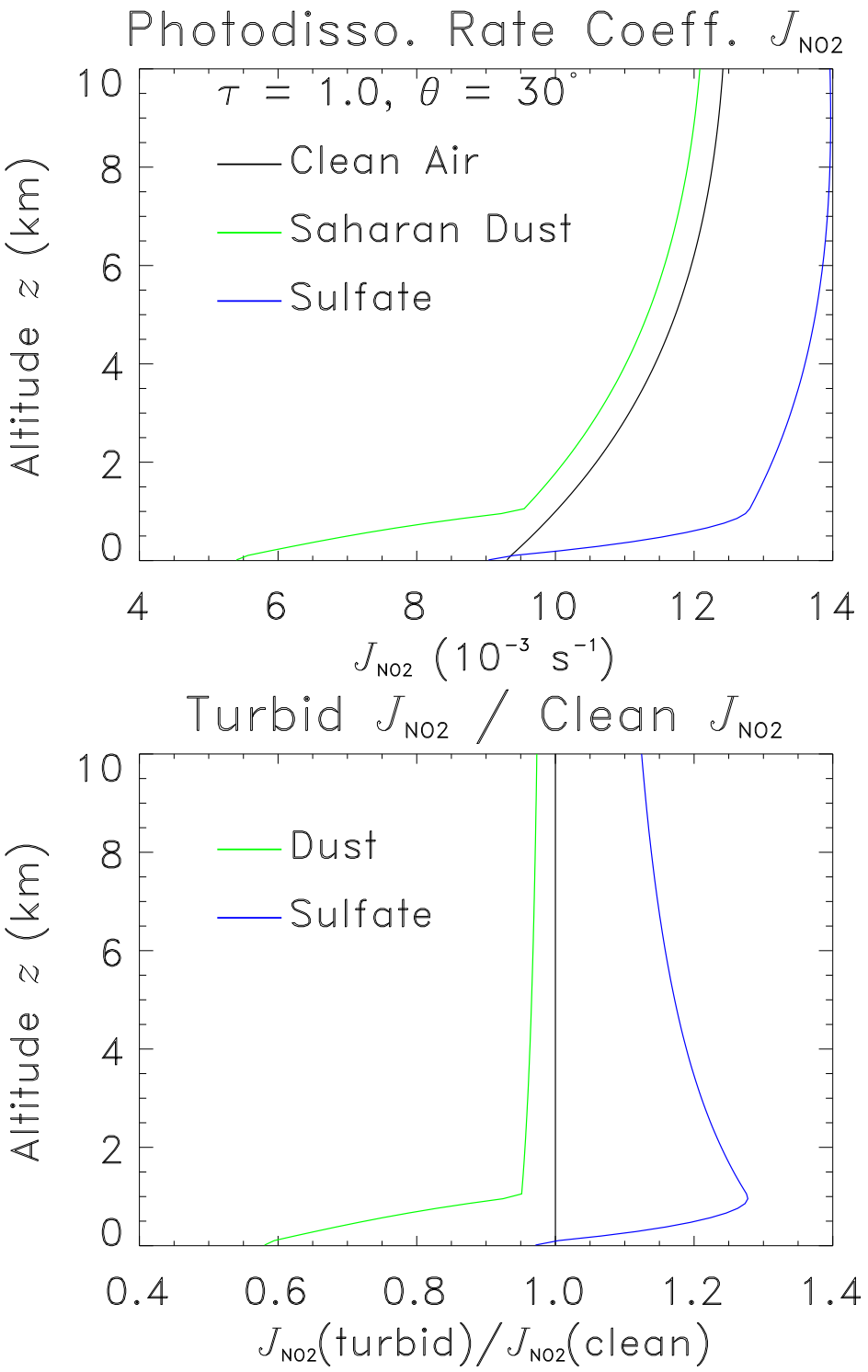

Figure 2: Vertical distribution of J_{NO_2} [s^{-1}] (36) for the conditions shown in Figure (1). (a) Absolute rates. (b) Rates normalized by clean sky rates.

ity of natural surfaces is no more than 90% nor less than 5%[4], so that the F_ν^J in Table 3 represent bounds on realistic systems.

The Collimated-Non-Reflecting scenario assumes all light travels unidirectionally in a tightly collimated direct beam with irradiance $F_\nu = F_\nu^\odot$. In this case the radiation field is the delta-function in the direction of the solar beam $I_\nu(\hat{\mathbf{\Omega}}) = F_\nu^\odot \delta(\hat{\mathbf{\Omega}} - \hat{\mathbf{\Omega}}_\odot)$. The closest approximation to this scenario in the natural environment is the pristine atmosphere high above the ocean in daylight. The actinic flux $F_\nu^J = F_\nu^\odot$ follows directly from (31). We define the actinic flux enhancement S of a medium as the ratio of the actinic flux to the actinic flux of a collimated beam with the same incident irradiance

$$S \equiv F_\nu^J / F_\nu^- \tag{38}$$

Table 3 shows S ranges from one for the direct solar beam to a maximum of four in a completely isotropic radiation field. Thus a collimated beam is the least efficient configuration of radiant energy for driving photochemistry. Scattering processes diffuse the radiation field, and, as a result, always enhance the photolytic efficiency of a given irradiance. Absorption in a medium (i.e., in the atmosphere or by the surface) always reduces F_ν^J and may lead to $S < 1$.

The Isotropic-Non-Reflecting scenario assumes isotropic downwelling radiance above a completely black surface. Under these conditions, the actinic flux is twice the incident irradiance because the photons are evenly distributed over the hemisphere rather than collimated. Moderately thick clouds ($\tau \gtrsim 3$) over a dark surface such as the ocean create a radiance field approximately like this. However, because clouds are efficient at diffusing downwelling irradiance, they are also efficient reflectors and this significantly reduces the incident irradiance F_ν^- relative to the total extraterrestrial irradiance $F_\nu^\odot$. Whether photochemistry is enhanced or diminished beneath real clouds depends on whether the actinic flux enhancement factor $F_\nu^J = 2$ compensates the reduced sub-cloud insolation due to photons up-scattering off the cloud and back to space.

The Collimated-Reflecting scenario is a very important limit in nature because the net effect on photochemistry can approach the theoretical photochemical enhancement of $S = 3$. In this limit, collimated downwelling radiation and diffuse upwelling radiation combine to drive photochemistry from both hemispheres. A clear atmosphere above bright surfaces (clouds, desert, snow) approaches this limit. These conditions describe a large fraction of the atmosphere, which is 50–60% cloud-covered. Moreover, the incident flux is not attenuated by cloud transmission, so $F_\nu^- \approx F_\nu^\odot$. The relatively high frequency of occurance of this scenario, combined with the large photochemical enhancement of $S = 3$, are unequalled by any other scenario.

We may also define the actinic flux efficiency E of a medium as the actinic flux relative to the actinic flux of an isotropic radiation field with the same incident irradiance

$$E \equiv \frac{F_\nu^J}{4F_\nu^-} \tag{39}$$

[4]Glaciers are the most reflective surfaces in nature, with $\rho_L(\nu) \lesssim 0.9$. Maximum cloud reflectance is $\lesssim 0.7$. Dark forests and ocean have $\rho_L(\nu) \gtrsim 0.05$. See discussion in §2.3.2 and Table 4.

Clearly $0 \leq E \leq 1$. Table 3 shows $E = 0.25$ for a collimated beam, and $E = 1$ for isotropic radiation. Just as scattering of the solar beam is required to increase E above 0.25, absorption must be present to reduce E beneath 0.25.

The Isotropic-Reflecting scenario shows that an isotropic radiation field is most efficient for driving photochemistry. The maximum four-fold increase in efficiency relative to the collimated field arises from the radiation field interacting with the particle from all directions, rather than from one direction only. This is geometrically equivalent to multiplying the molecular cross section by a factor of four, the ratio between the surface and cross-sectional areas of a sphere. Note that photochemistry itself is driven by molecular absorption which reduces F_ν^J from the values in Table 3.

In summary, we have learned that a reactant molecule with a spherically symmetric field of influence receives photochemical radiation much like Earth receives solar irradiance. In both cases the collimated beam intercepts one fourth of the total area of matter (molecule or Earth), while an equal flux of diffuse (or diurnal average) irradiance impinges on four times as much area. Since, in the geometric limit, absorption probability depends upon area, not direction, collimated beams have one fourth the photochemical potential as isotropic radiation.

2.1.6 Energy Density

Another quantity of interest is the density of radiant energy per unit volume of space. We call this quantity the energy density U_ν. The energy density is the number of photons per unit volume in the frequency range $[\nu, \nu + \mathrm{d}\nu]$ times the energy per photon, $\mathrm{h}\nu$. U_ν is simply related to the actinic flux F_ν^J (31) and thus to the mean intensity $\bar{I}_\nu$.

$$\begin{aligned} U_\nu &= \int_{4\pi} \mathrm{d}U_\nu \\ &= \frac{4\pi}{\mathrm{c}} \bar{I}_\nu \end{aligned} \tag{40}$$

The units of U_ν are $\mathrm{J\,m^{-3}\,Hz^{-1}}$.

2.1.7 Spectral vs. Broadband

Until now we have considered only spectrally dependent quantities such as the spectral radiance I_ν, spectral irradiance F_ν, spectral actinic flux F_ν^J, and spectral energy density U_ν. These quantities are called spectral and are given a subscript of ν, λ, or $\tilde{\nu}$ because they are expressed per unit frequency, wavelength, or wavenumber, respectively. Each spectral radiant quantity may be integrated over a frequency range to obtain the corresponding band-integrated radiant quantity. Band-integrated radiant fields are often called narrowband or broadband Depending on the size of the frequency range, broadband radiant are obtained

by integrating over all frequencies:

$$
\begin{aligned}
I &= \int_0^\infty I_\nu(\nu)\,\mathrm{d}\nu \\
F &= \int_0^\infty F_\nu(\nu)\,\mathrm{d}\nu \\
F^J &= \int_0^\infty F_\nu^J(\nu)\,\mathrm{d}\nu \\
F^\alpha &= \int_0^\infty F_\nu^\alpha(\nu)\,\mathrm{d}\nu \\
J &= \int_0^\infty J_\nu(\nu)\,\mathrm{d}\nu \\
U &= \int_0^\infty U_\nu(\nu)\,\mathrm{d}\nu \\
h &= \int_0^\infty h_\nu(\nu)\,\mathrm{d}\nu
\end{aligned}
$$

2.1.8 Thermodynamic Equilibria

Temperature plays a fundamental role in radiative transfer because T determines the population of excited atomic states, which in turn determines the potential for thermal emission. Thermal emission occurs as matter at any temperature above absolute zero undergoes quantum state transitions from higher energy to lower energy states. The difference in energy between the higher and lower level states is transferred via the electromagnetic field by photons. Thus an important problem in radiative transfer is quantifying the contribution to the radiation field from all emissive matter in a physical system. For the atmosphere the system of interest includes, e.g., clouds, aerosols, and the surface.

To develop this understanding we must discuss various forms of energetic equilibria in which a physical system may reside. Earth (and the other terrestrial planets, Mercury, Venus, and Mars) are said to be in planetary radiative equilibrium because, on an annual timescale the solar energy absorbed by the Earth system balances the thermal energy emitted to space by Earth. Radiation and matter inside a constant temperature enclosure are said to be in thermodynamic equilibrium, or TE.

Radiation in thermodynamic equilibrium with matter plays a fundamental role in radiation transfer. Such radiation is most commonly known as blackbody radiation. Kirchoff first deduced the properties of blackbody radiation.

Thermodynamic equilibrium (TE) is an idealized state, but, fortunately, the properties of radiation in TE can be shown to apply to a less restrictive equilibrium known as local thermodynamic equilibrium, or LTE.

2.1.9 Planck Function

The Planck function B_ν describes the intensity of blackbody radiation as a function of temperature and wavelength

$$B_\nu(T,\nu) = \frac{2\mathrm{h}\nu^3}{\mathrm{c}^2(\mathrm{e}^{\mathrm{h}\nu/\mathrm{k}T}-1)} \tag{41a}$$

$$B_\lambda(T,\lambda) = \frac{2\mathrm{hc}^2}{\lambda^5(\mathrm{e}^{\mathrm{hc}/\lambda\mathrm{k}T}-1)} \tag{41b}$$

Blackbodies emit isotropically—this considerably simplifies thermal radiative transfer. The correct predictions (41a) resolved one of the great mysteries in experimental physics in the late 19th century. In fact, this discovery marked the beginning of the science of quantum mechanics.

The relations (41a) and (41b) predict slightly different quantities. The former predicts the blackbody radiance per unit frequency, while the latter predicts the blackbody radiance per unit wavelength. Of course these quantities are related since the blackbody energy within any given spectral band must be the same regardless of which formula is used to describe it. Expressed mathematically, this constraint means

$$B_\nu \,\mathrm{d}\nu \;=\; -B_\lambda \,\mathrm{d}\lambda \tag{42}$$

Once again, the negative sign arises as a result of the opposite senses of increasing frequency versus increasing wavelength. We may derive (41b) from (41a) by using (9) in (42)

$$\begin{aligned} B_\nu &= -B_\lambda \frac{\mathrm{d}\lambda}{\mathrm{d}\nu} \\ &= \frac{B_\lambda \mathrm{c}}{\nu^2} \\ &= B_\lambda \mathrm{c}\left(\frac{\lambda^2}{\mathrm{c}^2}\right) \\ B_\nu &= \frac{\lambda^2}{\mathrm{c}} B_\lambda = \frac{\mathrm{c}}{\nu^2} B_\lambda \qquad (43) \\ B_\lambda &= \frac{\nu^2}{\mathrm{c}} B_\nu = \frac{\mathrm{c}}{\lambda^2} B_\nu \qquad (44) \end{aligned}$$

These relations are analogous to (30).

The Planck function (41) has interesting behavior in both the high and the low energy photon limits. In the high energy limit, known as Wien's limit, the photon energy greatly exceeds the ambient thermal energy

$$\mathrm{h}\nu_\mathrm{M} \gg \mathrm{k}T \tag{45}$$

In Wien's limit, (41) becomes

$$B_\nu(T,\nu) = \frac{2\mathrm{h}\nu^3}{\mathrm{c}^2}\mathrm{e}^{-\mathrm{h}\nu/\mathrm{k}T} \tag{46a}$$

$$B_\lambda(T,\lambda) = \frac{2\mathrm{hc}^2}{\lambda^5}\mathrm{e}^{-\mathrm{hc}/\lambda\mathrm{k}T} \tag{46b}$$

In the very low energy limit, known as the Rayleigh-Jeans limit, the photon energy is much less than the ambient thermal energy

$$\mathrm{h}\nu_\mathrm{M} \ll \mathrm{k}T \tag{47}$$

Thus in the Rayleigh-Jeans limit the arguments to the exponential in (41) are less than 1 so the exponentials may be expanded in Taylor series. Starting from (41a)

$$\begin{aligned} B_\nu(T,\nu) &\approx \frac{2\mathrm{h}\nu^3}{\mathrm{c}^2}\left(1+\frac{\mathrm{h}\nu}{\mathrm{k}T}-1\right)^{-1} \\ &= \frac{2\mathrm{h}\nu^3\mathrm{k}T}{\mathrm{c}^2\mathrm{h}\nu} \\ &= \frac{2\nu^2\mathrm{k}T}{\mathrm{c}^2} \end{aligned} \tag{48}$$

Similar manipulation of (41b) may be performed and we obtain

$$B_\nu(T,\nu) \approx \frac{2\nu^2\mathrm{k}T}{\mathrm{c}^2} \tag{49a}$$

$$B_\lambda(T,\lambda) \approx \frac{2\mathrm{c}\mathrm{k}T}{\lambda^4} \tag{49b}$$

The frequency of extreme emission is obtained by taking the partial derivative of (41a) with respect to frequency with the temperature held constant

$$\left.\frac{\partial B_\nu}{\partial \nu}\right|_T = \frac{2\mathrm{h}}{\mathrm{c}^2} \times \frac{1}{(\mathrm{e}^{\mathrm{h}\nu/\mathrm{k}T}-1)^2} \times \left(3\nu^2(\mathrm{e}^{\mathrm{h}\nu/\mathrm{k}T}-1) - \nu^3\frac{\mathrm{h}}{\mathrm{k}T}\mathrm{e}^{\mathrm{h}\nu/\mathrm{k}T}\right)$$

To solve for the frequency of maximum emission, ν_M, we set the RHS equal to zero so that one or more of the LHS factors must equal zero

$$\begin{aligned} \frac{2\mathrm{h}\nu_\mathrm{M}^2\left[3(\mathrm{e}^{\mathrm{h}\nu_\mathrm{M}/\mathrm{k}T}-1) - \frac{\mathrm{h}\nu_\mathrm{M}}{\mathrm{k}T}\mathrm{e}^{\mathrm{h}\nu_\mathrm{M}/\mathrm{k}T}\right]}{\mathrm{c}^2(\mathrm{e}^{\mathrm{h}\nu_\mathrm{M}/\mathrm{k}T}-1)^2} &= 0 \\ 3(\mathrm{e}^{\mathrm{h}\nu_\mathrm{M}/\mathrm{k}T}-1) - \frac{\mathrm{h}\nu_\mathrm{M}}{\mathrm{k}T}\mathrm{e}^{\mathrm{h}\nu_\mathrm{M}/\mathrm{k}T} &= 0 \\ \frac{\mathrm{h}\nu_\mathrm{M}}{\mathrm{k}T}\mathrm{e}^{\mathrm{h}\nu_\mathrm{M}/\mathrm{k}T} &= 3(\mathrm{e}^{\mathrm{h}\nu_\mathrm{M}/\mathrm{k}T}-1) \\ \frac{\mathrm{h}\nu_\mathrm{M}}{\mathrm{k}T} &= 3(1-\mathrm{e}^{-\mathrm{h}\nu_\mathrm{M}/\mathrm{k}T}) \end{aligned} \tag{50}$$

An analytic solution to (50) is impossible since ν_M cannot be factored out of this transcendental equation. If instead we solve $x = 3(1-\mathrm{e}^{-x})$ numerically we find that $x \approx 2.8215$ so that

$$\begin{aligned} \frac{\mathrm{h}\nu_\mathrm{M}}{\mathrm{k}T} &\approx 2.82 \\ \nu_\mathrm{M} &\approx 2.82\mathrm{k}T/\mathrm{h} \\ &\approx 5.88\times10^{10}\,T \qquad \mathrm{Hz} \end{aligned} \tag{51}$$

where the units of the numerical factor are $\mathrm{Hz\,K^{-1}}$. Thus the frequency of peak blackbody emission is directly proportional to temperature. This is known as Wien's Displacement Law.

A separate relation may be derived for the wavelength of maximum emission λ_{M} by an analogous procedure starting from (41b). The result is

$$\lambda_{\mathrm{M}} \approx 2897.8/T \qquad \mu\mathrm{m} \tag{52}$$

where the units of the numerical factor are $\mu\mathrm{m\,K}$. Note that (51) and (52) do not yield the same answer because they measure different quantities. The wavelength of maximum emission per unit wavelength, for example, is displaced by a factor of approximately 1.76 from the wavelength of maximum emission per unit frequency.

It is possible to use (51) to estimate the temperature of remotely sensed surfaces. For example, a satellite-borne tunable spectral radiometer may measure the emission of a newly discovered planet at all wavelengths of interest. Assuming the wavelength of peak measured emission is $\lambda_{\mathrm{M}}\,\mu\mathrm{m}$. Then a first approximation is that the planetary temperature is close to $2897.8/\lambda_{\mathrm{M}}$.

2.1.10 Hemispheric Quantities

In climate studies we are most interested in the irradiance passing upwards or downwards through horizontal surfaces, e.g., the ground or certain layers in the atmosphere. These hemispheric irradiances measure the radiant energy transport in the vertical direction. These hemispheric irradiances depend only on the corresponding hemispheric intensities. Let us assume the intensity field is azimuthally independent, i.e., $I_\nu = I_\nu(\theta)$ only. Then the azimuthal contribution to (28) is 2π and

$$\begin{aligned} F_\nu &= 2\pi \int_{u=-1}^{u=1} I_\nu u \,\mathrm{d}u \\ &= 2\pi \left(\int_{u=-1}^{u=0} I_\nu u \,\mathrm{d}u + \int_{u=0}^{u=1} I_\nu u \,\mathrm{d}u \right) \end{aligned} \tag{53}$$

We now introduce the change of variables $\mu = |u| = |\cos\theta|$. Referring to (23) we find

$$\mu = |\cos\theta| = \begin{cases} \cos\theta & : \quad 0 < \theta < \pi/2 \\ -\cos\theta & : \quad \pi/2 < \theta < \pi \end{cases} \tag{54a}$$

$$\mu = |u| = \begin{cases} u & : \quad 0 \le u < 1 \\ -u & : \quad -1 < u < 0 \end{cases} \tag{54b}$$

Most formal work on radiative transfer is written in terms of μ rather than u or θ. Substituting (54) into (53)

$$\begin{aligned} F_\nu &= 2\pi \left(\int_{\mu=1}^{\mu=0} I_\nu(-\mu)\,(-\mathrm{d}\mu) + \int_{\mu=0}^{\mu=1} I_\nu \mu \,\mathrm{d}\mu \right) \\ &= 2\pi \left(\int_{\mu=1}^{\mu=0} I_\nu \mu \,\mathrm{d}\mu + \int_{\mu=0}^{\mu=1} I_\nu \mu \,\mathrm{d}\mu \right) \\ &= 2\pi \left(- \int_{\mu=0}^{\mu=1} I_\nu \mu \,\mathrm{d}\mu + \int_{\mu=0}^{\mu=1} I_\nu \mu \,\mathrm{d}\mu \right) \\ &= -F_\nu^- + F_\nu^+ \\ &= F_\nu^+ - F_\nu^- \end{aligned} \tag{55}$$

where we have defined the hemispheric fluxes or half-range fluxes

$$F_\nu^+ = 2\pi \int_0^1 I_\nu(+\mu)\mu \,\mathrm{d}\mu \tag{56a}$$

$$F_\nu^- = 2\pi \int_0^1 I_\nu(-\mu)\mu \,\mathrm{d}\mu \tag{56b}$$

The hemispheric fluxes are positive-definite, and their difference is the net flux.

$$F_\nu = F_\nu^+ - F_\nu^- \tag{57}$$

$$\boxed{F_\nu = F_\nu^+ - F_\nu^-} \tag{58}$$

The superscripts $^+$ and $^-$ denote upwelling (towards the upper hemisphere) and downwelling (towards the lower hemisphere) quantities, respectively. The net flux F_ν is the difference between the upwelling and downwelling hemispheric fluxes, F_ν^+ and F_ν^-, which are both positive-definite quantities.

The hemispheric flux transport in isotropic radiation fields is worth examining in detail since this condition is often met in practice. It will be seen that isotropy considerably simplifies many of the troublesome integrals encountered. When I_ν has no directional dependence (i.e., it is a constant) then $F_\nu^+ = F_\nu^-$ (58). Thus the net radiative energy transport is zero in an isotropic radiation field, such as a cavity filled with blackbody radiation.

Let us compute the upward transport of radiation $B_\nu(T)$ (41a) emitted by a perfect blackbody such as the ocean surface. Since $B_\nu(T)$ is isotropic, the intensity may be factored out of the definition of the upwelling flux (56a) and we obtain

$$\begin{aligned} F_\nu^B &= 2\pi \int_0^1 B_\nu \mu \,\mathrm{d}\mu \\ &= 2\pi B_\nu \int_0^1 \mu \,\mathrm{d}\mu \\ &= 2\pi B_\nu \frac{\mu^2}{2}\bigg|_{\mu=0}^{\mu=1} \end{aligned}$$

$$\begin{aligned} &= 2\pi B_\nu \left(\tfrac{1}{2} - 0\right) \\ &= \pi B_\nu \end{aligned} \tag{59}$$

Thus the upwelling blackbody irradiance tranports π times the constant intensity of the radiation. Given that the upper hemisphere contains 2π steradians, one might naively expect the upwelling irradiance to be $2\pi B_\nu$. In fact the divergence of blackbody radiance above the emitting surface is $2\pi B_\nu$. But the vertical flux of energy is obtained by cosine-weighting the radiance over the hemisphere and this weight introduces the factor of $\frac{1}{2}$ difference between the naive and the correct solutions.

2.1.11 Stefan-Boltzmann Law

The frequency-integrated hemispheric irradiance emanating from a blackbody of great interest since it describes, e.g., the radiant power of most surfaces on Earth. Although we could integrate the B_ν (41a) directly to obtain the broadband intensity $B \equiv \int_0^\infty B_\nu(\nu)\,\mathrm{d}\nu$, it is traditional to integrate B_ν first over the hemisphere (59). By proceeding in this order, we shall obtain the total hemispheric blackbody irradiance F_B^+ in terms fundamental physical constants and the temperature of the body.

$$\begin{aligned} F_B^+ &= \pi \int_0^\infty B_\nu \,\mathrm{d}\nu \\ &= \pi \int_0^\infty \frac{2\mathrm{h}\nu^3}{\mathrm{c}^2(\mathrm{e}^{\mathrm{h}\nu/\mathrm{k}T} - 1)}\,\mathrm{d}\nu \\ &= \frac{2\pi\mathrm{h}}{\mathrm{c}^2} \int_0^\infty \frac{\nu^3}{\mathrm{e}^{\mathrm{h}\nu/\mathrm{k}T} - 1}\,\mathrm{d}\nu \end{aligned} \tag{60}$$

To simplify (60) we make the change of variables

$$\begin{aligned} x &= \frac{\mathrm{h}\nu}{\mathrm{k}T} \\ \nu &= \frac{\mathrm{k}Tx}{\mathrm{h}} \\ \mathrm{d}\nu &= \frac{\mathrm{k}T}{\mathrm{h}}\,\mathrm{d}x \\ \mathrm{d}x &= \frac{\mathrm{h}}{\mathrm{k}T}\,\mathrm{d}\nu \end{aligned}$$

This change of variables maps $\nu \in [0, \infty)$ to $x \in [0, \infty)$. Substituting this into (60) we obtain

$$\begin{aligned} F_B^+ &= \frac{2\pi\mathrm{h}}{\mathrm{c}^2} \int_0^\infty \left(\frac{\mathrm{k}T}{\mathrm{h}}\right)^3 \frac{x^3}{\mathrm{e}^x - 1} \frac{\mathrm{k}T}{\mathrm{h}}\,\mathrm{d}x \\ &= \frac{2\pi\mathrm{k}^4T^4}{\mathrm{c}^2\mathrm{h}^3} \int_0^\infty \frac{x^3}{\mathrm{e}^x - 1}\,\mathrm{d}x \end{aligned} \tag{61}$$

The definite integral in (61) is $\pi^4/15$. Proving this is a classic problem in mathematical physics which involves the Riemann zeta function (and thus prime number theory), the

Gamma function, and contour integration. The procedure used to obtain this result is interesting so we briefly summarize it here. The Riemann zeta function $\zeta(x)$ for real $x > 1$ may be defined as

$$\zeta(x) \equiv \frac{1}{\Gamma(x)} \int_0^\infty \frac{u^{x-1}}{\mathrm{e}^u - 1}\, \mathrm{d}u \tag{62}$$

Comparing (61) with the Riemann zeta function definition (62), we see that $x = 4$, i.e,

$$F_B^+ = \frac{2\pi \mathrm{k}^4 T^4}{\mathrm{c}^2 \mathrm{h}^3} \Gamma(4)\zeta(4) \tag{63}$$

The integral (62) is analytically solvable for the special case of integers $x = n$. We may transform the integrand from a rational fraction into a power series using algebraic manipulation:

$$\begin{aligned} \frac{u^{x-1}}{\mathrm{e}^u - 1} &= \frac{u^{x-1}}{\mathrm{e}^u - 1} \times \frac{\mathrm{e}^{-u}}{\mathrm{e}^{-u}} \\ &= \frac{u^{x-1}\mathrm{e}^{-u}}{1 - \mathrm{e}^{-u}} \\ &= u^{x-1}\mathrm{e}^{-u} \times \frac{1}{1 - \mathrm{e}^{-u}} \end{aligned} \tag{64}$$

The integration limits in (62) are $[0, \infty)$ so it is always true that $\mathrm{e}^{-u} < 1$ in (64), and thus in the integrand of (62).

Recall that the sum of an infinite power series with initial term a_0 and ratio r is

$$\begin{aligned} \sum_{k=0}^{\infty} a_0 r^k &= \lim_{k\to\infty} a_0 + a_0 r + a_0 r^2 + \cdots + a_0 r^{k-1} + a_0 r^k \\ &= a_0/(1-r) \quad \text{for } |r| < 1 \end{aligned} \tag{65}$$

Hence the last term in (64) is the sum of a power series (65) with initial term $a_0 = 1$ and ratio $r = \mathrm{e}^{-u}$.

$$\frac{1}{1 - \mathrm{e}^{-u}} = \sum_{k=0}^{\infty} \mathrm{e}^{-ku} \tag{66}$$

Substituting (66) into (64) we obtain

$$\begin{aligned} \frac{u^{x-1}}{\mathrm{e}^u - 1} &= u^{x-1}\mathrm{e}^{-u} \sum_{k=0}^{\infty} \mathrm{e}^{-ku} \\ &= \sum_{k=0}^{\infty} u^{x-1}\mathrm{e}^{-(k+1)u} \\ &= \sum_{k=1}^{\infty} u^{x-1}\mathrm{e}^{-ku} \end{aligned} \tag{67}$$

where the last step shifts the initial index to from zero to one.

Using the inifinite series representation (67) for the integrand of (62) yields

$$\zeta(x) = \frac{1}{\Gamma(x)} \int_0^\infty \left[\sum_{k=1}^\infty u^{x-1} \mathrm{e}^{-ku} \right] \mathrm{d}u$$

Integration and addition are commutative operations. Interchanging their order yields

$$\zeta(x) = \frac{1}{\Gamma(x)} \sum_{k=1}^\infty \left[\int_0^\infty u^{x-1} \mathrm{e}^{-ku} \, \mathrm{d}u \right] \tag{68}$$

We change variables from $u \in [0, +\infty]$ to $y \in [0, +\infty]$ with

$$\begin{aligned} y &= ku \\ \mathrm{d}y &= k \, \mathrm{d}u \\ u &= y/k \\ \mathrm{d}u &= k^{-1} \, \mathrm{d}y \end{aligned} \tag{69}$$

so that (68) becomes

$$\begin{aligned} \zeta(x) &= \frac{1}{\Gamma(x)} \sum_{k=1}^\infty \left[\int_0^\infty \left(\frac{y}{k} \right)^{x-1} \mathrm{e}^{-y} k^{-1} \, \mathrm{d}y \right] \\ &= \frac{1}{\Gamma(x)} \sum_{k=1}^\infty k^{-(x-1)} k^{-1} \left[\int_0^\infty y^{x-1} \mathrm{e}^{-y} \, \mathrm{d}y \right] \\ &= \frac{1}{\Gamma(x)} \sum_{k=1}^\infty k^{-x} [\Gamma(x)] \\ &= \sum_{k=1}^\infty k^{-x} \end{aligned} \tag{70}$$

where we replaced the integral in brackets with the Gamma function it defines. Hence the Riemann zeta function of a positive integer n is the sum of the reciprocals of the postive integers to the power n.

Contour integration in the complex plane gives analytic closed-form solutions to $\Sigma_1^\infty k^{-n}$ (70) for positive, even integers n. Our immediate concern is $n = 4$. Consider the complex function (Carrier et al., 1983, p. 97)

$$f(z) = \frac{\pi \cot \pi z}{z^4} \tag{71}$$

This function

1. Is analytic throughout the complex plane
2. Has first order poles at all integer values on the real axis (except the origin)
3. Has a fifth order pole at the origin

4. Satisfies $\lim_{|R|\to\infty} f(z) = 0$ where $z = R\mathrm{e}^{\mathrm{i}\theta}$

Therefore (71) obeys the residue theorem for suitably chosen contours. In other words, fxm.
Having shown

$$\zeta(4) \;=\; \pi^4/90 \tag{72}$$

Using $\Gamma(4) = 3! = 3 \times 2 \times 1 = 6$ and $\zeta(4) = \pi^4/90$ from (72), Equation (63) becomes

$$\begin{aligned} F_B^+ &= \frac{2\pi \mathrm{k}^4}{\mathrm{c}^2\mathrm{h}^3} \times 6 \times \frac{\pi^4}{90} \times T^4 \\ &= \frac{2\pi^5 \mathrm{k}^4}{15\mathrm{c}^2\mathrm{h}^3} T^4 \end{aligned}$$

This is known as the Stefan-Boltzmann Law of radiation, and is usually written as

$$F_B^+ \;=\; \sigma T^4 \qquad \text{where} \tag{73}$$

$$\sigma \;\equiv\; \frac{2\pi^5 \mathrm{k}^4}{15\mathrm{c}^2\mathrm{h}^3} \tag{74}$$

σ is known as the Stefan-Boltzmann constant and depends only on fundamental physical constants. The value of σ is $5.67032 \times 10^{-8}\,\mathrm{W\,m^{-2}\,K^{-4}}$. The thermal emission of matter depends very strongly (quartically) on T (73). This rather surprising result has profound implications for Earth's climate.

We derived F_B^+ (73) directly so that the Stefan-Boltzmann constant would fall naturally from the derivation. For completeness we now present the broadband blackbody intensity B

$$\begin{aligned} B &= \int_0^\infty B_\nu(\nu)\,\mathrm{d}\nu \\ &= \frac{2\pi^4 \mathrm{k}^4}{15\mathrm{c}^2\mathrm{h}^3} T^4 \\ &= F_B^+/\pi = \sigma T^4/\pi \end{aligned} \tag{75}$$

The factor of π difference between B and F_B^+ is at first confusing. One must remember that B is the broadband (spectrally-integrated) intensity and that F_B^+ is the broadband hemispheric irradiance (spectrally-and-angularly-integrated).

2.1.12 Luminosity

The total thermal emission of a body (e.g., star or planet) is called its luminosity, L. The luminosity is thermal irradiance integrated over the surface-area of a volume containing the body. The luminosity of bodies with atmospheres is usually taken to be the total outgoing thermal emission at the top of the atmosphere. If the time-mean thermal radiation field of a body is spherically symmetric, then its luminosity is easily obtained from a time-mean measurement of the thermal irradiance normal to any unit area of the surrounding surface. This technique is used on Earth to determine the intrinsic luminosity of stars whose distance $D_\odot$ is known (e.g., through parallax) including our own.

$$L_\odot \;=\; 4\pi D_\odot^2 F_\odot \tag{76}$$

The meaning of the solar constant $F_\odot$ is made clear by (76). $F_\odot$ is the solar irradiance that would be measured normal to the Earth-Sun axis at the top of Earth's atmosphere. The mean Earth-Sun distance is $\sim 1.5 \times 10^{11}\,\mathrm{m}$ and $F_\odot \approx 1367\,\mathrm{W\,m^{-2}}$ so $L_\odot = 3.9 \times 10^{26}\,\mathrm{W}$. Note that L has dimensions of power, i.e., $\mathrm{J\,s^{-1}}$.

An independent means of estimating the luminosity of a celestial body is to integrate the surface thermal irradiance over the surface area of the body. For planets without atmospheres, L is simply the integrated surface emission. Assuming the effective temperature (4) of our Sun is T_E, the radius $r_\odot$ at which this emission must originate is defined by combining (73) with (76)

$$\begin{aligned} 4\pi r_\odot^2 \sigma T_\odot^4 &= 4\pi D_\odot^2 F_\odot \\ r_\odot^2 &= \frac{D_\odot^2 F_\odot}{\sigma T_\odot^4} \\ r_\odot &= \frac{D_\odot}{T_\odot^2}\sqrt{\frac{F_\odot}{\sigma}} \end{aligned} \tag{77}$$

For the Sun-Earth system, $T_\odot \approx 5800\,\mathrm{K}$ so $r_\odot = 6.9 \times 10^8\,\mathrm{m}$. Solar radiation received by Earth appears to originate from a portion of the solar atmosphere known as the photosphere.

2.1.13 Extinction and Emission

Radiation and matter have only two forms of interactions, extinction and emission. Lambert[5], first proposed that the extinction (i.e., reduction) of radiation traversing an infinitesimal path $\mathrm{d}s$ is linearly proportional to the incident radiation and the amount of interacting matter along the path

$$\frac{\mathrm{d}I_\nu}{\mathrm{d}s} = -k(\nu) I_\nu \qquad \text{Extinction only} \tag{78}$$

Here $k(\nu)$ is the extinction coefficient, a measurable property of the medium, and s is the absorber path length. $k(\nu)$ is proportional to the local density of the medium and is positive-definite.

The term extinction coefficient and the exact definition of $k(\nu)$ are somewhat ambiguous until their physical dimensions are specified. Path length, for example, can be measured in terms of column mass path $M\,[\mathrm{kg\,m^{-2}}]$, number path of molecules $N\,[\#\,\mathrm{m^{-2}}]$, and geometric distance $s\,[\mathrm{m}]$. Each path measure has a commensurate extinction coefficient: the mass extinction coefficient $\psi_\mathrm{e}\,[\mathrm{m^2\,kg^{-1}}]$ (i.e., optical cross-section per unit mass), the number extinction coefficient $\kappa_\mathrm{e}\,[\mathrm{m^2\,molecule^{-1}}]$ (i.e., optical cross-section per molecule), the volume extinction coefficient $k_\mathrm{e}\,[\mathrm{m^2\,m^{-3}}]$=$[\mathrm{m^{-1}}]$ (i.e., optical cross-section per unit concentration). These coefficients are inter-related by

$$\begin{aligned} \psi_\mathrm{e}\,[\mathrm{m^2\,kg^{-1}}] &= \frac{k_\mathrm{e}\,[\mathrm{m^{-1}}]}{\rho\,[\mathrm{kg\,m^{-3}}]} \\ \kappa_\mathrm{e}\,[\mathrm{m^2\,molecule^{-1}}] &= \frac{\psi_\mathrm{e}\,[\mathrm{m^2\,kg^{-1}}] \times \mathcal{M}\,[\mathrm{kg\,mol^{-1}}]}{\mathcal{N}\,[\mathrm{molecule\,mol^{-1}}]} \\ k_\mathrm{e}\,[\mathrm{m^{-1}}] &= \kappa_\mathrm{e}\,[\mathrm{m^2\,molecule^{-1}}] \times n\,[\mathrm{molecule\,m^{-3}}] \end{aligned} \tag{79}$$

[5]Beer is usually credited with first formulating this law, but actually the similarly-named Bougher deserves the credit.

We will develop the formalism of radiative transfer in this chapter in terms using the geometric path and volume extinction coefficient (s, k_e) formalism. Our intent is to be concrete, rather than leaving the choice of units unstated. However, there is nothing fundamental about (s, k_e). In Section 4.1.1 we state our preference for working in mass-path units (M, ψ_e).

Extinction includes all processes which reduce the radiant intensity. As will be described below, these processes include absorption and scattering, both of which remove photons from the beam. Similarly the radiative emission is also proportional to the amount of matter along the path

$$\frac{\mathrm{d}I_\nu}{\mathrm{d}s} = k(\nu)S_\nu \qquad \text{Emission only} \tag{80}$$

where S_ν is known as the source function. The source function plays an important role in radiative transfer theory. We show in §2.2.1 that if S_ν is known, then the full radiance field I_ν is determined by an integration of S_ν with the appropriate boundary conditions. Emission includes all processes which increase the radiant intensity. As will be described below, these processes include thermal emission and scattering which adds photons to the beam. Determination of $k(\nu)$, which contains all the information about the electromagnetic properties of the media, is the subject of active theoretical, laboratory and field research.

Extinction and emission are linear processes, and thus additive. Since they are the only two processes which alter the intensity of radiation,

$$\begin{aligned} \frac{\mathrm{d}I_\nu}{\mathrm{d}s} &= -k_\mathrm{e}I_\nu + k_\mathrm{e}S_\nu \\ \frac{1}{k_\mathrm{e}}\frac{\mathrm{d}I_\nu}{\mathrm{d}s} &= -I_\nu + S_\nu \end{aligned} \tag{81}$$

Equation (81) is the equation of radiative transfer in its simplest differential form.

2.1.14 Optical Depth

We define the optical path $\tilde{\tau}$ between points P_1 and P_2 as

$$\begin{aligned} \tilde{\tau}(P_1, P_2) &= \int_{P_1}^{P_2} k_\mathrm{e}\,\mathrm{d}s \\ \mathrm{d}\tilde{\tau} &= k_\mathrm{e}\,\mathrm{d}s \end{aligned} \tag{82}$$

The optical path measures the amount of extinction a beam of light experiences traveling between two points. When $\tilde{\tau} > 1$, the path is said to be optically thick.

The most frequently used form of optical path is the optical depth. The optical depth τ is the vertical component of the optical path $\tilde{\tau}$, i.e., τ measures extinction between vertical levels. For historical reasons, the optical depth in planetary atmospheres is defined $\tau = 0$ at the top of the atmosphere and $\tau = \tau^*$ at the surface. This convention reflects the astrophysical origin of much of radiative transfer theory. Much like pressure, τ is a positive-definite coordinate which increases monotonically from zero at the top of the atmosphere to its surface value. Consider the optical depth between two levels $z_2 > z_1$, and then allow

$z_2 \to \infty$

$$\begin{aligned} \tau(z_1, z_2) &= \int_{z'=z_1}^{z'=z_2} k_\mathrm{e}\, \mathrm{d}z' \\ \tau(z, \infty) &= \int_{z'=z}^{z'=\infty} k_\mathrm{e}\, \mathrm{d}z' \qquad (83) \\ &= \int_{z'=z}^{z'=\infty} k_\mathrm{e}\, \mathrm{d}z' \qquad (84) \end{aligned}$$

Equation (84) is the integral definition of optical depth. The differential definition of optical depth is obtained by differentiating (84) with respect to the lower limit of integration and using the fundamental theorem of differential calculus

$$\begin{aligned} \mathrm{d}\tau &= [k_\mathrm{e}(\infty) - k_\mathrm{e}(z)]\, \mathrm{d}z \\ &= -k_\mathrm{e}(z)\, \mathrm{d}z \qquad (85) \end{aligned}$$

where the second step uses the convention that $k_\mathrm{e}(\infty) = 0$. By convention, τ is positive-definite, but (85) shows that $\mathrm{d}\tau$ may be positive or negative. If this seems confusing, consider the analogy with atmospheric pressure: pressure increases monotonically from zero at the top of the atmosphere, and we often express physical concepts such as the temperature lapse rate in terms of negative pressure gradients.

2.1.15 Geometric Derivation of Optical Depth

The optical depth of a column containing spherical particles may be derived by appealing to intuitive geometric arguments. Consider a concentration of $N\,\mathrm{m}^{-3}$ identical spherical particles of radius r residing in a rectangular chamber measuring one meter in the x and y dimensions and of arbitrary height. If the chamber is uniformly illuminated by a collimated beam of sunlight from one side, how much energy reaches the opposite side?

For this thought experiment, we will neglect the effects of scattering[6]. Moreover, we will assume that the particles are partially opaque so that the incident radiation which they do not absorb is transmitted without any change in direction. Finally, assume the particles are homogeneously distributed in the horizontal so that the radiative flux $F(z)$ is a function only of height in the chamber. Let us denote the power per unit area of the incident collimated beam of sunlight as $F_\odot$. Our goal is to compute $F(z)$ as a function of N and of r.

Since each particle absorbs incident energy in proportion to its geometric cross-section, the total absorption of radiation per particle is proportional to $\pi r^2 Q_\mathrm{e}$, where $Q_\mathrm{e} = 1$ for perfectly absorbing particles. If $Q_\mathrm{e} < 1$, then each particle removes fewer photons than suggested by its geometric size[7]. Conversely, if $Q_\mathrm{e} > 1$ each particle removes more photons

[6]The effects of diffraction will not be explicitly included either, but are implicit in the assumption of the horizontal homogeneity of the radiative flux.

[7]Although intuition suggests a spherical particle should not remove more energy from a collimated light beam than it can geometrically intercept, this is not the case. As discussed later, diffraction around the particle is important. In fact, for $r \gg \lambda$, $Q_\mathrm{e} \to 2$. However, most of the extinction due to diffraction occurs as scattering, not absorption.

than suggested by its geometric size. Each particle encountered removes $\pi r^2 Q_e F(z)\,\mathrm{W\,m^{-2}}$ from the incident beam. The maximum flux which can be removed from the beam is, of course, $F_\odot$.

In a section of height Δz, the collimated beam passing through the chamber will encounter a total of $N\Delta z$ particles. The number of particles encounted times the flux removed per particle gives the change in the radiative flux of the beam between the entrance and the rear wall

$$\begin{aligned} \Delta F &= -\pi r^2 Q_e F N \Delta z \\ \frac{\Delta F}{F} &= -\pi r^2 Q_e N \Delta z \end{aligned} \tag{86}$$

If we take the limit as $\Delta z \to 0$ then (86) becomes

$$\begin{aligned} \frac{1}{F}\,\mathrm{d}F &= -\pi r^2 Q_e N\,\mathrm{d}z \\ \mathrm{d}(\ln F) &= -\pi r^2 Q_e N\,\mathrm{d}z \end{aligned} \tag{87}$$

Let us define the volume extinction coefficient k as

$$k \equiv \pi r^2 Q_e N \tag{88}$$

Finally we define the optical depth τ in terms of the extinction

$$\tau \equiv k\Delta z \tag{89}$$

$$\tau = \pi r^2 Q_e N \Delta z \tag{90}$$

The dimensions of k are inverse meters $[\mathrm{m^{-1}}]$, or, perhaps more intuitively, square meters of effective surface area per cubic meter of air $[\mathrm{m^2\,m^{-3}}]$. Therefore τ is dimensionless. It can be helpful to remember that All quantities which compose τ are positive by convention, therefore τ itself is positive-definite.

We are now prepared to solve (87) for $F(\tau)$. From the theory of first order differential equations, we know that F must be an exponential function whose solution decays from its initial value with an e-folding constant of τ

$$F(\tau) = F_\odot \mathrm{e}^{-\tau} \tag{91}$$

Thus, in the limit of geometrical optics, the optical depth measures the number of e-foldings undergone by the radiative flux of a collimated beam passing through a given medium. This result is one form of the extinction law.

The exact value of $Q_e(r, \lambda)$ depends on the composition of the aerosol. However, there is a limiting value of Q_e as particles become large compared to the wavelength of light.

$$\lim_{r \gg \lambda} Q_e = 2 \tag{92}$$

Thus particles larger than 5–10 μm extinguish twice as much visible light as their geometric cross-section suggests.

To gain more insight into the usefulness of the optical depth, we can express τ (90) in terms of the aerosol mass M, rather than number concentration N. For a monodisperse aerosol of density ρ, the mass concentration is

$$M = \frac{4}{3}\pi r^3 \rho N \tag{93}$$

If we substitute

$$\pi r^2 N = \frac{3M}{4r\rho}$$

into (90) we obtain

$$\tau = \frac{3MQ_e\Delta z}{4r\rho} \tag{94}$$

Typical cloud particles have $r \sim 10\,\mu\text{m}$ so that for visible solar radiation with $\lambda \sim 0.5\,\mu\text{m}$ we may employ (92) to obtain

$$\tau = \frac{3M\Delta z}{2r\rho} \tag{95}$$

Thus τ increases linearly with M for a given r. Note however, that a given mass M produces an optical depth that is inversely proportional to the radius of the particles!

2.1.16 Stratified Atmosphere

We obtain the radiative transfer equation in terms of optical path by substituting (82) into (81)

$$\frac{\mathrm{d}I_\nu}{\mathrm{d}\tilde{\tau}} = -I_\nu + S_\nu \tag{96}$$

A stratified atmosphere is one in which all atmospheric properties, e.g., temperature, density, vary only in the vertical. As shown in the non-existant Figure, the photon path increment $\mathrm{d}s$ at polar angle θ in a stratified atmosphere is related to the vertical path increment $\mathrm{d}z$ by $\mathrm{d}z = \cos\theta\,\mathrm{d}s$ or $\mathrm{d}s = u^{-1}\,\mathrm{d}z$. In other words, the optical path traversed by photons is proportional to the vertical path divided by the cosine of the trajectory.

$$\mathrm{d}\tilde{\tau} = u^{-1}\,\mathrm{d}\tau \tag{97a}$$

$$\mathrm{d}\tau = u\,\mathrm{d}\tilde{\tau} \tag{97b}$$

Substituting (97a) into (96) we obtain

$$u\frac{\mathrm{d}I_\nu}{\mathrm{d}\tau} = -I_\nu + S_\nu \tag{98}$$

This is the differential form of the radiative transfer equation in a plane parallel atmosphere and is valid for all angles. The solution of (98) is made difficult because S_ν depends on I_ν. A more tractable set of equations may be obtained by considering the form of the boundary conditions. For many (most) problems of atmospheric interest, we know I_ν over an entire hemisphere at each boundary of a "slab". Considering the entire atmosphere as a slab, for

example, we know that, at the top of the atmosphere, sunlight is the only incident intensity from the hemisphere containing the sun. Or, at the surface, we have constraints on the upwelling intensity due to thermal emission or the surface reflectivity. When combined, these two hemispheric boundary conditions span a complete range of polar angle, and are thus sufficient to solve (98). However, in practice it is difficult to apply half a boundary condition. Moreover, we are often interested in knowing the hemispheric flows of radiation because many instruments (e.g., pyranometers) are designed to measure hemispheric irradiance and many models (e.g., climate models) require hemispheric irradiance to compute surface exchange properties. For these reasons we will decouple (98) into its constituent upwelling and downwelling radiation components.

Using the definitions of the half-range intensities (25) in (98) we obtain

$$-u\frac{\mathrm{d}I_\nu^-}{\mathrm{d}\tau} = I_\nu^- - S_\nu^- \qquad 0 < \theta < \pi/2, u = \cos\theta > 0 \tag{99a}$$

$$-u\frac{\mathrm{d}I_\nu^+}{\mathrm{d}\tau} = I_\nu^+ - S_\nu^+ \qquad \pi/2 < \theta < \pi, u = \cos\theta < 0 \tag{99b}$$

where we have simply multiplied (98) by -1 in order to place the negative sign on the LHS for reasons that will be explained shortly. The definitions of S_ν^- and S_ν^+ are exactly analogous to (25).

We now change variables from u to μ (54). Replacing u by μ in (99a) is allowed since $\mu = u > 0$ in this hemisphere. In the upwelling hemisphere where $\pi/2 < \theta < \pi$, $u < 0$ so that $\mu = -u$ (54). This negative sign cancels the negative sign on the LHS of (99b), resulting in

$$-\mu\frac{\mathrm{d}I_\nu^-}{\mathrm{d}\tau} = I_\nu^- - S_\nu^- \tag{100a}$$

$$\mu\frac{\mathrm{d}I_\nu^+}{\mathrm{d}\tau} = I_\nu^+ - S_\nu^+ \tag{100b}$$

These are the equations of radiative transfer in slab geometry for downwelling ($0 < \theta < \pi/2$) and upwelling ($\pi/2 < \theta < \pi$) intensities, respectively. The only mathematical difference between (100a) and (100b) is the negative sign. A helpful mnemonic is that the negative sign on the LHS is associated with I_ν^- while the implicit unary positive sign is associated with I_ν^+. Of course the I_ν and S_ν terms on the RHS are prefixed with opposited signs since they represent opposing, but positive definite, physical processes (absorption and emission).

Equation (99) states that $I^\pm$ depends explicitly only on $I^\pm$ and on $S^\pm$, but has no explicit dependence on $I^\mp$ or on $S^\mp$. Thus it may appear that I^+ and I^- are completely decoupled from eachother. However, we shall see that in problems involving scattering, $S^\pm$ depends explicitly on $I^\mp$ because scattering may change the trajectory of photons from upwelling to downwelling and visa versa. By coupling I^+ to I^-, scattering allows the entire radiance field to affect the radiance field at every point and in every direction (modulo the speed of light, of course). Thus scattering changes the solutions to (100) from being locally-dependent to depending on the global radiation field.

As a special case of (98), consider a stratified, non-scattering atmosphere in thermodynamic equilibrium. Then the source function equals the Planck function $S_\nu = B_\nu = B_\nu(T)$ and we have

$$u\frac{\mathrm{d}I_\nu}{\mathrm{d}\tau} = -I_\nu + B_\nu \tag{101}$$

Equation (101) is the basis of radiative transfer in the thermal infrared, where scattering effects are often negligible. The solution to (101) is described in §2.2.2.

2.2 Integral Equations

2.2.1 Formal Solutions

It is useful to write down the formal solution to (98) before making additional assumptions about the form of the source function S_ν.

$$\begin{aligned} u\frac{\mathrm{d}I_\nu}{\mathrm{d}\tau} &= -I_\nu + S_\nu \\ u\,\mathrm{d}I_\nu &= -I_\nu\,\mathrm{d}\tau + S_\nu\,\mathrm{d}\tau \\ u\,\mathrm{d}I_\nu + I_\nu\,\mathrm{d}\tau &= S_\nu\,\mathrm{d}\tau \\ \mathrm{d}I_\nu + \frac{I_\nu}{u}\,\mathrm{d}\tau &= u^{-1}S_\nu\,\mathrm{d}\tau \end{aligned} \tag{102}$$

Multiplying (102) by the integrating factor $\mathrm{e}^{\tau/u}$

$$\begin{aligned} \mathrm{e}^{\tau/u}\,\mathrm{d}I_\nu + \frac{\mathrm{e}^{\tau/u}I_\nu}{u}\,\mathrm{d}\tau &= u^{-1}\mathrm{e}^{\tau/u}S_\nu\,\mathrm{d}\tau \\ \mathrm{d}(\mathrm{e}^{\tau/u}\,I_\nu) &= u^{-1}\mathrm{e}^{\tau/u}S_\nu\,\mathrm{d}\tau \\ \frac{\mathrm{d}(\mathrm{e}^{\tau/u}\,I_\nu)}{\mathrm{d}\tau} &= u^{-1}\mathrm{e}^{\tau/u}S_\nu \end{aligned} \tag{103}$$

The LHS side of (103) is a complete differential. The boundary condition which applies to this first degree differential equation depends on the direction the radiation is traveling. Thus we denote the solutions to (103) as $I_\nu(\tau,+\mu)$ and $I_\nu(\tau,-\mu)$ for upwelling and downwelling radiances, respectively. We shall assume that the upwelling intensity at the surface, $I_\nu(\tau^*,+\mu)$, and the downwelling intensity at the top of the atmosphere, $I_\nu(0,-\mu)$, are known quantities. Since μ is positive-definite (54), $+\mu$ and $-\mu$ uniquely specify the angles for which these boundary conditions apply.

The solution for upwelling radiance is obtained by replacing u in (103) by $-\mu$ because $u<0$ for upwelling intensities.

$$\frac{\mathrm{d}(\mathrm{e}^{-\tau/\mu}\,I_\nu^+)}{\mathrm{d}\tau} = -\mu^{-1}\mathrm{e}^{-\tau/\mu}S_\nu^+ \tag{104}$$

We could have arrived at (104) by starting from (100b), and proceeding as above except using $\mathrm{e}^{-\tau/\mu}$ as the integrating factor. We now integrate from the surface to level τ (i.e.,

along a path of decreasing τ') and apply the boundary condition at the surface

$$\begin{aligned}
\mathrm{e}^{-\tau'/\mu} I_\nu(\tau', +\mu)\Big|_{\tau'=\tau^*}^{\tau'=\tau} &= -\mu^{-1} \int_{\tau'=\tau^*}^{\tau'=\tau} \mathrm{e}^{-\tau'/\mu} S_\nu^+ \, \mathrm{d}\tau' \\
\mathrm{e}^{-\tau/\mu} I_\nu(\tau, +\mu) - \mathrm{e}^{-\tau^*/\mu} I_\nu(\tau^*, +\mu) &= \mu^{-1} \int_\tau^{\tau^*} \mathrm{e}^{-\tau'/\mu} S_\nu^+ \, \mathrm{d}\tau' \\
\mathrm{e}^{-\tau/\mu} I_\nu(\tau, +\mu) &= \mathrm{e}^{-\tau^*/\mu} I_\nu(\tau^*, +\mu) + \mu^{-1} \int_\tau^{\tau^*} \mathrm{e}^{-\tau'/\mu} S_\nu^+ \, \mathrm{d}\tau' \\
I_\nu(\tau, +\mu) &= \mathrm{e}^{(\tau-\tau^*)/\mu} I_\nu(\tau^*, +\mu) + \mu^{-1} \int_\tau^{\tau^*} \mathrm{e}^{(\tau-\tau')/\mu} S_\nu^+ \, \mathrm{d}\tau'
\end{aligned}$$

Note that $\tau^* > \tau$ and $\tau' > \tau$ so that both of the transmission factors reduce a beam's intensity between its source (at τ^* or τ') and where it is measured (at τ). The physical meaning of the transmission factors is more clear if we write all transmission factors as negative exponentials.

$$I_\nu(\tau, +\mu) = \mathrm{e}^{-(\tau^*-\tau)/\mu} I_\nu(\tau^*, +\mu) + \mu^{-1} \int_\tau^{\tau^*} \mathrm{e}^{-(\tau'-\tau)/\mu} S_\nu(\tau', +\mu) \, \mathrm{d}\tau' \tag{105}$$

The first term on the RHS is the contribution of the boundary (e.g., Earth's surface) to the upwelling intensity at level τ. This contribution is attenuated by the optical path of the radiation between the ground and level τ. The second term on the RHS is the contribution of the atmosphere to the upwelling intensity at level τ. The net upward emission of each parcel of air between the surface and level τ is $S_\nu^+(\tau')$, but this internally emitted radiation is attenuated along the slant path between τ' and τ. The μ^{-1} factor in front of the integral accounts for the slant path of the emitting mass in the atmosphere.

The solution for downwelling radiance is obtained by replacing u in (103) by μ because $\mu = u$ in the downwelling hemisphere. The resulting expression must be integrated from the upper boundary down to level τ, and a boundary condition applied at the top.

$$\begin{aligned}
\frac{\mathrm{d}(\mathrm{e}^{\tau/\mu} I_\nu^-)}{\mathrm{d}\tau} &= \mu^{-1} \mathrm{e}^{\tau/\mu} S_\nu^- \\
\mathrm{e}^{\tau'/\mu} I_\nu(\tau', -\mu)\Big|_{\tau'=0}^{\tau'=\tau} &= \mu^{-1} \int_{\tau'=0}^{\tau'=\tau} \mathrm{e}^{\tau'/\mu} S_\nu^- \, \mathrm{d}\tau' \\
\mathrm{e}^{\tau/\mu} I_\nu(\tau, -\mu) - I_\nu(0, -\mu) &= \mu^{-1} \int_0^\tau \mathrm{e}^{\tau'/\mu} S_\nu^- \, \mathrm{d}\tau' \\
\mathrm{e}^{\tau/\mu} I_\nu(\tau, -\mu) &= I_\nu(0, -\mu) + \mu^{-1} \int_0^\tau \mathrm{e}^{\tau'/\mu} S_\nu^- \, \mathrm{d}\tau' \\
I_\nu(\tau, -\mu) &= \mathrm{e}^{-\tau/\mu} I_\nu(0, -\mu) + \mu^{-1} \int_0^\tau \mathrm{e}^{(-\tau+\tau')/\mu} S_\nu^- \, \mathrm{d}\tau' \\
I_\nu(\tau, -\mu) &= \mathrm{e}^{-\tau/\mu} I_\nu(0, -\mu) + \mu^{-1} \int_0^\tau \mathrm{e}^{-(\tau-\tau')/\mu} S_\nu(\tau', -\mu) \, \mathrm{d}\tau'
\end{aligned} \tag{106}$$

The upwelling and downwelling intensities in a stratified atmosphere are fully described by (105) and (106). Such formal solutions to the equation of radiative transfer are of great

heuristic value but limited practical use until the source function is known. Note that we have assumed a source function and boundary conditions which are azimuthally independent, but that the derivation of (105) and (106) does not rely on this assumption. It is straightforward to relax this assumption and replace $I_\nu(\tau,\mu)$ by $I_\nu(\tau,\mu,\phi)$ and $S_\nu(\tau,\mu)$ by $S_\nu(\tau,\mu,\phi)$ in the above.

2.2.2 Thermal Radiation In A Stratified Atmosphere

Consider a purely absorbing, stratified atmosphere in thermodynamic equilibrium. Then the source function equals the Planck function $S_\nu = B_\nu = B_\nu(T)$ (41) and the radiative transfer equation is given by (101). It is important to remember that B_ν is the complete source function only because we are explicitly neglecting all scattering processes. Thus we need only define the boundary conditions in order to use (105) and (106) to fully specify I_ν. We assume that the surface emits blackbody radiation into the upper hemisphere

$$I_\nu(\tau^*,+\mu) = B_\nu[T(\tau^*)] \tag{107}$$

For brevity we shall define $B^*_\nu = B_\nu[T(\tau^*)]$. At the top of the atmosphere, we assume there is no downwelling thermal radiation.

$$I_\nu(0,-\mu) = 0 \tag{108}$$

The solutions for upwelling and downwelling intensities are then obtained by using $S_\nu(\tau',\mu) = B_\nu(\tau')$ (the Planck function is isotropic) and substituting (107) and (108) into (105) and (106), respectively

$$I_\nu(\tau,+\mu) = \mathrm{e}^{-(\tau^*-\tau)/\mu}B_\nu(\tau^*) + \mu^{-1}\int_\tau^{\tau^*} \mathrm{e}^{-(\tau'-\tau)/\mu}B_\nu(\tau')\,\mathrm{d}\tau' \tag{109}$$

$$I_\nu(\tau,-\mu) = \mu^{-1}\int_0^{\tau} \mathrm{e}^{-(\tau-\tau')/\mu}B_\nu(\tau')\,\mathrm{d}\tau' \tag{110}$$

The first term on the RHS of (109) is the thermal radiation emitted by the surface, attenuated by absorption in the atmosphere until it contributes to the upwelling intensity at level τ. The second term on the RHS contains the upwelling intensity arriving at τ contributed from the attenuated atmospheric thermal emission from each parcel between the surface and τ. The μ^{-1} factor in front of the integral accounts for the slant path of the thermally emitting atmosphere. The RHS of (110) is similar but contains no boundary contribution since the vacuum above the atmosphere is assumed to emit no thermal radiation. The upwelling and downwelling intensities in a stratified, thermal atmosphere are fully described by (109) and (110).

2.2.3 Angular Integration

Once the solutions for the hemispheric intensities are known, it is straightforward to obtain the hemispheric fluxes by performing the angular integrations (56a)–(56b).

$$F^-_\nu(\tau) = 2\pi\int_{\mu=0}^{\mu=1} I_\nu(\tau,-\mu)\mu\,\mathrm{d}\mu \tag{111}$$

Consider first the downwelling flux in a non-scattering, thermal, isotropic, stratified atmosphere obtained by substituting (110) into (111) and interchanging the order of integration

$$\begin{aligned} F_\nu^-(\tau) &= 2\pi \int_{\mu=0}^{\mu=1} \left(\mu^{-1} \int_{\tau'=0}^{\tau'=\tau} \mathrm{e}^{-(\tau-\tau')/\mu} B_\nu(\tau')\,\mathrm{d}\tau' \right) \mu\,\mathrm{d}\mu \\ &= 2\pi \int_{\tau'=0}^{\tau'=\tau} \int_{\mu=0}^{\mu=1} \mathrm{e}^{-(\tau-\tau')/\mu} B_\nu(\tau')\,\mathrm{d}\mu\,\mathrm{d}\tau' \\ &= 2\pi \int_{\tau'=0}^{\tau'=\tau} B_\nu(\tau') \left(\int_{\mu=0}^{\mu=1} \mathrm{e}^{-(\tau-\tau')/\mu}\,\mathrm{d}\mu \right) \mathrm{d}\tau' \end{aligned} \tag{112}$$

Notice that two factors of μ cancelled each other out: The reduction in irradiance due to non-normal incidence (μ) exactly compensates the increased irradiance due to emission by the entire slant column which is μ^{-1} times greater than emission from a vertical column.

In terms of exponential integrals defined in Appendix 10.7, the inner integral in parentheses in (112) is $E_2(\tau - \tau')$ (603c).

$$F_\nu^-(\tau) = 2\pi \int_{\tau'=0}^{\tau'=\tau} B_\nu(\tau') E_2(\tau - \tau')\,\mathrm{d}\tau' \tag{113}$$

Similar terms arise when we consider the horizontal upwelling flux obtained by substituting (109) into (56a) and we obtain

$$\begin{aligned} F_\nu^+(\tau) &= 2\pi \int_{\mu=0}^{\mu=1} I_\nu(\tau, +\mu)\mu\,\mathrm{d}\mu \\ &= 2\pi \int_{\mu=0}^{\mu=1} \left(\mathrm{e}^{-(\tau^*-\tau)/\mu} B_\nu(\tau^*) + \mu^{-1} \int_\tau^{\tau^*} \mathrm{e}^{-(\tau'-\tau)/\mu} B_\nu(\tau')\,\mathrm{d}\tau' \right) \mu\,\mathrm{d}\mu \\ &= 2\pi B_\nu(\tau^*) \int_{\mu=0}^{\mu=1} \mathrm{e}^{-(\tau^*-\tau)/\mu} \mu\,\mathrm{d}\mu + 2\pi \int_\tau^{\tau^*} B_\nu(\tau') \left(\int_{\mu=0}^{\mu=1} \mathrm{e}^{-(\tau'-\tau)/\mu}\,\mathrm{d}\mu \right) \mathrm{d}\tau' \\ &= 2\pi B_\nu(\tau^*) E_3(\tau^* - \tau) + 2\pi \int_{\tau'=\tau^*}^{\tau'=\tau} B_\nu(\tau') E_2(\tau' - \tau)\,\mathrm{d}\tau' \end{aligned} \tag{114}$$

Subtracting (113) from (114) we obtain the net flux at any layer in a non-scattering, thermal, stratified atmosphere

$$\begin{aligned} F_\nu(\tau) &= F_\nu^+(\tau) - F_\nu^-(\tau) \\ &= 2\pi \left[B_\nu(\tau^*) E_3(\tau^* - \tau) + \int_\tau^{\tau^*} B_\nu(\tau') E_2(\tau' - \tau)\,\mathrm{d}\tau' - \int_0^\tau B_\nu(\tau') E_2(\tau - \tau')\,\mathrm{d}\tau' \right] \end{aligned} \tag{115}$$

Equations (113) and (114) may not seem useful at this point but their utility becomes apparent in §2.3.4 where we define the flux transmissivity.

2.2.4 Thermal Irradiance

Assume a non-scattering planetary surface at temperature T emits blackbody radiation such that $I_\nu(\tau^*, +\mu) = B_\nu(T)$ (107). What is the total upwelling thermal irradiance from the

surface? From (56a) we have

$$\begin{aligned} F_\nu^+ &= 2\pi \int_0^1 B_\nu(T)\mu \,\mathrm{d}\mu \\ &= 2\pi B_\nu(T) \int_0^1 \mu \,\mathrm{d}\mu \\ &= 2\pi B_\nu(T) \left[\frac{\mu^2}{2}\right]_0^1 \\ &= 2\pi B_\nu(T) \left(\frac{1}{2} - 0\right) \\ F_\nu^+ &= \pi B_\nu(T) \\ \frac{1}{\pi} F_\nu^+ &= B_\nu(T) \end{aligned} \tag{116}$$

Notice the isotropy of the Planck function allows the factor of 2 from the azimuthal integration to cancel the mean value of the cosine weighting function over a hemisphere. Moving the remaining factor of π from the azimuthal integration to the LHS conveniently sets the RHS equal to the Planck function.

We integrate (116) over frequency to obtain the total upwelling thermal irradiance

$$\begin{aligned} \frac{1}{\pi} \int_0^\infty F_\nu^+ \,\mathrm{d}\nu &= \int_0^\infty B_\nu(T) \,\mathrm{d}\nu \\ \frac{1}{\pi} F^+ &= \int_0^\infty B_\nu(T) \,\mathrm{d}\nu \\ \frac{1}{\pi} F^+ &= \frac{\sigma T^4}{\pi} \\ F^+ &= \sigma T^4 \end{aligned} \tag{117}$$

Thus the factor of π from the azimuthal integration nicely cancels the factor of π from the Stefan-Boltzmann Law. Equation (117) applies to any surface whose emissivity is 1. Consider, e.g., a thick cloud with cloud base and cloud top temperatures $T(z_\mathrm{B}) = T_\mathrm{B}$ and $T(z_\mathrm{T}) = T_\mathrm{T}$, respectively. Then the upwelling thermal flux at cloud top and the downwelling flux at cloud bottom will be $F^-(z_\mathrm{B}) = \sigma T_\mathrm{B}^4$ and $F^+(z_\mathrm{T}) = \sigma T_\mathrm{T}^4$, respectively.

2.2.5 Grey Atmosphere

Consider an atmosphere transparent to solar radiation and partially opaque to thermal radiation governed by (101). The exact solution, including angular dependence, is given in §2.2.2. The hemispheric fluxes and net flux may only be obtained exactly by accounting for the angular dependence as in §2.2.3. We may eliminate the angular dependence of the net flux by making the simplifying assumption that the hemispheric up and downwelling irradiances equal a constant times the corresponding intensity. A number of methods exist to determine this constant, called the diffusivity factor (e.g., §2.2.15). These methods are all related to the two-stream approximation.

One such method (Salby, 1996, p. 232) is to identify an effective inclination $\bar{\mu}$ along which all radiation is assumed to travel. With this assumption, the contribution to upwelling irradiance from the lower boundary, the first term on the RHS of 115), is

$$2E_3(\tau^* - \tau) \quad = \quad \exp\left(-\frac{\tau^* - \tau}{\bar{\mu}}\right) \tag{118}$$

Inspection (or differentiation) shows that the atmosphere within one optical depth makes the dominant contribution to (118). For $\Delta\tau = \tau^* - \tau = 1$, the diffusivity factor

$$\bar{\mu}^{-1} \quad \approx \quad \frac{5}{3} \tag{119}$$

The hypothetical collimated beam of radiation is inclined to the zenith by $\arccos(3/5) \approx 53.13°$. This is equivalent to a collimated beam of radiation travelling vertically through an optical depth equal to five thirds the vertical optical depth traversed by the diffuse radiation.

Using this assumption (118), the upwelling hemispheric irradiance (56a) for blackbody radiation is

$$\begin{aligned}
F_\nu^+ &= 2\pi \int_0^1 I_\nu(+\mu)\mu \, \mathrm{d}\mu \\
&\approx 2\pi \int_0^1 I_\nu(+\bar{\mu})\mu \, \mathrm{d}\mu \\
&= 2\pi\bar{\mu} I_\nu(+\bar{\mu}) \int_0^1 \mu \, \mathrm{d}\mu \\
&= 2\pi I_\nu(+\bar{\mu}) \left[\frac{\mu^2}{2}\right]_0^1 \\
&= 2\pi I_\nu(+\bar{\mu}) \left[\frac{1}{2} - 0\right] \\
&= \pi I_\nu(+\bar{\mu})
\end{aligned} \tag{120}$$

An analogous relationship holds for the downwelling irradiance.

Based on (119) and (120), the irradiance structure of the thermal atmosphere may approximated by performing a direct angular integration of (100). With our approximation, radiances I integrate directly to irradiances F modulo the diffusivity factor $\bar{\mu}$. (101)

$$-\bar{\mu}\frac{\mathrm{d}F_\nu^-}{\mathrm{d}\tau} = F_\nu^- - \pi F_\nu^B \tag{121a}$$

$$\bar{\mu}\frac{\mathrm{d}F_\nu^+}{\mathrm{d}\tau} = F_\nu^+ - \pi F_\nu^B \tag{121b}$$

It is instructive to examine an idealized grey atmosphere, where the fluxes of interest have no spectral dependence. Although this is far from true in Earth's atmosphere, the solution is straightforward and sheds light on the radiative equilibrium temperature profile and the greenhouse effect. We simplify (121) in two ways. First, we introduce a scaled

optical depth $\mathrm{d}\tilde{\tau} = \bar{\mu}^{-1}\mathrm{d}\tau = \frac{5}{3}\mathrm{d}\tau$. Second, we drop the frequency dependence, which is equivalent to integrating over a broad range of frequencies. For heuristic purposes, think of this integration as being over the relatively narrow $\lambda = 5$–$20\,\mu\mathrm{m}$ range where most of Earth's terrestrial radiative energy resides.

$$-\frac{\mathrm{d}F^-}{\mathrm{d}\tilde{\tau}} = F^- - \pi B \tag{122a}$$

$$\frac{\mathrm{d}F^+}{\mathrm{d}\tilde{\tau}} = F^+ - \pi B \tag{122b}$$

In the absence of dynamical, chemical, and latent heating, the energy deposition in a parcel of air is entirely radiative. Under these conditions the idealize grey atmosphere described by (122) will adjust to a temperature profile determined by radiative equilibrium. Let the time rate of change of temperature T of a parcel be denoted by $h\,[\mathrm{K\,s^{-1}}]$, the parcel warming rate[8] or cooling rate. The warming rate is the rate of net energy deposition divided by the specific heat capacity at constant pressure $\mathrm{c_p}\,[\mathrm{J\,kg^{-1}\,K^{-1}}]$ times the density $\rho\,[\mathrm{kg\,m^{-3}}]$

$$\begin{aligned} h \equiv \frac{\mathrm{d}T}{\mathrm{d}t} &= \frac{1}{\rho \mathrm{c_p}}\frac{\mathrm{d}F}{\mathrm{d}z} \\ \frac{\mathrm{K}}{\mathrm{s}} &= \left(\frac{\mathrm{kg}}{\mathrm{m}^3} \times \frac{\mathrm{J}}{\mathrm{kg\,K}}\right)^{-1} \times \frac{\mathrm{J}}{\mathrm{m}^2\,\mathrm{s}} \times \frac{1}{\mathrm{m}} \end{aligned} \tag{123}$$

The forcing term on the RHS, $\mathrm{d}F/\mathrm{d}z$ is the radiative flux divergence, the vertical gradient of net radiative flux. Absorption and emission are the only mechanisms which contribute to the flux divergence. In terms of hemispheric fluxes,

$$\frac{\mathrm{d}F}{\mathrm{d}z} = \frac{\mathrm{d}}{\mathrm{d}z}(F^- - F^+) \tag{124}$$

By definition, the time variation of net radiative heating vanishes ($\mathrm{d}T/\mathrm{d}t = 0$) at all levels of an atmosphere in radiative equilibrium. By (124), we see that the vertical gradient in net radiative flux must also vanish in radiative equilibrium. Setting (124) to zero and integrating we obtain

$$F^- - F^+ = F_0 \tag{125}$$

The net radiative flux $F(z) = F_0$ is constant in radiative equilibrium.

Adding and subtracting (122), we obtain

$$\frac{\mathrm{d}}{\mathrm{d}\tilde{\tau}}(F^+ - F^-) = F^+ + F^- - 2\pi B \tag{126a}$$

$$\frac{\mathrm{d}}{\mathrm{d}\tilde{\tau}}(F^+ + F^-) = F^+ - F^- = F_0 \tag{126b}$$

[8] Conventionally h is called the heating rate, which is a misnomer since the dimensions of $\mathrm{d}T/\mathrm{d}t$ are $\mathrm{K\,s^{-1}}$. Thus we use the less common but more accurate terminology "warming rate". We reserve "heating rate" for a measure power dissipation, i.e., energy per unit time, in $\mathrm{J\,s^{-1}}$, $\mathrm{J\,m^{-3}\,s^{-1}}$, or $\mathrm{J\,kg^{-1}\,s^{-1}}$.

Defining $\psi = F^+ - F^-$ and $\phi = F = F^+ - F^-$,

$$\frac{\mathrm{d}\phi}{\mathrm{d}\tilde{\tau}} = \psi - 2\pi B \tag{127a}$$

$$\frac{\mathrm{d}\psi}{\mathrm{d}\tilde{\tau}} = \phi = F_0 \tag{127b}$$

Since $\phi = F^+ - F^-$ is constant, (127b) shows that $\mathrm{d}\phi/\mathrm{d}\tilde{\tau} = 0$ and thus

$$\psi = 2\pi B \tag{128}$$

Substituting this into (127b),

$$\begin{aligned} \frac{\mathrm{d}}{\mathrm{d}\tilde{\tau}}(2\pi B) &= F_0 \\ \frac{\mathrm{d}B}{\mathrm{d}\tilde{\tau}} &= \frac{F_0}{2\pi} \\ B(\tilde{\tau}) &= \frac{F_0\tilde{\tau}}{2\pi} + C_1 \end{aligned} \tag{129}$$

We evaluate the constant of integration by using the boundary condition at the top of the atmosphere. By definition $F^- = 0$ and $\tilde{\tau} = 0$ at TOA. This implies that $\phi = \psi(0) = F^+(0) = F_0$. We must therefore have $B(0) = \phi/2\pi$ by (128). Using this result in (133),

$$\begin{aligned} B(0) &= \frac{\phi}{2\pi} = \frac{F_0(0)}{2\pi} + C_1 \\ C_1 &= \frac{\phi}{2\pi} = \frac{F_0}{2\pi} \end{aligned} \tag{130}$$

Substituting (130) back into (133) shows

$$\begin{aligned} B(\tilde{\tau}) &= \frac{F_0\tilde{\tau}}{2\pi} + \frac{F_0}{2\pi} \\ &= \frac{F_0}{2\pi}(\tilde{\tau} + 1) \end{aligned} \tag{131}$$

The thermal absorption and emission in a grey atmosphere increase linearly with optical depth from TOA to the surface.

The upwelling irradiance at the surface is $F^+(\tilde{\tau}^*) = \pi B(T_\mathrm{s})$ where $T_\mathrm{s}\,[\mathrm{K}]$ is the surface skin temperature. The atmospheric temperature just above the surface is given by (131) as $B(\tilde{\tau}^*) = \frac{F_0}{2\pi}(\tilde{\tau}^* + 1)$. Thus there is a temperature discontinuity between the near-surface air and the ground.

Climate models typically express h (124) in terms of the flux gradient with respect to

pressure by invoking the hydrostatic equilibrium condition (456)

$$\begin{aligned} h \equiv \frac{\mathrm{d}T}{\mathrm{d}t} &= \frac{1}{\rho c_\mathrm{p}} \frac{\mathrm{d}F}{[-(\rho g)^{-1}\mathrm{d}p]} \\ &= -\frac{g}{c_\mathrm{p}} \frac{\mathrm{d}F}{\mathrm{d}p} \qquad (132) \\ &= -\frac{g}{c_\mathrm{p}} \frac{(F_k^- - F_k^+) - (F_{k+1}^- - F_{k+1}^+)}{p_k - p_{k+1}} \\ &= \frac{g}{c_\mathrm{p}} \frac{(F_k^- - F_{k+1}^-) + (F_{k+1}^+ - F_k^+)}{p_{k+1} - p_k} \qquad (133) \end{aligned}$$

where the subscript denotes the kth vertical interface level in the atmosphere.

2.2.6 Scattering

Energy interacting with matter undergoes one of two processes, scattering or absorption. Scattering occurs when a photon reflects off matter without absorption. The direction of the photon after the interaction is usually not the same as the incoming direction. The case where the scattered photons are homogeneously distributed throughout all 4π steradians is called isotropic scattering. In general, the angular dependence of the scattering is described by the phase function of the interaction. The phase function p is closely related to the probability that photons incoming from the direction $\hat{\mathbf{\Omega}}' = (\theta', \phi')$ will (if scattered) scatter into outgoing direction $\hat{\mathbf{\Omega}} = (\theta, \phi)$. It is usually assumed that p depends only on the scattering angle Θ between incident and emergent directions.

$$\cos\Theta = \hat{\mathbf{\Omega}}' \cdot \hat{\mathbf{\Omega}} \qquad (134)$$

The case where incident and emergent directions are equal, i.e., $\Omega' = \Omega$ corresponds to $\Theta = 0$. When the scattered direction continues moving in the forward hemisphere (relative to the plane defined by $\hat{\mathbf{\Omega}}'$), it is called forward scattering, and corresponds to $\Theta < \pi/2$. When scattered radiation has been reflected back into the hemisphere from whence it arrived, it is called back scattering, and corresponds to $\Theta > \pi/2$. The case where incident and emergent directions are opposite, i.e., $\hat{\mathbf{\Omega}}' = -\hat{\mathbf{\Omega}}$, corresponds to $\Theta = \pi$.

The Cartesian components of Ω' and Ω are straigtforward to obtain in spherical polar coordinates.

$$\hat{\mathbf{\Omega}} = \sin\theta\cos\phi\,\hat{\mathbf{i}} + \sin\theta\sin\phi\,\hat{\mathbf{j}} + \cos\theta\,\hat{\mathbf{k}} \qquad (135)$$

$$\hat{\mathbf{\Omega}}' = \sin\theta'\cos\phi'\,\hat{\mathbf{i}} + \sin\theta'\sin\phi'\,\hat{\mathbf{j}} + \cos\theta'\,\hat{\mathbf{k}} \qquad (136)$$

The scattering angle Θ is simply related to the inner product of $\hat{\mathbf{\Omega}}'$ and $\hat{\mathbf{\Omega}}$ by the cosine law

$$\begin{aligned} \cos\Theta &= \hat{\mathbf{\Omega}}' \cdot \hat{\mathbf{\Omega}} \\ &= \sin\theta'\cos\phi'\sin\theta\cos\phi + \sin\theta'\sin\phi'\sin\theta\sin\phi + \cos\theta' + \cos\theta \\ &= \sin\theta'\sin\theta\,(\cos\phi'\cos\phi + \sin\phi'\sin\phi) + \cos\theta'\cos\theta \\ &= \sin\theta'\sin\theta\cos(\phi' - \phi) + \cos\theta'\cos\theta \qquad (137) \end{aligned}$$

2.2.7 Phase Function

Accurate treatment of the angular scattering of radiation, i.e., the phase function, is, perhaps, makes rigorous demands of radiative transfer applications. A correspondingly large body of literature is devoted to this topic. Essential references include van de Hulst (1957), Joseph et al. (1976), Wiscombe and Grams (1976), Wiscombe (1977), Wiscombe (1979, edited/revised 1996), and Boucher (1998).

The phase function $p(\cos\Theta)$ is normalized so that the total probability of scattering is unity

$$\frac{1}{4\pi}\int_{\Omega} p(\cos\Theta)\,\mathrm{d}\Omega = 1 \tag{138a}$$

$$\frac{1}{4\pi}\int_{\phi=0}^{\phi=2\pi}\int_{\theta=0}^{\theta=\pi} p(\theta',\phi';\theta,\phi)\,\sin\theta\,\mathrm{d}\theta\,\mathrm{d}\phi = 1 \tag{138b}$$

The dimensions of the phase function are somewhat ambiguous. If the $(4\pi)^{-1}$ factor in (138) is assumed to be steradians, then p is a true probability and is dimensionless. However, if the $(4\pi)^{-1}$ factor is considered to be numeric and dimensionless (i.e., a probability), then p has units of (dimensionless) probability per (dimensional) steradian, sr^{-1}. The latter convention best expresses the physical meaning of the phase function and is adopted in this text. It is therefore important to remember that factors of $(4\pi)^{-1}$ which multiply the scattering integral in the radiative transfer equation are considered to be dimensionless in the formulations which follow, e.g., (152). Furthermore, the units of p are probability per steradian, sr^{-1}.

Scattering may depend on the absolute directions $\hat{\boldsymbol{\Omega}}'$ and $\hat{\boldsymbol{\Omega}}$ themselves, rather than just their relative orientations as measured by the angle Θ between them. This might be the case, for example, in a broken sea-ice field. For the time being, however, we shall assume that the phase function depends only on Θ.

In atmospheric problems, the phase function may often be independent of the azimuthal angle ϕ, and depend only on θ. In this case the phase function normalization (138b) simplifies to

$$\frac{1}{2}\int_{\theta=0}^{\theta=\pi} p(\theta';\theta)\,\sin\theta\,\mathrm{d}\theta \;=\; 1 \tag{139}$$

In accord with the discussion above, the factor of $1/2$ is dimensionless, as is the RHS.

2.2.8 Legendre Basis Functions

The phase function (138) specifies the angular distribution of scattering. Solution of any radiative transfer equation involving scattering depends on it. Numerical approaches aim for a suitable approximation or discretization which represents $p(\Theta)$ to some desired level of accuracy. The optimal basis functions for representing $p(\Theta)$ are the Legendre polynomials.

The Legendre polynomial expansion of the phase function is

$$p(\cos\Theta) \;=\; \sum_{n=0}^{n=N}(2n+1)\chi_n P_n(\cos\Theta) \tag{140}$$

An expansion of order N contains $N+1$ terms. The zeroth order polynomial and coefficient are identically 1.

The Legendre polynomials are orthonormal on the interval $[-1, 1]$. The factor of $2n+1$ that appears in the numerator of the Legendre expansion (146) also appears in the denominator of the Legendre polynomial orthonormality property:

$$\frac{1}{2}\int_{u=-1}^{u=1} P_n(u)P_k(u)\,\mathrm{d}u = \frac{1}{2n+1}\delta_{n,k} \tag{141a}$$

$$\frac{1}{2}\int_{u=-1}^{u=1} P_n(\cos\Theta)P_k(\cos\Theta)\,\mathrm{d}(\cos\Theta) = \frac{1}{2n+1}\delta_{n,k} \tag{141b}$$

Some other properties of Legendre polynomials are discussed in §10.5.

The expansion coefficients χ_n are defined by the projection of the corresponding Legendre polynomial onto the phase function.

$$\chi_n = \frac{1}{2}\int_{u=-1}^{u=1} P_n(u)p(u)\,\mathrm{d}u \tag{142a}$$

$$= \frac{1}{2}\int_{\Theta=\pi}^{\Theta=0} P_n(\cos\Theta)p(\cos\Theta)\,\mathrm{d}(\cos\Theta) \tag{142b}$$

$$= \frac{1}{2}\int_{\Theta=0}^{\Theta=\pi} P_n(\cos\Theta)p(\cos\Theta)\sin\Theta\,\mathrm{d}\Theta \tag{142c}$$

map the phase function into a series of Legendre polynomials. The χ_n are also called the phase function moments. Radiative transfer programs like DISORT (Stamnes et al., 1988) usually require that directional information be specified as a Legendre polynomial expansion.

The Legendre expansion for simple, smoothly varying and symmetric phase functions is highly accurate with just few terms. For instance, a single moment Legendre expansion exactly describes Rayleigh scattering. However, the expansions of asymmetric phase functions converge much more slowly. The strongly peaked forward scattering lobes which appear at large size parameter may require hundreds of moments for accurate representation.

Computing the χ_n using quadrature methods significantly increases accuracy and reduces time. Wiscombe (1977) recommends Gauss-Lobatto quadrature for highly asymmetric phase functions:

$$\chi_n = \frac{1}{2}\sum_{l=1}^{l=L} H_l P_n(\cos\Theta_l)p(\cos\Theta_l)\sin\Theta_l \tag{143}$$

where L is the number of Gauss-Lobatto abscissae. Lobatto quadrature is discussed more thorought in § 10.6.

2.2.9 Henyey-Greenstein Approximation

Computation of the exact phase function of scatterers is laborious but desirable when the objective is to predict directional radiances. However, phase function approximations often suffice when hemispheric fluxes are the objective. The Henyey-Greenstein Phase Function

approximates the full phase function in terms of its first Legendre moment, i.e., its asymmetry parameter g.

$$p(\cos\Theta) \quad = \quad \frac{1-g^2}{(1+g^2-2g\cos\Theta)^{3/2}} \tag{144}$$

The n'th moment in the Legendre expansion of (144) is, conveniently, g^n.

$$\chi_n \quad = \quad g^n \tag{145}$$

Applying (145) in (146) gives

$$p(\cos\Theta) \quad = \quad \sum_{n=0}^{n=N}(2n+1)g^n P_n(\cos\Theta) \tag{146}$$

This convenient property (145) makes numerical quadrature of the Legendre expansion coefficients unnecessary once the first moment, $g = \chi_1$, is known.

2.2.10 Direct and Diffuse Components

When working with half-range intensities it is convenient to decompose the downwelling intensity I^- into the sum of a direct component, $I_{\rm s}^-(\tau,\hat{\mathbf{\Omega}})$, and a diffuse component, $I_{\rm d}^-(\tau,\hat{\mathbf{\Omega}})$ such that

$$I_\nu^-(\tau,\hat{\mathbf{\Omega}}) \quad = \quad I_{\rm s}^-(\tau,\hat{\mathbf{\Omega}}) + I_{\rm d}^-(\tau,\hat{\mathbf{\Omega}}) \tag{147}$$

where we have suppressed the ν subscript on the RHS to simplify notation. The direct component refers to any photons contributing from a collimated source which have not (yet) been scattered. Typically the collimated source is solar radiation, and so we subscript the direct component with s for "solar". There may be a corresponding direct component of intensity in the upwelling direction $I_{\rm s}^+$ if the reflectance at the lower surface is specular, e.g., ocean glint. In such situations it is straightforward to define

$$I_\nu^+(\tau,\hat{\mathbf{\Omega}}) \quad = \quad I_{\rm s}^+(\tau,\hat{\mathbf{\Omega}}) + I_{\rm d}^+(\tau,\hat{\mathbf{\Omega}}) \tag{148}$$

Of course there exist planetary atmospheres somewhere which are illuminated by multiple stars. We shall neglect upwelling solar beams for the time being. For consistency, though, we shall shall use $I_{\rm d}^+$ rather than I^+ in equations in which $I_{\rm d}^-$ also appears.

It is plain that $I_{\rm s}^-(\tau,\hat{\mathbf{\Omega}})$ is zero in all directions except that of the collimated beam. Moreover, the intensity in the direct beam is, by definition, subject only to extinction by Bougher's law (i.e., there is no emission). Thus the direct beam component of the downwelling intensity is the irradiance incident at the top of the atmosphere, attenuated by the extinction law (91),

$$\begin{aligned} I_{\rm s}^-(\tau,\hat{\mathbf{\Omega}}) \quad &= \quad F_\odot \mathrm{e}^{-\tau/\mu_0}\delta(\hat{\mathbf{\Omega}}-\hat{\mathbf{\Omega}}_\odot) \\ &= \quad F_\odot \mathrm{e}^{-\tau/\mu_0}\delta(\mu-\mu_0)\delta(\phi-\phi_0) \end{aligned} \tag{149}$$

2.2.11 Source Function

The source function for thermal emission S_ν^{t} is

$$\begin{aligned} S_\nu^{\mathrm{t}} &= \frac{j(\nu)}{k(\nu)} \\ &= \frac{\alpha(\nu)}{k(\nu)} B_\nu(T) \\ &= \frac{k(\nu)-\alpha(\nu)}{k(\nu)} B_\nu(T) \\ &= (1-\varpi) B_\nu(T) \end{aligned} \tag{150}$$

With knowledge of the phase function $p(\hat{\mathbf{\Omega}}', \hat{\mathbf{\Omega}})$ as well as the scattering and absorption coefficients of the particular extinction process, we can determine the contribution of scattering to the total source function S_ν. Consider the change in radiance $\mathrm{d}I_\nu(\hat{\mathbf{\Omega}})$ occuring over a small change in path $\mathrm{d}\tilde{\tau}$ due to a scattering process with phase function $p(\hat{\mathbf{\Omega}}', \hat{\mathbf{\Omega}})$. The scattering contribution to $\mathrm{d}I_\nu(\hat{\mathbf{\Omega}})$ from every incident direction $\hat{\mathbf{\Omega}}'$ is proportional the radiance of the incident beam, $I_\nu(\hat{\mathbf{\Omega}}')$, the probability that extinction of $I_\nu(\hat{\mathbf{\Omega}}')$ at location $\tilde{\tau}$ is due to scattering (not to absorption), and to the normalized phase function $p(\hat{\mathbf{\Omega}}', \hat{\mathbf{\Omega}})/4\pi$ (138).

$$\begin{aligned} \frac{\mathrm{d}I_\nu(\hat{\mathbf{\Omega}})}{\mathrm{d}\tilde{\tau}} &= I_\nu(\hat{\mathbf{\Omega}}') \frac{\sigma(\nu)}{\sigma(\nu)+\alpha(\nu)} \frac{p(\hat{\mathbf{\Omega}}', \hat{\mathbf{\Omega}})}{4\pi} \\ &= \frac{\varpi}{4\pi} I_\nu(\hat{\mathbf{\Omega}}') p(\hat{\mathbf{\Omega}}', \hat{\mathbf{\Omega}}) \end{aligned} \tag{151}$$

The source function for scattering S_ν^{s} is obtained by integrating (151) over all possible incident directions $\hat{\mathbf{\Omega}}'$ that contribute the exiting radiance in direction $\hat{\mathbf{\Omega}}$

$$S_\nu^{\mathrm{s}} = \frac{\varpi}{4\pi} \int_{\Omega'} I_\nu(\tilde{\tau}, \hat{\mathbf{\Omega}}') p(\tilde{\tau}, \hat{\mathbf{\Omega}}', \hat{\mathbf{\Omega}}) \, \mathrm{d}\Omega' \tag{152}$$

The LHS and RHS of (152) must have equal dimensions. This is easily verified: ϖ is dimensionless, $(4\pi)^{-1}$ is dimensionless (cf. §2.2.7), I_ν and S_ν^{s} both have dimensions of intensity, the dimensions of p are sr^{-1} and the cancel the dimensions of $\mathrm{d}\Omega'$ which are sr.

All terms in (152) are functions of position and scattering process. If there are n distinct scattering processes (e.g., Rayleigh scattering, aerosol scattering, cloud scattering) then we must know the properties of each individual process (e.g., σ_i, p_i) and sum their contributions to obtain to total scattering source function $S_\nu^{\mathrm{s}} = \sum_{i=1}^{i=n} S_{\nu,i}^{\mathrm{s}}$. We neglect such details for now and merely remind the reader that applications need to consider multiple extinction processes at the same time.

The total source function is obtained by adding the source functions for thermal emission (150) and for scattering (152)

$$\begin{aligned} S_\nu &= S_\nu^{\mathrm{t}} + S_\nu^{\mathrm{s}} \\ S_\nu &= (1-\varpi) B_\nu(T) + \frac{\varpi}{4\pi} \int_{\Omega'} I_\nu(\tilde{\tau}, \hat{\mathbf{\Omega}}') p(\tilde{\tau}, \hat{\mathbf{\Omega}}', \hat{\mathbf{\Omega}}) \, \mathrm{d}\Omega' \end{aligned} \tag{153}$$

Although (153) is complete for sources within a medium, additional terms may need to be added to account for boundary sources, such as surface reflection. Boundary sources are discussed in §2.3.

2.2.12 Radiative Transfer Equation in Slab Geometry

Inserting (153) into (96) we obtain the radiative transfer equation including absorption, thermal emission and scattering

$$\begin{aligned}\frac{\mathrm{d}I_\nu}{\mathrm{d}\tilde{\tau}} &= -I_\nu + S_\nu \\ &= -I_\nu + (1-\varpi)B_\nu(T) + \frac{\varpi}{4\pi}\int_{\Omega'} I_\nu(\tilde{\tau},\hat{\mathbf{\Omega}}')p(\tilde{\tau},\hat{\mathbf{\Omega}}',\hat{\mathbf{\Omega}})\,\mathrm{d}\Omega'\end{aligned} \tag{154}$$

This is a general form for the equation of radiative transfer in one dimension, and the jumping off point for our discussion of various solution techniques. The physics of thermal emission, absorption, and scattering are all embodied in (154). The most appropriate solution technique for (154) depends on the boundary conditions of the particular problem, the fields required in the solution (e.g., if irradiance is required but radiance is not), and the required accuracy of the solution.

We are most interested in solving the radiative transfer equations in a slab geometry. To do this we transform from the path optical depth coordinate $\tilde{\tau}$ to the vertical optical depth coordinate τ. Applying the procedure described in (96)–(100) to (154) we obtain the radiative transfer equation for the half range intensities in a slab geometry

$$\begin{aligned}-\mu\frac{\mathrm{d}I^-(\tau,\hat{\mathbf{\Omega}})}{\mathrm{d}\tau} &= I^-(\tau,\hat{\mathbf{\Omega}}) - (1-\varpi)B - \frac{\varpi}{4\pi}\int_+ I^+(\tau,\hat{\mathbf{\Omega}}')p(+\hat{\mathbf{\Omega}}',-\hat{\mathbf{\Omega}})\,\mathrm{d}\Omega' \\ &\quad - \frac{\varpi}{4\pi}\int_- I^-(\tau,\hat{\mathbf{\Omega}}')p(-\hat{\mathbf{\Omega}}',-\hat{\mathbf{\Omega}})\,\mathrm{d}\Omega'\end{aligned} \tag{155a}$$

$$\begin{aligned}\mu\frac{\mathrm{d}I^+(\tau,\hat{\mathbf{\Omega}})}{\mathrm{d}\tau} &= I^+(\tau,\hat{\mathbf{\Omega}}) - (1-\varpi)B - \frac{\varpi}{4\pi}\int_+ I^+(\tau,\hat{\mathbf{\Omega}}')p(+\hat{\mathbf{\Omega}}',+\hat{\mathbf{\Omega}})\,\mathrm{d}\Omega' \\ &\quad - \frac{\varpi}{4\pi}\int_- I^-(\tau,\hat{\mathbf{\Omega}}')p(-\hat{\mathbf{\Omega}}',+\hat{\mathbf{\Omega}})\,\mathrm{d}\Omega'\end{aligned} \tag{155b}$$

If we substitute (147) into (155a) we obtain

$$\begin{aligned}&-\mu\frac{\mathrm{d}I_\mathrm{d}^-(\tau,\hat{\mathbf{\Omega}})}{\mathrm{d}\tau} - \mu\frac{\mathrm{d}I_\mathrm{s}^-(\tau,\hat{\mathbf{\Omega}})}{\mathrm{d}\tau} = \\ &\quad I_\mathrm{d}^-(\tau,\hat{\mathbf{\Omega}}) + I_\mathrm{s}^-(\tau,\hat{\mathbf{\Omega}}) - (1-\varpi)B - \frac{\varpi}{4\pi}\int_- I_\mathrm{s}^-(\tau,\hat{\mathbf{\Omega}}')p(-\hat{\mathbf{\Omega}}',-\hat{\mathbf{\Omega}})\,\mathrm{d}\Omega' \\ &\quad - \frac{\varpi}{4\pi}\int_+ I_\mathrm{d}^+(\tau,\hat{\mathbf{\Omega}}')p(+\hat{\mathbf{\Omega}}',-\hat{\mathbf{\Omega}})\,\mathrm{d}\Omega' - \frac{\varpi}{4\pi}\int_- I_\mathrm{d}^-(\tau,\hat{\mathbf{\Omega}}')p(-\hat{\mathbf{\Omega}}',-\hat{\mathbf{\Omega}})\,\mathrm{d}\Omega'\end{aligned}$$

The direct beam (150) satisfies the extinction law (91) so that $-\mu\,\mathrm{d}I_\mathrm{s}^-/\mathrm{d}\tau = I_\mathrm{s}^-$. Thus the

second terms on the LHS and the RHS of (156) cancel eachother and we are left with

$$-\mu\frac{\mathrm{d}I_{\mathrm{d}}^{-}(\tau,\hat{\mathbf{\Omega}})}{\mathrm{d}\tau} = I_{\mathrm{d}}^{-}(\tau,\hat{\mathbf{\Omega}}) - (1-\varpi)B - S^{*}(\tau,-\hat{\mathbf{\Omega}}) - \frac{\varpi}{4\pi}\int_{+} I_{\mathrm{d}}^{+}(\tau,\hat{\mathbf{\Omega}}')p(+\hat{\mathbf{\Omega}}',-\hat{\mathbf{\Omega}})\,\mathrm{d}\Omega' - \frac{\varpi}{4\pi}\int_{-} I_{\mathrm{d}}^{-}(\tau,\hat{\mathbf{\Omega}}')p(-\hat{\mathbf{\Omega}}',-\hat{\mathbf{\Omega}})\,\mathrm{d}\Omega' \tag{156}$$

where S^{*} is called the single-scattering source function. S^{*} is defined by the integral containing the direct beam on the RHS of (156)

$$\begin{aligned} S^{*}(\tau,-\hat{\mathbf{\Omega}}) &= \frac{\varpi}{4\pi}\int_{-} I_{\mathrm{s}}^{-}(\tau,\hat{\mathbf{\Omega}}')p(-\hat{\mathbf{\Omega}}',-\hat{\mathbf{\Omega}})\,\mathrm{d}\Omega' \\ &= \frac{\varpi}{4\pi}\int_{-} F_{\odot}\mathrm{e}^{-\tau/\mu_0}\delta(\hat{\mathbf{\Omega}}',\hat{\mathbf{\Omega}}_{\odot})p(-\hat{\mathbf{\Omega}}',-\hat{\mathbf{\Omega}})\,\mathrm{d}\Omega' \\ &= \frac{\varpi}{4\pi}F_{\odot}\mathrm{e}^{-\tau/\mu_0}p(-\hat{\mathbf{\Omega}}_{\odot},-\hat{\mathbf{\Omega}}) \end{aligned} \tag{157}$$

Note that (156) is an equation for the diffuse downwelling radiance, not for the total downwelling radiance. The relation between the diffuse and total radiance is given by (147). The direct component is always known (150) once the optical depth has been determined.

Likewise, inserting (147) and (150) into (155b), we obtain the equation for the diffuse upwelling intensity

$$\mu\frac{\mathrm{d}I_{\mathrm{d}}^{+}(\tau,\hat{\mathbf{\Omega}})}{\mathrm{d}\tau} = I_{\mathrm{d}}^{+}(\tau,\hat{\mathbf{\Omega}}) - (1-\varpi)B - S^{*}(\tau,+\hat{\mathbf{\Omega}}) - \frac{\varpi}{4\pi}\int_{+} I_{\mathrm{d}}^{+}(\tau,\hat{\mathbf{\Omega}}')p(+\hat{\mathbf{\Omega}}',+\hat{\mathbf{\Omega}})\,\mathrm{d}\Omega' - \frac{\varpi}{4\pi}\int_{-} I_{\mathrm{d}}^{-}(\tau,\hat{\mathbf{\Omega}}')p(-\hat{\mathbf{\Omega}}',+\hat{\mathbf{\Omega}})\,\mathrm{d}\Omega' \tag{158}$$

where

$$\begin{aligned} S^{*}(\tau,+\hat{\mathbf{\Omega}}) &= \frac{\varpi}{4\pi}\int_{-} I_{\mathrm{s}}^{-}(\tau,\hat{\mathbf{\Omega}}')p(-\hat{\mathbf{\Omega}}',+\hat{\mathbf{\Omega}})\,\mathrm{d}\Omega' \\ &= \frac{\varpi}{4\pi}\int_{-} F_{\odot}\mathrm{e}^{-\tau/\mu_0}\delta(\hat{\mathbf{\Omega}}',\hat{\mathbf{\Omega}}_{\odot})p(-\hat{\mathbf{\Omega}}',+\hat{\mathbf{\Omega}})\,\mathrm{d}\Omega' \\ &= \frac{\varpi}{4\pi}F_{\odot}\mathrm{e}^{-\tau/\mu_0}p(-\hat{\mathbf{\Omega}}_{\odot},+\hat{\mathbf{\Omega}}) \end{aligned} \tag{159}$$

2.2.13 Azimuthal Mean Radiation Field

Often we are not concerned with the azimuthal dependence of the radiation field. In some cases this is because the azimuthal dependence is very weak. For example, heavily overcast skies, or diffuse reflectance from a uniform surface. In other cases the azimuthal dependence may not be weak, but there insufficient information to fully determine the solutions. For example, the full surface BRDF or the shapes of clouds are not available. The azimuthal dependence of a radiative quantity $X(\phi)$ is removed by applying the azimuthal mean operator

$$\bar{X}_{\phi} = \frac{1}{2\pi}\int_{0}^{2\pi} X(\phi)\,\mathrm{d}\phi \tag{160}$$

For future reference we present also the polar angle integration operator which will be used to formulate the two stream equations.

$$\begin{aligned} \bar{X}_\theta &= \int_0^\pi X(\theta)\sin\theta\,\mathrm{d}\theta \\ \bar{X}_\mu &= \int_0^1 X(\mu)\,\mathrm{d}\mu \end{aligned} \tag{161}$$

Applying (160) to (25) and (138), we obtain the azimuthal mean hemispheric intensity, phase function, and single-scattering source function respectively,

$$I^\pm(\tau,\mu) = \frac{1}{2\pi}\int_0^{2\pi} I^\pm(\tau,\mu,\phi)\,\mathrm{d}\phi \tag{162}$$

$$p(\pm\mu';\pm\mu) = \frac{1}{2\pi}\int_0^{2\pi} p(\pm\mu',\phi';\pm\mu,\phi)\,\mathrm{d}\phi \tag{163}$$

$$S^*(\tau,\pm\mu) = \frac{\varpi}{4\pi}F_\odot \mathrm{e}^{-\tau/\mu_0} p(-\mu_0,\pm\mu) \tag{164}$$

No additional symbols are used to indicate azimuthal mean quantities. The presence of only the polar angle (θ or μ) on the LHS of (162) indicates that azimuthal mean quantities are involved.

Applying (160) to the full radiative transfer equations for slab geometry, (156) and (158), we obtain the radiative transfer equations for the azimuthal mean intensity in slab geometry

$$\begin{aligned} -\mu\frac{\mathrm{d}I_\mathrm{d}^-(\tau,\mu)}{\mathrm{d}\tau} &= I_\mathrm{d}^-(\tau,\mu) - (1-\varpi)B - \frac{\varpi}{4\pi}F_\odot \mathrm{e}^{-\tau/\mu_0} p(-\mu_0,-\mu) \\ &- \frac{\varpi}{2}\int_+ I_\mathrm{d}^+(\tau,\mu')p(+\mu',-\mu)\,\mathrm{d}\mu' - \frac{\varpi}{2}\int_- I_\mathrm{d}^-(\tau,\mu')p(-\mu',-\mu)\,\mathrm{d}\mu' \end{aligned} \tag{165a}$$

$$\begin{aligned} \mu\frac{\mathrm{d}I_\mathrm{d}^+(\tau,\mu)}{\mathrm{d}\tau} &= I_\mathrm{d}^+(\tau,\mu) - (1-\varpi)B - \frac{\varpi}{4\pi}F_\odot \mathrm{e}^{-\tau/\mu_0} p(-\mu_0,+\mu) \\ &- \frac{\varpi}{2}\int_+ I_\mathrm{d}^+(\tau,\mu')p(+\mu',+\mu)\,\mathrm{d}\mu' - \frac{\varpi}{2}\int_- I_\mathrm{d}^-(\tau,\mu')p(-\mu',+\mu)\,\mathrm{d}\mu' \end{aligned} \tag{165b}$$

The azimuthal mean equations (165) are very similar to the full equations (156) and (158). While the remainder of the terms in (165) contain only one azimuthally dependent intensity, the scattering integrals contain two, p and $I^\pm$. This causes the factor of $\varpi/4\pi$ in front of the scattering integrals has to become a factor of $\varpi/2$.

We apply the two stream formalism introduced in §2.4 to the radiative transfer equation for the azimuthal mean radiation field (165). Recall that the two stream formalism is obtained by applying three successive approximations. The approximation is achieved in three stages. First, we operate on both sides of (165a) with the hemispheric averaging operator (161). The procedure for (165a) is identical.

$$\begin{aligned} -\int_0^1 \mu\frac{\mathrm{d}I_\mathrm{d}^-(\tau,\mu)}{\mathrm{d}\tau}\,\mathrm{d}\mu &= \int_0^1 I_\mathrm{d}^-(\tau,\mu)\,\mathrm{d}\mu - (1-\varpi)\int_0^1 B\,\mathrm{d}\mu - \frac{\varpi}{4\pi}F_\odot \mathrm{e}^{-\tau/\mu_0}\int_0^1 p(-\mu_0,-\mu)\,\mathrm{d}\mu \\ &- \frac{\varpi}{2}\int_0^1\int_+ I_\mathrm{d}^+(\tau,\mu')p(+\mu',-\mu)\,\mathrm{d}\mu'\,\mathrm{d}\mu - \frac{\varpi}{2}\int_0^1\int_- I_\mathrm{d}^-(\tau,\mu')p(-\mu',-\mu)\,\mathrm{d}\mu'\,\mathrm{d}\mu \end{aligned} \tag{166}$$

Further approximations are required to simplify equations (173). These approximations allow us to decouple products of functions with μ dependence. The first approximation, (167), replaces the continuous value μ on the LHS of (165) by a suitable hemispheric mean value $\bar{\mu}$.

$$\int_0^1 \mu \frac{\mathrm{d}I_\mathrm{d}^-(\tau,\mu)}{\mathrm{d}\tau}\,\mathrm{d}\mu \;\approx\; \bar{\mu}\frac{\mathrm{d}}{\mathrm{d}\tau}\int_0^1 I_\mathrm{d}^-(\tau,\mu)\,\mathrm{d}\mu = \bar{\mu}\frac{\mathrm{d}I_\mathrm{d}^-(\tau)}{\mathrm{d}\tau} \tag{167}$$

Extracting $\bar{\mu}$ from the integral on the LHS of (167) is an approximation whose validity worsens as the correlation between μ and $I_\mathrm{d}^\pm(\tau,\mu)$ increases.

The first two terms on the RHS of (166) are simple hemispheric integrals of hemispherically-varying intensities. We will replace $I^\pm(\tau,\mu)$ by the hemispheric mean intensity $I^\pm(\tau)$ (205). The Planck function is isotropic and so may be pulled outside the hemispheric integral which promptly vanishes since $\int_0^1 \mathrm{d}\mu = 1$. Thus the hemispherically integrated intensities which result explicitly are replaced by the hemispheric mean intensity (205) associated with $\bar{\mu}$.

The final three terms on the RHS of (166) involve products of the phase function and the intensity. We approximate the scattering integrals by applying the hemispheric integral over μ to the intensities, and then extracting the intensities from original integrals over μ'.

$$\begin{aligned}\int_0^1\int_+ p(+\mu',-\mu)I_\mathrm{d}^+(\tau,\mu')\,\mathrm{d}\mu' &\approx \int_0^1 I_\mathrm{d}^+(\tau,\mu')\,\mathrm{d}\mu\int_+ p(+\mu',-\mu)\,\mathrm{d}\mu' \\ &= I_\mathrm{d}^+(\tau)\int_+ p(+\mu',-\mu)\,\mathrm{d}\mu'\end{aligned} \tag{168}$$

These terms define the backscattered fraction of the radiation field. Equation (168), for example, represents the fraction of upwelling energy backscattered into the downwelling direction. This is one of four similar terms that appear in the coupled equations (166). We define the azimuthal mean backscattering function $b(\mu)$ as

$$b(\mu) \;\equiv\; \frac{1}{2}\int_0^1 p(-\mu',\mu)\,\mathrm{d}\mu' = \frac{1}{2}\int_0^1 p(\mu',-\mu)\,\mathrm{d}\mu' \tag{169}$$

The complement of the backscattering function is the forward scattering function f.

$$f(\mu) = 1 - b(\mu) \;\equiv\; \frac{1}{2}\int_0^1 p(-\mu',-\mu)\,\mathrm{d}\mu' = \frac{1}{2}\int_0^1 p(\mu',\mu)\,\mathrm{d}\mu' \tag{170}$$

Pairs of the terms in (169)–(170) are identical due to reciprocity relations. Reciprocity relations state that photon paths are reversible.

The hemispheric mean backscattering coefficient b is the hemispheric integral of (169)

$$b \;\equiv\; \int_0^1 b(\mu)\,\mathrm{d}\mu \tag{171}$$

$$= \frac{1}{2}\int_0^1\int_0^1 p(-\mu',\mu)\,\mathrm{d}\mu'\,\mathrm{d}\mu \tag{172}$$

The hemispheric mean forward scattering coefficient is defined analogously.

The result of these two steps is

$$-\bar{\mu}\frac{\mathrm{d}I_{\mathrm{d}}^{-}(\tau)}{\mathrm{d}\tau} = I_{\mathrm{d}}^{-}(\tau) - (1-\varpi)B - \frac{\varpi}{4\pi}F_{\odot}\mathrm{e}^{-\tau/\mu_0}p(-\mu_0,-\mu) - \frac{\varpi}{2}\int_{+} I_{\mathrm{d}}^{+}(\tau)p(+\mu',-\mu)\,\mathrm{d}\mu' - \frac{\varpi}{2}\int_{-} I_{\mathrm{d}}^{-}(\tau)p(-\mu',-\mu)\,\mathrm{d}\mu' \tag{173a}$$

$$\bar{\mu}\frac{\mathrm{d}I_{\mathrm{d}}^{+}(\tau)}{\mathrm{d}\tau} = I_{\mathrm{d}}^{+}(\tau) - (1-\varpi)B - \frac{\varpi}{4\pi}F_{\odot}\mathrm{e}^{-\tau/\mu_0}p(-\mu_0,+\mu) - \frac{\varpi}{2}\int_{+} I_{\mathrm{d}}^{+}(\tau)p(+\mu',+\mu)\,\mathrm{d}\mu' - \frac{\varpi}{2}\int_{-} I_{\mathrm{d}}^{-}(\tau)p(-\mu',+\mu)\,\mathrm{d}\mu' \tag{173b}$$

These are the hemispheric mean, azimuthal mean, two stream equations for the radiation field in slab geometry. It should be clear that these equations (173) are not derived simply by performing a hemispheric integral (161) on (165). A strict hemispheric averaging operation would applies to the product of the phase function and and the intensity, not to each separately, so that extracting $I_{\mathrm{d}}^{\pm}$ from the scattering integrals is an approximation, as is the definition of $\bar{\mu}$.

2.2.14 Anisotropic Scattering

Armed with techniques introduced in solving the two stream equations for an isotropically scattering medium §2.4.1, we now solve analytically the coupled two stream equations for an anisotropic medium. First we recast (??) into a simpler notation

$$\bar{\mu}\frac{\mathrm{d}I_{\nu}^{+}(\tau)}{\mathrm{d}\tau} = I_{\nu}^{+}(\tau) - \varpi(1-b)I_{\nu}^{+}(\tau) - \varpi b I_{\nu}^{-}(\tau) - (1-\varpi)B_{\nu} - S_{\nu}^{*+} \tag{174a}$$

$$-\bar{\mu}\frac{\mathrm{d}I_{\nu}^{-}(\tau)}{\mathrm{d}\tau} = I_{\nu}^{-}(\tau) - \varpi(1-b)I_{\nu}^{-}(\tau) - \varpi b I_{\nu}^{+}(\tau) - (1-\varpi)B_{\nu} - S_{\nu}^{*-} \tag{174b}$$

For the remainder of the derivation we drop the ν subscript and the explicit dependence of $I^{\pm}$ on τ. Adding and subtracting we obtain

$$\frac{\mathrm{d}(I^{+}+I^{-})}{\mathrm{d}\tau} = -(\alpha-\beta)(I^{+}-I^{-}) \tag{175a}$$

$$\frac{\mathrm{d}(I^{+}-I^{-})}{\mathrm{d}\tau} = -(\alpha+\beta)(I^{+}+I^{-}) \tag{175b}$$

where we have defined

$$\alpha \equiv -[1-\varpi(1-b)]/\bar{\mu} \tag{176a}$$

$$\beta \equiv \varpi b/\bar{\mu} \tag{176b}$$

2.2.15 Diffusivity Approximation

The angular integration required to convert the intensity field into a hemispheric irradiance is a time consuming aspect of numerical models and should be avoided where possible.

According to (56a)–(56b)

$$\frac{1}{\pi}F_\nu^+ = 2\int_0^1 I_\nu(+\mu)\mu\,\mathrm{d}\mu \tag{177a}$$

$$\frac{1}{\pi}F_\nu^- = 2\int_0^1 I_\nu(-\mu)\mu\,\mathrm{d}\mu \tag{177b}$$

The factor of π has been moved to the LHS so that, when the source function is thermal, the RHS is the integral Planck function (116). These angular integrals may be reduced to a calculation of the intensity at certain quadrature points (zenith angles) in each hemisphere with surprising accuracy. The location of the optimal quadrature points may be arrived at through both theoretical and empirical methods.

Two point full Gaussian quadrature (§10.5) tells us the optimal angles to evaluate (177) at are $u = \pm 3^{-1/2}$, $\theta = \pm 54.7356°$.

$$\frac{1}{\pi}F_\nu^+ \simeq \frac{2}{\sqrt{3}}I_\nu(+3^{-1/2}) \tag{178a}$$

$$\frac{1}{\pi}F_\nu^- \simeq \frac{2}{\sqrt{3}}I_\nu(-3^{-1/2}) \tag{178b}$$

The relation in Equation (178) is exact when $I_\nu(\mu)$ is a polynomial of degree < 2. For two point Gaussian quadrature the quadrature weights happen to be unity, but not so for three point (or higher order) Gaussian quadrature. Here is the four point quadrature version of (178)

$$\begin{aligned}
u_1 = -u_4 &= 0.339981 \\
u_2 = -u_3 &= 0.861136 \\
A_1 = A_4 &= 0.652145 \\
A_2 = A_3 &= 0.347855 \\
\frac{1}{2\pi}F_\nu^+ &\simeq A_1 u_1 I_\nu(u_1) + A_2 u_2 I_\nu(u_2) \\
\frac{1}{2\pi}F_\nu^- &\simeq A_3 u_3 I_\nu(u_3) + A_4 u_4 I_\nu(u_4)
\end{aligned} \tag{179}$$

What is often used to evaluate (177) instead of Gaussian quadrature is a diffusivity approximation. Instead of choosing optimal quadrature angles μ_k, the diffusivity approximation relies on choosing the optimal effective absorber path. Thus the diffusivity factor, D, is defined by

$$\frac{1}{\pi}F_\nu^+ \simeq I_\nu(u = +D^{-1}) \tag{180a}$$

$$\frac{1}{\pi}F_\nu^- \simeq I_\nu(u = -D^{-1}) \tag{180b}$$

Comparing (180) to (178) and (177) shows that D replaces, simultaneously, the quadrature angle, its weight, the factor of μ in (177), and a factor of 2 from the azimuthal integration.

The angle $\theta_D = \arccos D^{-1}$ may be interpreted as the mean slant path of radiation in an isotropic, non-scattering atmosphere.

The reasons for subsuming so many factors into D are historical. Nevertheless, (180) is much more common than (178) in the literature. Heating rate calculations in isotropic, non-scattering atmospheres show that using $D = 1.66$ results in errors $< 2\%$ (Goody and Yung, 1989, p. 221).

In applying (180), D only affects the optical depth factor of the intensity. Thus computing the intensity in (180) at the angle $\theta = \theta_D$ is formally equivalent to computing the intensity in the vertical direction $\theta = 0$ but through an atmosphere in which the absorber densities have been increased by a factor of D.

2.2.16 Transmittance

The transmittance between two points measures the transparency of the atmosphere between those points. The transmittance $\tilde{T}$ from point P_1 to point P_2 is the likelihood a photon traveling in direction $\hat{\mathbf{\Omega}}$ at P_1 will arrive at P_2 without having interacted with the matter in between.

$$\tilde{T}(P_1, P_2) = \exp[-\tilde{\tau}(P_1, P_2)] \tag{181}$$

We have left implicit the dependence on frequency. In a stratified atmosphere, we are interested in the transmission of light traveling from layer z' to layer z at angle θ from the vertical, thus

$$T(z', z; \mu) = \exp[-\tau(z', z)/\mu] \tag{182}$$

Thus, in common with absorptance $\mathcal{A}$ and reflectance R, the transmittance $T \in [0, 1]$[9]

The vertical gradient of T is frequently used to formulate solutions of the radiative transfer equation in non-scattering, thermal atmospheres.

$$\begin{aligned} \frac{\partial}{\partial z'} T(z', z; \mu) &= \frac{\partial}{\partial z'} \exp[-\tau(z', z; \mu)/\mu] \\ \frac{\partial T(z', z; \mu)}{\partial z'} &= -\frac{1}{\mu} \exp[-\tau(z', z; \mu)/\mu] \frac{\partial \tau(z', z; \mu)}{\partial z'} \\ &= -\frac{1}{\mu} T(z', z; \mu) \frac{\partial \tau}{\partial z'} \end{aligned} \tag{183}$$

Inverting the above, we obtain

$$\mu^{-1} T(z', z; \mu) = -\frac{\partial T(z', z; \mu)}{\partial z'} \frac{\partial z'}{\partial \tau} \tag{184}$$

The integral solutions for the upwelling and downwelling intensities in a non-scattering, thermal, stratified atmosphere (109)–(110) may be rewritten in terms of T. (110) from τ to

[9] This text distinguishes between transmittance and transmission. The former measures the potential for the latter to occur. Thus a transmittance of unity means the transmission of energy is very high. A similar rule holds for reflectance and reflection and for absorptance and absorption.

z. To do this we use

$$\begin{aligned} z(\tau = \tau^*) &= 0 \\ z(\tau = 0) &= \infty \\ T(0, z; \mu) &= \mathrm{e}^{-(\tau^* - \tau)/\mu} \\ T(z', z; \mu) &= \mathrm{e}^{-(\tau' - \tau)/\mu} \\ T(z, z'; \mu) &= \mathrm{e}^{-(\tau - \tau')/\mu} \\ \frac{\partial T(z', z; \mu)}{\partial z'} &= -\frac{\partial T(z, z'; \mu)}{\partial z'} \end{aligned} \tag{185}$$

The last relation simply states that the transmission decreases as the distance between z', z increases and visa versa. Substituting the above into (109) and (110) yields

$$\begin{aligned} I_\nu(z, +\mu) &= T(0, z; \mu) B_\nu(0) + \mu^{-1} \int_z^0 T(z', z; \mu) B_\nu(z') \, (-\mathrm{d}z') \\ I_\nu(z, -\mu) &= \mu^{-1} \int_\infty^z T(z, z'; \mu) B_\nu(z') \, (-\mathrm{d}z') \end{aligned}$$

Rearranging terms we obtain

$$I_\nu(z, +\mu) = T(0, z; \mu) B_\nu(0) + \mu^{-1} \int_0^z T(z', z; \mu) B_\nu(z') \, \mathrm{d}z' \tag{186a}$$

$$I_\nu(z, -\mu) = \mu^{-1} \int_z^\infty T(z, z'; \mu) B_\nu(z') \, \mathrm{d}z' \tag{186b}$$

Substituting (184) in the above leads to

$$I_\nu(z, +\mu) = T(0, z; \mu) B_\nu(0) + \int_0^z \frac{\partial T(z', z; \mu)}{\partial z'} B_\nu(z') \, \mathrm{d}z' \tag{187a}$$

$$I_\nu(z, -\mu) = -\int_z^\infty \frac{\partial T(z, z'; \mu)}{\partial z'} B_\nu(z') \, \mathrm{d}z' \tag{187b}$$

If T is known, then Equations (187a)–(187b) are suitable for use in quadrature formulae to obtain irradiances.

2.3 Reflection, Transmission, Absorption

Perhaps the most useful metrics of the radiative properties of entire systems are the quantities reflection, transmission, and absorption. These metrics describe normalized properties of a system and thus are somewhat more fundamental than absolute quantities (like transmitted irradiance), which may, for example, change depending on time of day. We shall define the reflection, transmission, and absorption first of the radiance field, and then integrate these definitions with the appropriate weighting to obtain the R, T, and $\mathcal{A}$ pertinent to fluxes. We shall introduce a painful but necessary menagerie of terminology to describe the various species of R, T, and $\mathcal{A}$.

Molotch et al. (2004) show how remotely sensed surface reflectance differs significantly from that derived from snow-age models. Using the more realistic albedos improved models of snowmelt by providing more accurate net surface shortwave radiation estimates. This term, $F_{\mathrm{SW}}^{\mathrm{sfc}}$, dominates the snow-melt energy budget.

Wang et al. (2005) derived a simple functional fit to the desert surface albedo observed by MODIS.

2.3.1 BRDF

The bidirectional reflectance distribution function (BRDF) ρ is the ratio of the reflected intensity to the energy in the incident beam. As such, ρ is a function of frequency, incident angle, and scattered angle

$$\rho(\nu, -\hat{\mathbf{\Omega}}', \hat{\mathbf{\Omega}}) \equiv \frac{\mathrm{d}I_{\nu r}^{+}(\hat{\mathbf{\Omega}})}{I_{\nu}^{-}(\hat{\mathbf{\Omega}}')\cos\theta'\,\mathrm{d}\Omega'} \tag{188}$$

The dimensions of ρ are sr^{-1} and they convert irradiance to intensity. The reflected intensity in any particular direction $\hat{\mathbf{\Omega}}$ is the sum of contributions from all incident directions $\hat{\mathbf{\Omega}}'$ that have a finite probability of reflecting into $\hat{\mathbf{\Omega}}$.

$$\begin{aligned} I_{\nu r}^{+}(\hat{\mathbf{\Omega}}) &= \int_{-\hat{\mathbf{\Omega}}'} \mathrm{d}I_{\nu r}^{+}(\hat{\mathbf{\Omega}}) \\ &= \int_{-\hat{\mathbf{\Omega}}'} I_{\nu}^{-}(\hat{\mathbf{\Omega}}')\rho(\nu, -\hat{\mathbf{\Omega}}', \hat{\mathbf{\Omega}})\cos\theta'\,\mathrm{d}\Omega' \end{aligned} \tag{189}$$

The dependence of $\rho(\nu, -\hat{\mathbf{\Omega}}', \hat{\mathbf{\Omega}})$ on two directions and on frequency makes it a difficult property to measure.

2.3.2 Lambertian Surfaces

Fortunately many surfaces found in nature obey simpler reflectance properties first characterized by Lambert. A Lambertian surface is one whose reflectance is independent of both incident and reflected directions. The reflectance of a Lambertian surface depends only on frequency

$$\rho(\nu, -\hat{\mathbf{\Omega}}', \hat{\mathbf{\Omega}}) = \rho_{\mathrm{L}}(\nu) \tag{190}$$

The intensity reflected from a Lambertian surface is given by inserting (190) into (188) and then using (56b)

$$\begin{aligned} I_{\nu r}^{+}(\hat{\mathbf{\Omega}}) &= \int_{-\hat{\mathbf{\Omega}}'} I_{\nu}^{-}(\hat{\mathbf{\Omega}}')\rho_{\mathrm{L}}(\nu)\cos\theta'\,\mathrm{d}\Omega' \\ &= \rho_{\mathrm{L}}(\nu)\int_{-\hat{\mathbf{\Omega}}'} I_{\nu}^{-}(\hat{\mathbf{\Omega}}')\cos\theta'\,\mathrm{d}\Omega' \\ &= \rho_{\mathrm{L}}(\nu)F_{\nu}^{-} \end{aligned} \tag{191}$$

As expected, the intensity reflected from a Lambertian surface depends only on the incident irradiance, and not at all on the details of the angular distribution of the incident intensity field.

The irradiance reflected from a Lambertian surface $F^+_{\nu r}$ is the cosine-weighted integral of the reflected intensity (191) over all reflected angles

$$\begin{aligned} F^+_{\nu r} &= \int_{\hat{\mathbf{\Omega}}} I^+_\nu(\hat{\mathbf{\Omega}}) \cos\theta \, \mathrm{d}\Omega \\ &= \int_{\hat{\mathbf{\Omega}}} \rho_{\mathrm{L}}(\nu) F^-_\nu \cos\theta \, \mathrm{d}\Omega \end{aligned}$$

Neither F^-_ν and $\rho_{\mathrm{L}}(\nu)$ depend on the emergent angle $\hat{\mathbf{\Omega}}$ so the integral reduces to the familiar integral of $\cos\theta$ over the hemisphere (59) which is $\boldsymbol{\pi}$.

$$F^+_{\nu r} = \boldsymbol{\pi} \rho_{\mathrm{L}}(\nu) F^-_\nu \tag{192}$$

The reflected irradiance may not exceed the incident irradiance or the requirement of energy conservation will be violated. Therefore (192) shows that

$$\rho_{\mathrm{L}}(\nu) \leq \boldsymbol{\pi}^{-1} \tag{193}$$

with equality holding only for a perfectly reflective (non-absorbing) Lambertian surface.

Many researchers prefer the Lambertian BRDF to have an upper limit of 1, not $\boldsymbol{\pi}^{-1}$ (193). Thus it is common to encounter in the literature BRDF defined as $r = \boldsymbol{\pi}\rho$.

2.3.3 Albedo

The reflectance of a surface illuminated by a collimated source such as the Sun or a laser is of great interest in planetary studies and in remote sensing. For an incident collimated beam of intensity $F_\odot$, the diffusely reflected intensity is

$$\begin{aligned} I^+_{\nu r}(\hat{\mathbf{\Omega}}) &= \int_{-\hat{\mathbf{\Omega}}'} F_\odot \delta(\hat{\mathbf{\Omega}}' - \hat{\mathbf{\Omega}}_\odot) \rho(\nu, -\hat{\mathbf{\Omega}}', \hat{\mathbf{\Omega}}) \cos\theta' \, \mathrm{d}\Omega' \\ &= F_\odot \rho(\nu, -\hat{\mathbf{\Omega}}_\odot, \hat{\mathbf{\Omega}}) \cos\theta_0 \end{aligned} \tag{194}$$

Integrating (194) over all reflected angles we obtain the diffusely reflected hemispheric irradiance

$$\begin{aligned} F^+_{\nu r} &= \int_{+\hat{\mathbf{\Omega}}} F_\odot \rho(\nu, -\hat{\mathbf{\Omega}}_\odot, \hat{\mathbf{\Omega}}) \cos\theta_0 \cos\theta \, \mathrm{d}\Omega \\ &= F_\odot \cos\theta_0 \int_{+\hat{\mathbf{\Omega}}} \rho(\nu, -\hat{\mathbf{\Omega}}_\odot, \hat{\mathbf{\Omega}}) \cos\theta \, \mathrm{d}\Omega \end{aligned} \tag{195}$$

The flux reflectance or plane albedo is the ratio of the reflected (diffuse) irradiance (195) to the incident (collimated) irradiance (150)

$$\begin{aligned} \rho(\nu, -\hat{\mathbf{\Omega}}_\odot, 2\boldsymbol{\pi}) &= \frac{F^+_{\nu r}}{F^-_\nu} \\ &= \int_{+\hat{\mathbf{\Omega}}} \rho(\nu, -\hat{\mathbf{\Omega}}_\odot, \hat{\mathbf{\Omega}}) \cos\theta \, \mathrm{d}\Omega \end{aligned} \tag{196}$$

Table 4: Surface Albedo[a]

Surface Type	Reflectance
Glacier	0.9
Snow	0.8
Sea-ice	0.6
Clouds	0.2–0.7
Desert	0.2–0.3
Savannah	0.2–0.25
Forest	0.05–0.1
Ocean	0.05–0.1
Planetary	0.3

[a]Sources: Bird Entrails (2000)

The 2π indicates that the plane albedo pertains to the entire reflected hemisphere.

When the reflecting body is of finite size then the corresponding ratio of reflected to incident fluxes is more complicated because it contains "edge effects", e.g., diminishing contributions from planetary limbs. First we consider the reflection, called the spherical albedo, planetary albedo or Bond albedo, of an entire planetary disk illuminated by collimated sunlight.

The directional reflectance $\rho(\nu, -2\pi, \hat{\mathbf{\Omega}})$ is the

$$F^+_{\nu r}(\hat{\mathbf{\Omega}}) = \int_{-\hat{\mathbf{\Omega}}'} F^-_\nu(-\hat{\mathbf{\Omega}}')\rho(\nu, -2\pi, \hat{\mathbf{\Omega}}) \cos\theta' \, \mathrm{d}\Omega' \tag{197}$$

The flux reflectance of a Lambertian surface to collimated light is found by subsituting (190) in (196)

$$\begin{aligned} \rho(\nu, -\hat{\mathbf{\Omega}}_\odot, 2\pi) &= \int_{+\hat{\mathbf{\Omega}}} \rho_\mathrm{L}(\nu) \cos\theta \, \mathrm{d}\Omega \\ &= \pi\rho_\mathrm{L}(\nu) \end{aligned} \tag{198}$$

which agrees with (192).

The BRDF must be integrated over all possible angles of reflectance in order to obtain the flux reflectance, $\rho(\nu, -\hat{\mathbf{\Omega}}', 2\pi)$. Representative flux reflectances of various surfaces in the Earth system are presented in Table 4.

2.3.4 Flux Transmission

The flux transmission T_ν^F between two layers is (twice) the cosine-weighted integral of the spectral transmission

$$\begin{aligned} T_\nu^F(z',z) &= 2\int_0^1 T(z',z;\mu)\mu\,\mathrm{d}\mu \\ T_\nu^F(z',z) &= 2\int_0^1 \exp[-\tau(z',z)/\mu]\mu\,\mathrm{d}\mu \end{aligned} \tag{199}$$

We can rewrite (199) in terms of exponential integrals (603d)

$$T_\nu^F(z',z) = 2E_3[\tau(z',z)] \tag{200}$$

The factor of 2 ensures that expressions for the hemispheric fluxes in non-scattering, thermal atmospheres closely resemble the equations for intensities, as will be shown next.

The vertical gradient of the flux transmission is frequently used to formulate solutions of the radiative transfer equation in non-scattering, thermal atmospheres. It is obtained by differentiating (200) then applying (602a)

$$\begin{aligned} \frac{\partial}{\partial z'}T_\nu^F(z',z) &= 2\frac{\partial}{\partial z'}E_3[\tau(z',z)]\frac{\partial T_\nu^F(z',z)}{\partial z'} \\ \frac{\partial T_\nu^F(z',z)}{\partial z'} &= 2[-E_2(z',z)]\frac{\partial \tau(z',z;\mu)}{\partial z'} \\ &= -2E_2(z',z)\frac{\partial \tau}{\partial z'} \end{aligned} \tag{201}$$

The integral solutions for the upwelling and downwelling fluxes in a non-scattering, thermal, stratified atmosphere (113) and (114) may be rewritten in terms of T_ν^F. The procedure for doing so is analogous to the procedure applied to intensities in §2.2.16. First, we change the independent variable in (113) and (114) from τ to z.

$$\begin{aligned} F_\nu^+(z) &= 2\pi B_\nu(0)E_3(z) + 2\pi\int_{z'=0}^{z'=z} B_\nu(z')E_2(z-z')\,\mathrm{d}z' \\ F_\nu^-(z) &= 2\pi\int_{z'=z}^{z'=\infty} B_\nu(z')E_2(z'-z)\,\mathrm{d}z' \end{aligned}$$

Substituting (201) into the above yields

$$\frac{1}{\pi}F_\nu^+(z) = B_\nu(0)T_\nu^F(0,z) + \int_{z'=0}^{z'=z} B_\nu(z')\frac{\partial T_\nu^F(z',z)}{\partial z'}\,\mathrm{d}z' \tag{202a}$$

$$\frac{1}{\pi}F_\nu^-(z) = -\int_{z'=z}^{z'=\infty} B_\nu(z')\frac{\partial T_\nu^F(z',z)}{\partial z'}\,\mathrm{d}z' \tag{202b}$$

The analogy between (202a)–(202b) and (187a)–(187b) is complete. T_ν^F plays the same role in former that T plays in the latter.

Equations (202a)–(202b) are particularly useful because they contain no explicit reference to the angular integration. The polar integration, however, is still implicit in the definition of T_ν^F (199). The hemispherical irradiances may be determined without any angular integration if the diffusivity approximation is applied to (202a)–(202b). This is accomplished by replacing T_ν^F by the vertical spectral transmission T through a factor D (180) times as much mass

$$T_\nu^F(z', z) \simeq T(z', z; \arccos D^{-1}) \tag{203}$$

Determination of T requires the use of a spectral gaseous extinction database in conjunction with either a line-by-line model, a narrow band model, or a broadband emissivity approach.

2.4 Two-Stream Approximation

The two-stream approximation to the radiative transfer equation assumes that up- and downwelling radiances travel at mean inclinations $\bar{\mu}^+$ and $\bar{\mu}^-$, respectively. With this assumption, the hemispheric intensities $I_\nu^\pm$ in the azimuthally averaged radiative transfer equation (165) lose their explicit dependence on μ and depend solely on optical depth. For an isotropically scattering atmosphere in a slab geometry, the two-stream approximation may be written

$$\bar{\mu}^+ \frac{\mathrm{d}I_\nu^+(\tau)}{\mathrm{d}\tau} = I_\nu^+(\tau) - \frac{\varpi}{2} I_\nu^+(\tau) - \frac{\varpi}{2} I_\nu^-(\tau) - (1-\varpi) B_\nu[T(\tau)] \tag{204a}$$

$$-\bar{\mu}^- \frac{\mathrm{d}I_\nu^-(\tau)}{\mathrm{d}\tau} = I_\nu^-(\tau) - \frac{\varpi}{2} I_\nu^+(\tau) - \frac{\varpi}{2} I_\nu^-(\tau) - (1-\varpi) B_\nu[T(\tau)] \tag{204b}$$

These equations are no longer exact, but only approximations. Nevertheless, and as we shall show, the two-stream approximation yields remarkably accurate solutions for a wide variety of scenarios including the most important ones in planetary atmospheres. We emphasize that the solutions to the two-stream equation, $I_\nu^\pm$, are hemispheric mean intensities each associated with a hemispheric mean direction $\bar{\mu}^\pm$. In this interpretation of $I_\nu^\pm(\tau)$,

$$I_\nu^\pm(\tau) = \frac{\int_0^1 I_\nu^\pm(\tau, \mu)\, \mathrm{d}\mu}{\int_0^1 \mathrm{d}\mu} = \int_0^1 I_\nu^\pm(\tau, \mu)\, \mathrm{d}\mu \tag{205}$$

As emphasized by (205), $I_\nu^\pm$ are not isotropic intensities in each hemisphere.

We now re-define the other important properties of the radiation field to be consistent with the two-stream approximation. Perhaps most important is the hemispheric irradiance. Starting from (56) we obtain

$$\begin{aligned} F_\nu^\pm(\tau) &= 2\pi \int_0^1 I_\nu^\pm(\tau, \mu) \mu \, \mathrm{d}\mu \\ &\approx 2\pi \bar{\mu} I_\nu^\pm(\tau) \end{aligned} \tag{206}$$

where $\approx$ indicates that (206) is an approximation. Equation (206) reveals one interesting physical interpretation of the two-stream approximation: the radiance field comprises only two discrete streams travelling at angles $\bar{\mu}^\pm$. Mathematically, this radiance field could be represented by the union of the two delta-functions representing collimated beams travelling

in the $\bar{\mu}^{\pm}$ directions. This interpretation (presumably) gives the "two stream" method its name. Physically, it is more appropriate to interpret the two-stream radiance field as being continuously distributed in each hemisphere (205), such that the angular moments (e.g., in the definition of irradiance) have the properties in (206).

A common mis-understanding of the two-stream approximation is that the radiance field is isotropic in each hemisphere. If two-stream radiance were isotropic in each hemisphere then the appropriate measure of hemispheric irradiance would be $F_{\nu}^{\pm} = \pi I_{\nu}^{\pm}$ (59) as opposed to $F_{\nu}^{\pm} = 2\pi\bar{\mu}^{\pm} I_{\nu}^{\pm}$ (206). In fact, assuming the intensity field varies linearly with μ (and is thus anisotropic) is a reasonable interpretation of the two-stream approximation.

The mean intensity $\bar{I}_{\nu}$ (20) for an azimuthally independent, isotropically scattering radiation field is

$$\begin{aligned} \bar{I}_{\nu}(\tau) &= \frac{1}{2}\int_{-1}^{1} I_{\nu}(\tau,u)\,\mathrm{d}u \\ &= \frac{1}{2}\int_{0}^{1} I_{\nu}^{+}(\tau,\mu) + I_{\nu}^{-}(\tau,\mu)\,\mathrm{d}\mu \\ &\approx \frac{1}{2}[I_{\nu}^{+}(\tau) + I_{\nu}^{-}(\tau)] \end{aligned} \tag{207}$$

Although $\bar{I}_{\nu}(\tau)$ (207) appears independent of $\bar{\mu}$, the two-stream intensities in (207) do depend on $\bar{\mu}$.

Continuing to write the two-stream approximations for radiative quantities of interest, we turn now to the source function. The source function S_{ν} (153) for an azimuthally independent, isotropically scattering ($p = 1$) radiation field is

$$\begin{aligned} S_{\nu}(\tau) &= (1-\varpi)B_{\nu}[T(\tau)] + \frac{\varpi}{2}\int_{-1}^{1} I_{\nu}(\tau,u)\,\mathrm{d}u \\ &\approx (1-\varpi)B_{\nu}[T(\tau)] + \frac{\varpi}{2}[I_{\nu}^{+}(\tau) + I_{\nu}^{-}(\tau)] \end{aligned} \tag{208}$$

The final term on the RHS is the two-stream mean intensity $ntnmnfrq$ (207). $\bar{I}_{\nu}$ appears in S_{ν} (208) due to the assumption of isotropic scattering. For more general phase functions, S_{ν} will not contain $\bar{I}_{\nu}$.

A comment on vertical homogeneity is appropriate here. The Planck function in (208) varies continuously with τ, whereas ϖ is assumed to be constant in a given layer over which (208) is discretized. Thus τ-dependence appears explicitly for B_{ν}, and is absent for ϖ. More generally, the radiation field (intensity, irradiance, source function, etc.) varies continuously with τ. The discretization of τ (or, in general, all spatial coordinates) is required in order to solve for the continuously varying radiation field. The discretization determines the scale over which the properties of the matter in the medium may change.

The radiative heating rate h_{ν} in the two-stream approximation may be obtained in at least two distinct forms.

$$\begin{aligned} h_{\nu}(\tau) &= -\frac{\partial F_{\nu}}{\partial z} \\ &= 4\pi\bar{I}_{\nu}(\tau)\alpha - 4\pi\alpha B_{\nu}[T(\tau)] \\ &\approx 2\pi\alpha[I_{\nu}^{+}(\tau) + I_{\nu}^{-}(\tau)] - 4\pi\alpha B_{\nu}[T(\tau)] \end{aligned} \tag{209}$$

The first term on the RHS represents the rate of absorption of radiative energy, while the second term is the rate of radiative emission. Note that (209) depends on the absorption cross section α rather that the single scattering albedo ϖ. This emphasizes that scattering has no direct effect on heating.

Together the relations for F_ν, $\bar{I}_\nu$, S_ν, and h_ν in (206)–(209) define a complete and self-consistent set of radiative properties under the two-stream approximation. We turn now to obtaining the two-stream intensities $I^\pm_\nu(\tau)$ from which these quantities may be computed.

2.4.1 Two-Stream Equations

We shall simplify both the physics and nomenclature of (204) before attempting an analytical solution. First, for algebraic simplicity we set $\bar{\mu}^+ = \bar{\mu}^- = \bar{\mu}$. Also, we neglect the thermal source term $B_\nu[T(\tau)]$. With these assumptions, (204) becomes

$$\bar{\mu}\frac{\mathrm{d}I^+_\nu(\tau)}{\mathrm{d}\tau} = I^+_\nu(\tau) - \frac{\varpi}{2}I^+_\nu(\tau) - \frac{\varpi}{2}I^-_\nu(\tau) \tag{210a}$$

$$-\bar{\mu}\frac{\mathrm{d}I^-_\nu(\tau)}{\mathrm{d}\tau} = I^-_\nu(\tau) - \frac{\varpi}{2}I^+_\nu(\tau) - \frac{\varpi}{2}I^-_\nu(\tau) \tag{210b}$$

For the remainder of the derivation we drop the ν subscript and the explicit dependence of $I^\pm$ on τ. Adding and subtracting the equations in (210) we obtain

$$\bar{\mu}\frac{\mathrm{d}(I^+ - I^-)}{\mathrm{d}\tau} = I^+ + I^- - \varpi(I^+ + I^-) = (1-\varpi)(I^+ + I^-) \tag{211a}$$

$$\bar{\mu}\frac{\mathrm{d}(I^+ + I^-)}{\mathrm{d}\tau} = I^+ - I^- \tag{211b}$$

These may be rewritten as first order, coupled equations in $Y^\pm$ where

$$Y^\pm \equiv I^+ \pm I^- \tag{212a}$$

$$I^\pm = \tfrac{1}{2}(Y^+ \pm Y^-) \tag{212b}$$

Using (212a) in (211)

$$\frac{\mathrm{d}Y^-}{\mathrm{d}\tau} = \frac{(1-\varpi)}{\bar{\mu}}Y^+ \tag{213a}$$

$$\frac{\mathrm{d}Y^+}{\mathrm{d}\tau} = \frac{1}{\bar{\mu}}Y^- \tag{213b}$$

We differentiate (213) with respect to τ to uncouple the equations,

$$\frac{\mathrm{d}^2Y^-}{\mathrm{d}\tau^2} = \frac{(1-\varpi)}{\bar{\mu}}\frac{\mathrm{d}Y^+}{\mathrm{d}\tau} = \frac{(1-\varpi)}{\bar{\mu}}\frac{1}{\bar{\mu}}Y^- = \frac{1-\varpi}{\bar{\mu}^2}Y^-$$

$$\frac{\mathrm{d}^2Y^+}{\mathrm{d}\tau^2} = \frac{1}{\bar{\mu}}\frac{\mathrm{d}Y^-}{\mathrm{d}\tau} = \frac{1}{\bar{\mu}}\frac{(1-\varpi)}{\bar{\mu}}Y^+ = \frac{1-\varpi}{\bar{\mu}^2}Y^+$$

The uncoupled quantities $Y^\pm$ satisfy the same second order ordinary differential equation

$$\frac{\mathrm{d}^2Y^\pm}{\mathrm{d}\tau^2} = \Gamma^2 Y^\pm \tag{214}$$

where

$$\Gamma^2 \equiv \frac{(1-\varpi)}{\bar{\mu}^2} \tag{215}$$

Elementary differential equation theory teaches us that the solutions to (214) are

$$Y^{\pm}(\tau) = C_1^{\pm} e^{\Gamma\tau} + C_2^{\pm} e^{-\Gamma\tau} \tag{216}$$

The general forms of $I^{\pm}$ are obtained by inserting (216) into (212b)

$$I^{+}(\tau) = C_1 e^{\Gamma\tau} + C_2 e^{-\Gamma\tau} \tag{217a}$$
$$I^{-}(\tau) = C_3 e^{\Gamma\tau} + C_4 e^{-\Gamma\tau} \tag{217b}$$

Equation (217) suggests that there are four unknown constants of integration C_1–C_4. This is a consequence of solving for the hemispheric intensities (25) separately in two equations (210) rather solving the full radiative transfer equation (154) for the full domain intensity I. As discussed in §2.1.16, the motivation for solving the half-range equations is that the physical boundary condition (at least in planetary science applications) is usually known for half the angular domain at both the top and the bottom of the atmosphere. These two independent boundary conditions for the first order equations for the hemispheric intensities (210) mean there must be two additional relationships among the unknowns C_1–C_4. Note that the boundary conditions themselves are still unspecified.

To obtain the relationships among C_1–C_4 we substitute the general solution forms (217) into the governing equations (210). It can be shown (after much tedious algebra) that

$$C_2 = \rho_\infty C_4$$
$$C_3 = \rho_\infty C_1$$

where

$$\rho_\infty \equiv \frac{1-\sqrt{1-\varpi}}{1+\sqrt{1-\varpi}} \tag{218}$$

With these additional constraints, (217) becomes

$$I^{+}(\tau) = C_1 e^{\Gamma\tau} + \rho_\infty C_4 e^{-\Gamma\tau} \tag{219a}$$
$$I^{-}(\tau) = \rho_\infty C_1 e^{\Gamma\tau} + C_4 e^{-\Gamma\tau} \tag{219b}$$

where now only the constants C_1 and C_4 remain to be determined by the particular boundary conditions of the problem.

The most relevant two-stream problem that is easily tractable is that of an isotropic, downwelling hemispheric radiation field of intensity $\mathcal{I}$ illuminating a homogeneous slab which overlies a black surface (so that upwelling intensity at the lower boundary is zero).

$$I^{+}(\tau = \tau^*) = 0 \tag{220a}$$
$$I^{-}(\tau = 0) = \mathcal{I} \tag{220b}$$

Substituting (220) into the solutions for the case of an isotropically scattering medium (219) we obtain

$$I^+(\tau = \tau^*) = 0 = C_1 \mathrm{e}^{\Gamma\tau^*} + \rho_\infty C_4 \mathrm{e}^{-\Gamma\tau^*}$$
$$I^-(\tau = 0) = \mathcal{I} = \rho_\infty C_1 + C_4$$

which lead to

$$C_1 = \frac{\rho_\infty \mathcal{I} \mathrm{e}^{-\Gamma\tau^*}}{\rho_\infty^2 \mathrm{e}^{-\Gamma\tau^*} - \mathrm{e}^{\Gamma\tau^*}} = \frac{\rho_\infty \mathcal{I}}{\rho_\infty^2 - \mathrm{e}^{2\Gamma\tau^*}} \tag{221a}$$

$$C_4 = \frac{\mathcal{I} \mathrm{e}^{\Gamma\tau^*}}{\mathrm{e}^{\Gamma\tau^*} - \rho_\infty^2 \mathrm{e}^{-\Gamma\tau^*}} = \frac{\mathcal{I}}{1 - \rho_\infty^2 \mathrm{e}^{-2\Gamma\tau^*}} \tag{221b}$$

It will prove convenient to define the denominators of (221b) as

$$\mathcal{D} = \mathrm{e}^{\Gamma\tau^*} - \rho_\infty^2 \mathrm{e}^{-\Gamma\tau^*} \tag{222a}$$

$$\mathcal{D}^* = 1 - \rho_\infty^2 \mathrm{e}^{-2\Gamma\tau^*} \tag{222b}$$

where $\mathcal{D}^* = \mathrm{e}^{-\Gamma\tau^*}\mathcal{D}$. The initial forms of C_1 and C_4 contain both positive and negative exponentials and are pleasingly symmetrical. These forms have been divided top and bottom by $\mathrm{e}^{-\Gamma\tau^*}$ to obtain the final forms on the RHS for reasons that will be discussed shortly.

Substituting (221) and (222) into (219) we can finally write the intensities at any optical depth τ in terms of the known quantities τ^* and ϖ

$$I^+(\tau) = \frac{\rho_\infty \mathcal{I}}{\mathcal{D}} [\mathrm{e}^{\Gamma(\tau^* - \tau)} - \mathrm{e}^{-\Gamma(\tau^* - \tau)}] = \frac{\rho_\infty \mathcal{I}}{\mathcal{D}^*} [\mathrm{e}^{-\Gamma\tau} - \mathrm{e}^{-2\Gamma(\tau^* - \tau/2)}] \tag{223a}$$

$$I^-(\tau) = \frac{\mathcal{I}}{\mathcal{D}} [\mathrm{e}^{\Gamma(\tau^* - \tau)} - \rho_\infty^2 \mathrm{e}^{-\Gamma(\tau^* - \tau)}] = \frac{\mathcal{I}}{\mathcal{D}^*} [\mathrm{e}^{-\Gamma\tau} - \rho_\infty^2 \mathrm{e}^{-2\Gamma(\tau^* - \tau/2)}] \tag{223b}$$

Two forms of the solution are presented. The initial forms on the RHS are differences between positive and negative exponential terms. In this form, the solutions may appear to depend only on the distance from the lower boundary $(\tau^* - \tau)$ but notice that the $\mathcal{D}$ term (222a) depends on the absolute layer thickness (τ^*) as well. This solution form is not recommended for computational implementation because the positive exponentials are difficult to handle for large optical depths. Moreover, the difference between the exponential terms quickly leads to a loss of numerical precision as $\tau \to \infty$.

The final forms on the RHS of (223) contain only negative exponentials and are numerically well-behaved as $\tau \to \infty$. Since $0 < \tau < \tau^*$, it is clear that all exponentials in (223) and (222a) are negative exponentials and thus well-conditioned for computational applications. There are no physical processes which would lead to positive exponential terms in the solutions, so it is always worthwhile doublechecking for accuracy or stability any formulae which contain positive exponentials.

As expected, the solutions (223) are proportional to the incident intensity $\mathcal{I}$, which is the only source of energy in the problem since we neglected the thermal source term while constructing the governing equations (210). The upwelling radiance is proportional to the parameter ρ_∞. The physical meaning of ρ_∞ is elucidated by noting that $I^+ \to \rho_\infty \mathcal{I}$ as $\tau^* \to \infty$. Thus ρ_∞ is the maximum reflectance of semi-infinite layer of matter with the same optical properties as the layer in question.

2.4.2 Layer Optical Properties

The solutions for the intensities (223) allow us to derive the other optical properties of the layer using (206)–(209). The total flux reflectance $\rho(\nu, -2\pi, 2\pi)$ is the ratio of reflected irradiance to all incident irradiance.

$$\begin{aligned} R(\nu) &\equiv \rho(\nu, -2\pi, 2\pi) \equiv \frac{F_\nu^+(\tau=0)}{F_\nu^-(\tau=0)} \approx \frac{2\pi\bar{\mu} I_\nu^+(\tau=0)}{2\pi\bar{\mu} I_\nu^-(\tau=0)} = \frac{I_\nu^+(\tau=0)}{I_\nu^-(\tau=0)} \\ &= \frac{\rho_\infty \mathcal{I}}{\mathcal{D}^*}(1-\mathrm{e}^{-2\Gamma\tau^*}) \times \left[\frac{\mathcal{I}}{\mathcal{D}^*}(1-\rho_\infty^2 \mathrm{e}^{-2\Gamma\tau^*})\right]^{-1} \\ &= \frac{\rho_\infty}{\mathcal{D}^*}(1-\mathrm{e}^{-2\Gamma\tau^*}) = \frac{\rho_\infty}{\mathcal{D}}(\mathrm{e}^{\Gamma\tau^*} - \mathrm{e}^{-\Gamma\tau^*}) \\ &= \frac{\rho_\infty(1-\mathrm{e}^{-2\Gamma\tau^*})}{1-\rho_\infty^2 \mathrm{e}^{-2\Gamma\tau^*}} = \frac{\rho_\infty(\mathrm{e}^{\Gamma\tau^*} - \mathrm{e}^{-\Gamma\tau^*})}{\mathrm{e}^{\Gamma\tau^*} - \rho_\infty^2 \mathrm{e}^{-\Gamma\tau^*}} \end{aligned} \tag{224}$$

where we have used the definition of $\mathcal{D}^*$ (222b) in the last step.

The total flux transmittance $T(\nu)$ is the ratio of transmitted irradiance to incident irradiance. [10]

$$\begin{aligned} T(\nu) &\equiv T(\nu, -2\pi, -2\pi) \equiv \frac{F_\nu^-(\tau=\tau^*)}{F_\nu^-(\tau=0)} \approx \frac{2\pi\bar{\mu} I_\nu^-(\tau=\tau^*)}{2\pi\bar{\mu} I_\nu^-(\tau=0)} = \frac{I_\nu^-(\tau=\tau^*)}{I_\nu^-(\tau=0)} \\ &= \frac{\mathcal{I}}{\mathcal{D}^*}(\mathrm{e}^{-\Gamma\tau^*} - \rho_\infty^2 \mathrm{e}^{-\Gamma\tau^*}) \times \left[\frac{\mathcal{I}}{\mathcal{D}^*}(1-\rho_\infty^2 \mathrm{e}^{-2\Gamma\tau^*})\right]^{-1} \\ &= \frac{(1-\rho_\infty^2)\mathrm{e}^{-\Gamma\tau^*}}{\mathcal{D}^*} = \frac{1-\rho_\infty^2}{\mathcal{D}} \\ &= \frac{(1-\rho_\infty^2)\mathrm{e}^{-\Gamma\tau^*}}{1-\rho_\infty^2 \mathrm{e}^{-2\Gamma\tau^*}} = \frac{1-\rho_\infty^2}{\mathrm{e}^{\Gamma\tau^*} - \rho_\infty^2 \mathrm{e}^{-\Gamma\tau^*}} \end{aligned} \tag{225}$$

The first expressions in (224) and (225) were derived using the $\mathcal{D}^*$ forms of the solutions (223) and contain no positive exponential terms which blow up as $\tau^* \to \infty$. The second expressions, on the other, hand, are numerically ill-conditioned as $\tau^* \to \infty$.

Conservation of energy requires that the total flux absorptance $\mathcal{A}(\nu)$ is one minus the sum of the transmittance and the reflectance

$$\begin{aligned} \mathcal{A}(\nu) &\equiv \mathcal{A}(\nu, -2\pi) \equiv \frac{F_\nu^-(0) - F_\nu^-(\tau^*) + F_\nu^+(\tau^*) - F_\nu^+(0)}{F_\nu^-(0)} \approx \frac{I_\nu^-(0) - I_\nu^-(\tau^*) + I_\nu^+(\tau^*) - I_\nu^+(0)}{I_\nu^-(0)} \\ &= 1 - T(\nu) - R(\nu) \end{aligned} \tag{226}$$

2.4.3 Conservative Scattering Limit

The preceding section evaluated $R(\nu)$ and $T(\nu)$ for the entire layer for a non-conservative scattering ($\varpi \neq 1$) atmosphere. When $\varpi = 1$ the two-stream equations take a simpler form

[10] A non-reflecting lower boundary ensures there is no ambiguity to the meaning of transmittance. A reflecting lower boundary artificially enhances the apparent transmittance by allowing surface-reflected radiation to scatter off the bottom of the layer and thus be counted as transmitted radiation.

with the result:

$$\begin{aligned} R(\nu) &\equiv \rho(\nu, -2\boldsymbol{\pi}, 2\boldsymbol{\pi}) \equiv \frac{I_\nu^+(\tau=0)}{I_\nu^-(\tau=0)} \\ &= \frac{\mathcal{I}(\tau^*-\tau)}{2\bar{\mu}+\tau^*} \times \left[\frac{\mathcal{I}(2\bar{\mu}+\tau^*-\tau)}{2\bar{\mu}+\tau^*}\right]^{-1} \\ &= \frac{\tau^*-\tau}{2\bar{\mu}+\tau^*-\tau} \\ &= \frac{\tau^*}{2\bar{\mu}+\tau^*} \end{aligned} \tag{227}$$

$$\begin{aligned} T(\nu) &\equiv T(\nu, -2\boldsymbol{\pi}, -2\boldsymbol{\pi}) \equiv \frac{I_\nu^-(\tau=\tau^*)}{I_\nu^-(\tau=0)} \\ &= \frac{\mathcal{I}(2\bar{\mu}+\tau^*-\tau)}{2\bar{\mu}+\tau^*} \times \frac{1}{\mathcal{I}} \\ &= \frac{2\bar{\mu}+\tau^*-\tau}{2\bar{\mu}+\tau^*} \\ &= \frac{2\bar{\mu}}{2\bar{\mu}+\tau^*} \end{aligned} \tag{228}$$

2.5 Example: Solar Heating by Uniformly Mixed Gases

In hydrostatic balance, the density of a uniformly mixed species i is

$$\rho_i(z) = \rho_i(z=0)\mathrm{e}^{-z/H} \tag{229}$$

$$\tag{230}$$

The optical depth of a purely absorbing species with volume absorption coefficient k_a is (84)

$$fxm \tag{231}$$

2.6 Exercises for Chapter 2

1. Consider a vertically homogeneous stratiform liquid water cloud extending from $z =$ 1–2 km above the surface, i.e., the cloud is 1 km thick. Assume the sun is directly overhead and let $F(z)$ denote the downwelling flux (in $\mathrm{W\,m^{-2}}$) in the direct solar beam. At the top of the cloud $F(z=2) = F_\odot$. In the middle of the cloud it is found that $F(z=1.5) = F_\odot/2$.

   (a) What causes $F(z)$ to decrease from the top to the middle of the cloud?
   Answer: Absorption and scattering by cloud droplets.

   (b) What is $F(z=1)$, i.e., the downwelling flux exiting the bottom of the cloud? Answer: $F_\odot/4$

   (c) What is the extinction optical depth of the cloud τ_e? Answer: $\ln 2$

   (d) Assuming the cloud droplets are uniform in size, what additional information about the cloud is needed to estimate the droplet radius? Answer: The mass or number concentration of cloud droplets and their density (i.e., the density of water, $1\,\mathrm{g\,cm^{-3}}$). Also, the extinction efficiency Q_e must be known, but it can be assumed to be 2.

3 Remote Sensing

3.1 Rayleigh Limit

The size parameter χ is the ratio of particle circumference to wavelength, times the real part of the refractive index of the surrounding medium n_r

$$\begin{aligned}\chi &= \mathrm{k} r n_\mathrm{r} &(232)\\ &= 2\pi r n_\mathrm{r}/\lambda &(233)\end{aligned}$$

For particles in air, $n_\mathrm{r} \approx 1$ so $\chi \approx 2\pi r/\lambda$. The Rayleigh limit is the regime where the wavelength is large compared to the particle size, $\lambda \gg r$, or, equivalently, where $\chi \to 0$. Note that this regime applies equally to visible light interacting with nanoparticles, and to microwave radiation interacting with cloud droplets. The absorption and scattering efficiencies reduce to simple, closed form expressions in the Rayleigh limit

$$\lim_{\chi\to 0} Q_\mathrm{a} = -4\chi\,\Im\left(\frac{n^2-1}{n^2+2}\right) \tag{234a}$$

$$\lim_{\chi\to 0} Q_\mathrm{s} = \frac{8\chi^4}{3}\left|\frac{n^2-1}{n^2+2}\right|^2 \tag{234b}$$

where $\Im(z)$ is the imaginary part of z. We see that $Q_\mathrm{a} > Q_\mathrm{s}$ as $\chi \to 0$. Thus we may rewrite (543) as

$$\begin{aligned}\tilde{k}(z) &= \int_0^\infty -4\left(\frac{2\pi r}{\lambda}\right)\Im\left(\frac{n^2-1}{n^2+2}\right)\pi r^2 n_\mathrm{n}(r,z)\,\mathrm{d}r\\ &= -\frac{8\pi^2}{\lambda}\Im\left(\frac{n^2-1}{n^2+2}\right)\int_0^\infty r^3 n_\mathrm{n}(r,z)\,\mathrm{d}r\\ &= -\frac{8\pi^2}{\lambda}\Im\left(\frac{n^2-1}{n^2+2}\right)\frac{3}{4\pi\rho}\int_0^\infty \frac{4\pi\rho}{3} r^3 n_\mathrm{n}(r,z)\,\mathrm{d}r\\ &= -\frac{6\pi}{\rho\lambda}\Im\left(\frac{n^2-1}{n^2+2}\right) M_0(z) &(235)\end{aligned}$$

where in the last step we have replaced the integrand by the total mass concentration, $M_0\,\mathrm{kg\,m^{-3}}$. If the cloud particles are liquid droplets then the density ρ and index of refraction n are well known and M_0 is referred to as the liquid water content. Assuming the extinction by cloud droplets dominates the volume extinction coefficient then we may integrate over the thickness of the cloud to determine the total optical depth. Referring to (545c) we have

$$\begin{aligned}\tilde{\tau}_\mathrm{e} &= -\frac{6\pi}{\rho\lambda}\Im\left(\frac{n^2-1}{n^2+2}\right)\int_{\Delta z} M_0(z)\,\mathrm{d}z\\ &= -\frac{6\pi}{\rho\lambda}\Im\left(\frac{n^2-1}{n^2+2}\right) M_0^\Sigma &(236)\end{aligned}$$

where M_0^Σ is the path-integrated water content in the cloud, called the liquid water path. It is notable that $\tilde{\tau}_\mathrm{e}$ explicitly depends on the total condensed water mass, but not on the

cloud droplet size. In contrast, (95) shows that $\tilde{\tau}_e$ in visible wavelengths depends on both M_0^Σ and r. If the microwave optical depth of the cloud is known, through any independent measurement, then we may use it to obtain M_0^Σ by inverting (236). Fortunately $\tilde{\tau}_e(\lambda)$ may be independently estimated through estimating the microwave brightness temperature of clouds.

3.2 Anomalous Diffraction Theory

The full Mie theory solutions are amenable to approximations in certain limits, the Rayleigh approximation (§3.1) for example. Scattering and absorption by particles with indices of refraction near unity ($n \approx 1$) may be treated with anomalous diffraction theory (ADT) in the regime of large size parameters $\chi \gg 1$. ADT, described in van de Hulst (1957), estimates particle-radiation interaction in this regime by considering the effect refraction has on the phase delay between scattered and diffracted waves. Consider incident plane waves of the form

$$\begin{aligned}
\mathbf{E}_c(\mathbf{r},t) &= \mathbf{E}_0 \exp[\mathrm{i}(\mathbf{k}\cdot\mathbf{r} - \omega t)] \\
&= \mathbf{E}_0 \exp[\mathrm{i}(\mathbf{k}\cdot\mathbf{r} - \mathrm{i}\omega t + \phi)] \\
\mathbf{E}(\mathbf{r},t) &= \Re(\mathbf{E}_c) \\
&= E_0 \cos(\mathbf{k}\cdot\mathbf{r} - \omega t + \phi) \\
&= E_{0,x}\cos(\mathbf{k}\cdot\mathbf{r} - \omega t + \phi_x)\hat{\mathbf{i}} + E_{0,y}\cos(\mathbf{k}\cdot\mathbf{r} - \omega t + \phi_y)\hat{\mathbf{j}} + E_{0,z}\cos(\mathbf{k}\cdot\mathbf{r} - \omega t + \phi_z)\hat{\mathbf{k}}
\end{aligned} \tag{237}$$

where the phase angle ϕ is an arbitrary angular offset. Of course plane waves which explicitly include ϕ satisfy Maxwell's equations (474). ϕ is often omitted from plane wave solutions since, being a constant offset, it has no effect on the physical properties of the solution. We include ϕ in (237) because it will prove useful to examine the phase delay which accrues in plane waves due to particle scattering.

After particle scattering, the electric field is comprised of two waves: the incident plane wave $\mathbf{E}_0$ which travels unrefracted through the particle (because $n \approx 1$), and the scattered wave, $\mathbf{E}_s$ which has been diffracted by the edge of the particle.

$$E = E_0 + E_s \tag{238}$$

We assume that rays suffer no reflection or deviations at the particle boundaries since $n \approx 1$. Thus the particle changes $\mathbf{E}_s$ only in phase, not in amplitude. The change in phase may be determined by considering the geometric path length through the particle. Collimated rays passing through the particle of radius r a distance a (the impaction parameter) from the center define chords of length $2a\sin\psi$ from the entry point to the exit point. The angle ψ lays between the radius to the point where the light ray enters the sphere, and the line segment (of length a) joining the center of the sphere to the chord the ray travels through the sphere.

$$\psi = \cos^{-1} a/r \tag{239}$$

Thus the angle between the entry and exit points and the center of the particle is 2ψ. The phase lag $\Delta\phi$ is determined by the phase of the electric field measured on a plane behind

the particle but normal to the propagation of the incident wave. The electric field measured within the geometric shadow of the particle has suffered a phase lag relative to the field outside the geometric shadow, which has not interacted with the particle. The path length traveled within the particle is a

$$a = 2r \sin\psi \tag{240}$$

The phase lag $\Delta\phi$ suffered during particle transit is a times the difference in propagation speeds times the spatial wavenumber $\mathrm{k} = 2\pi/\lambda$ (12). We assume the particle is suspended in air so the propagation speeds differ by a factor of $n - 1$.

$$\begin{aligned} \Delta\phi &= a \times (n-1) \times \mathrm{k} \\ &= 2r \sin\psi \times (n-1) \times \mathrm{k} \\ &= \rho \sin\psi \end{aligned} \tag{241}$$

where ρ is the phase delay suffered by a ray crossing the full diameter of the particle

$$\begin{aligned} \rho &= 2r(n-1)(2\pi/\lambda) \\ &= 2\chi(n-1) \end{aligned} \tag{242}$$

The phase delay (241) causes a radially varying reduction the electric field amplitude behind the particle, so that

$$E_\mathrm{s} = E_0 \mathrm{e}^{-\mathrm{i}\Delta\phi} - 1 \tag{243}$$

We shall determine the extinction efficiency due to the particle by examining the scattering amplitude function $S(\Theta)$ at the scattering angle $\Theta = 0$. The amplitude function $S(0)$ is the integral over the geometric shadow region of the ratio of the scattered wave to the incident wave.

$$S(0) = \frac{\mathrm{k}^2}{2\pi} \int_A \frac{E_\mathrm{s}}{E_0} \,\mathrm{d}A$$

Following van de Hulst (1957), we employ polar coordinates within the geometric shadow region and begin by integrating over the impact parameter (239)

$$a = r \cos\psi$$

from the center of the particle to the edge. The element of area is a ring of radius a about the center of the particle. The elemental area is $2\pi a \,\mathrm{d}a$ and area

$$\begin{aligned} S(0) &= \frac{\mathrm{k}^2}{2\pi} \int_0^r (1 - \mathrm{e}^{-\mathrm{i}\rho\sin\psi})(2\pi a) \,\mathrm{d}a \\ &= \mathrm{k}^2 \int_0^r (1 - \mathrm{e}^{-\mathrm{i}\rho\sin\psi})\, a \,\mathrm{d}a \end{aligned} \tag{244}$$

The first term in the integrand represents the incident wave. The exponential term which represents the scattered wave is more difficult to integrate. We now change integration variables from impact parameter to entry angle using (244),

$$\begin{aligned} a &= r\cos\psi \\ \psi &= \cos^{-1}(a/r) \\ \mathrm{d}a &= -r\sin\psi\,\mathrm{d}\psi \end{aligned}$$

The change of variables maps $a \in [0, r]$ to $\psi \in [0, \pi/2]$. Thus

$$\begin{aligned} S(0) &= \mathrm{k}^2 \int_0^{\pi/2} (1 - \mathrm{e}^{-\mathrm{i}\rho\sin\psi})(r\cos\psi)(r\sin\psi)\,\mathrm{d}\psi \\ &= \mathrm{k}^2 r^2 \int_0^{\pi/2} (1 - \mathrm{e}^{-\mathrm{i}\rho\sin\psi})\cos\psi\sin\psi\,\mathrm{d}\psi \\ &\equiv \mathrm{k}^2 r^2 K(w) \end{aligned} \tag{245}$$

where $w \equiv \mathrm{i}\rho$. The first term in the integrand in $K(w)$ (245) is a simple trigonometric function. The second term may be integrated by parts with the formula $\int u\,\mathrm{d}v = uv - \int v\,\mathrm{d}u$ where

$$\begin{aligned} u &= \sin\psi \\ \mathrm{d}v &= \mathrm{e}^{-w\sin\psi}\cos\psi\,\mathrm{d}\psi \\ v &= -\frac{\mathrm{e}^{-w\sin\psi}}{w} \\ \mathrm{d}u &= \cos\psi\,\mathrm{d}\psi \end{aligned} \tag{246}$$

Using these standard techniques we obtain

$$\begin{aligned} K(w) &= \int_0^{\pi/2} \sin\psi\cos\psi\,\mathrm{d}\psi - (uv - \int v\,\mathrm{d}u) \\ &= \int_0^{\pi/2} \frac{\sin 2\psi}{2}\,\mathrm{d}\psi - \left[-\sin\psi\frac{\mathrm{e}^{-w\sin\psi}}{w}\right]_0^{\pi/2} + \int_0^{\pi/2} \frac{\mathrm{e}^{-w\sin\psi}}{w}\cos\psi\,\mathrm{d}\psi \\ &= \left[-\frac{\cos 2\psi}{4}\right]_0^{\pi/2} - \left(-\frac{\mathrm{e}^{-w}}{w} - 0\right) + \frac{1}{w}\left[-\frac{\mathrm{e}^{-w\sin\psi}}{w}\right]_0^{\pi/2} \\ &= \frac{-(-1) - [-(1)]}{4} + \frac{\mathrm{e}^{-w}}{w} + \frac{\mathrm{e}^{-w} - 1}{w^2} \\ &= \frac{1}{2} + \frac{\mathrm{e}^{-w}}{w} + \frac{\mathrm{e}^{-w} - 1}{w^2} \end{aligned} \tag{247}$$

With $K(w)$ known we can finally determine the scattering function and the extinction efficiency in the anomalous diffraction limit

$$\begin{aligned} S(0) &= \chi^2 K(w) \\ Q_\mathrm{e} &= \frac{4}{\chi^2}\,\Re\left[S(0)\right] \\ &= 4\,\Re\left[K(w)\right] \end{aligned} \tag{248}$$

For non-absorbing spheres, n is real so (248) becomes

$$Q_{\mathrm{e}} = 2 - \frac{4}{\rho}\sin\rho + \frac{4}{\rho^2}(1-\cos\rho) \tag{249}$$

Following a similar procedure (Liou, 2002) leads to the ADT approximation for absorption efficiency

$$Q_{\mathrm{a}} = 1 + \frac{2}{b}\mathrm{e}^{-b} + \frac{2}{b^2}(\mathrm{e}^{-b}-1) \tag{250}$$

where $b = 4\chi n_{\mathrm{i}}$.

3.3 Geometric Optics Approximation

Nussenzveig (2003) estimate the fraction of absorption due to Mie resonance effects. First, they summarize previous studies (Nussenzveig, 1992; van de Hulst, 1957) which show Mie scattering in transparent spheres results in quasi-periodic resonances with approximate period $\delta\chi$. For water-based liquid aerosols typical of the atmosphere, the period is of order unity in size parameter space. A more precise estimate is

$$\mu \equiv \sqrt{n_{\mathrm{r}}^2 - 1} \tag{251}$$

$$\delta\chi \approx \frac{\arctan\mu}{\mu} \tag{252}$$

Nussenzveig (2003) estimate the absorption due to resonance effects based on complex angular momentum (CAM) theory. Let R be the fractional contribution of resonances to the total mean density of states. In the asymptotic limit as $\chi \gg 1$,

$$R = (\mu/n_{\mathrm{r}})^3, \quad \text{for } \chi \ll 1 \tag{253}$$

For H_2O, $n_{\mathrm{r}} = 1.33$ so $R \sim 29\%$. Let $\langle Q_{\mathrm{a,r}}\rangle$ be the mean absorption efficiency due to resonances across the approximate resonance period $\delta\chi$. Nussenzveig argues that, since each resonance adds to the absorption efficiency, R is a good estimate of $\langle Q_{\mathrm{a,r}}\rangle/Q_{\mathrm{a}}$, the fractional contribution of resonances to the overall absorption efficiency.

A second estimate of $\langle Q_{\mathrm{a,r}}\rangle/Q_{\mathrm{a,r}}$ can be obtained from the geometric optics approximation (GOA). A fundamental result of GOA (Bohren and Huffman, 1983) is that

$$Q_{\mathrm{a,g}} = \frac{8}{3}n_{\mathrm{r}}^2(1-R)n_{\mathrm{i}}\chi, \quad \text{for } n_{\mathrm{i}}\chi \ll 1 \tag{254}$$

Nussenzveig (2003) combines (254) with Wentzel-Kramers-Brillouin (WKB) theory to show

$$\frac{\langle Q_{\mathrm{a,r}}\rangle}{Q_{\mathrm{a,g}}} = \frac{3}{4}\frac{\arctan\mu}{n_{\mathrm{r}}^3 - \mu^3}\left[\left(\frac{\mu}{\arctan\mu}\right)^2 - 1\right] \quad \text{for } \chi \gg 1,\ n_{\mathrm{i}} \ll 1 \tag{255}$$

For $n_{\mathrm{r}} = 1.33$, (255) yields $\langle Q_{\mathrm{a,r}}\rangle/Q_{\mathrm{a,g}} \sim 16\%$, similar to the estimate based on R (253).

Dave recommended a size parameter resolution for Mie integrations of $\Delta\chi \approx 0.1$. Markel (2002) shows this leads to an underestimate of the absorptance of soot in water spheres by about a factor of two.

3.4 Single Scattered Intensity

In clear sky conditions it is reasonable to assume that most of the majority photons measured by Downward looking satellite instruments measure upwelling radiation reflected by the surface plus any photons scattered by the atmosphere into the satellite viewing geometry. In clear sky conditions it is reasonable to approximate the solar radiance measured by a satellite as consisting entirely of singly-scattered photons.

The upwelling intensity measured by a downward-looking instrument mounted, e.g., on an aircraft or satellite, is formally described by the exact solution for upwelling radiance presented in (105). The full, multiple scattering source function with thermal emission S_ν^+ (153) is difficult to obtain and we shall instead make the single-scattering approximation. In the single-scattering approximation, we replace $S_\nu^+(\tau, \hat{\mathbf{\Omega}})$ by the single-scattering source function $S^*(\tau, \hat{\mathbf{\Omega}})$ (159).

In the single-scattering approximation, the upwelling intensity leaving the surface consists solely of reflected photons (194) from the direct downwelling beam (150)

$$\begin{aligned} I_\nu^+(\tau^*, \hat{\mathbf{\Omega}}) &= \int_{-\hat{\mathbf{\Omega}}'} I_\mathrm{s}^-(\tau^*, \hat{\mathbf{\Omega}}')\rho(\nu, -\hat{\mathbf{\Omega}}', \hat{\mathbf{\Omega}}) \cos\theta' \, \mathrm{d}\Omega' \\ &= \int_{-\hat{\mathbf{\Omega}}'} F_\odot \mathrm{e}^{-\tau^*/\mu_0} \delta(\hat{\mathbf{\Omega}}' - \hat{\mathbf{\Omega}}_\odot)\rho(\nu, -\hat{\mathbf{\Omega}}', \hat{\mathbf{\Omega}})\mu' \, \mathrm{d}\Omega' \\ &= \mu_0 F_\odot \mathrm{e}^{-\tau^*/\mu_0} \rho(\nu, -\hat{\mathbf{\Omega}}_\odot, \hat{\mathbf{\Omega}}) \end{aligned} \tag{256}$$

3.5 Satellite Orbits

Assume a satellite is in a circular orbit about Earth so that its Cartesian position $\mathbf{r}$ at radial distance r as a function of time t is

$$\mathbf{r} = r(\sin\omega t\hat{\mathbf{i}} + \cos\omega t\hat{\mathbf{j}}) \tag{257}$$

where ω is the angular velocity. As its name implies, ω measures the rapidity with which the angular coordinate changes (in radians per second, denoted s^{-1}). Let τ denote the orbital period of the satellite. We assume the orbital speed v of a satellite in a circular orbit is a constant. Circular geometry dictates that

$$\tau = 2\pi r/v \tag{258}$$

By definition

$$\begin{aligned} \omega &= 2\pi\tau^{-1} \\ &= 2\pi\left(\frac{2\pi r}{v}\right)^{-1} \\ &= v/r \end{aligned} \tag{259}$$

The acceleration $\mathbf{a}$ of the satellite is the second derivative of the position.

$$\mathbf{v} = r\omega(\cos\omega t\hat{\mathbf{i}} - \sin\omega t\hat{\mathbf{j}}) \tag{260}$$

$$\mathbf{a} = -r\omega^2(\sin\omega t\hat{\mathbf{i}} + \cos\omega t\hat{\mathbf{j}}) \tag{261}$$

$$= -\omega^2\mathbf{r} \tag{262}$$

It is easy to show that $\mathbf{v} \cdot \mathbf{r} = 0$ because they are orthogonal. Thus the velocity of an object in a circular trajectory is tangential to the radial vector. In plane polar coordinates, $\mathbf{r} = r\hat{\mathbf{r}}$ so

$$\mathbf{a} = -r\omega^2\hat{\mathbf{r}} \tag{263}$$

Moreover, (263) shows that the acceleration of an object in a circular trajectory is opposite in direction to the radial vector.

Since the orbit is circular, the magnitudes of $\mathbf{r}$, $\mathbf{v}$, and $\mathbf{a}$ are all constant with time and only their direction changes. This can be verified by computing the vector magnitudes, e.g.,

$$\begin{aligned} a \equiv |\mathbf{a}| &= \sqrt{\mathbf{a} \cdot \mathbf{a}} \\ &= r\omega^2\sqrt{\sin^2 \omega t + \cos^2 \omega t} \\ &= r\omega^2 \end{aligned} \tag{264}$$

a is known as the centripetal acceleration. Substituting (259) into (264) we obtain

$$\begin{aligned} a &= r(v/r)^2 \\ &= v^2/r \\ \mathbf{a} &= -\frac{v^2}{r}\hat{\mathbf{r}} \end{aligned} \tag{265}$$

According to Newton's Second Law (??), the gravitational force $\mathbf{F}$ (??) holding the satellite in orbit must exactly balance (265). Let m and $M_\oplus$ denote the mass of the satellite and of Earth, respectively. Then

$$\begin{aligned} \mathbf{F} &= m\mathbf{a} \\ -\frac{\mathrm{G}mM_\oplus}{r^2}\hat{\mathbf{r}} &= -m\frac{v^2}{r}\hat{\mathbf{r}} \\ \frac{\mathrm{G}mM_\oplus}{r^2} &= m\frac{v^2}{r} \\ \frac{\mathrm{G}M_\oplus}{r^2} &= \frac{v^2}{r} \\ v^2 &= \frac{\mathrm{G}M_\oplus}{r} \\ v &= \sqrt{\frac{\mathrm{G}M_\oplus}{r}} \end{aligned} \tag{266}$$

We note that r is the distance from Earth's center of mass, not its surface, to the satellite. Hence satellite's speed increases slowly as its distance from Earth decreases. The orbital period τ is determined by substituting (266) into (258)

$$\begin{aligned} \tau &= 2\pi r\sqrt{\frac{r}{\mathrm{G}M_\oplus}} \\ \tau^2 &= \frac{4\pi^2 r^3}{\mathrm{G}M_\oplus} \end{aligned} \tag{267}$$

Hence the satellite period squared is proportional to the cube of the orbital size. This relationship is known as Kepler's Law in honor of its discoverer, the astronomer Johannes Kepler.

3.6 Aerosol Characterization

The wavelength and size dependence of aerosol optical properties are generally well-predicted if the aerosol composition and shape are known. However, in situ aerosol composition and size are often difficult or impossible to obtain in the field. Thus indirect estimates of particle size and composition are often derived from the measurements that are available. Many field sites and experiments are equipped to measure the spectrally resolved, column-integrated, aerosol extinction optical depth $\tau_{\mathrm{e}}^{\mathrm{aer}}(\lambda_i)$ where i denotes the spectral channel. The following sections discuss techniques for inferring aerosol optical depth from surface measurements, and the subsequent uses of $\tau_{\mathrm{e}}^{\mathrm{aer}}(\lambda_i)$ to calibrate radiometry, and to infer information about aerosol size distribution and composition.

3.6.1 Measuring Aerosol Optical Depth

Surface radiometry is incapable of directly measuring aerosol optical depth (AOD)[11] because aerosol is vertically distributed in the atmosphere. We now describe how AOD is inferred from surface measurements. This will enable us to qualify what is usually meant by the phrase "measured optical depth" as it appears in the literature. Upward pointing radiometers may measure one or more parts of the radiance field. Downwelling total solar irradiance F^{-} is traditionally measured by global solar pyranometers. The downwelling direct beam irradiance F_{s}^{-} is most accurately measured by a normal incidence pyrheliometer (NIP). Downwelling diffuse irradiance F_{d}^{-} is measured by shaded pyranometers. Instruments that measure all three irradiances also exist. A class of instruments called shadowband radiometers do this by periodically blocking the detector from the direct solar beam using an occluding device called a shadowband.

3.6.2 Aerosol Indirect Effects on Climate

Greater than the direct radiative effect of aerosols on climate is the uncertainty are the effects on climate of changes in cloud due to aerosols. These changes are collectively known as Aerosol Indirect Effects (AIE). The first AIE is the droplet size effect or albedo effect described by Twomey (1977). The second AIE is the so-called cloud lifetime effect or LWC effect. Other AIEs include the cloud glaciation effect.

Dust may suppress precipitation (Rosenfeld et al., 2001; Rudich et al., 2002) including tropical storms and hurricanes () or enhance precipitation (Levin and Ganor, 1996; Wurzler et al., 2000).

3.6.3 Aerosol Effects on Snow and Ice Albedo

Snow and ice always contain a number of particulate and bubble inclusions. The effect on reflectance is non-negligible when the particles are substantially darker than the snow or ice. Warren and Wiscombe (1980) and Wiscombe and Warren (1980) show that Mie theory is an appropriate, but not exact, tool with which to model these effects. Light et al. (1998) present updated data on these effects.

[11] AOD implicitly refers to aerosol extinction optical depth $\tau_{\mathrm{e}}^{\mathrm{aer}}$, the sum of aerosol absorption optical depth $\tau_{\mathrm{a}}^{\mathrm{aer}}$ and aerosol scattering optical depth $\tau_{\mathrm{s}}^{\mathrm{aer}}$.

3.6.4 Ångström Exponent

The sensitivity of the particle extinction efficiency to wavelength i.e., $|\partial Q_{\rm e}(r,\lambda)/\partial\lambda|$, generally increases with decreasing particle size. This sensitivity holds true any paritcle composition, and may be easily demonstrated using Mie codes. An empirical measure of this sensitivity is obtained by defining the Ångström exponent or Ångström parameter α.

$$\alpha \;=\; \frac{\ln[\tau_{\rm e}(\lambda_1)/\tau_{\rm e}(\lambda_2)]}{\ln(\lambda_1/\lambda_2)} \tag{268}$$

Typical values of α are $\alpha > 2$ for small carbonaceous aerosols (smoke) and urban pollution (sulfate) to $\alpha \approx 0$ for large dust particles.

4 Gaseous Absorption

4.1 Line Shape

Three fundamental processes interact to determine the observed shape of spectral lines. These are the natural line width, pressure broadening, and Doppler broadening. Natural line width, which arises from the Heisenberg uncertainty principle, is unimportant in planetary atmospheres. Pressure- and Doppler-broadening effects dominate line shapes here. However, the processes determining natural line widths and pressure broadening of lines are statistically identical, so these two processes have the same analytical form. In planetary atmospheres, Doppler broadening is intermediate in importance between natural line shape and pressure broadening or collision broadening. At pressures weaker than about 1 mb collisions become infrequent enough that the line shapes transition from Lorentzian to Doppler. In this transitional regime the line shape is a convolution of Lorentzian and Doppler shapes. This convolution is known as the Voigt line shape.

4.1.1 Line Shape Factor

The fundamental property of a discrete line transition is the spectral absorption cross section, $\alpha(\nu)$, which measures the strength of the transition as a function of frequency (or wavelength, etc.). As discussed in Section 2.1.13, the units of $\alpha(\nu)$ depend on the application, and they must be consistent with the units of the absorber path, U. The absorber mass path is integral of the absorber amount u along the path.

$$U(P_1,P_2) = \int_{P_1}^{P_2} u(s)\,{\rm d}s \tag{269}$$

Thus, if $\alpha(\nu)$ is expressed in units of $\mathrm{m^2\,kg^{-1}}$, then U and ρ should be expressed in units of $\mathrm{kg\,m^{-2}}$ and $\mathrm{kg\,m^{-3}}$, respectively. We adopt the convention that, when referrring to gaseous absorption, $\alpha(\nu)$ is the number absorption coefficient and is expressed in $\mathrm{m^2\,molecule^{-1}}$. Closely related is the volume absorption coefficient $k_{\rm a}\,[\mathrm{m^{-1}}]$

$$k_{\rm a}(\nu) \;=\; \alpha(\nu)N_0 \tag{270}$$

where N_0 is the number concentration [molecule m^{-3}] of the species.

The value of $\alpha(\nu)$ depends on the absorber type. For a single spectral line, $\alpha(\nu)$ is obtained by converting the parameters in the HITRAN compilation (Rothman et al., 1998) to the local temperature and pressure. For a continuum absorption process, e.g., O_3 Chappuis bands, $\alpha(\nu)$ is usually obtained from a standard table (which may include a parameterized temperature dependence). The JPL compilation (DeMore et al., 1994) is the standard reference for absorption cross sections of photochemical species.

Given these definitions, the optical depth due to absorption between points P_1 and P_2 is

$$\begin{aligned} \tau_\mathrm{a}(P_1, P_2) &= \int_{P_1}^{P_2} \alpha(\nu) u(s)\, \mathrm{d}s \\ &= \alpha(\nu) \int_{P_1}^{P_2} u(s)\, \mathrm{d}s \\ &= \alpha(\nu) U(P_1, P_2) \end{aligned} \tag{271}$$

Comparing this to (82) we see that $\alpha(\nu)$ is the extinction due to absorption.

The integrated strength of a transition is called the line strength or line intensity and is denoted by S

$$S = \int_0^\infty \alpha(\nu)\, \mathrm{d}\nu \tag{272}$$

The dimensions of S are thus the dimensions of the absorption coefficient times the dimensions of frequency (or wavelength), e.g., $\mathrm{m}^2\,\mathrm{kg}^{-1}\,\mathrm{Hz}$ or $\mathrm{m}^2\,\mathrm{kg}^{-1}\,\mathrm{m}$. The relation between $\alpha(\nu)$ and the line strength is called the line shape factor $\Phi(\nu - \nu_0)$

$$\alpha(\nu) = S\Phi(\nu - \nu_0) \tag{273a}$$

$$S = \alpha(\nu)/\Phi(\nu - \nu_0) \tag{273b}$$

$$\Phi(\nu - \nu_0) = \alpha(\nu)/S \tag{273c}$$

where ν_0 is the central frequency of the unperturbed transition. Thus $\Phi(\nu - \nu_0)$ relates the frequency-integrated absorption amount (i.e., line strength) to the specific absorption a distance $\nu - \nu_0$ from the line center. The shape factor for each transition (i.e., line) is normalized to unity

$$\int_0^\infty \Phi(\nu - \nu_0)\, \mathrm{d}\nu = 1 \tag{274}$$

The dimensions of Φ are inverse frequency or wavelength, e.g., $(\mathrm{s}^{-1})^{-1}$, Hz^{-1}, or m^{-1}.

In this section we do not need to specify the which set of self-consistent dimensions we choose for u, U, and $\alpha(\nu)$. Nevertheless, for concreteness we list the three most common choices. First, we may employ dimensions relative to absorber number concentration

$$\begin{aligned} u &= n && \text{molecule}\,\mathrm{m}^{-3} \\ U &= N && \text{molecule}\,\mathrm{m}^{-2} \\ \alpha(\nu) &= k_\mathrm{a}(\nu) && \mathrm{m}^2\,\text{molecule}^{-1} \end{aligned} \tag{275}$$

where $k_{\rm a}(\nu)$ is a number absorption coefficient. Alternatively, we may employ dimensions relative to absorber mass concentration

$$\begin{aligned} u &= m & \mathrm{kg\,m^{-3}} \\ U &= M_0^{\Sigma} & \mathrm{kg\,m^{-2}} \\ \alpha(\nu) &= \psi(\nu) & \mathrm{m^2\,kg^{-1}} \end{aligned} \qquad \text{where}$$

$\psi(\nu)$ is a mass absorption coefficient. (276)

Finally, we may employ dimensions relative to absorber number

$$\begin{aligned} u &= m & \mathrm{kg\,m^{-3}} \\ U &= M_0^{\Sigma} & \mathrm{kg\,m^{-2}} \\ \alpha(\nu) &= \psi(\nu) & \mathrm{m^2\,kg^{-1}} \end{aligned} \qquad \text{where}$$

$\psi(\nu)$ is a mass absorption coefficient. (277)

We prefer to work in units absorption per unit mass (277) because, at least in models, the mass of absorbers is more readily available than the number of absorbers.

4.1.2 Natural Line Shape

Radiative transitions from an upper to a lower state may occur spontaneously, in a process known as spontaneous emission or spontaneous decay. The time intervals t between spontaneous emission are described by a Poisson distribution

$$p_{\rm P}(t) = \frac{1}{\tau_e}\mathrm{e}^{-t/\tau_e} \tag{278}$$

where τ_e is the mean lifetime of the excited state.

The time-dependent Schroedinger equation predicts that the relation between the time intervals between such decays and the energy of the decays gives rise to a continuous, rather than discrete, profile of absorption. The resulting profile is called the natural line shape and is described by

$$\Phi_{\rm n}(\nu-\nu_0) = \frac{\alpha_{\rm n}}{\pi[(\nu-\nu_0)^2+\alpha_{\rm n}^2]} \tag{279}$$

where $\alpha_{\rm n}$ is the natural line shape half width at half-maximum (HWHM). This is seen by noting that $\Phi_{\rm n}(\nu=\nu_0) = (\pi\alpha_{\rm n})^{-1}$ is the full maximum value of $\Phi_{\rm n}(\nu)$, while $\Phi_{\rm n}(\nu = \nu_0+\alpha_{\rm n}) = (2\pi\alpha_{\rm n})^{-1}$.

Natural broadening is one of two important broadening processes that are described by the Lorentz line shape, $\Phi_{\rm L}(\nu-\nu_0)$. The Lorentz line shape is defined identically to (279) as

$$\Phi_{\rm L}(\nu-\nu_0) = \frac{\alpha_{\rm L}}{\pi[(\nu-\nu_0)^2+\alpha_{\rm L}^2]} \tag{280}$$

The Lorentz profile (280) may also be written in terms of the full width at half-maximum $\gamma_{\rm L} = 2\alpha_{\rm n}$ as

$$\Phi_{\rm L}(\nu-\nu_0) \;=\; \frac{\gamma_{\rm L}/2}{\pi[(\nu-\nu_0)^2+(\gamma_{\rm L}/2)^2]} \tag{281}$$

The HWHM of a Lorentz profile is often written in terms of a parameter $\Gamma_{\rm L}$ such that

$$\Phi_{\rm L}(\nu-\nu_0) \;=\; \frac{\Gamma_{\rm L}/4\pi}{\pi[(\nu-\nu_0)^2+(\Gamma_{\rm L}/4\pi)^2]} \tag{282}$$

The full meaning of $\Gamma_{\rm L}$ is described below in §4.1.3.

The Lorentz line shape describes the relative absorption as a function of distance from line center. A separate parameter, the line strength, S (272), defines the abolute absorption. Thus $\Phi_{\rm L}(\nu-\nu_0)$ must be normalized such that its integral over all frequencies is unity.

$$\begin{aligned}
\int_0^\infty \Phi_{\rm L}(\nu-\nu_0)\,{\rm d}\nu &= \int_0^\infty \frac{\alpha_{\rm n}}{\pi[(\nu-\nu_0)^2+\alpha_{\rm n}^2]}\,{\rm d}\nu \\
&= \frac{\alpha_{\rm n}}{\pi}\int_0^\infty \frac{1}{(\nu-\nu_0)^2+\alpha_{\rm n}^2}\,{\rm d}\nu \\
&= \frac{\alpha_{\rm n}}{\pi}\frac{1}{1/\alpha_{\rm n}^2}\frac{1/\alpha_{\rm n}^2}{1}\int_0^\infty \frac{1}{(\nu-\nu_0)^2+\alpha_{\rm n}^2}\,{\rm d}\nu \\
&= \frac{1}{\pi\alpha_{\rm n}}\int_0^\infty \frac{1}{\frac{1}{\alpha_{\rm n}^2}(\nu-\nu_0)^2+1}\,{\rm d}\nu
\end{aligned}$$

We now make the change of variable

$$\begin{aligned}
y &= (\nu-\nu_0)/\alpha_{\rm n} \\
\nu &= \nu_0+\alpha_{\rm n} y \\
{\rm d}y &= {\rm d}\nu/\alpha_{\rm n} \\
{\rm d}\nu &= \alpha_{\rm n}\,{\rm d}y
\end{aligned}$$

This change of variables maps $\nu \in [0,\infty)$ to $y \in [-\nu_0/\alpha_{\rm n},\infty)$. Since $\nu_0 \gg 1$, and the integrand is peaked near the origin, we will replace the lower limit of integration by $-\infty$.

$$\begin{aligned}
\int_0^\infty \Phi_{\rm L}(\nu-\nu_0)\,{\rm d}\nu &= \frac{1}{\pi\alpha_{\rm n}}\int_{-\infty}^\infty \frac{1}{y^2+1}\alpha_{\rm n}\,{\rm d}y \\
&= \frac{1}{\pi}\int_{-\infty}^\infty \frac{1}{y^2+1}\,{\rm d}y \\
&= \frac{1}{\pi}\Big[\tan^{-1}y\Big]_{-\infty}^{\infty} \\
&= \frac{1}{\pi}\left[\frac{\pi}{2}-\left(-\frac{\pi}{2}\right)\right] \\
&= 1
\end{aligned} \tag{283}$$

Thus the Lorentz line shape (280) is correctly normalized.

Some insight into the origin of natural broadening may be obtained from simple examination of the Heisenberg uncertainty principle which may be expressed as the fundamental uncertainty relating two conjugate coordinates such as position and momentum, or, in our case, time and energy:

$$\Delta t \Delta E \sim \hbar \tag{284}$$

When a molecule is in an excited state it has a probability of spontaneously decaying to the lower state. Its actual state is uncertain on the timescale Δt, during which it may be in a superposition of allowed states. Corresponding to this uncertainty, then, is an uncertainty in energy $\Delta E = \mathrm{h}\Delta\nu$ so that

$$\begin{aligned} \Delta t\, \mathrm{h}\Delta\nu &\sim \mathrm{h}/2\pi \\ \Delta\nu &\sim \frac{1}{2\pi\Delta t} \end{aligned} \tag{285}$$

If we identify Δt with τ_e, the mean lifetime of the excited state, and $\Delta\nu$ with α_n, the natural half width, then

$$\alpha_\mathrm{n} = \frac{1}{2\pi\tau_e} \tag{286}$$

For spontaneous emission, τ_e is the reciprocal of the Einstein A coefficient (Shu, 1991). A typical value of τ_e is 10^{-8} s. This is an extremely long time relative to the typical mean time between (optical) collisions in a planetary atmosphere, order 10^{-10} s. In practice, therefore, the line shapes we are concerned with are dominated by collisional effects.

4.1.3 Pressure Broadening

Collisions between molecules are the most important cause of line broadening in the lower atmosphere. Statistically, collisions in a gas of molecules of uniform speeds take place at random time intervals about a mean value. As with spontaneous decay, the probability distribution of time intervals between collisions is therefore a Poisson distribution (278). In reality, molecular velocities are not uniform but obey the Maxwell distribution

$$p_\mathrm{M}(v)\,\mathrm{d}v = \left(\frac{M}{2\pi\mathrm{k}T}\right)^{1/2} \exp\left(-\frac{Mv^2}{2\mathrm{k}T}\right)\,\mathrm{d}v \tag{287}$$

$p_\mathrm{M}(v)$ is the probability that a molecule of mass M at temperature T has a velocity in $[v, v+\mathrm{d}v]$. In all other respects, collision-induced line broadening, or pressure broadening of lines is equivalent to (279) and is thus governed by a Lorentz line shape (280).

$$\Phi_p(\nu-\nu_0) = \frac{\alpha_p}{\pi[(\nu-\nu_0)^2+\alpha_p^2]} \tag{288}$$

where the half width at half-maximum intensity due to pressure (collision) broadening, α_p is called the pressure-broadened line width. Because α_p charaterizes collisional interactions, its value depends on the concentrations and masses of all the molecular species which are present. Thus its determination is somewhat involved.

Molecular collisions occur in two senses, the kinetic and the optical. A collision might change the kinetic energy of one or both of the molecules, but this is not neccessary. Collisions that do alter the kinetic energy of one or both of the particpants are kinetic collisions. Collisions may also cause a radiative excitation or de-excitation of the radiative energy levels of either or both of the molecules involved. Collisional de-excitation, for example, might release one vibrational quanta of energy without changing the kinetic energy of either of the molecules. Collisions that alter the rotational or vibrational quanta of one or both of the particpants are called optical collisions. Rotational energy levels are, in general, much smaller than translational energy levels and thus optical collisions may occur more frequently than kinetic collisions.

Many methods of determining the pressure-broadened line shape have been proposed. A particularly satisfying model is that of molecules radiating with constant intensity between elastic collisions that change the phase of the emitted wavetrain randomly. The radiation is a delta-function in frequency with harmonic time dependence

$$f(t) \quad = \quad \mathrm{e}^{\mathrm{i}\nu_0 t} \tag{289}$$

ν_0 is the center of the unbroadened line. We may restate (289) in frequency space by taking its Fourier transform

$$\begin{aligned} F(\nu) \quad &\equiv \quad \int_{-\infty}^{\infty} f(t)\mathrm{e}^{-\mathrm{i}\nu t}\,\mathrm{d}t \qquad (290) \\ &= \quad \int_{-\infty}^{\infty} \mathrm{e}^{\mathrm{i}\nu_0 t}\mathrm{e}^{-\mathrm{i}\nu t}\,\mathrm{d}t \\ &= \quad \left[\frac{\mathrm{e}^{\mathrm{i}(\nu_0-\nu)t}}{\mathrm{i}(\nu_0-\nu)}\right] \\ &= \quad \frac{\mathrm{e}^{\mathrm{i}(\nu_0-\nu)\tau_\mathrm{c}}}{\mathrm{i}(\nu_0-\nu)} \qquad (291) \end{aligned}$$

The phase of the oscillation, and thus of $f(t)$ is reset randomly by each collision. The waiting period between collisions determines the length of each wavetrain. The probability of a collision occuring between time t and $t + \mathrm{d}t$ follows a Poisson distribution

$$p_\mathrm{P}(t)\,\mathrm{d}t \quad = \quad \mathrm{e}^{t/\tau_\mathrm{c}}\,\mathrm{d}t \tag{292}$$

Let τ_c and τ_o denote the mean times between kinetic collisions and optical collisions, respectively. By definition the mean collision frequency ν_col is the inverse of τ_c. The relationship between distance, rate, and time may be formulated to obtain τ_c

$$\tau_\mathrm{c} \quad = \quad \nu_\mathrm{col}^{-1} = \frac{\lambda}{\bar{v}_\mathrm{m}} \tag{293}$$

where $\bar{v}_\mathrm{m}$ is the thermal speed and λ is the mean free path, both of which are known properties of the thermodynamic state of the atmosphere. First, let us recall that Maxwell-Boltzmann statistics prescribe a square-root dependence of $\bar{v}_\mathrm{m}$ on T

$$\bar{v}_\mathrm{A} \quad = \quad \sqrt{\frac{8RT}{\pi}} = \sqrt{\frac{8\mathrm{R}^*T}{\pi\mathcal{M}}} \tag{294}$$

where $\mathcal{M}$ is the mean molecular weight of the gas, $\mathrm{R}^* = \mathcal{M}R$ is the universal gas constant, R is the specific gas constant, and T is the ambient temperature. Kinetic theory tells us (Seinfeld and Pandis, 1997, p. 457) that the mean free path λ_{AA} of molecular species A in a gas of molecular species A is inversely related to the total concentration of molecules and to their cross-sectional area for collisions, $\pi\sigma_{\mathrm{A}}^2/4$

$$\begin{aligned} \lambda_{\mathrm{AA}} &= \frac{1}{\pi\sqrt{2}N_{\mathrm{A}}\sigma_{\mathrm{A}}^2} \qquad (295) \\ &= \frac{\mathcal{M}}{\pi\sqrt{2}\rho\mathcal{N}\sigma_{\mathrm{A}}^2} \\ &= \frac{\mathcal{M}RT}{\pi\sqrt{2}p\mathcal{N}\sigma_{\mathrm{A}}^2} \\ &= \frac{\mathrm{R}^*T}{\pi\sqrt{2}p\mathcal{N}\sigma_{\mathrm{A}}^2} \qquad (296) \end{aligned}$$

where[12] we have re-expressed λ_{AA} in terms of p and T by using $N = \rho\mathcal{N}/\mathcal{M}$ and then applying the ideal gas law $\rho = p/(RT)$ (??) to (295). There are many subtle assumptions embedded in (295) that should be clarified before proceeding: First is that λ_{AA} is the mean free path of molecular species A in a gas of molecular species A, i.e., of a homogeneous gas of A. Often A is a trace species (e.g., CO_2) in air, represented by species B. The mean free path of A in B incorporates properties of both A and B (Seinfeld and Pandis, 1997, p. 457):

The pressure of an inhomogeneous gaseous mixture of A and B is due, mainly, to the presence of the bulk medium which, for our purposes is air represented by species B. Although the temperatures T of both gases in a mixture are equal in thermodynamic equilibrium, their densities and partial pressures are unequal. Hence the expressions for pressure-broadened line shapes of A will contain molecular properties of A as well as bulk thermodynamics state (temperature, pressure) due mainly to B.

For a homogeneous gas of A, substituting (294) and (296) into (293) yields

$$\begin{aligned} \alpha_p &= \nu_{\mathrm{col}} = \frac{\bar{v}_{\mathrm{m}}}{\lambda} \\ &= \sqrt{\frac{8\mathrm{R}^*T}{\pi\mathcal{M}_{\mathrm{A}}}} \times \frac{\pi\sqrt{2}p\mathcal{N}\sigma_{\mathrm{A}}^2}{\mathrm{R}^*T} \\ &= \sqrt{\frac{8\mathrm{R}^*T}{\pi\mathcal{M}_{\mathrm{A}}}} \times \frac{\pi\sqrt{2}p\mathcal{N}\sigma_{\mathrm{A}}^2}{\mathrm{R}^*T} \\ &= 4\mathcal{N}\sigma_{\mathrm{A}}^2\sqrt{\frac{\pi}{\mathrm{R}^*\mathcal{M}_{\mathrm{A}}}}\frac{p}{\sqrt{T}} \\ &= \frac{4\mathcal{N}\sigma_{\mathrm{A}}^2}{\mathcal{M}_{\mathrm{A}}}\sqrt{\frac{\pi}{\mathrm{R}_{\mathrm{A}}}}\frac{p}{\sqrt{T}} \qquad (297) \end{aligned}$$

We see the interesting result that α_p decreases as T increases. This is because although thermal speed increases as $\sqrt{T}$ (294), the mean free path λ between collisions increases

[12] Unfortunately, terminology has placed in close proximity two symbols that are easy to confuse: N_{A} [# m^{-3}] is the number concentration of molecular species A, while $\mathcal{N}$ [# mol^{-1}] is Avagadro's constant.

Table 5: Temperature Dependence of α_p[a]

Molecule	Min	Mean	Median	Max
H_2O	0.28	0.66		0.97
CO_2	0.49	0.75		0.78
O_3	0.76	0.76	0.76	0.76
N_2O	0.64	0.78		0.82
CH_4	0.75	0.75		0.75
O_2	0.63	0.71		0.74
OH	0.50	0.66		0.66
SO_2	0.50	0.60		0.75

[a]Sources: Rothman et al. (1998), Liou (1992)

linearly as T (296). The net result of increasing T is therefore to decrease collision frequency ν_{col}, and α_p (297).

If we define

$$\begin{aligned} \alpha_{p,0} &\equiv 4\mathcal{N}\sigma_{\text{A}}^2\sqrt{\frac{\pi}{\text{R}^*\mathcal{M}_{\text{A}}}}\frac{\text{p}_0}{\sqrt{\text{T}_0}} \\ &\equiv \frac{4\mathcal{N}\sigma_{\text{A}}^2}{\mathcal{M}_{\text{A}}}\sqrt{\frac{\pi}{\text{R}_{\text{A}}}}\frac{\text{p}_0}{\sqrt{\text{T}_0}} \end{aligned} \tag{298}$$

then

$$\alpha_p(p,T) = \alpha_{p,0}\frac{p}{\text{p}_0}\left(\frac{\text{T}_0}{T}\right)^n \tag{299}$$

where $n = \frac{1}{2}$. The exponent n determining the temperature dependence in (299) is called the line width exponent. Two of the key line parameters measured in laboratory experiments are $\alpha_{p,0}$ and n. Both are tabulated in databases such as HITRAN (§5.5.1). Table 5 shows the mean, median, and range of the temperature-dependent exponent n for the pressure-broadened half width α_p of various optically active gases. For most optically active gases, $0.6 < \bar{n} < 0.8$. This range differs considerably from $n = \frac{1}{2}$ derived in (299), which is known as the classical value of n. This discrepancy arises becauses the optical cross section σ of the molecules have a temperature dependence.

Table 6 shows the mean, median, and range of the pressure-broadened half width α_p of various optically active gases.

Table 6: Pressure-Broadened Half Widths[a]

Molecule	Min	Mean	Median	Max
H_2O	0.0077	0.071		0.11
CO_2	0.055	0.071		0.095
O_3	0.049	0.069		0.084
N_2O	0.069	0.075		0.097
CH_4	0.018	0.054		0.16
O_2	0.028	0.043		0.060
OH	0.040	0.044		0.095
SO_2	0.10	0.11		0.15

[a]Units are $cm^{-1}\,atm^{-1}$ at 296 K. Sources: Rothman et al. (1998)

Pure kinetic theory must be combined with the optical cross section σ to determine α_p[13]

$$\alpha_p = \sum_i N_i^2 \left[\left(\frac{2kT}{\pi} \right) \left(\frac{1}{M} + \frac{1}{M_i} \right) \right]^{1/2} \tag{300}$$

where the summation is over all perturber species i (i.e., O_2, N_2, ...) and M is the mass of the absorber. Thus α_p depends quadratically (fxm: typo, must be linear) upon the number-density of collision partners and linearly upon the velocity of the molecules (note the factor of $\sqrt{kT}$). A scaling approximation is therefore frequently used to extrapolate $\alpha_p(T)$ based on some measured or tabulated value $\alpha_p(T_0)$

$$\alpha_p(T, p) \approx \alpha_p(T_0, p_0) \frac{p}{p_0} \left(\frac{T}{T_0} \right)^{1/2} \tag{301}$$

Atmospheric pressure changes by three orders of magnitude, from 1–1000 mb, from 50 km to the surface. Temperature changes by only a factor of 2 over the same altitude range. Since line widths (301) depend linearly on p, but only on the square root of T, pressure variation dominates vertical changes in α_p.

The mean time between optical collisions τ_o is then related to α_p by

$$\begin{aligned} \tau_o &= \frac{1}{2\pi\alpha_p} \\ \alpha_p &= \frac{1}{2\pi\tau_o} \\ \alpha_p &= \frac{\nu_{col}}{2\pi} \end{aligned} \tag{302}$$

[13](300) is taken from Goody and Yung (1989), p. 99. The equation appears to contain typos and should be viewed qualitatively until it is checked against a trustworthy reference on kinetic theory. For example, the quadratic dependence on the concentration of the perturber appears to be typo. Also the optical collision diameter σ is missing.

This is exactly analogous to the relation between τ_e and $\alpha_{\rm n}$ (286) because both processes are described by the Lorentz line shape.

When natural- and collision-broadening are considered simultaneously, it can be shown that the combined line shape is also a Lorentzian with HWHM $\Gamma_{\rm L}/4\pi$ (282). The parameter $\Gamma_{\rm L}$ is related to both the natural line width and the mean frequency of collisions $\nu_{\rm col} = \tau_{\rm c}^{-1}$ (302) by

$$\Gamma_{\rm L} \;=\; 4\pi\alpha_{\rm n} + 2\nu \tag{303}$$

These relations may be proved by examining the power spectrum of a sinusoidal electric field which is randomly interrupted $\nu_{\rm col}$ times per second. In practice in the lower atmosphere $\alpha_p \gg \alpha_{\rm n}$ so the Lorentz line width is nearly equivalent to the pressure-broadened line width. Therefore, Lorentz broadening and the Lorentz line width will hereafter refer to the Lorentzian line shape (280) due to the convolution of natural- and collision-broadening. With reference to (303) and (302)

$$\begin{aligned} \alpha_{\rm L} &= \Gamma_{\rm L}/4\pi \\ \alpha_{\rm L} &= \alpha_{\rm n} + \nu_{\rm col}/2\pi \\ \alpha_{\rm L} &= \alpha_{\rm n} + \alpha_p \end{aligned} \tag{304}$$

When discussing a given transition, it is convenient to translate the origin of the frequency axis to the line center. Rather than defining a new variable to do this, we continue to use ν. Thus we replace $\nu - \nu_0$ by ν alone. The intended meaning of ν should be clear from the context. Using this notation (280) becomes

$$\Phi_{\rm L}(\nu) \;=\; \frac{\alpha_{\rm L}}{\pi(\nu^2 + \alpha_{\rm L}^2)} \tag{305}$$

The absorption cross-section (273) for Lorentzian lines may now be written

$$\alpha(\nu) \;=\; \frac{S\alpha_{\rm L}}{\pi(\nu^2 + \alpha_{\rm L}^2)} \tag{306}$$

4.1.4 Doppler Broadening

Brownian motion causes molecules to constantly change their velocity relative to the photons which may interact with them. While the frequencies of resonant absorption are constant in the frame of motion of the molecule, this random motion broadens the range of resonant frequencies in the frame of a stationary observer. This form of line broadening is called Doppler broadening. The probability that the molecule and a stationary reference frame (an "observer") have relative velocity in $[v, v + {\rm d}v]$ is given by the Maxwell distribution (287)

$$p_{\rm M}(v)\,{\rm d}v \;=\; \left(\frac{M}{2\pi {\rm k}T}\right)^{1/2} \exp\left(-\frac{Mv^2}{2{\rm k}T}\right)\,{\rm d}v \tag{307}$$

We convert this Maxwellian PDF directly to the Doppler line shape PDF $\Phi_{\rm D}(\nu - \nu_0)$ by noting that each value of v describes a shift in line center $\Delta\nu \equiv \nu - \nu_0$. For $v/{\rm c} \ll 1$, the

relation between v and the Doppler shift $\Delta\nu$ is

$$\begin{aligned} \Delta\nu &= \nu_0 v/\mathrm{c} \\ v &= \mathrm{c}\Delta\nu/\nu_0 \\ \mathrm{d}\nu &= \mathrm{d}\Delta\nu = \frac{\nu_0}{\mathrm{c}}\,\mathrm{d}v \\ \mathrm{d}v &= \frac{\mathrm{c}}{\nu_0}\,\mathrm{d}\nu \end{aligned}$$

When we re-express $p_{\mathrm{M}}(v)$ (307) in terms of $\Delta\nu$ by imposing the condition

$$p_{\mathrm{M}}(v)\,\mathrm{d}v = p_{\mathrm{M}}(\Delta\nu)\,\mathrm{d}\Delta\nu \tag{308}$$

This relation between $p_{\mathrm{M}}(v)$ and $p_{\mathrm{M}}(\Delta\nu)$ is like that between $B_\lambda(\lambda)$ and $B_\nu(\nu)$ (42). Inserting (308) into (307) leads to

$$\begin{aligned} p_{\mathrm{M}}[v(\nu)]\,\mathrm{d}v &= \left(\frac{M}{2\pi\mathrm{k}T}\right)^{1/2} \exp\left(-\frac{M\mathrm{c}^2\Delta\nu^2}{2\nu_0^2\mathrm{k}T}\right) \frac{\mathrm{d}v}{\mathrm{d}\nu}\,\mathrm{d}\nu \\ &= \frac{\mathrm{c}}{\nu_0}\left(\frac{M}{2\pi\mathrm{k}T}\right)^{1/2} \exp\left[-\Delta\nu^2\left(\frac{2\nu_0^2\mathrm{k}T}{M\mathrm{c}^2}\right)^{-1}\right]\mathrm{d}\nu \end{aligned} \tag{309}$$

The RHS of (309) is now strictly a function of ν. We name this function the Doppler line shape, $\Phi_{\mathrm{D}}(\nu)$ and define the Doppler width $\tilde{\alpha}_{\mathrm{D}}$ as the square root of the portion of the exponential in parentheses

$$\tilde{\alpha}_{\mathrm{D}} = \frac{\nu_0}{\mathrm{c}}\sqrt{\frac{2\mathrm{k}T}{M}} \tag{310}$$

so that (309) becomes

$$\begin{aligned} \Phi_{\mathrm{D}}(\nu)\,\mathrm{d}\nu &= \frac{\mathrm{c}}{\nu_0}\left(\frac{M}{2\pi\mathrm{k}T}\right)^{1/2} \exp\left(-\frac{\Delta\nu^2}{\tilde{\alpha}_{\mathrm{D}}^2}\right)\mathrm{d}\nu \\ &= \frac{1}{\sqrt{\pi}}\frac{\mathrm{c}}{\nu_0}\left(\frac{M}{2\mathrm{k}T}\right)^{1/2} \exp\left(-\frac{\Delta\nu^2}{\tilde{\alpha}_{\mathrm{D}}^2}\right)\mathrm{d}\nu \\ &= \frac{1}{\tilde{\alpha}_{\mathrm{D}}\sqrt{\pi}} \exp\left[-\left(\frac{\nu-\nu_0}{\tilde{\alpha}_{\mathrm{D}}}\right)^2\right]\mathrm{d}\nu \end{aligned} \tag{311}$$

The normalization of (311) follows from the fact that it is simply a re-expression of the Maxwell distribution (307), which is already known to be normalized. The full maximum value of Φ_{D} is $\Phi_{\mathrm{D}}(\nu=\nu_0) = (\tilde{\alpha}_{\mathrm{D}}\sqrt{\pi})^{-1}$, and $\Phi_{\mathrm{D}}(\nu=\nu_0+\tilde{\alpha}_{\mathrm{D}}) = (\mathrm{e}\tilde{\alpha}_{\mathrm{D}}\sqrt{\pi})^{-1}$, so that $\tilde{\alpha}_{\mathrm{D}}$ is the half width at e^{-1} of the maximum of Φ_{D}. Care should be taken not to confuse $\tilde{\alpha}_{\mathrm{D}}$ with a half-width at half-maximum. The half width at half-maximum of $\Phi_{\mathrm{D}}(\nu)$ is

$$\alpha_{\mathrm{D}} = \tilde{\alpha}_{\mathrm{D}}\sqrt{\ln 2} \tag{312}$$

It is more appropriate to compare α_{L} (298) to α_{D} (312), since they are identical measures of line width, than to $\tilde{\alpha}_{\mathrm{D}}$ (310).

We recognize that (311) is a form of Gaussian distribution, although it is not expressed in the canonical form of a Gaussian

$$p_{\mathrm{G}}(\nu)\,\mathrm{d}\nu \;=\; \frac{1}{\sigma\sqrt{2\pi}}\exp\left[-\left(\frac{\nu-\nu_0}{\sigma\sqrt{2}}\right)^2\right]\mathrm{d}\nu \tag{313}$$

in which σ represents the standard deviation and ν_0 the mean value. Comparing (313) to (311) we see that the standard deviation of the Doppler line shape $\sigma_{\mathrm{D}} = \tilde{\alpha}_{\mathrm{D}}/\sqrt{2}$. Thus Doppler broadening alone allows absorptions to occur within $\tilde{\alpha}_{\mathrm{D}}/\sqrt{2}$ and $\sqrt{2}\tilde{\alpha}_{\mathrm{D}}$ of line center with efficiencies (relative to line center) of $1-\mathrm{e}^{-1} = 0.683$, and $1-\mathrm{e}^{-2} = 0.954$, respectively.

4.1.5 Voigt Line Shape

Line broadening processes occur simultaneously in nature. In particular, Collision-broadening occurs in tandem with Doppler broadening. If we assume these two processes are independent but occur simulateously, then the net line shape of the total process will be the collision-broadened line shape, shifted by the Doppler shift (308), and averaged over the Maxwell distribution (307). The resulting line shape is call the Voigt profile, $\Phi_{\mathrm{V}}(\nu)$.

$$\Phi_{\mathrm{V}}(\nu-\nu_0) \;=\; \int_{-\infty}^{\infty}\left(\frac{M}{2\pi\mathrm{k}T}\right)^{1/2}\exp\left(-\frac{Mv^2}{2\mathrm{k}T}\right)\frac{\alpha_{\mathrm{L}}}{\pi[(\nu-\nu_0+\nu_0 v/\mathrm{c})^2+\alpha_{\mathrm{L}}^2]}\,\mathrm{d}v \tag{314}$$

$$\;=\; \sqrt{\frac{M}{2\pi\mathrm{k}T}}\int_{-\infty}^{\infty}\exp\left(-\frac{Mv^2}{2\mathrm{k}T}\right)\frac{\alpha_{\mathrm{L}}}{\pi[(\nu-\nu_0+\nu_0 v/\mathrm{c})^2+\alpha_{\mathrm{L}}^2]}\,\mathrm{d}v \tag{315}$$

Analytic approximations to and asymptotic behavior of $\Phi_{\mathrm{V}}(\nu-\nu_0)$ are discussed in Goody and Yung (1989); Liou (1992).

With appropriate definitions (e.g., Liou, 1992, p.30)

$$\begin{aligned} t &= \sqrt{\ln 2}(\nu-\nu')/\tilde{\alpha}_{\mathrm{D}} \\ x &= \sqrt{\ln 2}(\nu-\nu_0)/\tilde{\alpha}_{\mathrm{D}} \\ \alpha_{\mathrm{D}} &= \sqrt{\ln 2}\tilde{\alpha}_{\mathrm{D}} \\ y &= \sqrt{\ln 2}\alpha_p/\alpha_{\mathrm{D}} \end{aligned} \tag{316}$$

we may re-express (315) as

$$\Phi_{\mathrm{V}}(\nu-\nu_0) \;=\; \frac{1}{\alpha_{\mathrm{D}}}\sqrt{\frac{\ln 2}{\pi}}K(x,y) \tag{317}$$

where the complex error function $K(x,y)$ is defined

$$K(x,y) \;=\; \frac{y}{\pi}\int_{-\infty}^{+\infty}\frac{\mathrm{e}^{-t^2}}{y^2+(x-t)^2}\,\mathrm{d}t \tag{318}$$

Efficient algorithms for evaluating $K(x,y)$ have been developed (Hui et al., 1978; Humlíček, 1982; Kuntz, 1997) to reduce computational expense in detailed line-by-line calculations.

5 Molecular Absorption

We now attempt to develop an introductory understanding of the location of absorption lines in gases. The science of atomic and molecular spectroscopy is extremely detailed and requires a quantum mechanical treatment for a satisfactory explanation of all phenomenon. Nevertheless, important insights as to the spectral location, temperature dependence, and relative population of radiative energy levels may be gained by resorting to a semi-classical treatment of the radiation field. In essence, our first task is to characterize the distribution of observed molecular transitions in the atmosphere, i.e., to characterize ΔE from Planck's relation

$$\Delta E = \mathrm{h}\nu \tag{319}$$

To begin, we enumerate the contributions to a molecule's total energy E_t. The total molecular energy comprises the tranlational kinetic energy $ngrtrn$, the electronic energy E_e, the vibrational energy E_v, the rotational energy E_r, and the nuclear energy E_n.

$$E_\mathrm{t} = E_\mathrm{t} + E_\mathrm{e} + E_\mathrm{v} + E_\mathrm{r} + E_\mathrm{n} \tag{320}$$

These energy components have been listed in order of decreasing magnitude. We are mainly interested in describing vibrational and rotational energy transitions in the next sections.

5.1 Mechanical Analogues

In the quantum mechanical view, radiative absorption occurs when an incident photon of energy level $\mathrm{h}\nu$ encounters a molecule with energy E_1. If $E_1 + \mathrm{h}\nu$ is "close enough" to an available energy state E_2 of the molecule, then absorption may occur. If absorption does occur, the energy of the photon is transferred to to the corresponding energetic mode or modes of the molecule. These molecular modes, e.g., spin, vibration, rotation, take their names from mechanical systems which form their classical analogues. To understand the distribution of energy levels in these modes it is thus useful to describe classical mechanical analogues which are known to behave like molecular systems.

Molecules may be thought of as rotating structures. When the molecular structure is fixed, i.e., the separation between the atoms does not change, we call the molecule obeys the rigid rotator model. Diatomic molecules, for example, may be visualized as barbell-shaped, with an atom at each end, separated by a massless but rigid rod. The separation of the atoms means their charges are separated. If the center of mass between the atoms does not coincide with the center of charge, then the molecule has a permanent dipole moment. Molecules comprised of a single element, e.g., N_2 or O_2, are called homonuclear. Homonuclear molecules are perfectly symmetric rigid rotators, and thus have no permanent dipole moment.

To continue with the quantum mechanical behavior of the rigid rotator molecule, we must determine the available energy states of the system. Let the atoms of masses M_1 and M_2 be separated by a distance r. Then the distances of each from the center of mass of the

system are

$$r_1 = \frac{M_1 r}{M_1 + M_2} = \frac{\tilde{M}}{M_2} r \tag{321}$$

$$r_2 = \frac{M_2 r}{M_1 + M_2} = \frac{\tilde{M}}{M_1} r \tag{322}$$

where the reduced mass $\tilde{M}$ of the system is

$$\tilde{M} \equiv \frac{M_1 M_2}{M_1 + M_2} \tag{323}$$

The moment of inertia I of the system about the center of mass is the total mass-weighted mean square distance from the axis of rotation

$$I = M_1 r_1^2 + M_2 r_2^2 \tag{324}$$

The angular momentum L of the system is the total mass-weighted product of the distance from the axis of rotation times the velocity. Denoting the angular frequency of the rotation by ω, the linear velocity of the atoms are ωr_1 and ωr_2.

$$\begin{aligned} L &= M_1 r_1 v_1 + M_2 r_2 v_2 \\ &= M_1 \omega r_1^2 + M_2 \omega r_2^2 \\ &= \omega (M_1 r_1^2 + M_2 r_2^2) \end{aligned}$$

The classical energy of a rigidly rotating dumbbell may be expressed in terms of I and L

$$\begin{aligned} E_{\mathrm{r}} &= \tfrac{1}{2} I \omega^2 \\ E_{\mathrm{r}} &= \frac{L^2}{2I} \end{aligned} \tag{325}$$

The quantum mechanical angular momentum operator, $\mathcal{L}$, quantizes the angular momentum component of the energy Hamiltonian. The eigenvalues of the square of the angular momentum operator, $\mathcal{L}^2$, are

$$\mathcal{L}^2 \psi = \hbar^2 J(J+1) \psi \tag{326}$$

where ψ is the wavefunction and J, an integer, is the rotational quantum number of the system. Substituting (326) into (325) we obtain the quantum mechanical energy of a rigid rotator

$$\begin{aligned} E_{\mathrm{r}} &= \frac{\hbar^2}{2I} J(J+1) \\ &= \frac{\mathrm{h}^2}{4\pi^2} \frac{1}{2I} \frac{\mathrm{c}}{\mathrm{c}} J(J+1) \\ &= \frac{\mathrm{h}}{8\pi^2 \mathrm{c} I} \mathrm{hc} J(J+1) \\ &= \mathrm{hc} B_{\mathrm{v}} J(J+1) \end{aligned} \tag{327}$$

where

$$B_{\mathrm{v}} = \frac{\mathrm{h}}{8\pi^2 \mathrm{c} I} \tag{328}$$

B_{v} is the rotational constant of the species. B_{v} is purely a function of the atomic masses and geometry of the species through I (324). The v subscript[14] indicates that B_{v} is a function of vibrational state.

Spectroscopists have adopted a variety of equivalent but usually unintuitive notations to describe the lower (lower energy) and upper (higher energy) states of transitions. The most common convention is that lower and upper state quantum numbers are superscripted by a double prime "″" and a single prime "′", respectively. Thus lower and upper vibrational and rotational quantum states are denoted by (v'', J'') and (v', J'), respectively. Examples of equivalent representations of emission include

$$\begin{aligned} \nu' &\rightarrow \nu \\ \nu &\leftarrow \nu' \\ (v', J') &\rightarrow (v'', J'') + \mathrm{h}\nu \\ (v'', J'') + \mathrm{h}\nu &\leftarrow (v', J') \end{aligned} \tag{329}$$

Due to destructive interference patterns between quantum mechanical wavefunctions, not all conceivable vibrotational transitions are allowed transitions. Rotational transitions are subject to the selection rule that

$$\Delta J = J' \pm J'' = \pm 1 \tag{330}$$

Transitions which break selection rules like (330) are called forbidden transitions.

Applying this rule to (327) we obtain the energy of photons released in purely rotational emission

$$\begin{aligned} \Delta E_{\mathrm{r}} &= \mathrm{hc}B_{\mathrm{v}}(J+1)(J+2) - \mathrm{hc}B_{\mathrm{v}}J(J+1) \\ \mathrm{h}\nu &= \mathrm{hc}B_{\mathrm{v}}[J^2 + 3J + 2 - (J^2 + J)] \\ \nu &= \mathrm{c}B_{\mathrm{v}}(2J+2) \\ &= 2\mathrm{c}B_{\mathrm{v}}(J+1) \end{aligned} \tag{331}$$

Thus lines in pure rotational bands are spaced linearly in frequency. Linear, symmetric molecules such as N_2, O_2, and CO_2 have no permanent dipole moments in their ground vibrational states because the center of mass coincides with the center of charge. These molecules therefore have no rotational bands in their ground vibrational state.

The factor of c on the RHS of (331) disappears if we work in wavenumber rather than frequency units. Using $\tilde{\nu} = \nu/\mathrm{c}$ results in

$$\tilde{\nu} = \Delta E_{\mathrm{r}} = 2B_{\mathrm{v}}(J+1) \tag{332}$$

This direct relation between wavenumber and quantum number is one reason spectroscopists prefer to work in wavenumber space.

[14] B_{v} is not to be confused with the Planck function, B_ν.

Table 7: Mechanical Analogues for Radiatively Important Atmospheric Gases[a]

Moments of Inertia	Class	Members
$I_A = 0, I_B = I_C \neq 0$	[b]Linear	$CO_2, N_2O, CO, NO, HF, HCl, HBr, HI, OCS$
$I_A \neq 0, I_B = I_C \neq 0$	Symmetric top	$CFCl_3, NH_3, CH_3Cl, C_2H_6, SF_6$
$I_A = I_B = I_C$	Spherical top	CH_4
$I_A \neq I_B \neq I_C$	Asymmetric top	$H_2O, O_3, SO_2, NO_2, HNO_3$

[a]Based on Goody and Yung (1989), p. 81, Rothman et al. (1998)
[b]Diatomic molecules and linear polyatomic molecules with integer J

5.1.1 Vibrational Transitions

A molecule composed of N atoms has K vibrational modes where

$$K = \begin{cases} 3N-3 & : \text{ Non-linear molecules} \\ 3N-2 & : \text{ Linear molecules} \end{cases} \tag{333}$$

Often modes are degenerate, and so have fewer distinct vibrational quantum numbers than indicated by (333). As shown in Table 7, linear molecules include all diatomic molecules (CO, NO, OH), as well as CO_2 and N_2O. Non-linear molecules include H_2O, O_3, CH_4, and $CFCl_3$.

The equation of motion for the position $\mathbf{r}$ of a classical oscillator of mass M oscillating with restoring force β is

$$\begin{aligned} M\frac{\mathrm{d}^2\mathbf{r}}{\mathrm{d}t^2} &= -\beta\mathbf{r} \\ \ddot{\mathbf{r}} + \frac{\beta}{M} &= 0 \\ \mathbf{r} &= A\sin\omega t + B\cos\omega t \\ \omega &= 2\pi\nu = \sqrt{\frac{\beta}{M}} \\ \nu &= \frac{1}{2\pi}\sqrt{\frac{\beta}{M}} \end{aligned} \tag{334}$$

where β is the constant of the linear restoring force, known as the spring constant or the bond strength. Since β is the restoring force divided by the displacement distance, its SI units are $\mathrm{N\,m^{-1}}$ (Newtons per meter) and its CGS units are $\mathrm{dyn\,cm^{-1}}$ (dynes per centimeter). The spring constant β depends only on the total particle mass, not on the mass distribution within the particle. The solution to a two particle sysytem where particle equilibrium separation is $\mathbf{r}$ is identical to (334) with the mass M replaced by the reduced mass $\tilde{M}$ (323)

$$\nu = \frac{1}{2\pi}\sqrt{\frac{\beta(M_1+M_2)}{M_1M_2}} \tag{335}$$

The bond strength β depends on the exact arrangement of nuclei within a molecule. For diatomic molecules β approximately fits the following progression: Single bond, double bond, and triple bond diatomic molecules have β of approximately 500, 1000, and 1500 $\mathrm{N\,m^{-1}}$(5×10^5, 10×10^5, and $15\times10^5\,\mathrm{dyn\,cm^{-1}}$) respectively.

Let us consider the aborption spectrum due to stretching of the carbon monoxide molecule. CO is approximately a triply bonded diatomic molecule with a bond strength of about $1900\,\mathrm{N\,m^{-1}}$. We will use (335) to predict the fundamental frequency ν_{CO} of the absorption spectrum. We shall include the details of the calculation to demonstrate the equivalence of the results obtained using SI and CGS units.

$$\begin{aligned}
\nu_{\mathrm{CO}} &\approx \frac{1}{2\pi}\sqrt{\frac{1900\,\mathrm{N\,m^{-1}}\times(12.0\times10^{-3}+16.0\times10^{-3})\,\mathrm{kg\,mol^{-1}}}{12.0\times10^{-3}\,\mathrm{kg\,mol^{-1}}\times16.0\times10^{-3}\,\mathrm{kg\,mol^{-1}}}} \\
&\approx \frac{1}{6.28}\sqrt{\frac{53.2\,\mathrm{N\,m^{-1}}}{192\times10^{-6}\,\mathrm{kg\,mol^{-1}}}} \approx 0.160\sqrt{2.77\times10^5\frac{\mathrm{kg\ m}}{\mathrm{s^2}}\times\frac{1}{\mathrm{m}}\times\frac{\mathcal{N}}{\mathrm{kg}}} \\
\nu_{\mathrm{CO}} &\approx 84.2\sqrt{\frac{1}{\mathrm{s^2}}\times\frac{6.02\times10^{23}}{1}} \approx 65.3\times10^{12}\,\mathrm{s^{-1}} = 65.3\,\mathrm{THz} \\
\lambda_{\mathrm{CO}} &= \frac{\mathrm{c}}{\nu_{\mathrm{CO}}} \approx \frac{3.00\times10^8\,\mathrm{m\,s^{-1}}}{65.3\times10^{12}\,\mathrm{s^{-1}}} = 4.59\times10^{-6}\,\mathrm{m} = 4.59\,\mu\mathrm{m} \\
\tilde{\nu}_{\mathrm{CO}} &= \frac{\nu_{\mathrm{CO}}}{100\mathrm{c}} \approx \frac{65.3\times10^{12}\,\mathrm{s^{-1}}}{100\,\mathrm{cm\,m^{-1}}\times3.00\times10^8\,\mathrm{m\,s^{-1}}} \approx 2182\,\mathrm{cm^{-1}}
\end{aligned} \tag{336}$$

The conversion of ν_{CO} to $\tilde{\nu}_{\mathrm{CO}}$ and λ_{CO} is straightforward, and shows that the stretching mode of the CO molecule produces an absorption spectrum in the infrared. For pedagogical reasons, let us repeat the derivation of ν_{CO} using CGS units to demonstrate that neither system is clearly superior in terms of its simplicity or ease of manipulation.

$$\begin{aligned}
\nu_{\mathrm{CO}} &\approx \frac{1}{2\pi}\sqrt{\frac{1.9\times10^6\,\mathrm{dyn\,cm^{-1}}\times(12.0+16.0)\,\mathrm{g\,mol^{-1}}}{12.0\,\mathrm{g\,mol^{-1}}\times16.0\,\mathrm{g\,mol^{-1}}}} \\
&\approx \frac{1}{6.28}\sqrt{\frac{53.2\times10^6\,\mathrm{dyn\,cm^{-1}}}{192\,\mathrm{g\,mol^{-1}}}} \approx 0.160\sqrt{27.7\times10^4\frac{\mathrm{g\,cm}}{\mathrm{s^2}}\times\frac{1}{\mathrm{cm}}\times\frac{\mathcal{N}}{\mathrm{g}}}
\end{aligned}$$

and the rest of the computation is identical to (336). It appears that CGS units, historically the system of choice for radiative transfer, are slightly more simple to work with than SI units because of the CGS-centric definition of atomic weights. However, in this era of automated computations, the slight advantage of CGS does not appear to outweigh the usefulness of consistently using SI units (336). All other things being equal, we recommend using SI units wherever practical in radiative transfer, a convention we follow in this text.

The vibrational energy of a quantum harmonic oscillator is

$$E_{\mathrm{v}} = \sum_{k=1}^{K}\mathrm{h}\nu_k(v_k+\tfrac{1}{2}) \tag{337}$$

where ν_k is the frequency of the kth mode, $\mathrm{h}\nu_k$ is the vibrational constant of the mode, and v_k is the vibrational quantum number of the mode. Like other quantum numbers, v

is an integer $v \in [0, 1, 2, \ldots]$. The term of $\frac{1}{2}$ in (337) is called the zero-point energy. The vibrational ground state of a molecule is reached when $v_k = 0$ for all K vibrational modes. The linear relation between v_k and E_v (337) is an approximation. In reality anharmonicities cause oscillations to deviate from linear behavior. This causes vibrational energy levels to become more closely spaced as v_k increases.

Allowed transitions must match applicable selection rules. The selection rule for vibrational transitions is

$$\Delta v \;=\; v' \pm v'' = \pm 1 \tag{338}$$

The fundamental transition refers to transitions between the first excited state ($v = 1$) and the vibrational ground state ($v = 0$). Using $\Delta v = \pm 1$ in (337) leads to

$$\begin{aligned} \Delta E_\mathrm{v} &= \mathrm{h}\nu_k(v + 1 + \tfrac{1}{2}) - \mathrm{h}\nu_k(v + \tfrac{1}{2}) \\ &= \mathrm{h}[\nu_k(v + \tfrac{3}{2}) - \nu_k(v + \tfrac{1}{2})] \\ &= \mathrm{h}\nu_k \end{aligned} \tag{339}$$

For simpler molecules such as diatomic molecules, the relation between the type of vibrational mode k (e.g., stretching, bending) and the fundamental energy of the mode (339) may depend on only a few parameters.

5.1.2 Isotopic Lines

The quantum mechanical analogue of (334) is

$$\nu_k \;=\; \frac{1}{2\pi}\sqrt{\frac{\beta}{\tilde{M}}} \tag{340}$$

where now β is the force constant of vibrational mode k which depends on the distribution of charge in the molecule but is completely independent of the mass distribution, and thus independent of isotope. Two distinct isotopes i and j of the same species will thus have differing equilibrium frequencies ν_i and ν_j for the same vibrational mode:

$$\frac{\nu_i}{\nu_j} \;=\; \sqrt{\frac{\tilde{M}_j}{\tilde{M}_i}} \tag{341}$$

For instance, the frequency shift for $^{13}\mathrm{C}^{16}\mathrm{O}$ relative to the $2140\,\mathrm{cm}^{-1}$ band of $^{12}\mathrm{C}^{16}\mathrm{O}$ is $47.7\,\mathrm{cm}^{-1}$.

5.1.3 Combination Bands

Transition selection rules for many important molecules (including all diatomic molecules), require that $\Delta v \neq 0$ and $\Delta J \neq 0$, i.e., vibrational transitions must occur simultaneously with rotational transitions. Thus simultaneous transitions of both vibrational and rotational states are the norm, not the exception, in the atmosphere. These simultaneous transitions

form what are called combination bands or vibration-rotation bands. The energy of such transitions is obtained by subtracting the lower energy state from the upper energy state

$$\tilde{\nu}_R = \tilde{\nu}_k + B'_{\rm v} J'(J'+1) - B''_{\rm v} J''(J''+1) J^2 \tag{342}$$

where $\tilde{\nu}_k$ is the energy of the pure vibrational transition (337). We have not cancelled like terms, as in the idealized case of (331), since $B'_{\rm v} \neq B''_{\rm v}$ in combination bands. Substituting $\Delta J = \pm 1$ into (342) leads to the energy spacings between the R-branch transitions and the P-branch transitions, respectively.

$$\tilde{\nu}_R = \tilde{\nu}_k + 2B'_{\rm v} + (3B'_{\rm v} - B''_{\rm v})J + (B'_{\rm v} - B''_{\rm v})J^2 \tag{343}$$

$$\tilde{\nu}_P = \tilde{\nu}_k - (B'_{\rm v} + B''_{\rm v})J + (B'_{\rm v} - B''_{\rm v})J^2 \tag{344}$$

There may be a number of absorption bands in addition to the fundamental bands of a molecule. These include overtone bands, combination bands, vibration-rotation bands, and harmonic coupling bands. Overtone bands occur at frequencies which are multiples of the fundamental frequencies. Combination bands are due to the interaction of two fundamental vibration bands. The combined frequency …Vibration-rotation bands have already been discussed. Harmonic coupling bands occur when interactions among closely spaced oscillation frequencies produces distinct, unexpected bands. This is relatively uncommon.

5.2 Partition Functions

The statistical weight g measures the number of available states in a given quantum configuration. Quantum theory teaches us that rotational energy levels are $2J+1$ degenerate owing to $2J+1$ indistinguishable orientations of the component of angular momentum in a fixed direction in space. The statistical weight for rotational levels is therefore

$$g_{\rm r} = 2J + 1 \tag{345}$$

In LTE, rotational states are populated according to Boltzmann statistics, so that the probability of occupancy is proportional to $\mathrm{e}^{-E_{\rm r}/{\rm k}T}$. At temperature T, the ratio of molecules in state J' to those in state J'' is therefore

$$\begin{aligned} \frac{N(J')}{N(J'')} &\equiv \frac{g_{J'}}{g_{J''}} \frac{\mathrm{e}^{-E_{\rm r}(J')/{\rm k}T}}{\mathrm{e}^{-E_{\rm r}(J'')/{\rm k}T}} \\ &= \frac{2J'+1}{2J''+1} \exp\left\{ -\frac{{\rm hc}B_{\rm v}}{{\rm k}T} [J'(J'+1) - J''(J''+1)] \right\} \end{aligned} \tag{346}$$

where now J' and J'' refer to any values of J, not just those satisfying selection rules. To examine the fractional abundance of molecules in state J relative to those in all other rotational states, we must sum (346) over all J'' while holding $J' = J$ fixed. This leads to

$$\frac{N(J)}{N} = \frac{2J+1}{Q_{\rm r}} \exp\left[-\frac{{\rm hc}B_{\rm v}}{{\rm k}T} J(J+1) \right] \tag{347}$$

where we have defined the rotational partition function $Q_{\rm r}$ as the total, probability-weighted number of available rotation states in the system

$$Q_{\rm r} = \sum_{J=1}^{\infty}(2J+1)\exp\left[-\frac{{\rm hc}B_{\rm v}}{{\rm k}T}J(J+1)\right] \tag{348}$$

For atmospheric cases of interest, ${\rm k}T \gg {\rm hc}B_{\rm v}$ so the exponential term becomes vanishingly small. To express and evaluate (348) as an integral, we make a change of variables

$$\begin{aligned} x &= \frac{{\rm hc}B_{\rm v}}{{\rm k}T}J(J+1) \\ {\rm d}x &= \frac{{\rm hc}B_{\rm v}}{{\rm k}T}(2J+1){\rm d}J \\ (2J+1){\rm d}J &= \frac{{\rm k}T}{{\rm hc}B_{\rm v}}{\rm d}x \end{aligned} \tag{349}$$

This maps $J \in [0,\infty)$ to $x \in [0,\infty)$. Thus x is considered a continuous function of J. Substituting (349) into (348) results in

$$\begin{aligned} Q_{\rm r} &\approx \int_0^{\infty}(2J+1)\exp\left[-\frac{{\rm hc}B_{\rm v}}{{\rm k}T}J(J+1)\right]\,{\rm d}J \\ &= \int_0^{\infty}\frac{{\rm k}T}{{\rm hc}B_{\rm v}}{\rm e}^{-x}\,{\rm d}x \\ &= \frac{{\rm k}T}{{\rm hc}B_{\rm v}}\left[-{\rm e}^{-x}\right]_0^{\infty} \\ &= \frac{{\rm k}T}{{\rm hc}B_{\rm v}}[-0-(-1)] \\ &= \frac{{\rm k}T}{{\rm hc}B_{\rm v}} \end{aligned} \tag{350}$$

Substituting (350) into (347) we obtain

$$\frac{N(J)}{N} = \frac{{\rm hc}B_{\rm v}(2J+1)}{{\rm k}T}\exp\left[-\frac{{\rm hc}B_{\rm v}}{{\rm k}T}J(J+1)\right] \tag{351}$$

Examination of (351) shows that $N(J)/N$ is small for $J \to 0$ and for $J \to \infty$ and maximal in between. The derivation of (351) neglected any vibrational-dependence of $B_{\rm v}$.

The vibrational partition function $Q_{\rm v}$ is defined by a procedure analogous to (346)–(350). Contrary to rotational states (345), vibrational states all have equal statistical weights

$$g_{\rm v} = g_0 \tag{352}$$

In LTE, Boltzmann's Law, (352) and (337) lead to

$$\begin{aligned} \frac{N(v')}{N(v'')} &\equiv \frac{g_{v'}}{g_{v''}}\frac{{\rm e}^{-E_{\rm v}(v')/{\rm k}T}}{{\rm e}^{-E_{\rm v}(v'')/{\rm k}T}} \\ &= \frac{g_0}{g_0}\exp\left\{-\left[\frac{{\rm h}\nu_0(v'+\frac{1}{2})}{{\rm k}T}-\frac{{\rm h}\nu_0(v''+\frac{1}{2})}{{\rm k}T}\right]\right\} \\ &= \exp\left[-\frac{{\rm h}\nu_0}{{\rm k}T}(v'-v'')\right] \end{aligned} \tag{353}$$

Notice that the statistical weight and the zero-point energy contribution of $\mathrm{h}\nu_0/2$ factor out of the relative abundance of molecules in a given vibrational level (353). Nevertheless, the zero-point energy does contribute to the total internal energy of the system and so is properly included in the definition of the vibrational partition function Q_v

$$\begin{aligned} Q_\mathrm{v} &= \sum_{v=0}^{\infty} \exp\left[-\frac{\mathrm{h}\nu_0}{\mathrm{k}T}(v+\tfrac{1}{2})\right] \\ &= \mathrm{e}^{-\mathrm{h}\nu_0/2\mathrm{k}T} \sum_{v=0}^{\infty} \left(\mathrm{e}^{-\mathrm{h}\nu_0/\mathrm{k}T}\right)^v \\ &= \frac{\mathrm{e}^{-\mathrm{h}\nu_0/2\mathrm{k}T}}{1-\mathrm{e}^{-\mathrm{h}\nu_0/\mathrm{k}T}} \end{aligned} \tag{354}$$

where in the last step we used the solution for an infinite geometric series whose ratio between terms $r < 1$,

$$\sum_{n=0}^{\infty} a_0 r^n = \frac{a_0}{1-r} \tag{355}$$

The fractional abundance of molecules in vibrational state v is thus

$$\begin{aligned} \frac{N(v)}{N} &= \frac{1}{Q_\mathrm{v}} \exp\left[-\frac{\mathrm{h}\nu_0}{\mathrm{k}T}(v+\tfrac{1}{2})\right] \\ &= \frac{1-\mathrm{e}^{-\mathrm{h}\nu_0/\mathrm{k}T}}{\mathrm{e}^{-\mathrm{h}\nu_0/2\mathrm{k}T}} \mathrm{e}^{-\mathrm{h}\nu_0/2\mathrm{k}T} \mathrm{e}^{-v\mathrm{h}\nu_0/\mathrm{k}T} \\ &= (1-\mathrm{e}^{-\mathrm{h}\nu_0/\mathrm{k}T}) \mathrm{e}^{-v\mathrm{h}\nu_0/\mathrm{k}T} \end{aligned} \tag{356}$$

Vibrational levels are so widely spaced that most molecules in the lower atmosphere are in $v = 0$ or $v = 1$ states.

It is common to approximate the total internal partition function of atmospheric transitions Q as the product of the vibrational and the rotational partition functions. Using (354) and (350) we obtain

$$\begin{aligned} Q &\approx Q_\mathrm{v} Q_\mathrm{r} \\ &\approx \frac{\mathrm{e}^{-\mathrm{h}\nu_0/2\mathrm{k}T}}{1-\mathrm{e}^{-\mathrm{h}\nu_0/\mathrm{k}T}} \frac{\mathrm{k}T}{\mathrm{hc}B_\mathrm{v}} \end{aligned}$$

In the high temperature limit where $\mathrm{k}T \gg \mathrm{h}\nu_0$ then we may use the behavior $\mathrm{e}^{-x} \approx 1 - x$ so this becomes

$$\begin{aligned} Q &\approx \frac{1-\frac{\mathrm{h}\nu_0}{2\mathrm{k}T}}{1-1+\frac{\mathrm{h}\nu_0}{\mathrm{k}T}} \frac{\mathrm{k}T}{\mathrm{hc}B_\mathrm{v}} \\ &\approx \frac{\frac{2\mathrm{k}T-\mathrm{h}\nu_0}{2\mathrm{k}T}}{\frac{\mathrm{h}\nu_0}{\mathrm{k}T}} \frac{\mathrm{k}T}{\mathrm{hc}B_\mathrm{v}} \\ &\approx \frac{2\mathrm{k}T-\mathrm{h}\nu_0}{2\mathrm{h}\nu_0} \frac{\mathrm{k}T}{\mathrm{hc}B_\mathrm{v}} \end{aligned}$$

5.3 Dipole Radiation

The probability $\mathcal{P}_{if}$ of absorption of a photon leading to a change in molecular state from state i to state f is

$$\mathcal{P}_{if} = t\left(\frac{\mathrm{e}^2}{\mathrm{hc}^3 m_\mathrm{e}^2}\right)\sum_{\alpha=1}^{2}\oint\left[\omega\mathcal{N}_\alpha(\mathbf{k})|\langle\psi_f|\mathrm{e}^{\mathrm{i}\mathbf{k}\cdot r}\mathbf{e}_\alpha(\hat{\mathbf{k}})\cdot\mathbf{p}|\psi_i\rangle|^2\right]_{fi}\mathrm{d}\Omega \tag{357}$$

The matrix element $\langle\psi_f|\mathrm{e}^{\mathrm{i}\mathbf{k}\cdot r}\mathbf{e}_\alpha(\hat{\mathbf{k}})\cdot\mathbf{p}|\psi_i\rangle$ determines the absorption probability. The dipole approximation retains only the first term in the expansion

$$\mathrm{e}^{\mathrm{i}\mathbf{k}\cdot r} = 1 + \mathrm{i}\mathbf{k}\cdot r + \cdots$$

so that the matrix element simplifies to

$$\langle\psi_f|\mathrm{e}^{\mathrm{i}\mathbf{k}\cdot r}\mathbf{e}_\alpha(\hat{\mathbf{k}})\cdot\mathbf{p}|\psi_i\rangle = \mathbf{e}_\alpha\cdot\langle\psi_f|\mathbf{p}|\psi_i\rangle \tag{358}$$

This matrix element is related to the line strength S as follows (Rothman et al., 1998, p. 709)....

5.4 Two Level Atom

Einstein created an elegant paradigm for analyzing the interaction of matter and radiation. His tool is called the two level atom. It consists of an ensemble of molecules with two discrete energy levels, E_1 and $E_2 > E_1$. The energy levels have statistical weights g_1 and g_2, respectively. There are n_1 molecules per unit volume in the state with E_1, and n_2 in the state with E_2. The frequency of transition between the two levels is $\mathrm{h}\nu_0 = E_2 - E_1$.

The five processes by which an idealized two-level molecule may change state are

$$\mathrm{n}_2 \xrightarrow{\mathrm{A}_{21}} \mathrm{n}_1 + \mathrm{h}\nu_0 \tag{359}$$

$$\mathrm{n}_1 + \mathrm{h}\nu_0 \xrightarrow{\mathrm{B}_{12}} \mathrm{n}_2 \tag{360}$$

$$\mathrm{n}_2 + \mathrm{h}\nu_0 \xrightarrow{\mathrm{B}_{21}} \mathrm{n}_1 + 2\mathrm{h}\nu_0 \tag{361}$$

$$\mathrm{n}_2 + \mathrm{M} + \mathrm{KE} \xrightarrow{\mathrm{C}_{21}} \mathrm{n}_1 + \mathrm{M} + \mathrm{KE}' + \mathrm{h}\nu_0 \tag{362}$$

$$\mathrm{n}_1 + \mathrm{M} + \mathrm{KE} \xrightarrow{\mathrm{C}_{12}} \mathrm{n}_2 + \mathrm{M} + \mathrm{KE}' \tag{363}$$

where M is a collision partner and KE and KE′ represent the kinetic energy of the two molecule system before and after the collision, respectively. The most frequent collision partners are, naturally, nitrogen and oxygen molecules.

The Einstein coefficient $A_{21}\,\mathrm{s}^{-1}$ is the transition probability per unit time for spontaneous emission. Spontaneous emission, as its name implies, requires no external stimulus. Thus decay of excited molecules occurs even in the absence of a radiation field. Each emission reduces the population of excited molecules and increases the population of ground state molecules by one. Hence

$$\frac{\mathrm{d}n_1}{\mathrm{d}t} = A_{21}n_2 \tag{364}$$

The Einstein coefficient B_{12} determines the rate of radiative absorption. B_{12} is also called the Einstein coefficient for stimulated absorption. More specifically, B_{12} is the proportionality constant between the mean intensity of the radiation field $\bar{I}_\nu$ and the probability per unit time of an absorption occuring. The transition probability per unit time for radiative absorption is $B_{12}\bar{I}_\nu$. B_{12} has units of $[\mathrm{s}^{-1}(\mathrm{W\,m^{-2}\,sr^{-1}\,Hz^{-1}})^{-1}]$. The rate of radiative absorptions per unit time per unit volume is

$$\begin{aligned}\frac{\mathrm{d}n_2}{\mathrm{d}t} &= n_1 \int_0^\infty \int_\Omega \alpha(\nu)\frac{I_\nu}{\mathrm{h}\nu}\,\mathrm{d}\Omega\,\mathrm{d}\nu \\ &= 4\pi n_1 \int_0^\infty \alpha(\nu)\frac{\bar{I}_\nu}{\mathrm{h}\nu}\,\mathrm{d}\nu \end{aligned} \tag{365}$$

where $\alpha(\nu)$ refers to absorption cross-section of the single transition available in the two-level atom. Comparing the final two expressions we see that

$$B_{12} = \frac{4\pi\alpha(\nu)}{\mathrm{h}\nu\Phi(\nu)} \tag{366}$$

B_{12} is intimately related to the line strength S of the molecular transition (Rothman et al., 1998, p. 709). In particular, B_{12} may be expressed in terms of the weighted transition-moment squared.

The Einstein coefficient B_{21} determines the rate of stimulated emission or induced emission. $B_{21}\bar{I}_\nu$ is transition probability per unit time for stimulated emission. B_{21} has the same dimensions as B_{12}.

$$\begin{aligned}\frac{\mathrm{d}n_1}{\mathrm{d}t} &= n_2 \int_0^\infty \int_\Omega \alpha^{\mathrm{s}}(\nu)\frac{I_\nu}{\mathrm{h}\nu}\,\mathrm{d}\Omega\,\mathrm{d}\nu \\ &= 4\pi n_2 \int_0^\infty \alpha^{\mathrm{s}}(\nu)\frac{\bar{I}_\nu}{\mathrm{h}\nu}\,\mathrm{d}\nu \end{aligned} \tag{367}$$

where $\alpha^{\mathrm{s}}(\nu)$ is the absorption cross-section for stimulated emission.

Gaseous absorption cross-sections $\alpha(\nu)$ are extremely narrow and so the integrals over frequency domain in (365) and (367) are determined by a small range of frequencies about ν_0, the line center frequency. Exact descriptions of line broadening about ν_0 are discussed in §4.1.2–§4.1.5. It is instructive to ignore the details of the finite shape of line transitions for now and to assume the line absorption cross section behaves as a delta-function with integrated cross section a_{12}

$$\alpha(\nu) \approx a_{12}\delta(\nu-\nu_0) \tag{368}$$

$$a_{12} = \frac{\pi \mathrm{e}^2}{m_\mathrm{e}\mathrm{c}} \tag{369}$$

where m_e is the electron rest mass, e is the electron charge, and f is the oscillator strength of the transition. With these definitions.

In thermodynamic equilibrium the number of transitions from state 1 to state 2 per unit time per unit volume equals the number of transitions from state 2 to state 1 per unit time

Table 8: HITRAN database[ab]

This Text	HITRAN	Description
$S_{i,0}$	$S_{\eta\eta'}$	Line strength
$\alpha_{i,0}$	γ_{air}	Pressure-broadened HWHM
	γ_{self}	Self-broadened HWHM
$\tilde{\nu}_0$	$\nu_{\eta\eta'}$	Transition frequency
$\tilde{\nu}_i''$	E_ν	Lower state energy
n	n	Exponent in temperature-dependence of pressure-broadened halfwidth
δ	δ	Air-broadened pressure shift of transition frequency $\tilde{\nu}_0$
$\tilde{\nu}$	ν	Frequency in wavenumbers

[a]Equivalance between symbols employed in this work and those used by Rothman et al. (1998), Appendix A.

[b]HITRAN data are tabulated at a temperature T_0 and pressure p_0 of 296 K and 101325.0 Pa, respectively.

per unit volume. Combining (364), (365), and (367) we obtain

$$\begin{aligned} \frac{\mathrm{d}n_1}{\mathrm{d}t} &= \frac{\mathrm{d}n_2}{\mathrm{d}t} \\ n_1 B_{12} \bar{I}_\nu &= n_2 A_{21} + n_2 B_{21} \bar{I}_\nu \end{aligned} \tag{370}$$

5.5 Line Strengths

We repeat the definition of line strength (272) for convenience

$$S = \int_0^\infty \alpha(\nu)\, \mathrm{d}\nu \tag{371}$$

In practice, (371) is either measured in the laboratory or predicted from ab initio methods.

5.5.1 HITRAN

The HITRAN ("high-resolution transmission") database provides the parameters required to computed absorption coefficients for all atmospheric transitions of interest. The HITRAN database is defined by Rothman et al. (1998), and its usage is defined in their Appendix A.

The idiosyncratic units of line parameters can be confusing. Most HITRAN data are provided in CGS units. For reference, Table 8 presents the equivalence between the symbols used in Rothman et al. (1998), their Appendix A, and our symbols.

The line strength $S_{i,0}$ (272) is tabulated in HITRAN in CGS units of wavenumbers times centimeter squared per molecule, $\mathrm{cm}^{-1}\,\mathrm{cm}^2\,\mathrm{molecule}^{-1}$, often written $\mathrm{cm\,atm}^{-1}$. Line strengths for weak lines can be less than $10^{-36}\,\mathrm{cm}^{-1}\,\mathrm{cm}^2\,\mathrm{molecule}^{-1}$, i.e., unrepresentable as IEEE single precision (4 byte) floating point numbers. Thus it is more robust to work with

$S_{i,0}$ units of per mole (rather than per molecule) in applications where using IEEE double precision (8 byte) floating point numbers is not an option either due to memory limitations or computational overhead. Following are the conversions from the tabulated values of $S_{i,0}$ in $\mathrm{cm^{-1}\,cm^2\,molecule^{-1}}$ to more useful units, including $\mathrm{cm^{-1}\,m^2\,molecule^{-1}}$, $\mathrm{cm^{-1}\,m^2\,mol^{-1}}$, and to fully SI units of $\mathrm{Hz\,m^2\,mol^{-1}}$ and $\mathrm{m\,m^2\,mol^{-1}}$.

$$S_{i,0}[\mathrm{cm^{-1}\,m^2\,molecule^{-1}}] = S_{i,0}[\mathrm{cm^{-1}\,cm^2\,molecule^{-1}}] \times 10^{-4} \tag{372a}$$

$$S_{i,0}[\mathrm{cm^{-1}\,m^2\,mol^{-1}}] = S_{i,0}[\mathrm{cm^{-1}\,cm^2\,molecule^{-1}}] \times 10^{-4} \times \mathcal{N} \tag{372b}$$

$$S_{i,0}[\mathrm{Hz\,m^2\,mol^{-1}}] = S_{i,0}[\mathrm{cm^{-1}\,cm^2\,molecule^{-1}}] \times 10^{-4} \times 100\mathrm{c} \times \mathcal{N} \tag{372c}$$

$$S_{i,0}[\mathrm{m\,m^2\,mol^{-1}}] = S_{i,0}[\mathrm{cm^{-1}\,cm^2\,molecule^{-1}}] \times 10^{-4} \times 100\lambda^2 \times \mathcal{N} \tag{372d}$$

where $\mathcal{N}$ is Avagadro's number. Equation (372d) is uncertain.

The energy of the lower state of each transition, E_i'', is required to determine the relative population of that state available for transitions. HITRAN supplies this energy in wavenumber units in the tabulated parameter $\tilde{\nu}_i''$ which is simply related to E_i'' by

$$E_i'' = \mathrm{hc}\tilde{\nu}_i'' \tag{373}$$

Of course, consistent with HITRAN and spectroscopic conventions, $\tilde{\nu}_i''$ is archived in CGS, $\mathrm{cm^{-1}}$.

All HITRAN data have been scaled from the conditions of the experiment to a temperature and pressure of 296 K and 1013.25 mb, respectively. Thus line strengths must typically be scaled from HITRAN-standard conditions, $S_{i,0}(\mathrm{T_0})$, to the atmospheric conditions of interest, $S_i(T)$.

$$S_i(T) = S_{i,0}(\mathrm{T_0}) \frac{Q(\mathrm{T_0})}{Q(T)} \frac{\mathrm{e}^{-\mathrm{hc}\tilde{\nu}_i/\mathrm{kT}}}{\mathrm{e}^{-\mathrm{hc}\tilde{\nu}_i/\mathrm{kT_0}}} \frac{1-\mathrm{e}^{-\mathrm{hc}\tilde{\nu}_{ij}/\mathrm{kT}}}{1-\mathrm{e}^{-\mathrm{hc}\tilde{\nu}_{ij}/\mathrm{kT_0}}} \tag{374}$$

where Q is the total internal partition function. The second, third and fourth factors on the RHS of (374) are the temperature-dependent scalings of, respectively, the total partition function, the Boltzmann factor for the lower state, and the stimulated emission factor. The scaling presented in (374) is general and contains no approximation.

The classical approximation (Rogers and Yau, 1989; Thomas and Stamnes, 1999) assumes that Q is the product of the rotational and the vibrational partition functions

$$Q(T) \approx Q_\mathrm{v}(T) Q_\mathrm{r}(T) \tag{375}$$

In this approximation, Q_v (354) and Q_r (350) are treated as independent components of Q. This allows Q to be computed as discussed in §5.2. Most high precision calculation improve this approach by using more exact methods described in Gamache et al. (1990) and Gamache et al. (2000).

For many applications, a simplified version of (374) is employed

$$\begin{aligned} S_i(T) &= S_{i,0}(\mathrm{T_0}) \left(\frac{\mathrm{T_0}}{T}\right)^m \exp\left[-\frac{E_i''}{\mathrm{k}}\left(\frac{1}{T}-\frac{1}{\mathrm{T_0}}\right)\right] \\ &= S_{i,0}(\mathrm{T_0}) \left(\frac{\mathrm{T_0}}{T}\right)^m \exp\left[\frac{E_i''}{\mathrm{k}}\left(\frac{1}{\mathrm{T_0}}-\frac{1}{T}\right)\right] \end{aligned} \tag{376}$$

where m is an empirical parameter of order unity and The parameterization (376) incorporates the temperature dependence of both partition functions and the stimulated emission factor into the single factor $(\mathrm{T}_0/T)^m$. The exact temperature dependence of Boltzmann factors is retained. If the parameter m is available, use of (376) offers decreased computational overhead relative to (374).

Pressure-broadened halfwidths $\alpha_{p,0}$ are also provided at the reference temperature and pressure, $\alpha_{p,0} \equiv \alpha_p(\mathrm{p}_0, \mathrm{T}_0)$. HITRAN literature refers to broadening features are as air-broadened (rather than pressure-broadened) because all parameters in the HITRAN database are normalized to Earth's natural isotopic mixing ratios. Thus while the broadening process is collision-broadening, the tabulated line width refers to collision-broadening by air of Earth's isotopic composition, hence the label. HITRAN actually provides two halfwidths, the self-broadened halfwidth $\alpha_{\mathrm{s},0}$ and the air-broadened or foreign-broadened halfwidth $\alpha_{\mathrm{f},0}$. Air-broadening accounts for collision-broadening by foreign molecules, i.e., all molecules except the species undergoing radiative transition. Thus air-broadening is, to a good approximation, due nitrogen and oxygen molecules. The other form of broadening, self-broadening refers to collision-broadening by molecules of the species undergoing the radiative transition. Because reasonances may develop between members of identical species, in general $\alpha_{\mathrm{s},0} \neq \alpha_{\mathrm{f},0}$. The pressure-broadened halfwidth of transitions of radiatively active species A at arbitrary pressure and temperature scales as

$$\alpha_p(p,T) = \left(\frac{\mathrm{T}_0}{T}\right)^n \left(\frac{p-p_\mathrm{A}}{\mathrm{p}_0}\alpha_{\mathrm{f},0} + \frac{p_\mathrm{A}}{\mathrm{p}_0}\alpha_{\mathrm{s},0}\right) \tag{377}$$

where n is an empirical fitting parameter supplied by HITRAN and p_A is the partial pressure of species A. Clearly self-broadening effects are appreciable only for species with signifcant partial pressures, i.e., O_2 and N_2. For minor trace gases, $p_\mathrm{A} \ll p$ and $p_\mathrm{A} \ll \mathrm{p}_0$ so $p - p_\mathrm{A} \approx p$ and $p_\mathrm{A}/\mathrm{p}_0 \approx 0$. For such gases, (377) simplifies to

$$\alpha(p,T) \approx \alpha_0 \frac{p}{\mathrm{p}_0}\left(\frac{\mathrm{T}_0}{T}\right)^n \tag{378}$$

which has no dependence on self-broadening.

Collision-broadening may also cause a pressure-shift of the line transition frequency away from the tabulated line center frequency $\tilde{\nu}_0 = \tilde{\nu}(\mathrm{p}_0)$ to a shifted frequency $\tilde{\nu}^* = \tilde{\nu}(p)$. HITRAN supplies a parameter $\delta(\mathrm{p}_0)$ in CGS wavenumbers per atmosphere ($\mathrm{cm}^{-1}\,\mathrm{atm}^{-1}$) with which to calculate the line center frequency change due to pressure-shifting.

$$\tilde{\nu}^*(p) = \tilde{\nu}_0 + \delta(\mathrm{p}_0)\frac{p}{\mathrm{p}_0} \tag{379}$$

The prescriptions for adjusting line centers (379) and half-widths (377) from $(\mathrm{p}_0, \mathrm{T}_0)$ to to arbitrary p and T should be used to determine the corrected line shape profile of each transition considered. In the lower atmosphere, application of (379) and (377) leads to a corrected Lorentzian profile (280)

$$\begin{aligned}
\Phi_\mathrm{L}(\tilde{\nu},\tilde{\nu}_0,p,T) &= \frac{1}{\pi}\frac{\alpha_\mathrm{L}(p,T)}{\{\tilde{\nu}-[\tilde{\nu}_0+p\delta(\mathrm{p}_0)/\mathrm{p}_0]\}^2+\alpha_\mathrm{L}(p,T)^2} \\
\Phi_\mathrm{L}(\nu,\nu_0,p,T) &= \frac{1}{\pi}\frac{\alpha_\mathrm{L}(p,T)}{(\nu-\nu^*)^2+\alpha_\mathrm{L}(p,T)^2}
\end{aligned} \tag{380}$$

Of course this section has only discussed application of HITRAN database parameters to atmospheres in LTE conditions. Application of HITRAN to nonlocal thermodynamic equilibrium conditions is discussed in Gamache and Rothman (1992).

It is necessary to compute statistics of S_i for use in narrow band models (§6). There is no reason not to apply the full approach of (374) when computing these statistics. Certain well-documented narrow band models use more approximate forms appropriate for specific applications. Briegleb (1992) uses

$$S_i(T) \quad = \quad S_{i,0}(\mathrm{T_0}) \left(\frac{\mathrm{T_0}}{T} \right)^{3/2} \frac{\mathrm{e}^{-\mathrm{hc}\tilde{\nu}_i/\mathrm{k}T}}{\mathrm{e}^{-\mathrm{hc}\tilde{\nu}_i/\mathrm{kT_0}}} \frac{1-\mathrm{e}^{-\mathrm{hc}\tilde{\nu}_{ij}/\mathrm{k}T}}{1-\mathrm{e}^{-\mathrm{hc}\tilde{\nu}_{ij}/\mathrm{kT_0}}} \tag{381}$$

which is a hybrid of (374) and (376) with $m = 1.5$.

5.6 Line-By-Line Models

5.6.1 Literature

The classic paper on the water vapor continuum is Clough et al. (1989). Fu and Liou (1992) compare a correlated-k method to line-by-line model results. Ellingson and Wiscombe (1996) describe the a field experiment to directly compared measured and modeled spectral radiances to both band and line-by-line models. Crisp (1997) uses a line-by-line model to determine atmospheric solar absorption. Sparks (1997) presents an economical algorithm for selecting variable wavelength grid resolution such that absorption coefficients may be computed to a given level of accuracy. Mlawer et al. (1997) compare a correlated-k model (rrtm) to the well-known line-by-line model lblrtm. Moncet and Clough (1997) describe a fully scattering line-by-line model. Walden et al. (1997) presents test-case spectra for evaluating line-by-line radiative transfer models in cold and dry atmospheres. Vogelmann et al. (1998) use observations to constrain magnitude of any non-Lorentzian continuum in the near-infrared. Partain et al. (2000) discuss the equivalance theorem. Quine and Drummond (2001) present an algorithm that computes absorption coefficients to a specified error tolerance by using a pre-computed lookup table of where interpolation is appropriate.

6 Band Models

Band models, also called narrow band models, discretize the radiative transfer equation intervals for which the line statistics and the Planck function are relatively constant. The literature describing these models extends back to Goody (1957). Band models have traditionally been applied to thermal source functions (187a)–(187b), but they may also be applied to the solar spectral region (Zender et al., 1997) (MODTRAN3) if additional assumptions are made.

6.1 Generic

The following presentation assumes that the absorption path is homogeneous, i.e., at constant temperature and pressure. Important corrections to these assumptions are necessary in inhomogeneous atmospheres. These corrections are discussed in §6.3.2.

This discussion makes use of an arbitrary frequency interval $\Delta\nu$ which represents the discretization interval of narrow band approximation. It is important to remember that $\Delta\nu$ is best determined empirically by comparison of the narrow band approximation to line-by-line approximations. Typically, $\Delta\nu$ is 5–10 cm^{-1}. Kiehl and Ramanathan (1983) showed $\Delta\nu = 5\,\mathrm{cm}^{-1}$ bands are optimal for CO_2. Briegleb (1992) uses $\Delta\nu = 5\,\mathrm{cm}^{-1}$ for CO_2, O_3, CH_4, N_2O, but $\Delta\nu = 10\,\mathrm{cm}^{-1}$ for H_2O. Kiehl (1997) recommends $\Delta\nu = 5\,\mathrm{cm}^{-1}$ for CO_2, $10\,\mathrm{cm}^{-1}$ for H_2O, 5–10 cm^{-1} for O_3, and $5\,\mathrm{cm}^{-1}$ for all other trace gases.

6.1.1 Beam Transmittance

The gaseous absorption optical depth $\tau_\mathrm{a}(\nu)$ is the product of the spectrally resolved molecular cross-section $\alpha(\nu)$ (535a) and the absorber path U (269)

$$\tau_\mathrm{a}(\nu) \quad = \quad \alpha(\nu)U \tag{382}$$

The transmittance $T(\nu)$ between two points in a homogeneous atmosphere is the negative exponential of $\tau_\mathrm{a}(\nu)$ (182),

$$\begin{aligned} T(\nu) &= \mathrm{e}^{-\tau_\mathrm{a}(\nu)} \\ &= \mathrm{e}^{-\alpha(\nu)U} \end{aligned} \tag{383}$$

Note that $T(\nu)$ is the spectrally and directionally resolved transmittance because (a) it pertains to a monochromatic frequency interval and (b) it applies to radiances, not to irradiances (which require an additional angular integration). Narrow band models are based on the mean transmittance $T_{\Delta\nu}$ of a narrow but finite frequency interval $\Delta\nu$ between $\nu_0 - \Delta\nu/2$ and $\nu_0 + \Delta\nu/2$.

$$\begin{aligned} T_{\Delta\nu} &= \frac{1}{\Delta\nu}\int_{\Delta\nu} T\,\mathrm{d}\nu \\ &= \frac{1}{\Delta\nu}\int_{\Delta\nu} \mathrm{e}^{-\tau_\mathrm{a}}\,\mathrm{d}\nu \end{aligned} \tag{384}$$

where ν_0 is the central frequency of the interval in question

Using (271), we rewrite (384) as

$$T_{\Delta\nu} = \frac{1}{\Delta\nu}\int_{\Delta\nu} \exp[-\alpha(\nu)U]\,\mathrm{d}\nu$$

If the lines are Lorentzian (i.e., pressure-broadened) then the transmittance may be written in terms of the line strength and absorber amount using (273a) and (305)

$$\alpha(\nu)U = \frac{S\alpha_\mathrm{L}U}{\pi(\nu^2 + \alpha_\mathrm{L}^2)} \tag{385}$$

Thus (384) becomes

$$T_{\Delta\nu} = \frac{1}{\Delta\nu}\int_{\Delta\nu} \exp\left[-\frac{S\alpha_\mathrm{L}U}{\pi(\nu^2 + \alpha_\mathrm{L}^2)}\right]\,\mathrm{d}\nu \tag{386}$$

6.1.2 Beam Absorptance

In analogy to T (181) we define the monochromatic beam absorptance $\mathcal{A}$

$$\begin{aligned} \mathcal{A} &= 1 - T \\ &= 1 - \exp[-\alpha(\nu)U] \end{aligned} \tag{387}$$

where $\alpha(\nu)$ is the absorption cross-section and U is the absorber path. As described in §6.1.1, we refer to $\mathcal{A}$ as the beam absorptance becuase it pertains to a monochromatic frequency, and refers to absorption of radiance, not irradiance.

The band absorptance $\mathcal{A}_{\Delta\nu}$ is the complement of the band transmittance

$$\begin{aligned} \mathcal{A}_{\Delta\nu} &= 1 - T_{\Delta\nu} \\ &= \frac{1}{\Delta\nu}\int_{\Delta\nu} \mathcal{A}\,\mathrm{d}\nu \\ &= \frac{1}{\Delta\nu}\int_{\Delta\nu} 1 - \mathrm{e}^{-\tau_\mathrm{a}}\,\mathrm{d}\nu \\ &= \frac{1}{\Delta\nu}\int_{\Delta\nu} 1 - \exp[-\alpha(\nu)U]\,\mathrm{d}\nu \end{aligned} \tag{388}$$

The relation between the band absorptance and band transmittance is the same as the relation between the monochromatic beam absorptance and the monochromatic beam transmittance (387). $\mathcal{A}_{\Delta\nu}$ measures the mean absorptance within a finite frequency (or wavelength) range comprising many lines. $\mathcal{A}_{\Delta\nu}$ does not include any contribution from outside the $\Delta\nu$ range. Thus $\mathcal{A}_{\Delta\nu}$ may neglect contribution from the far wings of some lines in the band. Moreover, it is important to remember that energy absorption follows the band absorptance only if the energy distribution within the band is close to linear.

If the line shape is Lorentzian (280), then (386) applies so that

$$\mathcal{A}_{\Delta\nu} = \frac{1}{\Delta\nu}\int_{\Delta\nu} 1 - \exp\left[-\frac{S\alpha_\mathrm{L}U}{\pi(\nu^2 + \alpha_\mathrm{L}^2)}\right]\,\mathrm{d}\nu \tag{389}$$

6.1.3 Equivalent Width

The spectrally integrated monochromatic beam absorptance of a line is called its equivalent width

$$\begin{aligned} W &= \int_{-\infty}^{+\infty} \mathcal{A}\,\mathrm{d}\nu \\ W(U) &= \int_{-\infty}^{+\infty} 1 - \exp[-\alpha(\nu)U]\,\mathrm{d}\nu \end{aligned} \tag{390}$$

Thus the absorber amount must be specified in order to determine the equivalent width. The lower limit of integration, $-\infty$, is actually an approximation which is mathematically convenient to retain so that (390) is analytically integrable for the important line shape functions. Recall that we are working with a frequency coordinate ν which is defined to be $\nu = 0$ at line center ν_0 (306). In practice the error caused by using the analytic expressions

resulting from $\int_{-\infty}^{+\infty}$ rather than those resulting from $\int_{-\nu_0}^{+\infty}$ is negligible except for lines in the microwave.

The name "equivalent width" reminds us that W is the width of a completely saturated rectangular line profile that has the same total absorptance. The relation between U and $W(U)$ is called the curve of growth. The curve of growth of a gas can be measured in the laboratory. The interpretation of the curve of growth played a very important role in advancing our understanding and representation of gaseous absorption.

If the line shape is Lorentzian (280), then (389) applies

$$W = \int_{-\infty}^{+\infty} 1 - \exp\left[-\frac{S\alpha_{\mathrm{L}}U}{\pi(\nu^2+\alpha_{\mathrm{L}}^2)}\right] \mathrm{d}\nu \tag{391}$$

6.1.4 Mean Absorptance

Although the spectrally resolved absorptance (387) and the band absorptance (388) are dimensionless, the equivalent width (390) has units of frequency (or wavelength). It is convenient to define a dimensionless mean absorptance for a transition line $\bar{\mathcal{A}}$

$$\begin{aligned} \bar{\mathcal{A}} &= \frac{1}{\bar{\delta}} \int_{-\infty}^{+\infty} \mathcal{A}\, \mathrm{d}\nu \\ &= \frac{1}{\bar{\delta}} \int_{-\infty}^{+\infty} 1 - \exp[-\alpha(\nu)U]\, \mathrm{d}\nu \\ &= \frac{W}{\bar{\delta}} \end{aligned} \tag{392}$$

where $\bar{\delta}$ is the mean line spacing between adjacent lines in a given band. Note that $\mathcal{A}_{\Delta\nu}$ (388) differs from $\bar{\mathcal{A}}$ (392). $\bar{\mathcal{A}}$ accounts for the absorptance due to a single line over the entire spectrum and renormalizes that to a mean absorptance within a specified frequency (or wavelength) range ($\bar{\delta}$). In contrast to $\mathcal{A}_{\Delta\nu}$, $\bar{\mathcal{A}}$ does not neglect any absorption in the far wings of a line. Therefore the sum of the average absorptances of all the lines centered within $\Delta\nu$ may exceed, by a small amount, the band absorptance computed from (388)

$$\sum_{i=1}^{i=N} \bar{\mathcal{A}}_i \geq \mathcal{A}_{\Delta\nu} \tag{393}$$

This difference should make it clear that $\bar{\mathcal{A}}$ is much more closely related to W than to $\mathcal{A}_{\Delta\nu}$.

For lines with Lorentzian profiles (280), $\bar{W}$ and $\bar{\mathcal{A}}$ are

$$W = \bar{\mathcal{A}}\bar{\delta} = \int_{-\infty}^{+\infty} 1 - \exp\left[-\frac{S\alpha_{\mathrm{L}}U}{\pi(\nu^2+\alpha_{\mathrm{L}}^2)}\right] \mathrm{d}\nu \tag{394}$$

We shall rewrite (394) in terms of three dimensionless variables, x, y, and u

$$\begin{aligned} x &= \nu/\bar{\delta} && \text{(395a)} \\ \nu &= \bar{\delta}x \\ \mathrm{d}x &= \bar{\delta}^{-1}\,\mathrm{d}\nu \\ \mathrm{d}\nu &= \bar{\delta}\,\mathrm{d}x \\ y &= \alpha_\mathrm{L}/\bar{\delta} && \text{(395b)} \\ \alpha_\mathrm{L} &= \bar{\delta}y \\ u &= \frac{SU}{2\pi\alpha_\mathrm{L}} && \text{(395c)} \\ \frac{SU}{\pi} &= 2\alpha_\mathrm{L}u \end{aligned}$$

This change of variables maps $\nu \in [-\infty, +\infty]$ to $x \in [-\infty, +\infty]$. We obtain

$$\begin{aligned} \bar{A} &= \frac{1}{\bar{\delta}}\int_{-\infty}^{+\infty} 1 - \exp\left[-(2\alpha_\mathrm{L}u)\left(\frac{\alpha_\mathrm{L}}{\bar{\delta}^2x^2 + \bar{\delta}^2y^2}\right)\right]\,(\bar{\delta}\,\mathrm{d}x) \\ &= \int_{-\infty}^{+\infty} 1 - \exp\left[-\frac{2\alpha_\mathrm{L}^2u}{\bar{\delta}^2(x^2+y^2)}\right]\,\mathrm{d}x \\ &= \int_{-\infty}^{+\infty} 1 - \exp\left[-\frac{2\bar{\delta}^2y^2u}{\bar{\delta}^2(x^2+y^2)}\right]\,\mathrm{d}x \\ &= \int_{-\infty}^{+\infty} 1 - \exp\left[-\frac{2uy^2}{x^2+y^2}\right]\,\mathrm{d}x \end{aligned} \qquad \text{(396)}$$

The solution to this definite integral may be written in terms of modified Bessel functions of the first kind $I_\nu(u)$ (see §10.4)

$$\begin{aligned} \bar{A} &= 2\pi yu\mathrm{e}^{-u}[I_0(u) + I_1(u)] \\ &\equiv 2\pi yL(u) \\ &= 2\pi\alpha_\mathrm{L}\bar{\delta}^{-1}L(u) \\ W &= 2\pi\alpha_\mathrm{L}L(u) \end{aligned} \qquad \text{(397)}$$

where $L(u)$ is the Ladenburg and Reiche function (Ladenburg and Reiche, 1913). The dimensionless optical path u (395) is therefore a key parameter in determining the gaseous absorptance. Two important limiting cases of (397) are $u \ll 1$ and $u \gg 1$.

For small optical paths, $SU \ll 1$ (269), or, equivalently, $u \ll 1$ (395c). This is the weak-line limit. In this limit the exponential in (394) or (396) may be replaced by the first two terms in its Taylor series expansion. Thus all line shapes have the same weak-line limit

$$\begin{aligned} W = \bar{A}\bar{\delta} &\approx \int_{-\infty}^{+\infty} \alpha(\nu)U\,\mathrm{d}\nu \\ &\approx SU\int_{-\infty}^{+\infty} \Phi_\mathrm{L}(\nu)\,\mathrm{d}\nu \\ &\approx SU \end{aligned} \qquad \text{(398)}$$

where we have use the generic normalization property of the line shape profile (283) in the final step.

For large optical paths, $SU \gg 1$ (269), or, equivalently, $u \gg 1$ (395c). This is the strong line limit. To examine this limit we first note that the line HWHM is much smaller than the frequencies where line absorptance is strong, i.e., $\alpha_L \ll \nu$ in (394). Equivalently, $y \ll x$ (395a)–(395b) so that y^2 may be neglected relative to x^2 in the denominator of (396)

$$\bar{\mathcal{A}} \approx \int_{-\infty}^{+\infty} 1 - \exp(-2uy^2/x^2)\,\mathrm{d}x$$

One further simplification is possible. Both terms in the integrand are symmetric about the origin so we may consider only positive x if we double the value of the integral.

$$\bar{\mathcal{A}} = 2\int_{0}^{+\infty} 1 - \exp(-2uy^2/x^2)\,\mathrm{d}x \tag{399}$$

The change of variables $z = 2uy^2x^{-2}$ maps $x \in (0, +\infty)$ to $z \in (+\infty, 0)$

$$z = 2uy^2x^{-2} \tag{400a}$$
$$x = (2u)^{1/2}yz^{1/2} \tag{400b}$$
$$\begin{aligned}\mathrm{d}x &= (2u)^{1/2}y(-\tfrac{1}{2})z^{-3/2}\,\mathrm{d}z \\ &= -2^{-1/2}u^{1/2}yz^{-3/2}\,\mathrm{d}z\end{aligned} \tag{400c}$$

Substituting this into (399) leads to

$$\begin{aligned}\bar{\mathcal{A}} &\approx 2\int_{+\infty}^{0}(1-\mathrm{e}^{-z})(-2^{-1/2}u^{1/2}y)z^{-3/2}\,\mathrm{d}z \\ &\approx 2^{1/2}u^{1/2}y\int_{0}^{+\infty}(1-\mathrm{e}^{-z})z^{-3/2}\,\mathrm{d}z \\ &\approx y\sqrt{2u}\int_{0}^{+\infty} z^{-3/2} - z^{-3/2}\mathrm{e}^{-z}\,\mathrm{d}z\end{aligned}$$

The first term in the integrand of (401) is directly integrable $\int z^{-3/2}\,\mathrm{d}z = -2z^{-1/2}$. The second term in the integrand of (401) is the complete gamma function $\Gamma(-1/2) =$. Section ?? describes the properties of gamma functions[15].

Combining these results we find that the mean absorptance of an isolated Lorentz line in the strong-line limit (401) reduces to

$$\begin{aligned}\bar{\mathcal{A}} &\approx y\sqrt{2u}\left(-2z^{-1/2}\Big|_{0}^{+\infty} - (-2\sqrt{\pi})\right) \\ &= y\sqrt{2u}(\infty + 2\sqrt{\pi}) \\ &= 2y\sqrt{2\pi u}\end{aligned} \tag{401}$$

[15]This section is currently in http://dust.ess.uci.edu/facts/aer/aer.pdf.

fxm: The first term must vanish, but how? Substituting (395b)–(395c) into (401)

$$\begin{aligned} \bar{\mathcal{A}} &\approx 2\left(\frac{\alpha_{\rm L}}{\bar{\delta}}\right)\sqrt{2\pi}\sqrt{\frac{SU}{2\pi\alpha_{\rm L}}} \\ W = \bar{\mathcal{A}}\bar{\delta} &= 2\sqrt{SU\alpha_{\rm L}} \end{aligned} \tag{402}$$

In the strong line limit we see that the mean absorptance $\bar{\mathcal{A}}$ of an isolated line increases only as the square-root of the mass path. Physically, the strong line limit is approached as the line core becomes saturated and any additional absorption must occur in the line wings. Put another way, transition lines do not obey the exponential extinction law on which our solutions to the radiative transfer equation are based. One important consequence of this result is that complicated gaseous spectra must either be decomposed into a multitude of monochromatic intervals, each narrow enough to resolve a small portion of a transition line, or some new statistical means must be developed which correctly represents line absorption in both the weak line and strong line limits.

In summary, the equivalent width W (390) of an isolated spectral line behaves distinctly differently in the two limits (398) and (402)

$$W = \bar{\mathcal{A}}\bar{\delta} = \begin{cases} SU & : \text{ Weak-line limit} \\ 2\sqrt{SU\alpha_{\rm L}} & : \text{ Strong-line limit} \end{cases} \tag{403}$$

6.2 Line Distributions

Inspection of realistic gaseous absorption spectra reveals that line strengths in complex bands occupy a seemingly continuous distribution space, with line strengths S varying over many orders of magnitude in a single band. A key point discussed further in Goody and Yung (1989) is that the variabilities in line spacing and in line widths within a band are negligible (and usually order of magnitude smaller) in comparison to the dynamic range of S. A band containing a suitably large number of lines, therefore, may be amenable to the approximation that the line strength distribution may be represented by a continuous function of S. The line strength distribution function $p(S)$ is the probability that a line in a given spectral region will have a line strength between S and $S + \mathrm{d}S$. The function $p(S)$ must be correctly normalized so that probability of a line having a finite, positive strength is unity

$$\int_0^\infty p(S)\,\mathrm{d}S = 1 \tag{404}$$

A number of functional forms for $p(S)$ have been proposed.

6.2.1 Line Strength Distributions

Goody (1952) proposed the exponential line strength distribution, now also known as the Goody distribution

$$p(S) = \bar{S}^{-1}\,\mathrm{e}^{-S/\bar{S}} \tag{405}$$

where $\bar{S}$ is a constant which, in the next section, we show to be equal to the mean line intensity. A prime advantage of (405) is its arithmetic tractability. The zeroth and first

moments of (405) are both solvable analytically. The following sections use this property to demonstrate the absorptive characteristics of line distributions. However, more complex distributions can improve upon the exponential distribution (405) by better representing the observed line shape distribution of many important species in Earth's atmosphere, such as H_2O.

Malkmus (1967) proposed an improved, albeit more complex, analytic form for the line strength distribution function. First we present a simplified, approximate version of this PDF which illustrates the essential differences between the Malkmus distribution and simpler line strength distributions.

$$p(S) \quad = \quad S^{-1}\,\mathrm{e}^{-S/\bar{S}} \tag{406}$$

The difference with (405) is the prefactor has changed from $\bar{S}^{-1}$ to S^{-1}. The S^{-1} dependence increases the number of weaker lines relative to stronger lines, which is an improvement over (405) and simpler distributions (such as the Elsasser or Godson distributions). The Malkmus distribution (406) is now perhaps the most commonly used line distribution function.

The astute reader will note that (406) is not normalizable on the interval $[0, +\infty)$ (cf. §6.2.2). A key point of the Malkmus distribution, therefore, is the truncation or tapering of $p(S)$ so that statistics of the resulting $p(S)$ are well-behaved. A straightforward line strength distribution function with most of the desired properties is the "truncated" distribution which is non-zero only between a fixed maximum and minimum line strength, S_M and $S_{\min}$, respectively. By convention, $S_{\min}$ is deprecated in favor of the ratio R_S between the maximum and minimum line strengths considered in the band

$$\begin{aligned} S_{\min} &= S_M/R_S \\ R_S &\equiv S_M/S_{\min} \end{aligned} \tag{407}$$

The line strength ratio R_S measures the dynamic range of line strengths considered in a band, which can be quite large, e.g., greater than 10^6 for H_2O bands. With this convention,

$$p(S) \quad = \quad \begin{cases} 0 & : \quad S < S_M/R_S \\ (S \ln R_S)^{-1} & : \quad S_M/R_S < S < S_M \\ 0 & : \quad S > S_M \end{cases} \tag{408}$$

Godson (1953) appears to have been the first to examine (408), although it is closely related to the full Malkmus distribution. The normalization of (408) is demonstrated in §6.2.2. Clearly (408) contains no contributions from lines weaker than S_M/R_S or stronger than S_M. The main disadvantage to (408) is that it is discontinuous, and thus more difficult to treat computationally.

Malkmus (1967) had the insight to identify the following continuous function

$$p(S) \quad = \quad \frac{\mathrm{e}^{-S/S_M} - \mathrm{e}^{-R_S S/S_M}}{S \ln R_S} \tag{409}$$

We shall call (409) the full Malkmus line strength distribution. In practice, (409) is only applied in the limit $R_S \to \infty$. Rather than simply truncating (406) so that $p(S)$ is non-zero only between some lower and upper bound (408), Malkmus (1967) developed (409) because it has many useful properties:

1. $p(S)$ is continuous
2. $p(S)$ has S^{-1} dependence over the bandwidth of interest
3. $p(S)$ approaches (408)
4. $p(S)$ is analytically integrable

Following Malkmus (1967), let us ellucidate the behavior of (409) in important limits. For large R_S and $S_M/R_S \ll S \ll S_M$ the bracketed term in (409) approaches unity so that $p(S) \approx (S \ln R_S)^{-1}$, i.e., the behavior is identical to (408). For $S \gg S_M$, $p(S) \approx (S \ln R_S)^{-1} \mathrm{e}^{-S/S_M}$. Thus for $S \gg S_M$, $p(S)$ is non-zero but much less than what extrapolating $(S \ln R_S)^{-1}$ into this region would yield. Finally, for large S_M and $S \ll S_M/R_S$, $p(S) \approx (R_S)^{-1}(R_S - 1)/S_M$. To summarize, the limits of (409) are as follows

$$p(S) \quad = \quad \begin{cases} (\ln R_S)^{-1}(R_S - 1)/S_M & : \quad S \ll S_M/R_S \\ (S \ln R_S)^{-1} & : \quad S_M/R_S \ll S \ll S_M \\ (S \ln R_S)^{-1} \mathrm{e}^{-S/S_M} & : \quad S \gg S_M \end{cases} \tag{410}$$

Thus (409) behaves like (408) everywhere except near the truncation points S_M/R_S and S_M. Beyond these points, (409) is sharply tapered so that lines in these regions do not influence the statistics of the line strength distribution very much.

6.2.2 Normalization

The normalization properties of the line strength distribution functions will now be shown. The exponential distribution (405) is easily shown to be normalized

$$\begin{aligned} \int_0^\infty \bar{S}^{-1} \, \mathrm{e}^{-S/\bar{S}} \, \mathrm{d}S &= \bar{S}^{-1} \left[-\bar{S} \mathrm{e}^{-S/\bar{S}} \right]_0^\infty \\ &= -0 - (-1) = 1 \end{aligned} \tag{411}$$

For heuristic purposes we first demonstrate that the approximate Malkmus distribution (406) is not normalizeable despite its apparent simplicity. With the substitution $x = S/\bar{S}$ we have

$$\int_0^\infty S^{-1} \, \mathrm{e}^{-S/\bar{S}} \, \mathrm{d}S \quad = \quad \int_0^\infty x^{-1} \, \mathrm{e}^{-x} \, \mathrm{d}x \tag{412}$$

The RHS resembles the complete gamma function of zero, $\Gamma(0)$ (??). However, $\Gamma(0)$ is indeterminate, a singularity between negative and positive infinities much like $\tan \frac{\pi}{2}$. Thus (406) is not normalizeable.

Next we consider the truncated Malkmus distribution (410). We integrate over the non-zero region, S_M/R_S to S_M, to demonstrate its normalization properties

$$\begin{aligned} \int_{S_M/R_S}^{S_M} (S \ln R_S)^{-1} \, \mathrm{d}S &= (\ln R_S)^{-1} [\ln S]_{S_M/R_S}^{S_M} \\ &= (\ln R_S)^{-1} [\ln S_M - \ln(S_M/R_S)] \\ &= (\ln R_S)^{-1} [\ln S_M - \ln S_M + \ln R_S] \\ &= 1 \end{aligned} \tag{413}$$

It is more challenging to prove that the full Malkmus distribution (409) is normalized. To begin, we simplify $p(S)$ (409) with the substituions $a = S_M^{-1}$, $b = R_S S_M^{-1}$, and thus $R_S = b/a$.

$$\int_0^\infty p(S)\,\mathrm{d}S \;=\; (\ln R_S)^{-1} \int_0^\infty S^{-1}(\mathrm{e}^{-aS} - \mathrm{e}^{-bS})\,\mathrm{d}S \tag{414}$$

We must show, therefore, that this rather complex definite integral always equals $\ln(b/a) = \ln R_S$. Since both terms in the integrand are of the same form, we shall explicitly evaluate $S^{-1}\mathrm{e}^{-aS}$ before subtracting the analogous term involving b. These terms are amenable to integration by parts with the change of variables

$$\begin{aligned} u &= \mathrm{e}^{-aS} \\ \mathrm{d}u &= -a\mathrm{e}^{aS}\,\mathrm{d}S \\ \mathrm{d}v &= S^{-1}\,\mathrm{d}S \\ v &= \ln S \end{aligned} \tag{415}$$

The result is

$$\begin{aligned} \ln R_S \int_0^\infty S^{-1}\mathrm{e}^{-aS}\,\mathrm{d}S &= \left[\mathrm{e}^{-aS}\ln S\right]_0^\infty - \int_0^\infty \ln S(-a\mathrm{e}^{-aS})\,\mathrm{d}S \\ &= \left[\mathrm{e}^{-aS}\ln S\right]_0^\infty + a\int_0^\infty \mathrm{e}^{-aS}\ln S\,\mathrm{d}S \end{aligned}$$

The first term on the RHS contains a singularity since $\ln(0)$ is undefined. This term however, will disappear once the similar term arising from the integration of $\int S^{-1}\mathrm{e}^{-bS}\,\mathrm{d}S$ is subtracted from (416). Now we change variables to isolate the parameter a from the dummy variable of integration. Letting $x = aS$, $S = x/a$, $\mathrm{d}x = a\,\mathrm{d}S$, and $\mathrm{d}S = a^{-1}\,\mathrm{d}x$ leads to

$$\begin{aligned} \ln R_S \int_0^\infty S^{-1}\mathrm{e}^{-aS}\,\mathrm{d}S &= \left[\mathrm{e}^{-aS}\ln S\right]_0^\infty + a\int_0^\infty \mathrm{e}^{-x}\ln(x/a)a^{-1}\,\mathrm{d}x \\ &= \left[\mathrm{e}^{-aS}\ln S\right]_0^\infty + \int_0^\infty \mathrm{e}^{-x}\ln x - \mathrm{e}^{-x}\ln a\,\mathrm{d}x \\ &= \left[\mathrm{e}^{-aS}\ln S\right]_0^\infty + \int_0^\infty \mathrm{e}^{-x}\ln x\,\mathrm{d}x - \ln a\left[-\mathrm{e}^{-x}\right]_0^\infty \\ &= \left[\mathrm{e}^{-aS}\ln S\right]_0^\infty + \int_0^\infty \mathrm{e}^{-x}\ln x\,\mathrm{d}x - \ln a[-0-(-1)] \\ &= \left[\mathrm{e}^{-aS}\ln S\right]_0^\infty + \int_0^\infty \mathrm{e}^{-x}\ln x\,\mathrm{d}x - \ln a \end{aligned} \tag{416}$$

There is no closed form solution to the second term on the RHS, $\int \mathrm{e}^{-x}\ln x\,\mathrm{d}x$, which is very close in appearance to the original integral (414). However, this term will also disappear once the integration involving b is subtracted from (416). Multiplying both sides by $(\ln R_S)^{-1}$,

and subtracting the integration involving b leads to

$$\begin{aligned}\int_0^\infty p(S)\,\mathrm{d}S &= \frac{1}{\ln R_S}\Big\{\left[\mathrm{e}^{-aS}\ln S\right]_0^\infty - \left[\mathrm{e}^{-bS}\ln S\right]_0^\infty \\ &\quad + \int_0^\infty \mathrm{e}^{-x}\ln x\,\mathrm{d}x - \int_0^\infty \mathrm{e}^{-x}\ln x\,\mathrm{d}x - \ln a + \ln b\Big\} \\ &= \frac{\ln b - \ln a}{\ln R_S} = \frac{\ln(b/a)}{\ln R_S} = \frac{\ln R_S}{\ln R_S} \\ &= 1 \end{aligned} \tag{417}$$

All the like terms in the numerator cancelled in the first step with the exception of $\ln R_S$.

6.2.3 Mean Line Intensity

The mean line intensity $\bar{S}$ of a line strength distribution $p(S)$ is defined as

$$\bar{S} = \int_0^\infty Sp(S)\,\mathrm{d}S \tag{418}$$

$\bar{S}$ is an important statistic of a line strength distribution and any realistic line strength distribution should adequately predict $\bar{S}$ when compared to observed line strengths. Thus many line strength distributions, e.g., the exponential distribution (405) contain $\bar{S}$ in their definition. The claim that $\bar{S}$ is, in fact, the mean strength of these distributions will now be proved.

The mean line intensity of the exponential distribution (405) is

$$\begin{aligned}\int_0^\infty Sp(S)\,\mathrm{d}S &= \int_0^\infty \frac{S}{\bar{S}}\mathrm{e}^{-S/\bar{S}}\,\mathrm{d}S \\ &= \frac{1}{\bar{S}}\int_0^\infty S\mathrm{e}^{-S/\bar{S}}\,\mathrm{d}S \\ &= \frac{1}{\bar{S}}\int_0^\infty \bar{S}x\mathrm{e}^{-x}\bar{S}\,\mathrm{d}x \\ &= \bar{S}\int_0^\infty x\mathrm{e}^{-x}\,\mathrm{d}x \\ &= \bar{S}\left[-x\mathrm{e}^{-x} - \mathrm{e}^{-x}\right]_0^\infty \\ &= \bar{S}\left[-0 - 0 - (0-1)\right] \\ &= \bar{S} \end{aligned} \tag{419}$$

This demonstrates $\bar{S}$ is the mean line strength of the exponential distribution.

The mean line intensity of the approximate Malkmus distribution, (406) is

$$\begin{aligned}\int_0^\infty Sp(S)\,\mathrm{d}S &= \int_0^\infty \frac{S}{\bar{S}}\,\mathrm{e}^{-S/\bar{S}}\,\mathrm{d}S \\ &= \int_0^\infty \mathrm{e}^{-S/\bar{S}}\,\mathrm{d}S \\ &= -\bar{S}\mathrm{e}^{-S/\bar{S}}\Big|_0^\infty \\ &= -\bar{S}(\mathrm{e}^{-\infty/\bar{S}} - \mathrm{e}^{-0/\bar{S}}) \\ &= \bar{S} \end{aligned} \tag{420}$$

This proves that $\bar{S}$ is also the mean line strength in the approximate Malkmus line distribution function (406).

The mean line intensity of the full Malkmus distribution is derived directly from (409)

$$\begin{aligned}\int_0^\infty Sp(S)\,\mathrm{d}S &= \int_0^\infty S \times \frac{\mathrm{e}^{-S/S_M} - \mathrm{e}^{-R_S S/S_M}}{S \ln R_S}\,\mathrm{d}S \\ &= (\ln R_S)^{-1} \int_0^\infty \mathrm{e}^{-S/S_M} - \mathrm{e}^{-R_S S/S_M}\,\mathrm{d}S \\ &= \frac{1}{\ln R_S}\left[-S_M\mathrm{e}^{-S/S_M} + \frac{S_M}{R_S}\mathrm{e}^{-R_S S/S_M}\right]_0^\infty \\ &= \frac{S_M}{\ln R_S}\left[-0 + 0 - (-1) - (R_S^{-1})\right] \\ &= \frac{S_M}{\ln R_S}(1 - R_S^{-1}) = \frac{S_M}{\ln R_S}\frac{R_S - 1}{R_S} \\ &= \frac{R_S - 1}{R_S \ln R_S} S_M \end{aligned} \tag{421}$$

This expression for $\bar{S}$ does not converge in the limit as $R_S \to \infty$. Thus the mean line strength of the Malkmus distribution (409) depends on the parameter R_S (??), the ratio between the strongest and weakest lines in a given band. It is clear from (421) that $\bar{S}$ decreases as R_S increases. Adequately representing the importance of weak lines is one of the chief advantages of the Malkmus distribution relative to other distributions.

The maximum line strength intensity S_M may be expressed in terms of the mean line strength S by inverting (421)

$$S_M = \frac{R_S \ln R_S}{R_S - 1}\bar{S} \tag{422}$$

6.2.4 Mean Absorptance of Line Distribution

This section develops the concept of mean absorptance of a band of non-overlapping lines, whereas §6.1.4 derived the mean absorptance $\bar{\mathcal{A}}$ of an isolated Lorentz line. Since the lines are assumed to be non-overlapping, we may weight the contribution of each line to the mean

absorptance (392) by the normalized line strength probability (404)

$$\begin{aligned} \bar{W} = \bar{\mathcal{A}}\bar{\delta} &= \int_0^\infty p(S) \left(\int_{-\infty}^{+\infty} \mathcal{A}\, \mathrm{d}\nu \right) \mathrm{d}S \\ &= \int_0^\infty p(S) \int_{-\infty}^{+\infty} 1 - \exp[-S\Phi U]\, \mathrm{d}\nu\, \mathrm{d}S \end{aligned} \tag{423}$$

Inserting the exponential line strength distribution function (405) for $p(S)$ in (423) and interchanging orders of integration yields

$$\begin{aligned} \bar{W} = \bar{\mathcal{A}}\bar{\delta} &= \int_0^\infty \bar{S}^{-1}\, \mathrm{e}^{-S/\bar{S}} \int_{-\infty}^{+\infty} 1 - \exp[-S\Phi U]\, \mathrm{d}\nu\, \mathrm{d}S \\ &= \bar{S}^{-1} \int_{-\infty}^{+\infty} \int_0^\infty \mathrm{e}^{-S/\bar{S}} - \exp\left(-\frac{S}{\bar{S}} - S\Phi U \right) \mathrm{d}S\, \mathrm{d}\nu \\ &= \bar{S}^{-1} \int_{-\infty}^{+\infty} \int_0^\infty \mathrm{e}^{-S/\bar{S}} - \exp\left(-S(\bar{S}^{-1} + U\Phi) \right) \mathrm{d}S\, \mathrm{d}\nu \\ &= \bar{S}^{-1} \int_{-\infty}^{+\infty} \left[-\bar{S}\mathrm{e}^{-S/\bar{S}} + (\bar{S}^{-1} + U\Phi)^{-1} \exp\left(-S(\bar{S}^{-1} + U\Phi) \right) \right]_0^\infty \mathrm{d}\nu \\ &= \bar{S}^{-1} \int_{-\infty}^{+\infty} \left[0 + 0 - \left(-\bar{S} \times 1 + (\bar{S}^{-1} + U\Phi)^{-1} \times 1 \right) \right] \mathrm{d}\nu \\ &= \bar{S}^{-1} \int_{-\infty}^{+\infty} \bar{S} - (\bar{S}^{-1} + U\Phi)^{-1}\, \mathrm{d}\nu \\ &= \bar{S}^{-1} \int_{-\infty}^{+\infty} \bar{S} - \frac{\bar{S}}{1 + \bar{S}U\Phi}\, \mathrm{d}\nu \\ &= \int_{-\infty}^{+\infty} 1 - \frac{1}{1 + \bar{S}U\Phi}\, \mathrm{d}\nu \\ &= \int_{-\infty}^{+\infty} \frac{1 + \bar{S}U\Phi - 1}{1 + \bar{S}U\Phi}\, \mathrm{d}\nu \\ &= \int_{-\infty}^{+\infty} \frac{\bar{S}U\Phi}{1 + \bar{S}U\Phi}\, \mathrm{d}\nu \end{aligned} \tag{424}$$

Thus the mean absorptance of the exponential line distribution depends straightforwardly on the line shape function. Substituting the Lorentz line shape $\Phi_\mathrm{L}(\nu) = \alpha_\mathrm{L}/[\pi(\nu^2 + \alpha_\mathrm{L}^2)]$ (280) into (424) we obtain

$$\begin{aligned} \bar{W} = \bar{\mathcal{A}}\bar{\delta} &= \int_{-\infty}^{+\infty} \frac{\alpha_\mathrm{L}}{\pi(\nu^2 + \alpha_\mathrm{L}^2)} \times \frac{\bar{S}U}{1 + \bar{S}U \frac{\alpha_\mathrm{L}}{\pi(\nu^2 + \alpha_\mathrm{L}^2)}}\, \mathrm{d}\nu \\ &= \frac{\bar{S}U\alpha_\mathrm{L}}{\pi} \int_{-\infty}^{+\infty} \frac{1}{\nu^2 + \alpha_\mathrm{L}^2} \times \frac{1}{\frac{\pi(\nu^2 + \alpha_\mathrm{L}^2) + \bar{S}U\alpha_\mathrm{L}}{\pi(\nu^2 + \alpha_\mathrm{L}^2)}}\, \mathrm{d}\nu \\ &= \frac{\bar{S}U\alpha_\mathrm{L}}{\pi} \int_{-\infty}^{+\infty} \frac{1}{\nu^2 + \alpha_\mathrm{L}^2} \times \frac{\pi(\nu^2 + \alpha_\mathrm{L}^2)}{\pi(\nu^2 + \alpha_\mathrm{L}^2) + \bar{S}U\alpha_\mathrm{L}}\, \mathrm{d}\nu \end{aligned}$$

$$
\begin{aligned}
&= \bar{S}U\alpha_{\mathrm{L}} \int_{-\infty}^{+\infty} \frac{1}{\pi(\nu^2+\alpha_{\mathrm{L}}^2)+\bar{S}U\alpha_{\mathrm{L}}}\,\mathrm{d}\nu \\
&= \frac{\bar{S}U\alpha_{\mathrm{L}}}{\pi} \int_{-\infty}^{+\infty} \frac{1}{\nu^2+\alpha_{\mathrm{L}}^2+\pi^{-1}\bar{S}U\alpha_{\mathrm{L}}}\,\mathrm{d}\nu
\end{aligned} \tag{425}
$$

Letting $a = \sqrt{\alpha_{\mathrm{L}}^2+\pi^{-1}\bar{S}U\alpha_{\mathrm{L}}} = \alpha_{\mathrm{L}}\sqrt{1+\bar{S}U/(\pi\alpha_{\mathrm{L}})}$ and noting that $\int (x^2+a^2)^{-1}\,\mathrm{d}x = a^{-1}\tan^{-1}(x/a)$,

$$
\begin{aligned}
\bar{W} = \bar{\mathcal{A}}\bar{\delta} &= \frac{\bar{S}U\alpha_{\mathrm{L}}}{\pi} \int_{-\infty}^{+\infty} \frac{1}{\nu^2+a^2}\,\mathrm{d}\nu \\
&= \frac{\bar{S}U\alpha_{\mathrm{L}}}{\pi}\frac{1}{a}\left[\tan^{-1}\frac{x}{a}\right]_{-\infty}^{+\infty} \\
&= \frac{\bar{S}U\alpha_{\mathrm{L}}}{\pi}\left[\alpha_{\mathrm{L}}\left(1+\frac{\bar{S}U}{\pi\alpha_{\mathrm{L}}}\right)^{1/2}\right]^{-1}\left[\frac{\pi}{2}-\left(-\frac{\pi}{2}\right)\right] \\
&= \bar{S}U\left(1+\frac{\bar{S}U}{\pi\alpha_{\mathrm{L}}}\right)^{-1/2} \\
\frac{\bar{W}}{\bar{\delta}} = \bar{\mathcal{A}} &= \frac{\bar{S}U}{\bar{\delta}}\left(1+\frac{\bar{S}U}{\pi\alpha_{\mathrm{L}}}\right)^{-1/2}
\end{aligned} \tag{426}
$$

In addition to U, the mean band absorptance $\bar{\mathcal{A}}$ depends on only two statistics of the band, namely $\bar{S}/\bar{\delta}$ and $\bar{S}/(\pi\alpha_{\mathrm{L}})$.

We recall that (426) is based on the idealized, continuous line strength distribution (405) rather than on real (observed) line strengths. Observed line strengths and positions are tabulated in the HITRAN database (§5.5.1). Therefore we may compute any desired statistics of the actual line strength distribution. Of particular interest is the observed mean absorptance of a band in both the weak and strong line limits. Summing (398) and (402) over the N lines in the given band

$$
W = \bar{\mathcal{A}}\bar{\delta} = \begin{cases} N^{-1}\sum_{i=1}^{N} S_i U & : \quad SU \ll 1 \\ N^{-1}\sum_{i=1}^{N} 2\sqrt{S_i U \alpha_{\mathrm{L},i}} & : \quad SU \gg 1 \end{cases} \tag{427}
$$

The weak and strong line limits of the mean absorptance of the exponential line strength distribution function (426) are

$$
\lim_{\bar{S}U\ll 1} \bar{W} = \bar{\mathcal{A}}\bar{\delta} \approx \bar{S}U \tag{428a}
$$

$$
\lim_{\bar{S}U\gg 1} \bar{W} = \bar{\mathcal{A}}\bar{\delta} \approx \bar{S}U\left(\frac{\bar{S}U}{\pi\alpha_{\mathrm{L}}}\right)^{-1/2} = \sqrt{\pi\bar{S}U\alpha_{\mathrm{L}}} \tag{428b}
$$

We now require (428) to equal (427) in the appropriate limits. In the weak line limit

$$
\begin{aligned}
\bar{S}U &= N^{-1}\sum_{i=1}^{N} S_i U \\
\frac{\bar{S}}{\bar{\delta}} &= (N\bar{\delta})^{-1}\sum_{i=1}^{N} S_i
\end{aligned} \tag{429}
$$

In the strong line limit

$$\begin{aligned}
\sqrt{\pi\bar{S}U\alpha_{\mathrm{L}}} &= N^{-1}\sum_{i=1}^{N} 2\sqrt{S_i U\alpha_{\mathrm{L},i}} \\
\pi\bar{S}U\alpha_{\mathrm{L}} &= \frac{4U}{N^2}\left(\sum_{i=1}^{N}\sqrt{S_i\alpha_{\mathrm{L},i}}\right)^2 \\
\frac{1}{\pi\bar{S}\alpha_{\mathrm{L}}} &= \frac{N^2}{4}\left(\sum_{i=1}^{N}\sqrt{S_i\alpha_{\mathrm{L},i}}\right)^{-2} \\
\frac{1}{\pi\bar{S}\alpha_{\mathrm{L}}}\times\bar{S}^2 &= \bar{S}^2\times\frac{N^2}{4}\left(\sum_{i=1}^{N}\sqrt{S_i\alpha_{\mathrm{L},i}}\right)^{-2} \\
\frac{\bar{S}}{\pi\alpha_{\mathrm{L}}} &= \frac{1}{N^2}\left(\sum_{i=1}^{N} S_i\right)^2\times\frac{N^2}{4}\left(\sum_{i=1}^{N}\sqrt{S_i\alpha_{\mathrm{L},i}}\right)^{-2} \\
\frac{\bar{S}}{\pi\alpha_{\mathrm{L}}} &= \frac{1}{4}\left(\sum_{i=1}^{N} S_i\Big/\sum_{i=1}^{N}\sqrt{S_i\alpha_{\mathrm{L},i}}\right)^2
\end{aligned} \tag{430}$$

The tractable analytic form of (426) led to its adoption as the dominant formulation for band models for many years. The mean band absorptances $\bar{\mathcal{A}}$ of other line strength distributions have forms similar to (426).

Inserting the Malkmus line strength distribution function (409) for $p(S)$ in (423) and interchanging orders of integration yields

$$\begin{aligned}
\bar{W} = \bar{\mathcal{A}}\bar{\delta} &= \int_0^{\infty}\frac{\mathrm{e}^{-S/S_M}-\mathrm{e}^{-R_S S/S_M}}{S\ln R_S}\int_{-\infty}^{+\infty} 1-\exp(-S\Phi U)\,\mathrm{d}\nu\,\mathrm{d}S \\
&= \frac{1}{\ln R_S}\int_{-\infty}^{+\infty}\int_0^{\infty}\frac{1}{S}(\mathrm{e}^{-S/S_M}-\mathrm{e}^{-SR_S/S_M})(1-\mathrm{e}^{-S\Phi U})\,\mathrm{d}S\,\mathrm{d}\nu \\
&= \frac{1}{\ln R_S}\int_{-\infty}^{+\infty}\int_0^{\infty}\frac{\mathrm{e}^{-S/S_M}}{S}-\frac{\mathrm{e}^{-SR_S/S_M}}{S}+\frac{\mathrm{e}^{-S(\Phi U+R_S/S_M)}}{S}-\frac{\mathrm{e}^{-S(\Phi U+1/S_M)}}{S}\,\mathrm{d}S\,\mathrm{d}\nu
\end{aligned}$$

The first two terms and the last two terms in the integrand are both of the form $S^{-1}(\mathrm{e}^{-aS}-\mathrm{e}^{-bS})$. In proving the Malkmus distribution is correctly normalized (414)–(417) we showed the value of this type of definite integral is $\ln(b/a)$. For the first two terms, $a = S_M^{-1}$ and $b = R_S/S_M$. For the final two terms, $a = \Phi U + R_S/S_M$ and $b = \Phi U + 1/S_M$. Therefore the integration over S is complete and results in

$$\begin{aligned}
\bar{W} = \bar{\mathcal{A}}\bar{\delta} &= \frac{1}{\ln R_S}\int_{-\infty}^{+\infty}\ln R_S + \ln\left(\frac{\Phi U+1/S_M}{\Phi U+R_S/S_M}\right)\mathrm{d}\nu \\
&= \frac{1}{\ln R_S}\int_{-\infty}^{+\infty}\ln R_S + \ln\left(\frac{1+S_M\Phi U}{R_S+S_M\Phi U}\right)\mathrm{d}\nu \\
&= \frac{1}{\ln R_S}\int_{-\infty}^{+\infty}\ln R_S + \ln\left[\left(\frac{1}{R_S}\right)\frac{1+S_M\Phi U}{1+S_M\Phi U/R_S}\right]\mathrm{d}\nu
\end{aligned}$$

$$= \frac{1}{\ln R_S}\int_{-\infty}^{+\infty} \ln R_S + \ln\left(\frac{1+S_M\Phi U}{1+S_M\Phi U/R_S}\right) - \ln R_S \,\mathrm{d}\nu$$
$$= \frac{1}{\ln R_S}\int_{-\infty}^{+\infty} \ln\left(\frac{1+S_M\Phi U}{1+S_M\Phi U/R_S}\right) \mathrm{d}\nu \tag{431}$$

The mean absorptance of the Malkmus distribution also depends simply on the line shape $\Phi(\nu)$. The mean absorptance of the exponential line distribution (424) is analogous to the Malkmus result (431). Note that the former is a rational function of the mean line intensity $\bar{S}$, while the latter depends logarithmically on $\bar{S}$. Moreover, the mean absorptance of the Malkmus distribution depends on the additional parameter R_S, the ratio between the maximum and minimum line strengths with the band. The dependence is problematic in that (431) is not self-evidently convergent as $R_S \to \infty$. We now show that for the most important line shapes, $\bar{\mathcal{A}}$(431) does converge in this limit.

Substituting the Lorentz line shape $\Phi_\mathrm{L}(\nu) = \alpha_\mathrm{L}/[\pi(\nu^2+\alpha_\mathrm{L}^2)]$ (280) into (424) we obtain

$$\bar{W} = \bar{\mathcal{A}}\bar{\delta} = \frac{1}{\ln R_S}\int_{-\infty}^{+\infty} \ln\left(\frac{1+\frac{S_M U\alpha_\mathrm{L}}{\pi(\nu^2+\alpha_\mathrm{L}^2)}}{1+\frac{S_M U\alpha_\mathrm{L}}{\pi(\nu^2+\alpha_\mathrm{L}^2)R_S}}\right)\mathrm{d}\nu$$
$$= \frac{1}{\ln R_S}\int_{-\infty}^{+\infty} \ln\left(\frac{S_M U\alpha_\mathrm{L}+\pi(\nu^2+\alpha_\mathrm{L}^2)}{S_M U\alpha_\mathrm{L}R_S^{-1}+\pi(\nu^2+\alpha_\mathrm{L}^2)}\right)\mathrm{d}\nu$$
$$= \frac{1}{\ln R_S}\int_{-\infty}^{+\infty} \ln\left(\frac{\nu^2+\alpha_\mathrm{L}^2+S_M U\alpha_\mathrm{L}/\pi}{\nu^2+\alpha_\mathrm{L}^2+S_M U\alpha_\mathrm{L}/(\pi R_S)}\right)\mathrm{d}\nu$$
$$= \frac{1}{\ln R_S}\int_{-\infty}^{+\infty} \ln\left(\nu^2+\alpha_\mathrm{L}^2+\frac{S_M U\alpha_\mathrm{L}}{\pi}\right) - \ln\left(\nu^2+\alpha_\mathrm{L}^2+\frac{S_M U\alpha_\mathrm{L}}{\pi R_S}\right)\mathrm{d}\nu \tag{432}$$

We simplify (432) by making the substitutions $c^2 = \alpha_\mathrm{L}^2 + S_M U\alpha_\mathrm{L}/\pi$ and $d^2 = \alpha_\mathrm{L}^2 + S_M U\alpha_\mathrm{L}/(\pi R_S)$, or, equivalenty

$$c = \alpha_\mathrm{L}\sqrt{1+\frac{S_M U}{\pi\alpha_\mathrm{L}}} \tag{433a}$$
$$d = \alpha_\mathrm{L}\sqrt{1+\frac{S_M U\alpha_\mathrm{L}}{\pi\alpha_\mathrm{L}R_S}} \tag{433b}$$

With these definitions, (432) becomes

$$\bar{W} = \bar{\mathcal{A}}\bar{\delta} = \frac{1}{\ln R_S}\int_{-\infty}^{+\infty} \ln(\nu^2+c^2) - \ln(\nu^2+d^2)\,\mathrm{d}\nu \tag{434}$$

This is the difference of two identical, standard integrals (e.g., Gradshteyn and Ryzhik, 1965, p. 205) and reduces to elementary functions

$$\int \ln(\nu^2+a^2)\,\mathrm{d}\nu = \nu\ln(\nu^2+a^2) - 2\nu + 2\nu\tan^{-1}\frac{\nu}{a} \tag{435}$$

It is straightforward to differentiate (435) and verify the result. Using (435) to complete the frequency integration in (434) results in

$$\bar{W} = \bar{\mathcal{A}}\bar{\delta} = (\ln R_S)^{-1}\left[\nu\ln(\nu^2+c^2) - 2\nu + 2c\tan^{-1}\frac{\nu}{c} - \nu\ln(\nu^2+d^2) + 2\nu - 2d\tan^{-1}\frac{\nu}{d}\right]_{-\infty}^{+\infty}$$
$$= (\ln R_S)^{-1}\left[2c\tan^{-1}\frac{\nu}{c} - 2d\tan^{-1}\frac{\nu}{d}\right]_{-\infty}^{+\infty}$$

The mutual cancellation of the 2ν terms is obvious, but the equivalence of the logarithmic terms may not be self-evident. Consider, however, that both c and d (433) are finite-valued as $\nu \to \pm\infty$, and it is clear that these terms must cancel. Evaluating the remaining terms leads to

$$\begin{aligned} \bar{W} = \bar{\mathcal{A}}\bar{\delta} &= (\ln R_S)^{-1}\left\{2c\frac{\pi}{2} - 2d\frac{\pi}{2} - \left[2c\left(-\frac{\pi}{2}\right) - 2d\left(-\frac{\pi}{2}\right)\right]\right\} \\ &= (\ln R_S)^{-1}(\pi c - \pi d + \pi c - \pi d) \\ &= (\ln R_S)^{-1}2\pi(c-d) \\ &= \frac{2\pi\alpha_{\mathrm{L}}}{\ln R_S}\left(\sqrt{1+\frac{S_M U}{\pi\alpha_{\mathrm{L}}}} - \sqrt{1+\frac{S_M U}{\pi\alpha_{\mathrm{L}} R_S}}\right) \end{aligned} \tag{436}$$

Although (436) does convey the behavior of the mean absorptance of the Malkmus band model with Lorentzian lines, the presence of the S_M term and the R_S term is undesirable because their values are interrelated and depend on the specific gaseous absorption band being considered. It would be more convenient to express the mean absorptance in terms of universal statistics applicable to all band models, so that $\bar{\mathcal{A}}$ and $\bar{W}$ may be easily intercompared among band models. The mean line strength $\bar{S}$ (418) appears in both the exponential (405) and Godson line strength distributions. We use (422) to replace S_M by $\bar{S}$ in (436)

$$\begin{aligned} \bar{W} = \bar{\mathcal{A}}\bar{\delta} &= \frac{2\pi\alpha_{\mathrm{L}}}{\ln R_S}\left(\sqrt{1+\frac{\bar{S}U}{\pi\alpha_{\mathrm{L}}}\frac{R_S\ln R_S}{R_S-1}} - \sqrt{1+\frac{\bar{S}U}{\pi\alpha_{\mathrm{L}} R_S}\frac{R_S\ln R_S}{R_S-1}}\right) \\ &= \frac{2\pi\alpha_{\mathrm{L}}}{\ln R_S}\left(\sqrt{1+\frac{\bar{S}U}{\pi\alpha_{\mathrm{L}}}\frac{R_S\ln R_S}{R_S-1}} - \sqrt{1+\frac{\bar{S}U}{\pi\alpha_{\mathrm{L}}}\frac{\ln R_S}{R_S-1}}\right) \end{aligned} \tag{437}$$

The weak line limit of the mean absorptance of the Malkmus line strength distribution function (437) is obtained by expanding the radical into a Taylor series and retaining only the first two terms $\lim_{x\ll 1}\sqrt{1+x} \approx 1 + x/2$

$$\begin{aligned} \lim_{\bar{S}U\ll 1}\bar{W} = \bar{\mathcal{A}}\bar{\delta} &\approx \frac{2\pi\alpha_{\mathrm{L}}}{\ln R_S}\left(1+\frac{\bar{S}U}{2\pi\alpha_{\mathrm{L}}}\frac{R_S\ln R_S}{R_S-1} - 1 - \frac{\bar{S}U}{2\pi\alpha_{\mathrm{L}}}\frac{\ln R_S}{R_S-1}\right) \\ &= \frac{2\pi\alpha_{\mathrm{L}}}{\ln R_S}\times\frac{\bar{S}U\ln R_S(R_S-1)}{2\pi\alpha_{\mathrm{L}}(R_S-1)} \\ &= \bar{S}U \end{aligned} \tag{438}$$

which is identical to (428a). The strong line limit of (437) is

$$\begin{aligned} \lim_{\bar{S}U\gg 1}\bar{W} = \bar{\mathcal{A}}\bar{\delta} &\approx \frac{2\pi\alpha_{\mathrm{L}}}{\ln R_S}\left(\sqrt{\frac{\bar{S}U}{\pi\alpha_{\mathrm{L}}}\frac{R_S\ln R_S}{R_S-1}} - \sqrt{\frac{\bar{S}U}{\pi\alpha_{\mathrm{L}}}\frac{\ln R_S}{R_S-1}}\right) \\ &= \frac{2\pi\alpha_{\mathrm{L}}}{\ln R_S}\sqrt{\frac{\bar{S}U\ln R_S}{\pi\alpha_{\mathrm{L}}}}\left(\sqrt{\frac{R_S}{R_S-1}} - \sqrt{\frac{1}{R_S-1}}\right) \end{aligned}$$

$$= 2\left(\frac{\pi\alpha_{\rm L}\bar{S}U}{\ln R_S}\right)^{1/2}\left(\frac{\sqrt{R_S}}{\sqrt{R_S-1}}-\frac{1}{\sqrt{R_S-1}}\right)$$
$$= 2\sqrt{\pi\alpha_{\rm L}\bar{S}U}\times\frac{\sqrt{R_S}-1}{\sqrt{(R_S-1)\ln R_S}} \quad (439)$$

Let us encapsulate the R_S-dependence into the function $\chi(R_S)$ and and also present $\chi^2(R_S)$ for future use.

$$\chi(R_S) = \frac{\sqrt{R_S}-1}{\sqrt{(R_S-1)\ln R_S}} \quad (440a)$$
$$[\chi(R_S)]^2 = \frac{(\sqrt{R_S}-1)(\sqrt{R_S}-1)}{(R_S-1)\ln R_S}$$
$$= \frac{(\sqrt{R_S}-1)(\sqrt{R_S}-1)}{(\sqrt{R_S}-1)(\sqrt{R_S}+1)\ln R_S}$$
$$\chi^2(R_S) = \frac{\sqrt{R_S}-1}{(\sqrt{R_S}+1)\ln R_S} \quad (440b)$$

where we have made use of the factoring $R_S-1=(\sqrt{R_S}-1)(\sqrt{R_S}+1)$. Rewriting (439) with $\chi(R_S)$ (440a)

$$\lim_{\bar{S}U\gg 1}\bar{W} = \bar{\mathcal{A}}\bar{\delta} \approx 2\sqrt{\pi\alpha_{\rm L}\bar{S}U}\chi(R_S) \quad (441)$$

The strong line limit of the Malkmus distribution of Lorentzian lines (441), and the strong line limit of an individual Lorentzian line (403), differ by the factor $\sqrt{\pi}\chi(R_S)$.

The advantage of encapsulating the R_S-dependence in the $\chi(R_S)$ function is that the weak and strong line limits of the Malkmus distribution may now be cast in exactly the same notation as the exponential distribution (428). First introduce a transformed mean line intensity $\tilde{\bar{S}}$ and mean line spacing $\tilde{\bar{\delta}}$ which are defined in terms of the line strength ratio of the Malkmus distribution

$$\tilde{\bar{S}} = \frac{\bar{S}}{\pi\chi^2} \leftrightarrow \bar{S} = \pi\tilde{\bar{S}}\chi^2 \quad (442a)$$
$$\tilde{\bar{\delta}} = \frac{\bar{\delta}}{\pi\chi^2} \leftrightarrow \bar{\delta} = \pi\tilde{\bar{\delta}}\chi^2 \quad (442b)$$

The definitions (442) ensure that $\bar{S}/\bar{\delta}=\tilde{\bar{S}}/\tilde{\bar{\delta}}$. In terms of the original mean line strength and spacing, and the transformed line strength and line spacing, the weak and strong line limits of the mean absorptance $\bar{\mathcal{A}}$ of the Malkmus line strength distribution applied to Lorentzian lines (437) is

$$\lim_{\bar{S}U\ll 1}\bar{W} = \bar{\mathcal{A}}\bar{\delta} \approx \frac{\bar{S}U}{\bar{\delta}} = \frac{\tilde{\bar{S}}U}{\tilde{\bar{\delta}}} \quad (443a)$$
$$\lim_{\bar{S}U\gg 1}\bar{W} = \bar{\mathcal{A}}\bar{\delta} \approx 2\sqrt{\pi\alpha_{\rm L}\bar{S}U}\chi(R_S) = 2\sqrt{\alpha_{\rm L}\tilde{\bar{S}}U} \quad (443b)$$

We now rewrite the mean absorptance (437) in terms of the transformed parameters $\tilde{\bar{S}}$ and $\tilde{\bar{\delta}}$ (442), making use of (440b)

$$\begin{aligned}
\frac{\bar{W}}{\bar{\delta}} = \bar{\mathcal{A}} &= \frac{2\pi\alpha_{\mathrm{L}}}{\bar{\delta}\ln R_S}\left(\sqrt{1+\frac{\bar{S}U}{\pi\alpha_{\mathrm{L}}}\frac{R_S\ln R_S}{R_S-1}}-\sqrt{1+\frac{\bar{S}U}{\pi\alpha_{\mathrm{L}}}\frac{\ln R_S}{R_S-1}}\right)\\
&= \frac{1}{\pi\tilde{\bar{\delta}}\chi^2}\frac{2\pi\alpha_{\mathrm{L}}}{\ln R_S}\left(\sqrt{1+\frac{\pi\chi^2\tilde{\bar{S}}U}{\pi\alpha_{\mathrm{L}}}\frac{R_S\ln R_S}{R_S-1}}-\sqrt{1+\frac{\pi\chi^2\tilde{\bar{S}}U}{\pi\alpha_{\mathrm{L}}}\frac{\ln R_S}{R_S-1}}\right)\\
&= \frac{(\sqrt{R_S}+1)\ln R_S}{\sqrt{R_S}-1}\frac{2\alpha_{\mathrm{L}}}{\tilde{\bar{\delta}}\ln R_S}\left(\sqrt{1+\frac{\tilde{\bar{S}}U}{\alpha_{\mathrm{L}}}\times\frac{\sqrt{R_S}-1}{(\sqrt{R_S}+1)\ln R_S}\times\frac{R_S\ln R_S}{(\sqrt{R_S}-1)(\sqrt{R_S}+1)}}\right.\\
&\quad\left.-\sqrt{1+\frac{\tilde{\bar{S}}U}{\alpha_{\mathrm{L}}}\times\frac{\sqrt{R_S}-1}{(\sqrt{R_S}+1)\ln R_S}\times\frac{\ln R_S}{(\sqrt{R_S}-1)(\sqrt{R_S}+1)}}\right)\\
&= \frac{2\alpha_{\mathrm{L}}}{\tilde{\bar{\delta}}}\left(\frac{\sqrt{R_S}+1}{\sqrt{R_S}-1}\right)\left(\sqrt{1+\frac{\tilde{\bar{S}}U}{\alpha_{\mathrm{L}}}\times\frac{R_S}{(\sqrt{R_S}+1)^2}}-\sqrt{1+\frac{\tilde{\bar{S}}U}{\alpha_{\mathrm{L}}}\times\frac{1}{(\sqrt{R_S}+1)^2}}\right)\\
&= \frac{2\alpha_{\mathrm{L}}}{\tilde{\bar{\delta}}}\left(\frac{\sqrt{R_S}+1}{\sqrt{R_S}-1}\right)\left(\sqrt{1+\frac{\tilde{\bar{S}}U}{\alpha_{\mathrm{L}}(1+1/\sqrt{R_S})^2}}-\sqrt{1+\frac{\tilde{\bar{S}}U}{\alpha_{\mathrm{L}}(1+\sqrt{R_S})^2}}\right)
\end{aligned}$$

The asymmetric nature of the optical path terms under the radicals in (444) is clear. For large R_S, the first absorptance term approaches a finite-valued function of $\tilde{\bar{S}}$, U, and α_{L}. The second absorptance term, on the other hand, approaches unity. Thus the mean absorptance $\bar{\mathcal{A}}$ asymptotes to a finite value as $R_S\to\infty$. Formally, this amounts to taking the limit as $\sqrt{R_S}\gg 1$

$$\begin{aligned}
\frac{\bar{W}}{\bar{\delta}} = \bar{\mathcal{A}} &\approx \frac{2\alpha_{\mathrm{L}}}{\tilde{\bar{\delta}}}\left(\frac{\sqrt{R_S}}{\sqrt{R_S}}\right)\left(\sqrt{1+\frac{\tilde{\bar{S}}U}{\alpha_{\mathrm{L}}(1+0)}}-\sqrt{1+0}\right)\\
&= \frac{2\alpha_{\mathrm{L}}}{\tilde{\bar{\delta}}}\left(\sqrt{1+\frac{\tilde{\bar{S}}U}{\alpha_{\mathrm{L}}}}-1\right)
\end{aligned}\tag{444}$$

To obtain $\bar{W}$ and $\bar{\mathcal{A}}$ in terms of $\bar{S}$ and $\bar{\delta}$ we use (440a) in (444)

$$\begin{aligned}
\frac{\bar{W}}{\bar{\delta}} = \bar{\mathcal{A}} &= 2\alpha_{\mathrm{L}}\times\frac{\pi\chi^2}{\bar{\delta}}\left(\sqrt{1+\frac{\bar{S}}{\pi\chi^2}\times\frac{U}{\alpha_{\mathrm{L}}}}-1\right)\\
&= \frac{2\pi\alpha_{\mathrm{L}}\chi^2}{\bar{\delta}}\left(\sqrt{1+\frac{\bar{S}U}{\pi\alpha_{\mathrm{L}}\chi^2}}-1\right)
\end{aligned}\tag{445}$$

The mean absorptance of the Malkmus-Lorentz distribution $\bar{\mathcal{A}}$ (445) is thus a straightforward function of $\bar{S}$, U, α_{L}, and the parameter χ (440a). Equation (445) is valid only in the limit $\sqrt{R_S} \gg 1$.

It is more computationally economical to choose a single value of χ than to determine a new value for each band considered. The traditional approach to this has been to choose χ such that the mean absorptance of the Malkmus distribution (445) equals the mean absorptance of the exponential distribution (426) in the weak and strong line limits. The weak and strong line limits of (445) are

$$\begin{aligned}\lim_{\bar{S}U \ll 1} \bar{W} = \bar{\mathcal{A}}\bar{\delta} &\approx 2\pi\alpha_{\mathrm{L}}\chi^2 \left(1 + \frac{\bar{S}U}{2\pi\alpha_{\mathrm{L}}\chi^2} - 1\right) \\ &= \bar{S}U \end{aligned} \tag{446a}$$

$$\begin{aligned}\lim_{\bar{S}U \gg 1} \bar{W} = \bar{\mathcal{A}}\bar{\delta} &\approx 2\pi\alpha_{\mathrm{L}}\chi^2 \left(\sqrt{\frac{\bar{S}U}{\pi\alpha_{\mathrm{L}}\chi^2}} - 1\right) \\ &\approx 2\pi\alpha_{\mathrm{L}}\chi^2 \sqrt{\frac{\bar{S}U}{\pi\alpha_{\mathrm{L}}\chi^2}} \\ &= 2\chi\sqrt{\pi\bar{S}U\alpha_{\mathrm{L}}} \end{aligned} \tag{446b}$$

Equations (446a) and (428a) are an identity and yield no information on the value of $\chi(R_S)$. Equating (446b) to (428b) yields

$$\begin{aligned} 2\chi\sqrt{\pi\bar{S}U\alpha_{\mathrm{L}}} &= \sqrt{\pi\bar{S}U\alpha_{\mathrm{L}}} \\ 2\chi &= 1 \\ \chi &= 1/2 \end{aligned} \tag{447}$$

Thus the value $\chi = \frac{1}{2}$ causes (446) to agree with (428). Substituting $\chi^2 = 1/4$ into (445) yields the traditional form of the mean absorptance of the Malkmus line strength distribution for Lorentzian lines

$$\frac{\bar{W}}{\bar{\delta}} = \bar{\mathcal{A}} = \frac{\pi\alpha_{\mathrm{L}}}{2\bar{\delta}} \left(\sqrt{1 + \frac{4\bar{S}U}{\pi\alpha_{\mathrm{L}}}} - 1\right) \tag{448}$$

As mentioned above, the choice $\chi^2 = \frac{1}{4}$ (447) implies a specific choice of R_S. Starting from (440b)

$$\begin{aligned} \frac{\sqrt{R_S} - 1}{(\sqrt{R_S} + 1)\ln R_S} &= \frac{1}{4} \\ \ln R_S &= 4\left(\frac{\sqrt{R_S} - 1}{\sqrt{R_S} + 1}\right) \\ R_S &= \exp\left[4\left(\frac{\sqrt{R_S} - 1}{\sqrt{R_S} + 1}\right)\right] \end{aligned} \tag{449}$$

which is a transcendental equation in R_S. The solution of (449) appears to be imaginary, which is inconsistent with the assumption that $\sqrt{R_S} \gg 1$ (444).

6.2.5 Transmittance

The band transmittance $T_{\Delta\nu}$ of the exponential distribution (405) is the negative exponential of (426)

$$T_{\Delta\nu} = \exp\left[-\frac{\bar{S}U}{\bar{\delta}}\left(1+\frac{\bar{S}U}{\pi\alpha_{\mathrm{L}}}\right)^{-1/2}\right] \tag{450}$$

The band transmittance $T_{\Delta\nu}$ of the Malkmus distribution (409) is

$$T_{\Delta\nu} = \exp\left\{-\frac{(S/\bar{\delta})_{\Delta\nu}}{2(S/\pi\alpha_{\mathrm{L}})_{\Delta\nu}}\left[\left(1+4w\left(\frac{S}{\pi\alpha_{\mathrm{L}}}\right)_{\Delta\nu}\right)^{1/2}-1\right]\right\} \tag{451}$$

The band flux transmittance $T^F_{\Delta\nu}$ is simplified by replacing the angular integration with a diffusivity factor, D.

$$T^F_{\Delta\nu} = \exp\left\{-\frac{(S/\bar{\delta})_{\Delta\nu}}{2(S/\pi\alpha_{\mathrm{L}})_{\Delta\nu}}\left[\left(1+4Dw\left(\frac{S}{\pi\alpha_{\mathrm{L}}}\right)_{\Delta\nu}\right)^{1/2}-1\right]\right\} \tag{452}$$

As discussed in §2.2.15, $D = 1.66$ gives the best agreement between (452) and models which integrate the RT equation directly

Applying the Malkmus model to shortwave spectral regions is also possible if we redefine the diffusivity factor. For solar radiative transfer in clear skies most of the downwelling radiation follows the path of the direct solar beam. Thus the downwelling radiation traverses a mass path which increases with the cosine of the solar zenith angle θ. Defining $\mu = \cos\theta$ we have

$$T^F_{\Delta\nu} = \exp\left\{-\frac{(S/\bar{\delta})_{\Delta\nu}}{2(S/\pi\alpha_{\mathrm{L}})_{\Delta\nu}}\left[\left(1+\frac{4w}{\mu}\left(\frac{S}{\pi\alpha_{\mathrm{L}}}\right)_{\Delta\nu}\right)^{1/2}-1\right]\right\} \tag{453}$$

The role of μ in (453) is analogous to the role of D in (452). Note that both μ and D are approximations to the angular integral. Diffuse radiation, i.e., thermal emission, upwelling (scattered) solar radiation and downwelling solar radiation beneath optically thick scatterers, is better characterized by $D = 1.66$ than by μ. Direct downwelling solar radiation, on the other hand, is better characterized by μ than by $D = 1.66$.

6.2.6 Multiplication Property

It is observed that the spectrally resolved transmittance of a mixture of N gases obeys the multiplication property. Let $T(1,2,\ldots N)$ be the spectral transmittance of a mixture of N gases, and $T(i)$ be the transmittance of the ith gas alone.

$$T(1,2,\ldots N) = \prod_{i=1}^{N} T(i) \tag{454}$$

The usefulness of the multiplication property of transmittance cannot be overstated. It is basic to the construction of efficient wide band (emissivity) models.

Equation (454) may be integrated over a finite frequency interval.

$$\begin{aligned} \int_{\Delta\nu} T(1,2,\ldots N)\,\mathrm{d}\nu &= \int_{\Delta\nu} \prod_{i=1}^{N} T(i)\,\mathrm{d}\nu \\ T_{\Delta\nu}(N) &= \int_{\Delta\nu} \prod_{i=1}^{N} T(i)\,\mathrm{d}\nu \\ &= \prod_{i=1}^{N} T_{\Delta\nu}(i) \end{aligned} \tag{455}$$

The final step is strictly valid only if the spectral transmittances of the N gases are uncorrelated over the range of $\Delta\nu$. This will always be the case if the lines in these gases are randomly distributed in the interval. Fortunately, this random band assumption is met by all important atmospheric bands. Henceforth we shall consider (455) valid unless otherwise specified.

6.3 Transmission in Inhomogeneous Atmospheres

Until now we have focused on methods designed to obtain accurate spectral mean absorptance and transmittance of one or many lines over homogeneous atmospheric paths, i.e., paths along which temperature, pressure, and gas mixing ratio do not vary. This is generally a reasonable assumpution only along horizontal atmospheric paths, i.e., at constant altitude. In realistic atmospheres, at least pressure and temperature will vary vertically, and cause corresponding changes in line strength and line width (374).

6.3.1 Constant mixing ratio

Exact, analytic solutions for mean transmission through inhomogeneous atmospheres exist for Lorentzian lines in the idealized case where the gas mixing ratio is uniform, the atmosphere is isothermal at temperature T, and where, therefore, the half-width depends only on pressure p. Let q be the gas mass mixing ratio, and ρ be the atmospheric mass density so that the total gas mass concentration is $q\rho$. The Lorentzian line shape has a linear dependence on pressure (298). We shall assume hydrostatic equilibrium applies,

$$\begin{aligned} \mathrm{d}p &= -\rho g\,\mathrm{d}z \\ \mathrm{d}z &= -(\rho g)^{-1}\,\mathrm{d}p \end{aligned} \tag{456}$$

and use (456) to change variables to pressure coordinates. Referring to (271) and (273a), we may write the absorption optical depth through a uniformly mixed layer in hydrostatic

equilibrium between heights z and z' as

$$\begin{aligned}
\tau_{\mathrm{a}}(z,z') &= \int_0^U S\Phi_{\mathrm{L}}(z'')\,\mathrm{d}U \\
&= \int_z^{z'} S\Phi_{\mathrm{L}}(z'')q\rho(z'')\,\mathrm{d}z'' \\
&= \int_z^{z'} \frac{S\alpha_{\mathrm{L}}(z'')q\rho(z'')}{\pi[\nu^2+\alpha_{\mathrm{L}}(z'')^2]}\,\mathrm{d}z'' \\
&= \int_p^{p'} \frac{S\alpha_{\mathrm{L}}(p'')q\rho(p'')}{\pi[\nu^2+\alpha_{\mathrm{L}}(p'')^2]}\left(-\frac{\mathrm{d}p''}{\rho g}\right) \\
&= \frac{Sq}{\pi g}\int_{p'}^{p} \frac{\alpha_{\mathrm{L}}(p'')}{\nu^2+\alpha_{\mathrm{L}}(p'')^2}\,\mathrm{d}p'' \\
&= \frac{Sq}{\pi g}\int_{\alpha_{\mathrm{L}}(p')}^{\alpha_{\mathrm{L}}(p)} \frac{\alpha_{\mathrm{L}}}{\nu^2+\alpha_{\mathrm{L}}^2}\,\mathrm{d}\alpha_{\mathrm{L}} \\
&= \frac{Sq}{\pi g}\left[\frac{1}{2}\ln\left(\nu^2+\alpha_{\mathrm{L}}^2\right)\right]_{\alpha_{\mathrm{L}}(p')}^{\alpha_{\mathrm{L}}(p)} \\
&= \frac{Sq}{2\pi g}\ln\frac{\nu^2+\alpha_{\mathrm{L}}(z)^2}{\nu^2+\alpha_{\mathrm{L}}(z')^2} \\
&\quad \ldots \text{fxm: find error in above!} \\
&= \frac{SU}{2\pi\alpha_{\mathrm{L}}(z)}\ln\frac{\nu^2+\alpha_{\mathrm{L}}(z)^2}{\nu^2+\alpha_{\mathrm{L}}(z')^2}
\end{aligned} \tag{457}$$

where we have used the simple relationship $U = qp/g$ to determine the mass path of a gas with constant mixing ratio q.

Near the top of the atmosphere, the line shape approaches the Doppler shape Φ_{D} (311). In an isothermal atmosphere $\tilde{\alpha}_{\mathrm{D}}$ does not depend on height. The optical depth from level z to space is

$$\tau_{\mathrm{a}}(z,z') = \frac{Sq}{2\pi g}\ln\frac{\nu^2+\alpha_{\mathrm{L}}(z)^2}{\nu^2+\tilde{\alpha}_{\mathrm{D}}^2} \tag{458}$$

6.3.2 van de Hulst-Curtis-Godson Approximation

The general problem is to account for the effects of inhomogeneous mass, temperature, and pressure paths on transmission. We shall attempt to determine a scaled absorber path $\tilde{U}$, scaled temperature $\tilde{T}$, and scaled pressure $\tilde{p}$ such that $\tilde{U}$, $\tilde{T}$, and $\tilde{p}$ yield optimal results when employed in our machinery for homogeneous paths, e.g., (450), (451). We shall show that the scaled parameters can be chosen to yield correct band transmittances in certain limits.

The extra degree of freedom permitted by each parameter means that $\tilde{U}$, $\tilde{T}$, and $\tilde{p}$ form a three-parameter scaling approximation. The researchers van de Hulst, Curtis, and Godson independently discovered the following scaling approximation, now known as the H-C-G approximation. First we note that absorption along a path in Earth's atmosphere is generally more affected by changes in p than by changes in T. This stands to reason since p

changes by many orders of magnitude from the surface to space, while T generally changes by less than 30%. Thus the usual practice, often adeequate, is to set $\tilde{T}$ equal to the mean temperature along a path,

$$\tilde{T} \;=\; \bar{T} \tag{459}$$

This leaves two parameters, $\tilde{U}$ and $\tilde{p}$, to account for the effects of inhomogeneity on path absorption. We first derive a single parameter scaling approximation based solely on $\tilde{U}$. This will prove useful afterwards in developing the two parameter H-C-G approximation.

Consider the absorption optical depth through an arbitrary inhomogeneous atmosphere whose mass absorption coefficient $\psi(p,T)$ (277) depends only on T and p. The optical path through this medium is (271)

$$\tau_\mathrm{a} \;=\; \int \psi(p,T)\,\mathrm{d}U \tag{460}$$

A one-parameter scaling approximation is exact if $\psi(p,T)$ can be separated into a frequency-dependent function $\eta(\nu)$ times a p-T dependent function $\Phi(p,T)$ (Goody and Yung, 1989, p. 224)

$$\begin{aligned} \psi(p,T) &= \Phi(p,T)\,\eta(\nu) \\ \Phi(p,T) &= \psi(p,T)/\eta(\nu) \end{aligned} \tag{461}$$

Applying this separation of variables (461) to (460) yields

$$\begin{aligned} \tau_\mathrm{a} &= \int \Phi(p,T)\,\eta(\nu)\,\mathrm{d}U \\ &= \int \Phi(p,T)\frac{\Phi(\tilde{p},\tilde{T})}{\Phi(\tilde{p},\tilde{T})}\,\eta(\nu)\,\mathrm{d}U \\ &= \int \frac{\Phi(p,T)}{\Phi(\tilde{p},\tilde{T})}\frac{\psi(\tilde{p},\tilde{T})}{\eta(\nu)}\,\eta(\nu)\,\mathrm{d}U \\ &= \int \psi(\tilde{p},\tilde{T})\frac{\Phi(p,T)}{\Phi(\tilde{p},\tilde{T})}\,\mathrm{d}U \end{aligned}$$

We see that $\psi(\tilde{p},\tilde{T})$ is independent of the variable of integration, U, since both $\tilde{p}$ and $\tilde{T}$ are path-mean quantities. Therefore $\psi(\tilde{p},\tilde{T})$ may be placed outside the integrand

$$\begin{aligned} \tau_\mathrm{a} &= \psi(\tilde{p},\tilde{T})\int \frac{\Phi(p,T)}{\Phi(\tilde{p},\tilde{T})}\,\mathrm{d}U \\ &= \psi(\tilde{p},\tilde{T})\tilde{U} \qquad \text{where} \\ \tilde{U} &\equiv \int \frac{\Phi(p,T)}{\Phi(\tilde{p},\tilde{T})}\,\mathrm{d}U \end{aligned} \tag{462}$$

The scaled absorber amount, $\tilde{U}$, together with the absorption coefficient evaluated for the scaled temperature and pressure, exactly predicts the absorption optical path (460).

The exact form of the scaling function $\Phi(p,T)$ is chosen to optimize the accuracy of (462). The definition (461) makes clear that $\Phi(p,T)$ is a weighting function that does not explicitly depend on frequency, and yet must somehow account for the temperature dependence of all the lines with the band. Line strengths are highly temperature dependent (374). Considering first Doppler lines, we note that the Doppler line width $\tilde{\alpha}_{\mathrm{D}}$ (310) has no pressure dependence, but does depend on $\sqrt{T}$. Both strong and weak Doppler lines within a given band will therefore be well-represented by identifying the scaling function $\Phi(p,T)$ with the line strength S

$$\Phi(p,T) \;=\; \sum_{i}^{N} S_i(T) \tag{463}$$

Thus $\Phi(p,T)$ has no explicit pressure dependence in this case.

Chou and Arking (1980) present a more formalized one-parameter scaling based on the presumption (appropriate for water vapor) that errors due to inhomogeneity are likely to bias line wing absorption more than line center absorption. Liou (1992), p. presents a detailed account of this scaling.

The H-C-G approximation, sometimes called the C-G approximation, …

6.4 Temperature Dependence

SWNB evaluates the temperature dependence of the random band parameters. Let T_0 be the temperature at which the line parameters (strengths, half-widths) are known. Typically $\mathrm{T}_0 = 296\,\mathrm{K}$, the reference temperature of the HITRAN database discussed in §5.5.1. The H-C-G approximation accounts for the influence of temperature and pressure inhomogeneity along the path on the absorption (460). The scaling functions $\Phi(T)$ and $\Psi(T)$ at an arbitrary temperature T are

$$\Phi(T) \;\equiv\; \sum_{i}^{N} S_i(T) \Big/ \sum_{i}^{N} S_i(\mathrm{T}_0) \tag{464}$$

$$\Psi(T) \;\equiv\; \left(\sum_{i}^{N} \sqrt{S_i(T)\alpha_{\mathrm{L}}(\mathrm{p}_0,T)} \right)^2 \Big/ \left(\sum_{i}^{N} \sqrt{S_i(\mathrm{T}_0)\alpha_{\mathrm{L}}(\mathrm{p}_0,\mathrm{T}_0)} \right)^2 \tag{465}$$

where $S_i(T)$ is scaled from $S_i(\mathrm{T}_0)$ using (374) and $\alpha_{\mathrm{L}}(\mathrm{p}_0,T)$ is scaled from $\alpha_{\mathrm{L}}(\mathrm{p}_0,\mathrm{T}_0)$ using (377).

The scaled absorber path $\tilde{U}$ is

$$\tilde{U} \;=\; \int q\Phi(T)\,\frac{\mathrm{d}p}{g} \tag{466}$$

The scaled pressure $\tilde{p}$ is

$$\tilde{p} \;=\; \frac{1}{\tilde{U}} \int q\Psi(T)\,\frac{p}{\mathrm{p}_0}\,\frac{\mathrm{d}p}{g} \tag{467}$$

Following Rodgers and Walshaw (1966), we fit the logarithms of $\Phi(T)$ and $\Psi(T)$ to quadratic polynomials in temperature

$$\ln \Phi(T) = a_\Phi (T - \mathrm{T}_0) + b_\Phi (T - \mathrm{T}_0)^2 \tag{468a}$$

$$\ln \Psi(T) = a_\Psi (T - \mathrm{T}_0) + b_\Psi (T - \mathrm{T}_0)^2 \tag{468b}$$

The linear term dominates (468a) since $\Phi(T)$ (463) depends mostly exponentially on T (374), i.e., $a_\Phi \gg b_\Phi$. On the other hand the quadratic term is important in (468b) since $\Psi(T)$ (??) contains significant nonlinear behavior. The coefficients a_Φ, b_Φ, a_Ψ, and b_Ψ are determined by least-squares fitting Φ and Ψ at discrete temperatures T_k over the temperature range of interest:

$$a_\Phi = \frac{\sum_k (T_k - \mathrm{T}_0) \ln \Phi(T_k) \sum_k (T_k - \mathrm{T}_0)^4 - \sum_k (T_k - \mathrm{T}_0)^2 \ln \Phi(T_k) \sum_k (T_k - \mathrm{T}_0)^3}{\sum_k (T_k - \mathrm{T}_0)^2 \sum_k (T_k - \mathrm{T}_0)^4 - \sum_k (T_k - \mathrm{T}_0)^3 \sum_k (T_k - \mathrm{T}_0)^3} \tag{469a}$$

$$b_\Phi = \frac{\sum_k (T_k - \mathrm{T}_0)^2 \ln \Phi(T_k) \sum_k (T_k - \mathrm{T}_0)^2 - \sum_k (T_k - \mathrm{T}_0) \ln \Phi(T_k) \sum_k (T_k - \mathrm{T}_0)^3}{\sum_k (T_k - \mathrm{T}_0)^2 \sum_k (T_k - \mathrm{T}_0)^4 - \sum_k (T_k - \mathrm{T}_0)^3 \sum_k (T_k - \mathrm{T}_0)^3} \tag{469b}$$

and a_Ψ and b_Ψ are defined analogously.

In practice SWNB adjusts all band parameters from the HITRAN-standard temperature (296 K) to 250 K, roughly the mass-weighted mean temperature of Earth's atmosphere. This reduces any biases caused by non-quadratic temperature-dependent behavior of the logarithms of $\Phi(T)$ and $\Psi(T)$ (469). $\Phi(T)$ and $\Psi(T)$ are evaluated exactly in the temperature range $180 < T_k < 320$ K with a 1 K resolution and the results are fit using (469). The expressions (469) are generally accurate to within 1% over this 140 K range.

6.5 Transmission in Spherical Atmospheres

Until this point we have assumed plane-parellel boundary conditions. That is we have assumed the increase in path length due to off-vertical transmission is given by the secant of the solar zenith angle times the vertical path. Planetary atmospheres are, of course, spherical and the plane parallel approximation must be corrected for spherical effects when the zenith angle is large. Horizontal irradiances must be corrected if the zenith angle is greater than about 80°.

6.5.1 Chapman Function

The earliest quantitative computations of the absorber path to space at arbitrary angles through a spherical atmosphere were made by Sidney Chapman. Let H be the scale height of the species, so that

$$n(z) \quad = \quad n(\mathrm{z}_0) \mathrm{e}^{-(z - \mathrm{z}_0)/H} \tag{470}$$

The scale height well-mixed gases in Earth's atmosphere is about 7 km. Let $r_\oplus$ be the Earth's radius, and z_0 be the altitude at which the absorber path is to begin. With the assumption that the species is distributed exponentially with altitude (470), the number path N from height z_0 to space at a polar angle θ_0 reduces to

$$N(\mathrm{z}_0, \theta_0) \quad = \quad \int_{z=\mathrm{z}_0}^{z=\infty} n(z) \left[1 - \frac{(r_\oplus + \mathrm{z}_0) \sin(\theta_0)}{(r_\oplus + z)^2} \right]^{-1/2} \mathrm{d}z$$

It can be shown that the number path N (471) is a function of a dimensionless measure called the radius of curvature of the absorber distribution X

$$X = (r_\oplus + \mathrm{z}_0)/H \tag{471}$$

According to Huestis, X varies from about 300 to 1300 on Earth. The Chapman function Ch (e.g., Rees, 1989) is defined implicitly by the RHS of (471). It directly relates $N(\mathrm{z}_0, \theta_0)$ to the scale height H and local number concentration $n(z)$ of a species via

$$N(\mathrm{z}_0, \theta_0) = Hn(\mathrm{z}_0)\mathrm{Ch}(X, \theta_0) \tag{472}$$

Note that Ch (472) depends only on X, not on the individual values of $r_\oplus$, z_0, and H.

7 Radiative Effects of Aerosols and Clouds

Interaction of radiation and matter occurs on three scales. On the molecular scale, the scattering and absorption of radiation is described by the ambient concentration, scattering cross sections, reasonant frequencies, and quantum states of the molecule. Interaction of radiation with bulk phase matter (e.g., the sea surface) is described by the change in the index of refraction of the media (e.g., Snell's law) and macroscopic thermodynamic properties such as $F^+ = \sigma T^4$ (117). In between these two scales is the interaction of radiation with atmospheric particulates, i.e., aerosols and hydrometeors. Particulates are, by definition, isolated bodies of condensed matter surrounded by a continuous media. We now turn our attention to describing the effects of particulates on the radiation field.

7.1 Single Scattering Properties

Three properties are required to exactly specify the radiative effects of particles. The properties define the total extinction (scattering plus absorption) due to the particle, the probability an interaction results in absorption rather than scattering, and, finally, the angular distribution of scattered photons as a function of the incident angle. By convention, the properties defining the above attributes are usually specified as the extinction optical depth τ_e, the single scattering albedo ϖ, and the asymmetry parameter g. These three parameters, τ_e, ϖ, and g, are known collectively as the single scattering properties of the particles. These properties depend in turn on the mass, size, and composition of the particle species.

A particle's chemical composition determines its index of refraction[16] n. The index of refraction is a dimensionless, complex number

$$n = n_\mathrm{r} + \mathrm{i}n_\mathrm{i} \tag{473}$$

All the physics describing the fundamental electromagnetic properties of the material are consolidated into n. n_r describes the scattering properties of the medium while n_i describes

[16]Care must be taken not to confuse the complex index of refraction n (dimensionless) with the size distribution n_n [$\#\,\mathrm{m}^{-3}\,\mathrm{m}^{-1}$]. The former is a function of wavelength for a given chemical composition, while the latter is a function of size for a given particle population. The meaning should be clear from the context.

the absorption properties of the medium. The literature disagrees about the sign convention for n_{i}. We choose to represent n_{i} as positive-definite, i.e., $n_{\mathrm{i}} > 0$. This convention is employed by Bohren and Huffman (1983), among others.

n_{r} and n_{i} are fundamental properties of matter and must be determined from laboratory studies (e.g., Hess et al., 1998; Patterson et al., 1977; Patterson, 1981; Perovich and Govoni, 1991; Tang, 1997; Volz, 1973; Bohren and Huffman, 1983), or from models constrained by field measurements (e.g., Colarco et al., 2002; Sinyuk et al., 2003). The HITRAN database (Rothman et al., 1998) contains a compilation of n for many aerosols of atmospheric interest.

7.1.1 Maxwell Equations

The macroscopic form of Maxwell's equations in Rationalized SI (MKSA) units is (Bohren and Huffman, 1983, p. 12)

$$\nabla \cdot \mathbf{D} = \rho_{\mathrm{F}} \qquad \text{Coulomb's law} \tag{474a}$$

$$\nabla \cdot \mathbf{B} = 0 \tag{474b}$$

$$\nabla \times \mathbf{E} + \frac{\partial \mathbf{B}}{\partial t} = 0 \qquad \text{Faradays's law} \tag{474c}$$

$$\nabla \times \mathbf{H} = \mathbf{J}_{\mathrm{F}} + \frac{\partial \mathbf{D}}{\partial t} \qquad \text{Maxwell's generalization of Ampere's law} \tag{474d}$$

where $\mathbf{E}$ is the electric field measured in Volts per meter [$\mathrm{V\,m^{-1}}$], $\mathbf{B}$ is the magnetic induction measured in Tesla [T], and $\mathbf{J}_{\mathrm{F}}$ is the free current density measured in Amperes per square meter [$\mathrm{A\,m^{-2}}$]. In this context, macroscopic refers to spatio-temporal averaging of the Maxwell equations in a vacuum. Clearly (474) applies to microscopic spaces, since it is expressed in terms of differentials, though it does not apply at the smallest molecular scales.

The electric displacement $\mathbf{D}$ and magnetic field $\mathbf{H}$ are defined by

$$\mathbf{D} = \varepsilon_0 \mathbf{E} + \mathbf{P} \tag{475a}$$

$$\mathbf{H} = \frac{\mathbf{B}}{\mu_0} - \mathbf{M} \tag{475b}$$

where $\mathbf{P}$ is the electric polarization (mean electric dipole moment per unit volume), $\mathbf{M}$ is the magnetization (mean magnetic dipole moment per unit volume). $\mathbf{P}$ is measured in [$\mathrm{C\,m^{-2}}$], and $\mathbf{M}$ is measured in [$\mathrm{A\,m^{-1}}$]. The scalar symbols are the free charge density ρ_{F}, measured in [$\mathrm{C\,m^{-3}}$], the permittivity of free space ε_0, measured in [$\mathrm{F\,m^{-1}}$], the permeability of free space μ_0, measured in [$\mathrm{H\,m^{-1}}$].

The constitutive equations in SI units are (Bohren and Huffman, 1983, p. 13)

$$\mathbf{J}_{\mathrm{F}} = \sigma \mathbf{E} \tag{476a}$$

$$\mathbf{B} = \mu \mathbf{H} \tag{476b}$$

$$\mathbf{P} = \varepsilon_0 \chi \mathbf{E} \tag{476c}$$

Here σ is the conductivity which is measured in Siemens [S], Amperes per volt [$\mathrm{A\,V^{-1}}$], or mhos per meter [$\mathrm{mho\,x^{-1}}$]. μ is the permeability measured in [$\mathrm{H\,m^{-1}}$]. χ is the electric susceptibility measured in Farads per meter [$\mathrm{F\,m^{-1}}$] or [$\mathrm{C\,V^{-1}\,m^{-1}}$]. Together, σ, μ, and χ are

known as the phenomenological coefficients—they define the medium under consideration. In a linear medium, these coefficients do not depend upon the electromagnetic field. In a homogeneous medium, these coefficients are independent of position. In an isotropic medium, these coefficients are independent of direction. The media we consider is assumed to be linear, homogeneous, and isotropic.

We shall now simplify the Maxwell equations (474) to the problem of scattering of radiation by matter described by the the constitutive equations (476). Subsituting (476c) into (475a) and (475a) into (474a), we obtain

$$\nabla \cdot \mathbf{D} = \nabla \cdot (\varepsilon_0 \mathbf{E} + \varepsilon_0 \chi \mathbf{E}) = \varepsilon_0 (1 + \chi) \nabla \cdot \mathbf{E} = \rho_{\mathrm{F}} \tag{477}$$

Subsituting (476b) into (474b) leads to

$$\nabla \cdot \mathbf{B} = \nabla \cdot (\mu \mathbf{H}) = \mu \nabla \cdot \mathbf{H} = \nabla \cdot \mathbf{H} = 0 \tag{478}$$

Subsituting (476b) into (474c) leads to

$$\nabla \times \mathbf{E} + \frac{\partial \mu \mathbf{H}}{\partial t} = 0 \tag{479}$$

Subsituting (476c) into (475a), and then sustituting (476a) and (475a) into (474d), we obtain

$$\nabla \times \mathbf{H} = \sigma \mathbf{E} + \frac{\partial (\varepsilon_0 \mathbf{E} + \varepsilon_0 \chi \mathbf{E})}{\partial t} = \sigma \mathbf{E} + \varepsilon_0 (1 + \chi) \frac{\partial \mathbf{E}}{\partial t} \tag{480}$$

where ε, the complex permittivity is defined by

$$\varepsilon = \varepsilon_0 (1 + \chi) + \mathrm{i} \frac{\sigma}{\omega} \tag{481}$$

We assume the time-variation of the electro-magnetic field is harmonic, i.e., of the form $\mathbf{E} \propto \exp(-\mathrm{i}\omega t)$ where ω is the angular frequency. The particular problem we wish to solve is the scattering of incident plane waves by a sphere. The harmonic plane wave definition (237) is

$$\mathbf{E}_{\mathrm{c}}(\mathbf{r}, t) = \mathbf{E}_0 \exp[\mathrm{i}(\mathbf{k} \cdot \mathbf{r} - \omega t)] \tag{482}$$

where the subscript c denotes complex plane wave. With this assumption, the Maxwell equations for the medium (477)–(480) impose a dispersive relationship upon wave characteristics of (237).

$$\nabla \cdot \mathbf{E}_{\mathrm{c}} = 0 \tag{483a}$$
$$\nabla \cdot \mathbf{H}_{\mathrm{c}} = 0 \tag{483b}$$
$$\nabla \times \mathbf{E}_{\mathrm{c}} = \mathrm{i}\omega\mu \mathbf{H}_{\mathrm{c}} \tag{483c}$$
$$\nabla \times \mathbf{H}_{\mathrm{c}} = -\mathrm{i}\omega\varepsilon \mathbf{E}_{\mathrm{c}} \tag{483d}$$

Electrodynamics texts are often written in CGS (Gaussian) units. The Maxwell equations in all common units appear in Jackson (1975) p. 818.

The coupled vector equations (483) will prove more tractable once they are reduced to coupled scalar equations. This will be accomplished by exercising (483) with some vector mathematics (560). First we take the curl of equations (483c) and (483d):

$$\begin{aligned}\nabla\times\nabla\times\mathbf{E}_c &= \nabla\times(\mathrm{i}\omega\mu\mathbf{H}_c)\\ &= \mathrm{i}\omega\mu\nabla\times\mathbf{H}_c\\ &= \mathrm{i}\omega\mu(-\mathrm{i}\omega\varepsilon\mathbf{E}_c)\\ &= \omega^2\mu\varepsilon\mathbf{E}_c \qquad (484a)\\ \nabla\times\nabla\times\mathbf{H}_c &= \nabla\times(-\mathrm{i}\omega\varepsilon\mathbf{E}_c)\\ &= -\mathrm{i}\omega\varepsilon\nabla\times\mathbf{E}_c\\ &= -\mathrm{i}\omega\varepsilon(\mathrm{i}\omega\mu\mathbf{H}_c)\\ &= \omega^2\mu\varepsilon\mathbf{H}_c \qquad (484b)\end{aligned}$$

We introduce the wavenumber k as

$$\mathrm{k}^2 = \omega^2\mu\varepsilon \qquad (485)$$

Applying (560j) to (484) results in

$$\begin{aligned}\nabla\times\nabla\times\mathbf{E}_c = \nabla(\nabla\cdot\mathbf{E}_c) - \nabla\cdot(\nabla\mathbf{E}_c) &= \omega^2\mu\varepsilon\mathbf{E}_c\\ \nabla(0) - \nabla\cdot(\nabla\mathbf{E}_c) + \omega^2\mu\varepsilon\mathbf{E}_c &= 0\\ \nabla^2\mathbf{E}_c + \mathrm{k}^2\mathbf{E}_c &= 0 \qquad (486a)\\ \nabla^2\mathbf{H}_c + \mathrm{k}^2\mathbf{H}_c &= 0 \qquad (486b)\end{aligned}$$

where the derivation of (486b) follows (486a). Thus both the electric and magnetic fields satisfy the vector wave equation (486a)–(486b), as well as the Maxwell equations for time-harmonic fields (483). In fact, any two vector fields $\mathbf{M}$ and $\mathbf{N}$ which satisfy (486) and (483) are valid electric and magnetic fields. In keeping with convention (Bohren and Huffman, 1983), we let $\mathbf{M}$ and $\mathbf{N}$ denote a candidate pair of solutions to the electro-magnetic field equations.

We shall apply a gauge transformation to simplify the Maxwell equations for a plane wave scattering from a sphere. This transformation identifies a scalar generating function which satisfies the scalar wave equation. This generating function then determines $\mathbf{M}$ and $\mathbf{N}$. The problem thus reduces to identifying the correct scalar field. Denote the scalar field by u and introduce a constant vector function $\mathbf{c}$ such that

$$\begin{aligned}\mathbf{M} &= \nabla\times(u\mathbf{c}) \qquad (487)\\ &= \nabla u\times\mathbf{c} + u\nabla\times\mathbf{c} \qquad (488)\end{aligned}$$

where (488) follows from the vector identity for the curl of a product (560v). The divergence of $\mathbf{M}$ (487) is zero since $\mathbf{M}$ is the curl of a vector field (560s)

$$\nabla\cdot\mathbf{M} = 0 \qquad (489)$$

The curl of $\mathbf{M}$ (487) is

$$\begin{aligned} \nabla \times \mathbf{M} &= \nabla \times [\nabla \times (u\mathbf{c})] \\ &= \nabla[\nabla \cdot (u\mathbf{c})] - \nabla^2(u\mathbf{c}) \quad (490) \\ &= \nabla \times (\nabla u \times \mathbf{c} + u\nabla \times \mathbf{c}) \quad (491) \end{aligned}$$

where (492) comes from the vector identity for the curl of a curl (560j) and (491) arises from direct subsitution of (488). Neither of these expressions is particularly appealing for direct evaluation. We proceed from (492) armed with the vector identities for the gradient of a divergence (560n) and the Laplacian of a vector (560k)

$$\begin{aligned} &= \nabla \times (\nabla u \times \mathbf{c} + u\nabla \times \mathbf{c}) \\ &= \nabla[\mathbf{c} \cdot \nabla u + u\nabla \cdot \mathbf{c}] - \nabla[\nabla \cdot (u\mathbf{c})] - \nabla \times [\nabla \times (u\mathbf{c})] \end{aligned}$$

Applying (560m) to (489)

$$fxm \quad (492)$$

…leads to the desired result

$$\nabla^2\mathbf{M} + \mathrm{k}^2\mathbf{M} = \nabla \times [\mathbf{c}(\nabla^2 u + \mathrm{k}^2 u)] \quad (493)$$

If u satisfies the scalar wave equation then the RHS of (494) vanishes and $\mathbf{M}$ must satisfy the vector wave equation.

$$\nabla^2\mathbf{M} + \mathrm{k}^2\mathbf{M} = 0 \quad (494)$$

As $\mathbf{M}$ was constructed from the curl of $\mathbf{c}$ (487) , so may we construct a new vector function $\mathbf{N}$ from the curl of $\mathbf{M}$

$$\mathbf{N} = \frac{\nabla \times \mathbf{M}}{\mathrm{k}} \quad (495)$$

The divergence of $\mathbf{N}$ vanishes since $\mathbf{N}$ is the curl of a vector field (560s). Hence $\mathbf{N}$ also satisfies the vector wave equation

$$\nabla^2\mathbf{N} + \mathrm{k}^2\mathbf{N} = 0 \quad (496)$$

This implies that

$$\nabla \times \mathbf{N} = \mathrm{k}\mathbf{M} \quad (497)$$

We constructed $\mathbf{M}$ and $\mathbf{N}$ to behave like electric and magnetic fields, respectively. First, they are construced from the curls of vector fields and so their divergence vanishes (560s), as (483a)–(483b). Second, relations (495) and (497) show that the curls of $\mathbf{M}$ and $\mathbf{N}$ are mutually proportional, as are (483c)–(483d). Third, relations (494) and (496) show that $\mathbf{M}$ and $\mathbf{N}$ satisfy the vector wave equations.

7.2 Separation of Variables

We now seek a function u which satisfies the scalar wave equation (the Helmholtz equation) in spherical coordinates

$$\nabla^2 u + \mathrm{k}^2 u = 0 \tag{498}$$

$$\frac{1}{r^2}\frac{\partial}{\partial r}\left(r^2\frac{\partial u}{\partial r}\right) + \frac{1}{r^2\sin\theta}\frac{\partial}{\partial\theta}\left(\sin\theta\frac{\partial u}{\partial\theta}\right) + \frac{1}{r^2\sin^2\theta}\frac{\partial^2 u}{\partial\phi^2} + \mathrm{k}^2 u = 0 \tag{499}$$

The separation of variables procedure attempts to find u as the product of three independent functions—one for each radial and angular coordinate:

$$u(r,\theta,\phi) = R(r)\Theta(\theta)\Phi(\phi) \tag{500}$$

where $R(r)$, $\Theta(\theta)$, and $\Phi(\phi)$ contain the radial, polar, and azimuthally dependent components of u. Substituting (500) into (499) and dividing by $R\Theta\Phi$ we obtain (Arfken, 1985, p. 115)

$$\frac{1}{Rr^2}\frac{\mathrm{d}}{\mathrm{d}r}\left(r^2\frac{\mathrm{d}R}{\mathrm{d}r}\right) + \frac{1}{\Theta r^2\sin\theta}\frac{\mathrm{d}}{\mathrm{d}\theta}\left(\sin\theta\frac{\mathrm{d}\Theta}{\mathrm{d}\theta}\right) + \frac{1}{\Phi r^2\sin^2\theta}\frac{\mathrm{d}^2\Phi}{\mathrm{d}\phi^2} = -\mathrm{k}^2 \tag{501}$$

The differentials are full, not partial.

7.2.1 Azimuthal Solutions

We isolate the second order derivative of Φ by multiplying (501) by $r^2\sin^2\theta$— this is ill-defined at the poles, a detail we neglect:

$$\frac{1}{\Phi}\frac{\mathrm{d}^2\Phi}{\mathrm{d}\phi^2} = r^2\sin^2\theta\left[-\mathrm{k}^2 - \frac{1}{Rr^2}\frac{\mathrm{d}}{\mathrm{d}r}\left(r^2\frac{\mathrm{d}R}{\mathrm{d}r}\right) - \frac{1}{\Theta r^2\sin\theta}\frac{\mathrm{d}}{\mathrm{d}\theta}\left(\sin\theta\frac{\mathrm{d}\Theta}{\mathrm{d}\theta}\right)\right] \tag{502}$$

Equation (502) has the interesting property that its LHS and RHS are equal yet depend on completely independent variables (ϕ and r,θ, respectively). This can be true for all values of r, θ, and ϕ if and only if both sides are constant—the so-called separation constant. Since the LHS is an azimuthal angle, we expect $\Phi(\phi)$ to be periodic, i.e., to repeat every 2π radians. Recognizing the LHS allows simple trigonometric solutions, we denote the separation constant by $-m^2$.

$$\frac{1}{\Phi}\frac{\mathrm{d}^2\Phi}{\mathrm{d}\phi^2} = -m^2$$

$$\frac{\mathrm{d}^2\Phi}{\mathrm{d}\phi^2} = -m^2\Phi$$

$$\Phi_m(\phi) = C_{1,m}\mathrm{e}^{\mathrm{i}m\phi} + C_{2,m}\mathrm{e}^{-\mathrm{i}m\phi} \tag{503}$$

$$\Phi_m(\phi) = C_{1,m}\cos m\phi + C_{2,m}\sin m\phi \tag{504}$$

where $C_{1,m}$ and $C_{2,m}$ are constants of integration determined by the boundary conditions. A requirement of our physical problem, Mie scattering, is that the resulting electromagnetic

fields be single-valued. In other words, a given azimuthal angle ϕ must be associated with only one functional value so that

$$\Phi(\phi + 2\pi) \quad = \quad \Phi(\phi) \tag{505}$$

Requirement (505) can be met only if m is an integer. Consider, for example $m = \frac{1}{2}$. In this hypothetical case, $\Phi(\phi)$ is double-valued since

$$\cos m\phi = \cos\tfrac{\phi}{2} \neq \cos\tfrac{\phi+2\pi}{2} = \cos(\tfrac{\phi}{2} + \pi) = -\cos\tfrac{\phi}{2} \tag{506}$$

This does not satisfy requirement (505). Hence the physical requirements of the Mie problem require that m is integral.

The symmetries involved in Mie scattering make it useful to distinguish the even and odd components of Φ. We note that $\cos m\phi$ and $\sin m\phi$ are symmetric and anti-symmetric, respectively, so that

$$C_{1,m}\cos m\phi = C_{1,m}\cos[(-m)\phi] \tag{507a}$$
$$C_{2,m}\sin m\phi = -C_{2,m}\sin[(-m)\phi] \tag{507b}$$

Following Bohren and Huffman (1983), p. 85, we subscript even functions with e and odd function with o.

$$\begin{aligned}\Phi_{\mathrm{e},m} &= C_{1,m}\cos m\phi \\ \Phi_{\mathrm{o},m} &= C_{2,m}\sin m\phi \\ \Phi_m(\phi) &= \Phi_{\mathrm{e},m} + \Phi_{\mathrm{o},m}\end{aligned} \tag{508a}$$

The negative sign arising from anti-symmetric functions (507b) may be subsumed into $C_{2,m}$ so that all linear all linear combinations of $\Phi_{\mathrm{e},m}$ and $\Phi_{\mathrm{o},m}$ are obtainable with positive integers m. Hence we may assume that m takes only positive (or zero) integer values.

Since $\cos m\phi$ and $\sin m\phi$ are orthonormal, any azimuthal function can be decomposed into a series of these basis functions

$$\Phi(\phi) \quad = \quad \sum_{m=0}^{\infty} C_{1,m}\cos m\phi + C_{2,m}\sin m\phi \tag{509}$$

7.2.2 Polar Solutions

The polar and radial components of (502) now must satisfy

$$\frac{1}{Rr^2}\frac{\mathrm{d}}{\mathrm{d}r}\left(r^2\frac{\mathrm{d}R}{\mathrm{d}r}\right) + \frac{1}{\Theta r^2\sin\theta}\frac{\mathrm{d}}{\mathrm{d}\theta}\left(\sin\theta\frac{\mathrm{d}\Theta}{\mathrm{d}\theta}\right) - \frac{m^2}{r^2\sin^2\theta} \quad = \quad -\mathrm{k}^2 \tag{510}$$

To separate the radial and polar terms, multiply (510) by r^2 and re-group

$$\begin{aligned}\frac{1}{R}\frac{\mathrm{d}}{\mathrm{d}r}\left(r^2\frac{\mathrm{d}R}{\mathrm{d}r}\right) + \frac{1}{\Theta\sin\theta}\frac{\mathrm{d}}{\mathrm{d}\theta}\left(\sin\theta\frac{\mathrm{d}\Theta}{\mathrm{d}\theta}\right) - \frac{m^2}{\sin^2\theta} &= -\mathrm{k}^2r^2 \\ \frac{1}{R}\frac{\mathrm{d}}{\mathrm{d}r}\left(r^2\frac{\mathrm{d}R}{\mathrm{d}r}\right) + \mathrm{k}^2r^2 &= -\frac{1}{\Theta\sin\theta}\frac{\mathrm{d}}{\mathrm{d}\theta}\left(\sin\theta\frac{\mathrm{d}\Theta}{\mathrm{d}\theta}\right) + \frac{m^2}{\sin^2\theta}\end{aligned} \tag{511}$$

The LHS and RHS of Equation (511) must each equal a (new) separation constant for the same reasons given for the separation constant in Equation (502). We label this separation constant Q.

$$\begin{aligned} -\frac{1}{\Theta \sin\theta}\frac{\mathrm{d}}{\mathrm{d}\theta}\left(\sin\theta\frac{\mathrm{d}\Theta}{\mathrm{d}\theta}\right)+\frac{m^2}{\sin^2\theta} &= Q \\ \frac{1}{\sin\theta}\frac{\mathrm{d}}{\mathrm{d}\theta}\left(\sin\theta\frac{\mathrm{d}\Theta}{\mathrm{d}\theta}\right)+\left[Q-\frac{m^2}{\sin^2\theta}\right]\Theta &= 0 \end{aligned} \tag{512}$$

The radial component is

$$\begin{aligned} \frac{1}{R}\frac{\mathrm{d}}{\mathrm{d}r}\left(r^2\frac{\mathrm{d}R}{\mathrm{d}r}\right)-\mathrm{k}^2r^2 &= Q \\ \frac{\mathrm{d}}{\mathrm{d}r}\left(r^2\frac{\mathrm{d}R}{\mathrm{d}r}\right)+[\mathrm{k}^2r^2-Q]R &= 0 \end{aligned} \tag{513}$$

It is a well-known result that the separation constant Q is quantized and takes positive integral values defined by $Q = n(n+1)$. The reasoning for this is fxm. Substituting this into (512) and (513) and we obtain

$$\frac{1}{\sin\theta}\frac{\mathrm{d}}{\mathrm{d}\theta}\left(\sin\theta\frac{\mathrm{d}\Theta}{\mathrm{d}\theta}\right)+\left[n(n+1)-\frac{m^2}{\sin^2\theta}\right]\Theta = 0 \tag{514}$$

$$\frac{\mathrm{d}}{\mathrm{d}r}\left(r^2\frac{\mathrm{d}R}{\mathrm{d}r}\right)+[\mathrm{k}^2r^2-n(n+1)]R = 0 \tag{515}$$

Equation (514) is the associated Legendre equation and its solutions are the associated Legendre polynomials. The solutions are Legendre polynomials of degree n and order m, denoted by $P_n^m(\cos\theta)$. Appendix 10.2 describes many properties of Legendre polynomials including series expansions and recurrence formulae.

Legendre polynomials are usually expressed in terms of $\mu = \cos\theta$. Note that the rest of this monograph uses $\mu = |\cos\theta|$ to refer to the zenith angle with respect to an entire atmosphere. The present section is concerned with the polar angle of a single particle, and for this use only, and to maintain consistency with other Mie theory presentations (e.g., Bohren and Huffman, 1983; Liou, 2002) we define $\mu = \cos\theta$.

$$\frac{\mathrm{d}}{\mathrm{d}\mu}\left[(1-\mu^2)\frac{\mathrm{d}\Theta}{\mathrm{d}\mu}\right]+\left[n(n+1)-\frac{m^2}{1-\mu^2}\right]\Theta = 0 \tag{516}$$

The associated Legendre polynomials of degree n and order m which satisfy (516) are denoted by $P_n^m(\mu)$.

7.2.3 Radial Solutions

We turn now to the solution of the radial equation (522), which we re-write as

$$r^2\frac{\mathrm{d}^2R}{\mathrm{d}r^2}+2r\frac{\mathrm{d}R}{\mathrm{d}r}+[\mathrm{k}^2r^2-n(n+1)]R = 0 \tag{517}$$

The algebraic form of (517) simplifies if we change independent variables from r to the dimensionless ρ

$$\rho = \mathrm{k}r \tag{518a}$$
$$r = \rho/\mathrm{k} \tag{518b}$$
$$\mathrm{d}r = \mathrm{k}^{-1}\,\mathrm{d}\rho \tag{518c}$$
$$\mathrm{d}\rho = \mathrm{k}\,\mathrm{d}r \tag{518d}$$

to yield

$$\begin{aligned}\left(\frac{\rho}{\mathrm{k}}\right)^2\left(\frac{1}{\mathrm{k}^{-1}}\right)^2\frac{\mathrm{d}^2R}{\mathrm{d}\rho^2}+2\left(\frac{\rho}{\mathrm{k}}\right)\left(\frac{1}{\mathrm{k}^{-1}}\right)\frac{\mathrm{d}R}{\mathrm{d}\rho}+\left[\mathrm{k}^2\left(\frac{\rho}{\mathrm{k}}\right)^2-n(n+1)\right]R &= 0\\ \rho^2\frac{\mathrm{d}^2R}{\mathrm{d}\rho^2}+2\rho\frac{\mathrm{d}R}{\mathrm{d}\rho}+[\rho^2-n(n+1)]R &= 0\end{aligned} \tag{519}$$

Equation (519) is not tractable in its present form. However, a re-defined radial function will transform (519) into Bessel's equation. Define Z by

$$R = \rho^{-1/2}Z \tag{520a}$$
$$Z = \sqrt{\rho}R \tag{520b}$$

and substitute it into (519) to obtain

$$\begin{aligned}\rho^2\frac{\mathrm{d}^2(\rho^{-1/2}Z)}{\mathrm{d}\rho^2}+2\rho\frac{\mathrm{d}(\rho^{-1/2}Z)}{\mathrm{d}\rho}+[\rho^2-n(n+1)](\rho^{-1/2}Z) &= 0\\ \rho^2\frac{\mathrm{d}}{\mathrm{d}\rho}\left(-\frac{\rho^{-3/2}}{2}Z+\rho^{-1/2}\frac{\mathrm{d}Z}{\mathrm{d}\rho}\right)+\cdots &\\ \cdots+2\rho\left(-\frac{\rho^{-3/2}}{2}Z+\rho^{-1/2}\frac{\mathrm{d}Z}{\mathrm{d}\rho}\right)+[\rho^2-n(n+1)]\rho^{-1/2}Z &= 0\\ \rho^2\left(\frac{3\rho^{-5/2}}{4}Z-\frac{\rho^{-3/2}}{2}\frac{\mathrm{d}Z}{\mathrm{d}\rho}-\frac{\rho^{-3/2}}{2}\frac{\mathrm{d}Z}{\mathrm{d}\rho}+\rho^{-1/2}\frac{\mathrm{d}^2Z}{\mathrm{d}\rho^2}\right)-\cdots &\\ \cdots-\rho^{-1/2}Z+2\rho^{1/2}\frac{\mathrm{d}Z}{\mathrm{d}\rho}+[\rho^2-n(n+1)]\rho^{-1/2}Z &= 0\\ \frac{3\rho^{-1/2}}{4}Z-\rho^{1/2}\frac{\mathrm{d}Z}{\mathrm{d}\rho}+\rho^{3/2}\frac{\mathrm{d}^2Z}{\mathrm{d}\rho^2}-\rho^{-1/2}Z+2\rho^{1/2}\frac{\mathrm{d}Z}{\mathrm{d}\rho}+[\rho^2-n(n+1)]\rho^{-1/2}Z &= 0\\ \frac{3}{4}Z-\rho\frac{\mathrm{d}Z}{\mathrm{d}\rho}+\rho^2\frac{\mathrm{d}^2Z}{\mathrm{d}\rho^2}-Z+2\rho\frac{\mathrm{d}Z}{\mathrm{d}\rho}+[\rho^2-n(n+1)]Z &= 0\\ \rho^2\frac{\mathrm{d}^2Z}{\mathrm{d}\rho^2}+\rho\frac{\mathrm{d}Z}{\mathrm{d}\rho}-\frac{Z}{4}+[\rho^2-n(n+1)]Z &= 0\\ \rho^2\frac{\mathrm{d}^2Z}{\mathrm{d}\rho^2}+\rho\frac{\mathrm{d}Z}{\mathrm{d}\rho}+[\rho^2-(n^2+n+\tfrac{1}{4})]Z &= 0\\ \rho^2\frac{\mathrm{d}^2Z}{\mathrm{d}\rho^2}+\rho\frac{\mathrm{d}Z}{\mathrm{d}\rho}+[\rho^2-(n+\tfrac{1}{2})^2]Z &= 0\end{aligned} \tag{521}$$

Equation (521) is Bessel's equation (Watson, 1958, p. 19) for half-integral values. The solutions are Bessel functions of half-integral order, $Z = Z_{n+1/2}(\rho)$. Appendix 10.4 describes many properties of Bessel functions, including modified Bessel functions, asymptotic limits, and recurrence formulae.

In terms of the radial coordinate r and wavenumber k, the solutions to (517) are

$$R(n; r, \mathrm{k}) = \frac{1}{\sqrt{\mathrm{k}r}} Z_{n+1/2}(\mathrm{k}r) \tag{522}$$

The general solution to our Helmholtz equation in spherical coordinates (499), is the product (500) of the radial, polar, and azimuthal solutions from (522), (514), and (504), respectively

$$u(n, m; r, \theta, \phi) = \frac{1}{\sqrt{\mathrm{k}r}} Z_{n+1/2}(\mathrm{k}r) P_n^m(\cos\theta)(C_{1,m}\cos m\phi + C_{2,m}\sin m\phi) \tag{523}$$

The physical environment of Mie scattering allows us to restrict the radial solutions $Z_{n+1/2}(\mathrm{k}r)$ to certain subsets of Bessel functions. It is advantageous to explain the rationale for doing so now before the nomenclature becomes even more cumbersome as it will once we expand the incident wave into spherical harmonics Section 10.7 and apply the boundary conditions Section 7.2.5. As described in Appendix 10.4, the spherical Bessel functions $z_n(\mathrm{k}r)$ (571b) are suitably normalized re-definitions of $Z_{n+1/2}(\mathrm{k}r)$. The two linearly independent sets of basis function which $z_n(\mathrm{k}r)$ represents are (1) $j_n(\mathrm{k}r)$ and $y_n(\mathrm{k}r)$, and (2) $h_n^{(1)}(\mathrm{k}r)$ and $h_n^{(2)}(\mathrm{k}r)$.

The first physical restriction is that the scattered electromagnetic field must be finite at the origin. $y_n(\mathrm{k}r)$ is unbounded at the origin so $j_n(\mathrm{k}r)$ must suffice for Mie solutions interior to the sphere. The second physical restriction is that the scattered electromagnetic field must be finite at large distances from the sphere, as $r \to \infty$. $j_n(\mathrm{k}r)$ is unbounded as $r \to \infty$ whereas the Hankel functions are well-behaved. Hence $h_n^{(1)}(\mathrm{k}r)$ and $h_n^{(2)}(\mathrm{k}r)$ will be used for Mie solutions exterior to the sphere.

Note that (523) depends on kr rather than r. The radius-to-wavelength ratio is physically meaningful in the Helmholtz equation, rather than the absolute radius or wavelength. Of course (523) only defines the generating function that accounts for the geometry of the scattering problem. In practice, the dielectric constant (i.e., index of refraction) does depend on the absolute wavelenth, and this information propogates into the solutions for the electric and magnetic fields which are coupled through the Maxwell equations. Some explications of Mie theory (e.g., Liou, 2002, p. 180) include refractive index dependence in the solution of the Helmholtz equation rather than waiting until applying the boundary conditions, as we shall do.

7.2.4 Expansion of Plane Wave into Spherical Harmonics

Consider the scattering of a linearly polarized plane wave (482) by a sphere of radius a centered at the origin of the Cartesian coordinate system. In this coordinate system, an incident plane wave may be written as

$$\mathbf{E}_\mathrm{i}(\mathbf{r}, t) = \mathbf{E}_0 \exp[\mathrm{i}(\mathbf{k}_\mathrm{i} \cdot \mathbf{r} - \omega t)] \tag{524}$$

where the subscript i denotes "incident". We may simplify the representation of $\mathbf{E}_\mathrm{i}(\mathbf{r},t)$ without loss of generality by picking our coordinate system to align with the incident plane wave. By convention we choose (1) the incident wave to propogate toward the z-direction, and (2) the direction of polarization of the incident electric vector is parallel to the x-axis. Under our assumptions, the incident plane waves have no components in the $\hat{\mathbf{j}}$ or $\hat{\mathbf{k}}$ directions because we assumed linear polarization in the $\hat{\mathbf{i}}$ direction. Hence, $\mathbf{E}_\mathrm{i}$ may be represented by the simple scalar E_0. Furthermore, the waves are traveling in the positive z-direction, so the wavenumber vector $\mathbf{k}_\mathrm{i}$ in (524) collapses to the scalar k, and its dot product with position simplifies $\mathbf{k}_\mathrm{i}\cdot\mathbf{r} = \mathrm{k}z$. Finally, we assume the incident field is constant in time so that $\mathbf{E}_\mathrm{i}(\mathbf{r},t) = \mathbf{E}_\mathrm{i}(\mathbf{r})$. Accordingly, (524) simplifies to

$$\mathbf{E}_\mathrm{i}(\mathbf{r}) \;=\; E_0 \mathrm{e}^{\mathrm{i}\mathrm{k}z}\hat{\mathbf{i}} \tag{525}$$

fxm

7.2.5 Boundary Conditions

7.2.6 Mie Theory

The solution of Maxwell's equations (474) for the geometry of the aerosol (usually considered to be spherical) in the medium of interest (e.g., air or ocean water) yields the connection between the index of refraction n and the single scattering properties τ_e, ϖ, and g. The complete solution to this important problem was derived independently by physicists Ludwig Lorenz in 1890 and Gustav Mie in 1908. The subject is usually called Mie theory in honor of the latter, but Lorenz-Mie theory would be more appropriate. In-depth discussions of Mie theory are presented in van de Hulst (1957), Hansen and Travis (1974), and Bohren and Huffman (1983).

Consider the scattering of a linearly polarized plane wave (237) by a sphere of radius r centered at the origin of the Cartesian coordinate system. The plane wave propogates toward the z-direction. The direction of polarization of the incident electric vector is along the x-axis. The subscripts i, p, and s refer to the incident wave, particle wave (i.e., the wave interior to the particle), and scattered wave, respectively.

$$\mathbf{E}_\mathrm{i}(\mathbf{r},t) = \sum_{n=1}^{\infty} E_n[\mathbf{M}_{o1n}^{(1)} - \mathrm{i}\mathbf{N}_{e1n}^{(1)}] \tag{526a}$$

$$\mathbf{H}_\mathrm{i}(\mathbf{r},t) = -\frac{\mathrm{k}_\mathrm{m}}{\omega\mu}\sum_{n=1}^{\infty} E_n[\mathbf{M}_{e1n}^{(1)} + \mathrm{i}\mathbf{N}_{o1n}^{(1)}] \tag{526b}$$

$$\mathbf{E}_\mathrm{p}(\mathbf{r},t) = \sum_{n=1}^{\infty} E_n[c_n\mathbf{M}_{o1n}^{(1)} - \mathrm{i}d_n\mathbf{N}_{e1n}^{(1)}] \tag{526c}$$

$$\mathbf{H}_\mathrm{p}(\mathbf{r},t) = -\frac{\mathrm{k}}{\omega\mu_\mathrm{p}}\sum_{n=1}^{\infty} E_n[d_n\mathbf{M}_{o1n}^{(1)} + \mathrm{i}c_n\mathbf{N}_{o1n}^{(1)}] \tag{526d}$$

$$\mathbf{E}_\mathrm{s}(\mathbf{r},t) = \sum_{n=1}^{\infty} E_n[\mathrm{i}a_n\mathbf{N}_{e1n}^{(3)} - b_n\mathbf{M}_{o1n}^{(3)}) \tag{526e}$$

$$\mathbf{H}_{\mathrm{s}}(\mathbf{r},t) = -\frac{\mathrm{k_m}}{\omega\mu}\sum_{n=1}^{\infty} E_n[\mathrm{i}b_n\mathbf{N}_{o1n}^{(3)} + a_n\mathbf{M}_{e1n}^{(3)}] \tag{526f}$$

where

$$E_n \;=\; \frac{\mathrm{i}^n(2n+1)}{n(n+1)}E_0 \tag{527}$$

and E_0, the amplitude of the incident electric field, is defined in (237). The superscripts (1) and (3) in (527) indicate the type of spherical Bessel function into which the electric and magnetic fields are decomposed. The complex wavenumbers within the particle, k, and the medium, $\mathrm{k_m}$, are defined by, respectively

$$\mathrm{k} = 2\pi n_{\mathrm{p}}/\lambda_0 \tag{528a}$$
$$\mathrm{k_m} = 2\pi n_{\mathrm{m}}/\lambda_0 \tag{528b}$$

The vector spherical harmonic expansions of $\mathbf{M}$ and $\mathbf{N}$ are

$$\mathbf{M}_{o1n} = \cos\phi\pi_n(\cos\theta)z_n(\rho)\hat{\boldsymbol{\theta}} - \sin\phi\tau_n(\cos\theta)z_n(\rho)\hat{\boldsymbol{\phi}} \tag{529a}$$
$$\mathbf{M}_{e1n} = \tag{529b}$$
$$\mathbf{N}_{o1n} = \tag{529c}$$
$$\mathbf{N}_{e1n} = \tag{529d}$$

where the definition of the coordinate ρ at which the radial Bessel functions are evaluated depends on the field location. Within the particle, the radial coordinate is the radial distance times the internal wavenumber, while the radial coordinate used to evaluate the incident and scattered fields (which are outside the particle)

$$\rho \;=\; \begin{cases} r\mathrm{k} & : \text{ Internal field} \\ r\mathrm{k_m} & : \text{ Incident and Scattered fields} \end{cases} \tag{530}$$

7.2.7 Resonances

Recent studies suggest that resonant absorption of sunlight by cloud droplets may constitute a significant and unaccounted-for solar energy sink in the atmosphere (e.g, Nussenzveig, 2003). Many studies refer to the impact of resonances on absorptance (e.g., Chýlek et al., 1978a,b; Bennett and Rosasco, 1978; Bohren and Huffman, 1983; Guimarães and Nussenzveig, 1994; Markel and Shalaev, 1999; Mitchell, 2000; Markel, 2002; Nussenzveig, 2003; Zender and Talamantes, 2006). Resolving all sharp resonances requires a resolution in size parameter $\chi = 2\pi r/\lambda$ (r—droplet radius, λ—incident wavelength) of about 10^{-7} (Chýlek et al., 1978a).

This section describes application of resonance enhancement by absorbing particles such as soot in otherwise weakly absorbing spheres such as liquid cloud droplets. Markel and Shalaev (1999) present an exact theory for this enhancement. Markel (2002) shows how resonances amplify this enhancement.

Markel and Shalaev (1999) present a general theory of energy absorption by absorbing spheres in weakly-absorbing media. The theory has three main assumptions:

1. fxm

The absorption enhancement factor G is the ratio of absorption α by an inclusion inside a relatively weakly absorbing medium to the absorption $\alpha^{(0)}$ of the same inclusion in a vacuum. For concreteness, we may henceforth refer to the absorbing inclusion as the soot cluster and the relatively weakly absorbing spherical medium as the cloud droplet.

$$G(r_{\mathrm{c}},\lambda) = \frac{\alpha(r_{\mathrm{c}},\lambda)}{\alpha^{(0)}(r_{\mathrm{n}},\lambda)} \tag{531}$$

where subscripts c and n refer to the cloud droplet and the soot inclusion, respectively. Hence r_{c} is the cloud droplet radius, r_{n} is the soot inclusion radius, and the cloud droplet size parameter $\chi_{\mathrm{c}} = 2\pi r_{\mathrm{c}}/\lambda$.

With the above assumptions, the enhancement factor G (531) depends only on the wavelength and the size of the cloud droplet, not on the size of the inclusion.

7.2.8 Optical Efficiencies

Mie theory predicts the optical efficiencies Q_x of particles of a given size at a given wavelength. Here x stands for a, s, or e which represent the processes of absorption, scattering, and extinction, respectively. The optical efficiency for each of these processes is the ratio between a particle's effective cross-sectional area for the specified interaction (absorption, scattering, or both) with light and its geometric cross sectional area.

$$Q_{\mathrm{a}}(r,\lambda) = \frac{\alpha(r,\lambda)}{\pi r^2} \tag{532a}$$

$$Q_{\mathrm{s}}(r,\lambda) = \frac{\sigma(r,\lambda)}{\pi r^2} \tag{532b}$$

$$Q_{\mathrm{e}}(r,\lambda) = \frac{k(r,\lambda)}{\pi r^2} \tag{532c}$$

Thus the optical efficiencies are dimensionless. In mie, the band-mean versions of Q_{a}, Q_{s}, and Q_{e} are named abs_fsh, sca_fsh, and ext_fsh, respectively.

These optical efficiencies are not independent of one another. Two of the efficiency factors, usually the extinction efficiency Q_{e} and the scattering efficiency Q_{s}, are predicted directly by Mie theory. The third efficiency factor, the absorption efficiency Q_{a}, is the residual that satisfies energy conservation

$$Q_{\mathrm{a}}(r,\lambda) \;=\; Q_{\mathrm{e}}(r,\lambda) - Q_{\mathrm{s}}(r,\lambda) \tag{533}$$

This relation states that extinction is the sum of absorption and scattering.

As mentioned previously (92), Mie theory shows that

$$\lim_{\chi\to\infty} Q_{\mathrm{e}}(r,\lambda) \;=\; 2 \tag{534}$$

7.2.9 Optical Cross Sections

As mentioned above, the optical efficiencies Q_x are the ratios between a particle's effective cross-sectional area for interacting with light (i.e., absorbing or scattering photons) and its geometric cross-sectional area. The interaction cross-sections per particle are

$$\alpha(r,\lambda) = \pi r^2 Q_{\mathrm{a}}(r,\lambda) \tag{535a}$$
$$\sigma(r,\lambda) = \pi r^2 Q_{\mathrm{s}}(r,\lambda) \tag{535b}$$
$$k(r,\lambda) = \pi r^2 Q_{\mathrm{e}}(r,\lambda) \tag{535c}$$

The relationship between the interaction cross-sections is exactly analogous to the relationship between the optical efficiencies (532), so that

$$k(r,\lambda) = \alpha(r,\lambda) + \sigma(r,\lambda) \tag{536}$$

The optical cross sections have dimensions of area per particle.

7.2.10 Optical Depths

Using (85) we see that a column of depth Δz [m] with a homogeneous particle concentration of $N(r)$ [m^{-3}] produces optical depths of

$$\tau_{\mathrm{a}}(r,\lambda) = \pi r^2 Q_{\mathrm{a}}(r,\lambda) N(r) \Delta z \tag{537a}$$
$$\tau_{\mathrm{s}}(r,\lambda) = \pi r^2 Q_{\mathrm{s}}(r,\lambda) N(r) \Delta z \tag{537b}$$
$$\tau_{\mathrm{e}}(r,\lambda) = \pi r^2 Q_{\mathrm{e}}(r,\lambda) N(r) \Delta z \tag{537c}$$

7.2.11 Single Scattering Albedo

The single scattering albedo is simply the probability that, given an interaction between the photon and particle, the particle will be scattered rather than absorbed. For a single particle size, this probability may easily be expressed in terms of the optical efficiencies (532), optical cross-sections (535), or optical depths (537)

$$\begin{aligned} \varpi(r,\lambda) &= Q_{\mathrm{s}}(r,\lambda)/Q_{\mathrm{e}}(r,\lambda) \\ &= \sigma(r,\lambda)/k(r,\lambda) \\ &= \tau_{\mathrm{s}}(r,\lambda)/\tau_{\mathrm{e}}(r,\lambda) \\ &= \frac{1-\tau_{\mathrm{a}}(r,\lambda)}{\tau_{\mathrm{e}}(r,\lambda)} \end{aligned} \tag{538}$$

In mie, the band-mean version of ϖ is named ss_alb_fsh.

7.2.12 Asymmetry Parameter

In mie, the band-mean version of g is named asm_prm_fsh.

7.2.13 Mass Absorption Coefficient

It is often a reasonable approximation to neglect the effects of particulate scattering of radiation for wavelengths longer than about $5\,\mu\mathrm{m}$, i.e., in the longwave spectral region. This approximation to longwave radiative transfer means that many longwave band models require only one parameter to account for the absorption (and emission) of radiation by particles, the mass absorption coefficient ψ.

7.3 Effective Single Scattering Properties

In nature, particles are not monodisperse but rather appear continuous size distributions. Therefore the single scattering properties of each particle size must be appropriately weighted and combined into the net or effective single scattering properties of the entire size distribution. These effective properties are the optical properties of an infinitely narrow spectral region.

The size distribution, $n_\mathrm{n}(r,z)\,[\#\,\mathrm{m}^{-3}\,\mathrm{m}^{-1}]$, describes the rate of change of particle concentration with particle size, and is a function of position, which we denote by z for height.

$$n_\mathrm{n}(r) = \frac{\mathrm{d}N(r)}{\mathrm{d}r} \tag{539}$$

The total particle concentration is the integral of the number size distribution

$$N_0 = \int_0^\infty n_\mathrm{n}(r)\,\mathrm{d}r \tag{540}$$

N_0 has dimensions of $[\#\,\mathrm{m}^{-3}]$, particle number per unit air volume.

The total cross-sectional area A_0 is the integral of the cross-sectional area weighted by the size distribution

$$A_0 = \int_0^\infty \pi r^2 n_\mathrm{n}(r)\,\mathrm{d}r \tag{541}$$

A_0 has dimensions of $[\mathrm{m}^2\,\mathrm{m}^{-3}]$, particle area per unit air volume. Since Maxwell's equations (474) are linear, the solutions to the equations, i.e., the optical efficiencies, are linear and additive. The appropriate weight for each property is the particle number distribution and a factor which depends on the particular property.

For the rest of this section we assume that the single scattering properties of the aerosol are known or can be obtained. Section 9 describes a computer program which computes these properties for arbitrary size distributions of spherical aerosols.

7.3.1 Effective Efficiencies

$$\tilde{Q}_\mathrm{a}(z,\lambda) = \frac{1}{A_0}\int_0^\infty \pi r^2 Q_\mathrm{a}(r,\lambda) n_\mathrm{n}(r,z)\,\mathrm{d}r \tag{542a}$$

$$\tilde{Q}_\mathrm{s}(z,\lambda) = \frac{1}{A_0}\int_0^\infty \pi r^2 Q_\mathrm{s}(r,\lambda) n_\mathrm{n}(r,z)\,\mathrm{d}r \tag{542b}$$

$$\tilde{Q}_\mathrm{e}(z,\lambda) = \frac{1}{A_0}\int_0^\infty \pi r^2 Q_\mathrm{e}(r,\lambda) n_\mathrm{n}(r,z)\,\mathrm{d}r \tag{542c}$$

The effective efficiencies, like the fundamental optical efficiencies (542), are dimensionless.

7.3.2 Effective Cross Sections

The effective cross sections are the the fundamental optical cross sections (535) integrated over the size distribution.

$$\tilde{\alpha}(z,\lambda) = A_0\tilde{Q}_\mathrm{a} = \int_0^\infty \pi r^2 Q_\mathrm{a}(r,\lambda) n_\mathrm{n}(r,z)\,\mathrm{d}r \tag{543a}$$

$$\tilde{\sigma}(z,\lambda) = A_0\tilde{Q}_\mathrm{s} = \int_0^\infty \pi r^2 Q_\mathrm{s}(r,\lambda) n_\mathrm{n}(r,z)\,\mathrm{d}r \tag{543b}$$

$$\tilde{k}(z,\lambda) = A_0\tilde{Q}_\mathrm{e} = \int_0^\infty \pi r^2 Q_\mathrm{e}(r,\lambda) n_\mathrm{n}(r,z)\,\mathrm{d}r \tag{543c}$$

The dimensions of the effective cross-sections are $[\mathrm{m}^2\,\mathrm{m}^{-3}]$, particle area per unit air volume. Hence, they are also known as the volume absorption, scattering, and extinction coefficients. These units are usually expressed as $[\mathrm{m}^{-1}]$—we feel that $[\mathrm{m}^2\,\mathrm{m}^{-3}]$ is much clearer.

7.3.3 Effective Specific Extinction Coefficients

As mentioned earlier, specific extinction is the extinction per unit mass of particle. Thus the specific extinction coefficients are the effective specific cross-sections (Section 7.3.2) divided by the total mass of particles M_0. For completeness, we list the explicit definition here:

$$\tilde{\psi}_\mathrm{a}(z,\lambda) = \frac{\tilde{\alpha}}{M_0} = \frac{A_0\tilde{Q}_\mathrm{a}}{M_0} = \frac{\int_0^\infty \pi r^2 Q_\mathrm{a}(r,\lambda) n_\mathrm{n}(r,z)\,\mathrm{d}r}{\int_0^\infty \frac{4\pi}{3}\rho r^3 n_\mathrm{n}(r,z)\,\mathrm{d}r} \tag{544a}$$

$$\tilde{\psi}_\mathrm{s}(z,\lambda) = \frac{\tilde{\sigma}}{M_0} = \frac{A_0\tilde{Q}_\mathrm{s}}{M_0} = \frac{\int_0^\infty \pi r^2 Q_\mathrm{s}(r,\lambda) n_\mathrm{n}(r,z)\,\mathrm{d}r}{\int_0^\infty \frac{4\pi}{3}\rho r^3 n_\mathrm{n}(r,z)\,\mathrm{d}r} \tag{544b}$$

$$\tilde{\psi}_\mathrm{e}(z,\lambda) = \frac{\tilde{k}}{M_0} = \frac{A_0\tilde{Q}_\mathrm{e}}{M_0} = \frac{\int_0^\infty \pi r^2 Q_\mathrm{e}(r,\lambda) n_\mathrm{n}(r,z)\,\mathrm{d}r}{\int_0^\infty \frac{4\pi}{3}\rho r^3 n_\mathrm{n}(r,z)\,\mathrm{d}r} \tag{544c}$$

7.3.4 Effective Optical Depths

$$\tilde{\tau}_\mathrm{a}(z) = \tilde{\alpha}\Delta z = \tilde{\psi}_\mathrm{a} w = \Delta z \int_0^\infty \pi r^2 Q_\mathrm{a}(r,\lambda) n_\mathrm{n}(r,z)\,\mathrm{d}r \tag{545a}$$

$$\tilde{\tau}_\mathrm{s}(z) = \tilde{\sigma}\Delta z = \tilde{\psi}_\mathrm{s} w = \Delta z \int_0^\infty \pi r^2 Q_\mathrm{s}(r,\lambda) n_\mathrm{n}(r,z)\,\mathrm{d}r \tag{545b}$$

$$\tilde{\tau}_\mathrm{e}(z) = \tilde{k}\Delta z = \tilde{\psi}_\mathrm{e} w = \Delta z \int_0^\infty \pi r^2 Q_\mathrm{e}(r,\lambda) n_\mathrm{n}(r,z)\,\mathrm{d}r \tag{545c}$$

7.3.5 Effective Single Scattering Albedo

$$\tilde{\varpi}(z,\lambda) = \tilde{\sigma}(z,\lambda)/\tilde{k}(z,\lambda) = \left(\int_0^\infty \pi r^2 Q_\mathrm{s}(r,\lambda) n_\mathrm{n}(r,z)\,\mathrm{d}r\right) \Big/ \tilde{k}(z,\lambda) \tag{546}$$

7.3.6 Effective Asymmetry Parameter

The effective asymmetry parameter $\tilde{g}$

$$\tilde{g}(z,\lambda) = \frac{\int_0^\infty \pi r^2 g(r,\lambda) Q_\mathrm{s}(r,\lambda) n_\mathrm{n}(r,z)\,\mathrm{d}r}{\int_0^\infty \pi r^2 Q_\mathrm{s}(r,\lambda) n_\mathrm{n}(r,z)\,\mathrm{d}r} \tag{547}$$

7.4 Mean Effective Single Scattering Properties

Atmospheric radiative transfer models (with the possible exception of line-by-line models) work by discretizing the spectral region of interest into a reasonable number of finite width spectral bands. These bands can be, and usually are, much wider that the spectral structure of the absorption and scattering features they contain. For example, many GCMs divide the solar spectrum into about twenty bands, and the infrared spectrum into about ten[17]. The appropriate optical properties for such finite bands are called the mean effective single scattering properties.

Naturally, we construct the mean effective properties as a weighted mean of the effective single scattering properties (Section 7.3). For the single scattering properities of atmospheric size distributions, the appropriate spectral weight is the specific flux or radiance. For solar or infrared radiative transfer, weight by the fractional solar or infrared flux, respectively. These procedures are sometimes called Rayleigh weighting or Planck weighting, respectively If possible, use the ambient temperature for determining infrared weights.

Other potential spectral weighting factors depend on the application. For example, the single scatter properties of the surface particle size distribution determine the surface reflectance. The spectral surface reflectance is a more optimal weight than the incident specific flux for determining the band average reflectance of snow and ice surfaces.

We denote the spectral weighting function by $W(\lambda)$. Spectral flux weighting in Earth's atmosphere may be done by setting

$$W(\lambda) \quad = \quad \begin{cases} F_\lambda^\odot(\lambda) & : \quad \lambda \lesssim 5\,\mu\mathrm{m} \\ B_\lambda(\lambda,T) & : \quad \lambda \gtrsim 5\,\mu\mathrm{m} \end{cases} \tag{548}$$

where $F_\lambda^\odot(\lambda)$ is the solar spectral irradiance and $B_\lambda(\lambda,T)$ is the specific blackbody radiance (41b). For brevity, we omit the explicit dependence of $W(\lambda)$ on any factor (e.g., altitude, atmospheric composition) except wavelength. The mean effective single scattering properties must be normalized by the integral of the spectral weighting function over the region of interest, W_0.

$$W_0 \equiv \int_{\lambda_\mathrm{min}}^{\lambda_\mathrm{max}} W(\lambda)\,\mathrm{d}\lambda \tag{549}$$

Unless the spectral weighting function is normalized, i.e., integrates to unity over the region of interest, the computation of (549) should be done once, outside the spectral integration loop.

[17] CAM uses nineteen solar bands and six-to-eight infrared bands. The Malkmus narrow band model SWNB2 covers the solar spectrum with 1690 bands.

7.4.1 Mean Effective Efficiencies

The mean effective efficiencies are the flux-weighted opacities of a size distribution of particles.

$$\bar{Q}_{\mathrm{a}}(z) = \frac{1}{A_0 W_0} \int_{\lambda_{\min}}^{\lambda_{\max}} \int_0^{\infty} \pi r^2 Q_{\mathrm{a}}(r,\lambda) n_{\mathrm{n}}(r,z) W(\lambda)\,\mathrm{d}r\,\mathrm{d}\lambda \tag{550a}$$

$$\bar{Q}_{\mathrm{s}}(z) = \frac{1}{A_0 W_0} \int_{\lambda_{\min}}^{\lambda_{\max}} \int_0^{\infty} \pi r^2 Q_{\mathrm{s}}(r,\lambda) n_{\mathrm{n}}(r,z) W(\lambda)\,\mathrm{d}r\,\mathrm{d}\lambda \tag{550b}$$

$$\bar{Q}_{\mathrm{e}}(z) = \frac{1}{A_0 W_0} \int_{\lambda_{\min}}^{\lambda_{\max}} \int_0^{\infty} \pi r^2 Q_{\mathrm{e}}(r,\lambda) n_{\mathrm{n}}(r,z) W(\lambda)\,\mathrm{d}r\,\mathrm{d}\lambda \tag{550c}$$

The mean effective efficiencies, like the effective efficiencies (542) and the fundamental optical efficiencies (532), are dimensionless. In mie, $\bar{Q}_{\mathrm{a}}$, $\bar{Q}_{\mathrm{s}}$, and $\bar{Q}_{\mathrm{e}}$, are named abs_fsh_ffc, sct_fsh_ffc, and ext_fsh_ffc, respectively.

7.4.2 Mean Effective Cross Sections

$$\bar{\alpha}(z) = A_0 \bar{Q}_{\mathrm{a}} = \frac{1}{W_0} \int_{\lambda_{\min}}^{\lambda_{\max}} \int_0^{\infty} \pi r^2 Q_{\mathrm{a}}(r,\lambda) n_{\mathrm{n}}(r,z) W(\lambda)\,\mathrm{d}r\,\mathrm{d}\lambda \tag{551a}$$

$$\bar{\sigma}(z) = A_0 \bar{Q}_{\mathrm{s}} = \frac{1}{W_0} \int_{\lambda_{\min}}^{\lambda_{\max}} \int_0^{\infty} \pi r^2 Q_{\mathrm{s}}(r,\lambda) n_{\mathrm{n}}(r,z) W(\lambda)\,\mathrm{d}r\,\mathrm{d}\lambda \tag{551b}$$

$$\bar{k}(z) = A_0 \bar{Q}_{\mathrm{e}} = \frac{1}{W_0} \int_{\lambda_{\min}}^{\lambda_{\max}} \int_0^{\infty} \pi r^2 Q_{\mathrm{e}}(r,\lambda) n_{\mathrm{n}}(r,z) W(\lambda)\,\mathrm{d}r\,\mathrm{d}\lambda \tag{551c}$$

The mean effective cross sections, like the effective cross section (543), and the fundamental optical cross sections (535), have dimensions of area. In mie, $\bar{\alpha}$, $\bar{\sigma}$, and $\bar{k}$, are named abs_cff_vlm, sca_cff_vlm, and ext_cff_vlm, respectively.

7.4.3 Mean Effective Specific Extinction Coefficients

$$\bar{\psi}_{\mathrm{a}}(z) = \frac{\bar{\alpha}}{M_0} = \frac{A_0 \bar{Q}_{\mathrm{a}}}{M_0} = \frac{\int_{\lambda_{\min}}^{\lambda_{\max}} \int_0^{\infty} \pi r^2 Q_{\mathrm{a}}(r,\lambda) n_{\mathrm{n}}(r,z) W(\lambda)\,\mathrm{d}r\,\mathrm{d}\lambda}{\int_{\lambda_{\min}}^{\lambda_{\max}} W(\lambda)\,\mathrm{d}\lambda \int_0^{\infty} \frac{4\pi}{3} \rho r^3 n_{\mathrm{n}}(r,z)\,\mathrm{d}r} \tag{552a}$$

$$\bar{\psi}_{\mathrm{s}}(z) = \frac{\bar{\sigma}}{M_0} = \frac{A_0 \bar{Q}_{\mathrm{s}}}{M_0} = \frac{\int_{\lambda_{\min}}^{\lambda_{\max}} \int_0^{\infty} \pi r^2 Q_{\mathrm{s}}(r,\lambda) n_{\mathrm{n}}(r,z) W(\lambda)\,\mathrm{d}r\,\mathrm{d}\lambda}{\int_{\lambda_{\min}}^{\lambda_{\max}} W(\lambda)\,\mathrm{d}\lambda \int_0^{\infty} \frac{4\pi}{3} \rho r^3 n_{\mathrm{n}}(r,z)\,\mathrm{d}r} \tag{552b}$$

$$\bar{\psi}_{\mathrm{e}}(z) = \frac{\bar{k}}{M_0} = \frac{A_0 \bar{Q}_{\mathrm{e}}}{M_0} = \frac{\int_{\lambda_{\min}}^{\lambda_{\max}} \int_0^{\infty} \pi r^2 Q_{\mathrm{e}}(r,\lambda) n_{\mathrm{n}}(r,z) W(\lambda)\,\mathrm{d}r\,\mathrm{d}\lambda}{\int_{\lambda_{\min}}^{\lambda_{\max}} W(\lambda)\,\mathrm{d}\lambda \int_0^{\infty} \frac{4\pi}{3} \rho r^3 n_{\mathrm{n}}(r,z)\,\mathrm{d}r} \tag{552c}$$

The mean effective specific extinction coefficients, like the effective specific extinction coefficients (544) have dimensions of area per unit mass. In mie, $\bar{\psi}_{\mathrm{a}}$, $\bar{\psi}_{\mathrm{s}}$, and $\bar{\psi}_{\mathrm{e}}$ are named abs_cff_mss, sca_cff_mss, and ext_cff_mss, respectively.

7.4.4 Mean Effective Optical Depths

$$\bar{\tau}_{\mathrm{a}} = \bar{\alpha}\Delta z = \bar{\psi}_{\mathrm{a}} w = \frac{\Delta z}{W_0}\int_{\lambda_{\min}}^{\lambda_{\max}}\int_0^{\infty} \pi r^2 Q_{\mathrm{a}}(r,\lambda) n_{\mathrm{n}}(r,z) W(\lambda)\,\mathrm{d}r\,\mathrm{d}\lambda \tag{553a}$$

$$\bar{\tau}_{\mathrm{s}} = \bar{\sigma}\Delta z = \bar{\psi}_{\mathrm{s}} w = \frac{\Delta z}{W_0}\int_{\lambda_{\min}}^{\lambda_{\max}}\int_0^{\infty} \pi r^2 Q_{\mathrm{s}}(r,\lambda) n_{\mathrm{n}}(r,z) W(\lambda)\,\mathrm{d}r\,\mathrm{d}\lambda \tag{553b}$$

$$\bar{\tau}_{\mathrm{e}} = \bar{k}\Delta z = \bar{\psi}_{\mathrm{e}} w = \frac{\Delta z}{W_0}\int_{\lambda_{\min}}^{\lambda_{\max}}\int_0^{\infty} \pi r^2 Q_{\mathrm{e}}(r,\lambda) n_{\mathrm{n}}(r,z) W(\lambda)\,\mathrm{d}r\,\mathrm{d}\lambda \tag{553c}$$

7.4.5 Mean Effective Single Scattering Albedo

$$\bar{\varpi}(z) = \bar{\sigma}(z)/\bar{k}(z) = \frac{1}{W_0 \bar{k}(z)}\int_{\lambda_{\min}}^{\lambda_{\max}}\int_0^{\infty} \pi r^2 Q_{\mathrm{s}}(r,\lambda) n_{\mathrm{n}}(r,z) W(\lambda)\,\mathrm{d}r\,\mathrm{d}\lambda \tag{554}$$

In mie, $\bar{\varpi}$ is named ss_alb.

7.4.6 Mean Effective Asymmetry Parameter

The mean effective asymmetry parameter $\bar{g}$

$$\bar{g}(z) = \frac{\int_{\lambda_{\min}}^{\lambda_{\max}}\int_0^{\infty} \pi r^2 g(r,\lambda) Q_{\mathrm{s}}(r,\lambda) n_{\mathrm{n}}(r,z) W(\lambda)\,\mathrm{d}r\,\mathrm{d}\lambda}{\int_{\lambda_{\min}}^{\lambda_{\max}}\int_0^{\infty} \pi r^2 Q_{\mathrm{s}}(r,\lambda) n_{\mathrm{n}}(r,z) W(\lambda)\,\mathrm{d}r\,\mathrm{d}\lambda} \tag{555}$$

In mie, $\bar{g}$ is named asm_prm.

7.5 Bulk Layer Single Scattering Properties

The real atmosphere is characterized by multiple species coexisting and interacting with the radiation field. The radiation field is determined by the combined optical properties of all the radiatively active constituents. Knowing only the individual radiative properties of the constituents is not helpful as the radiation field is not in any sense linear, i.e., the additive result of the radiation fields produced by each constituent individually. Instead the individual radiative properties of all constituents, gases, particles, and boundary surfaces must be combined into what we shall call the bulk single scattering properties or layer single scattering properties. Combination of optical properties proceeds as in the previous section.

7.5.1 Addition of Optical Properties

Let N denote the number of radiatively active species in a volume. If we assume that these species do not interact with eachother then the scattering and absorbing properties of the medium are additive. This may be called the independent scatterers assumption. The combination rules that result from this assumption were described by Cess (1985).

The independent scatterers assumption has many critics. Melnikova (2008) believes that enough interactions occur on the scale of interstitial aerosol and gases in clouds, that the independent scatterers assumption significantly underestimates the effective optical depth (and thus absorption) of these media. Knyazikhin et al. (2002) may also question the assumption.

7.5.2 Bulk Optical Depths

Optical depths add linearly. With reference to (545),

$$\tau_\mathrm{a} = \sum_{i=1}^{N} \tilde{\tau}_{\mathrm{a},i} \tag{556a}$$

$$\tau_\mathrm{s} = \sum_{i=1}^{N} \tilde{\tau}_{\mathrm{s},i} \tag{556b}$$

$$\tau_\mathrm{e} = \sum_{i=1}^{N} \tilde{\tau}_{\mathrm{e},i} \tag{556c}$$

7.5.3 Bulk Single Scattering Albedo

With reference to (546), (545) and (556c),

$$\varpi = \frac{1}{\tau_\mathrm{e}} \sum_{i=1}^{N} \tilde{\varpi}_i \tilde{\tau}_{\mathrm{e},i} \tag{557}$$

7.5.4 Bulk Asymmetry Parameter

With reference to (555), (546), (545), (556c), and (557),

$$g = \frac{1}{\varpi \tau_\mathrm{e}} \sum_{i=1}^{N} \tilde{g}_i \tilde{\varpi}_i \tilde{\tau}_{\mathrm{e},i} \tag{558}$$

7.5.5 Diagnostics

When the radiation field is known, it is possible to diagnose the contribution of individual elements to bulk properties such as heating. For instance, the contribution of given-size particles to the net radiative heating of a layer is the difference between the absorption and the emission of the particles.

$$q_\mathrm{R}(r,z) = 4\pi \int_0^\infty \pi r^2 Q_\mathrm{a}(r,\lambda)[\bar{I}_\nu(z,\lambda) - B_\nu(T_\mathrm{a},\lambda)]\mathrm{d}\lambda \tag{559}$$

8 Global Radiative Forcing

Figure 3 shows the balance between incident, reflected, and absorbed solar radiation observed by the ERBE satellite system from 1985–1989.

Figure 4 shows the balance between terrestrial radiation emitted by the surface, trapped by the atmosphere, and escaping to space as observed by the ERBE satellite system from 1985–1989.

Figure 5 shows the temperature and OLR response to ENSO in terms of Hovmöller diagrams.

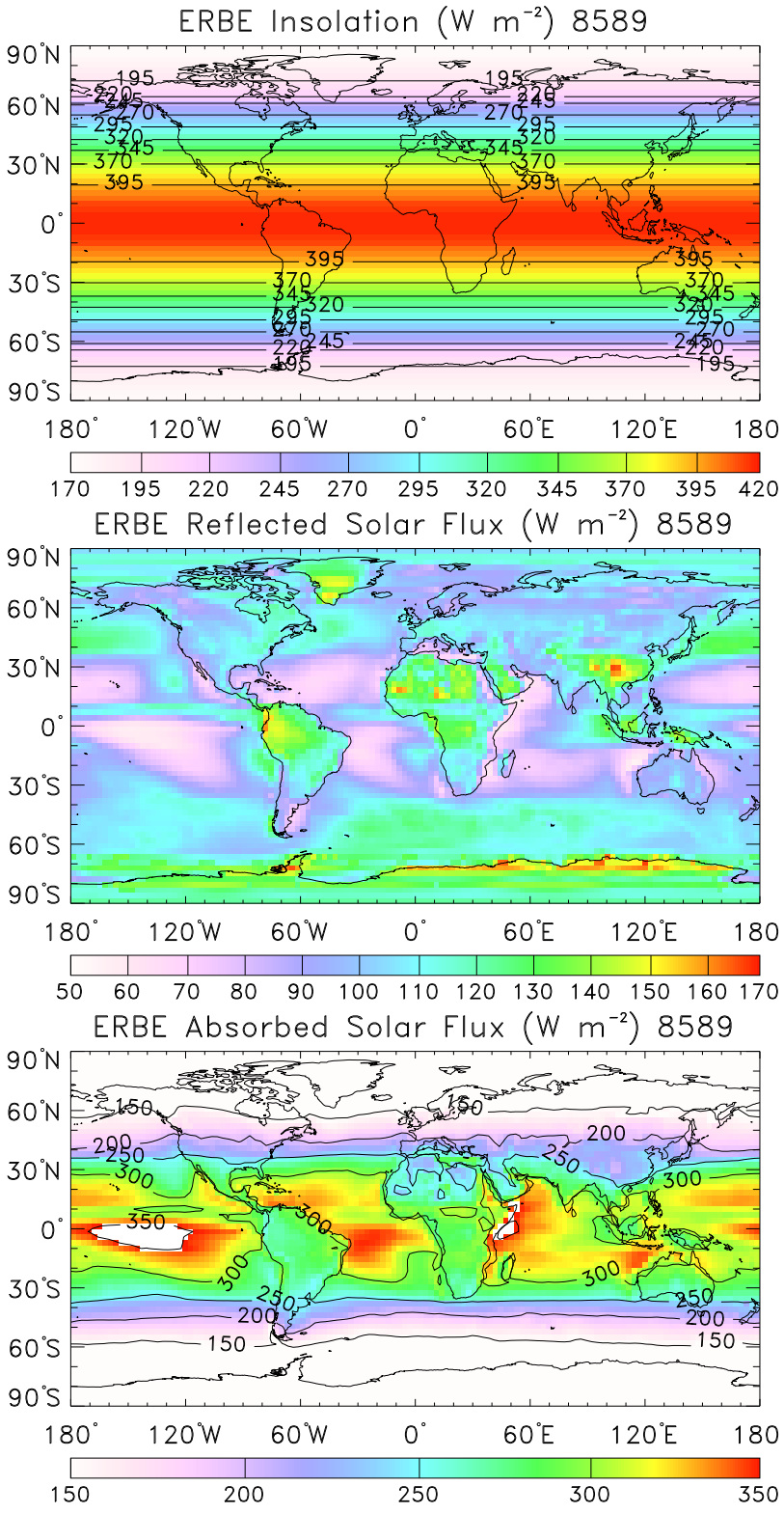

Figure 3: Geographic distribution of 1985–1989 climatological mean (a) insolation ${}^{\mathrm{TOA}}_{\mathrm{cld}}F^{\downarrow}_{\mathrm{SW}}$, (b) reflected shortwave irradiance ${}^{\mathrm{TOA}}_{\mathrm{cld}}F^{\uparrow}_{\mathrm{SW}}$, and (c) absorbed shortwave radiation ${}^{\mathrm{TOA}}_{\mathrm{cld}}F_{\mathrm{SW}}$ [$\mathrm{W\,m^{-2}}$] from ERBE observations.

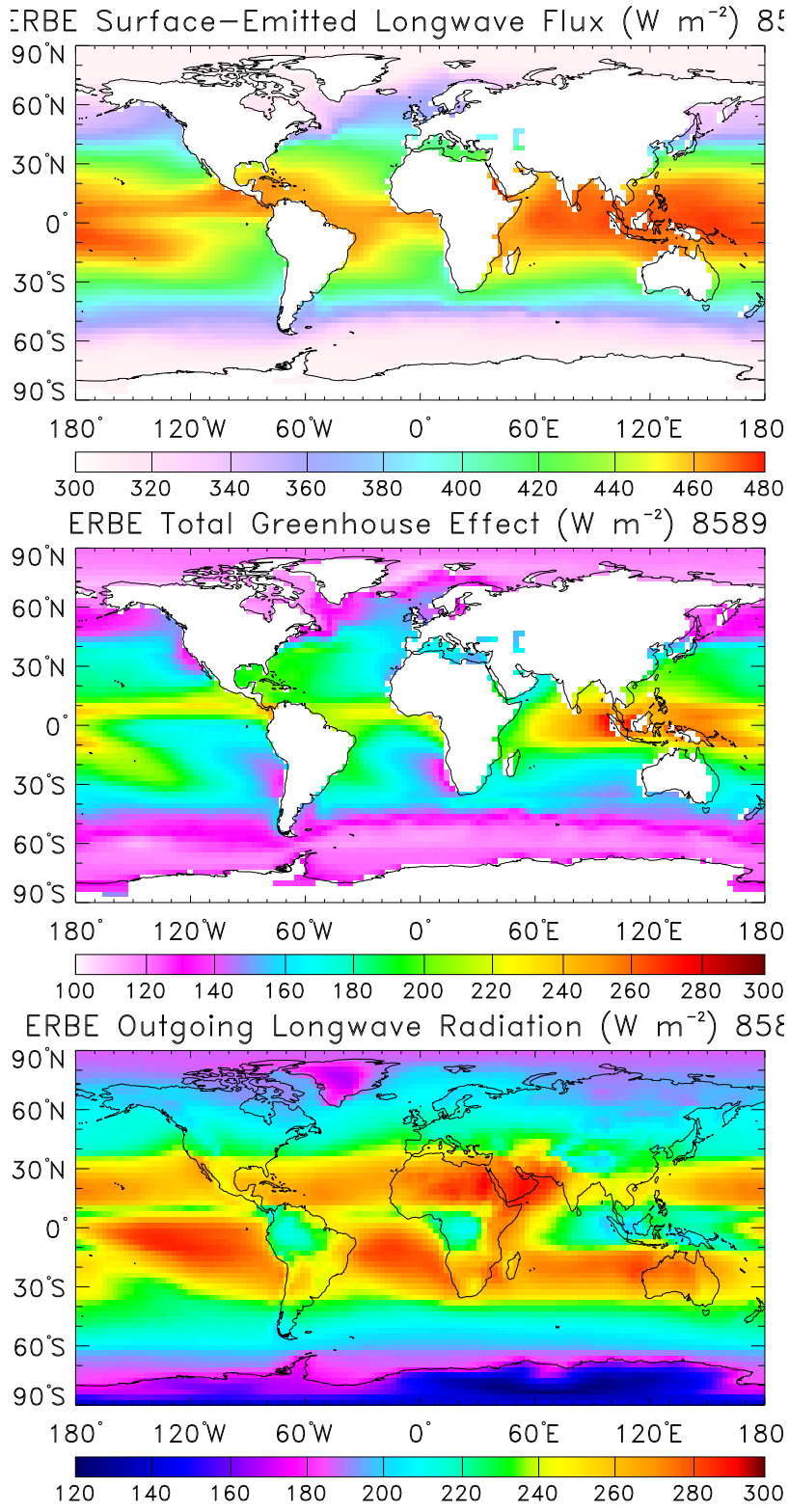

Figure 4: Geographic distribution of 1985–1989 climatological mean terrestrial radiation (a) emitted by the surface ${}^{\mathrm{sfc}}_{\mathrm{cld}}F^{\uparrow}_{\mathrm{LW}}$, (b) trapped by the atmosphere G_{c}, and (c) escaping to space ${}^{\mathrm{TOA}}_{\mathrm{cld}}F^{\uparrow}_{\mathrm{LW}}$ in [W m^{-2}] from ERBE observations.

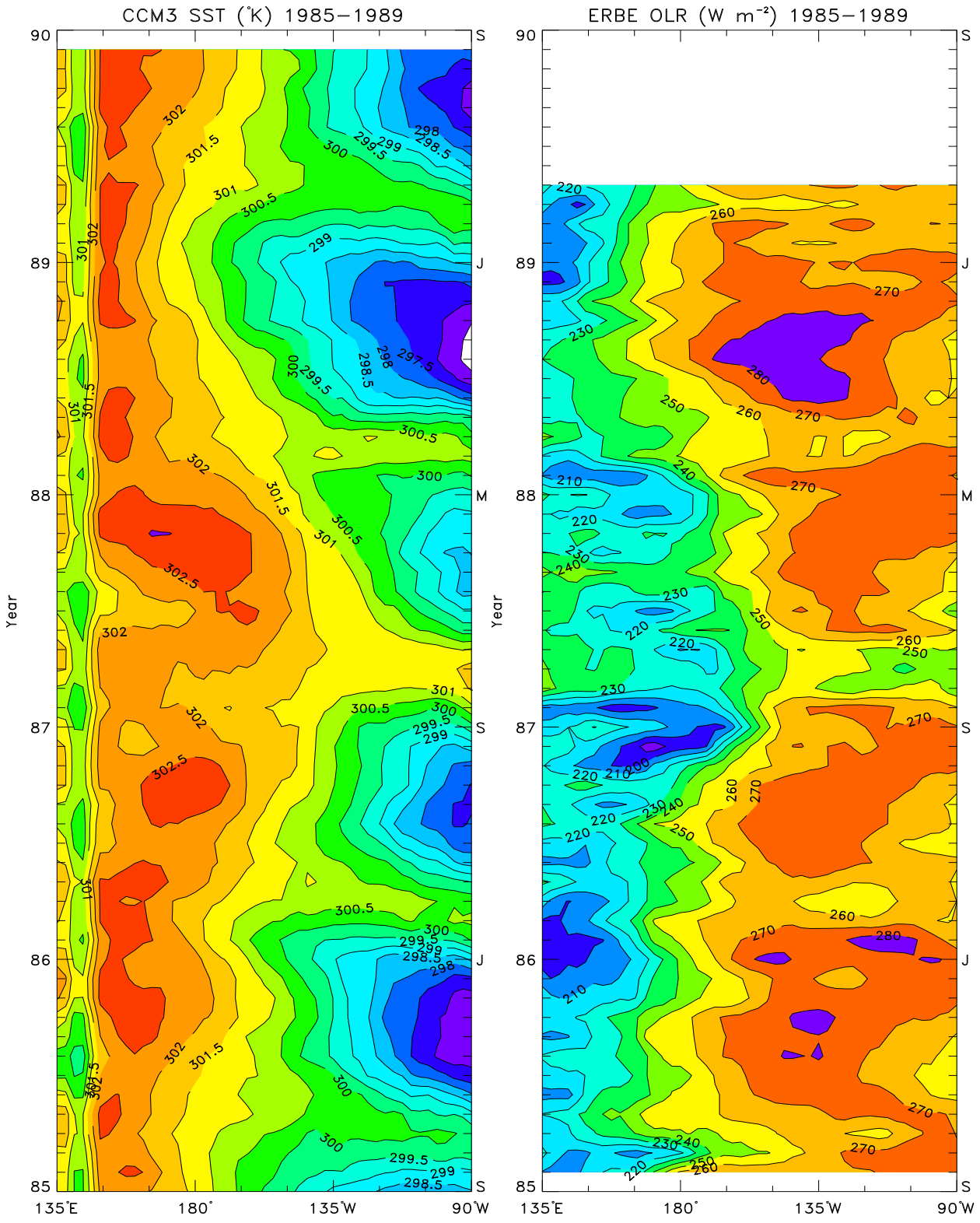

Figure 5: Hovmöller diagrams of (a) sea surface temperature [K] and (b) outgoing longwave radiation [$\mathrm{W\,m^{-2}}$] over the Equatorial Pacific (averaged 10 °S–10 °N). Month 1 is January 1985. Contour intervals are 0.5 K and 10 $\mathrm{W\,m^{-2}}$, respectively.

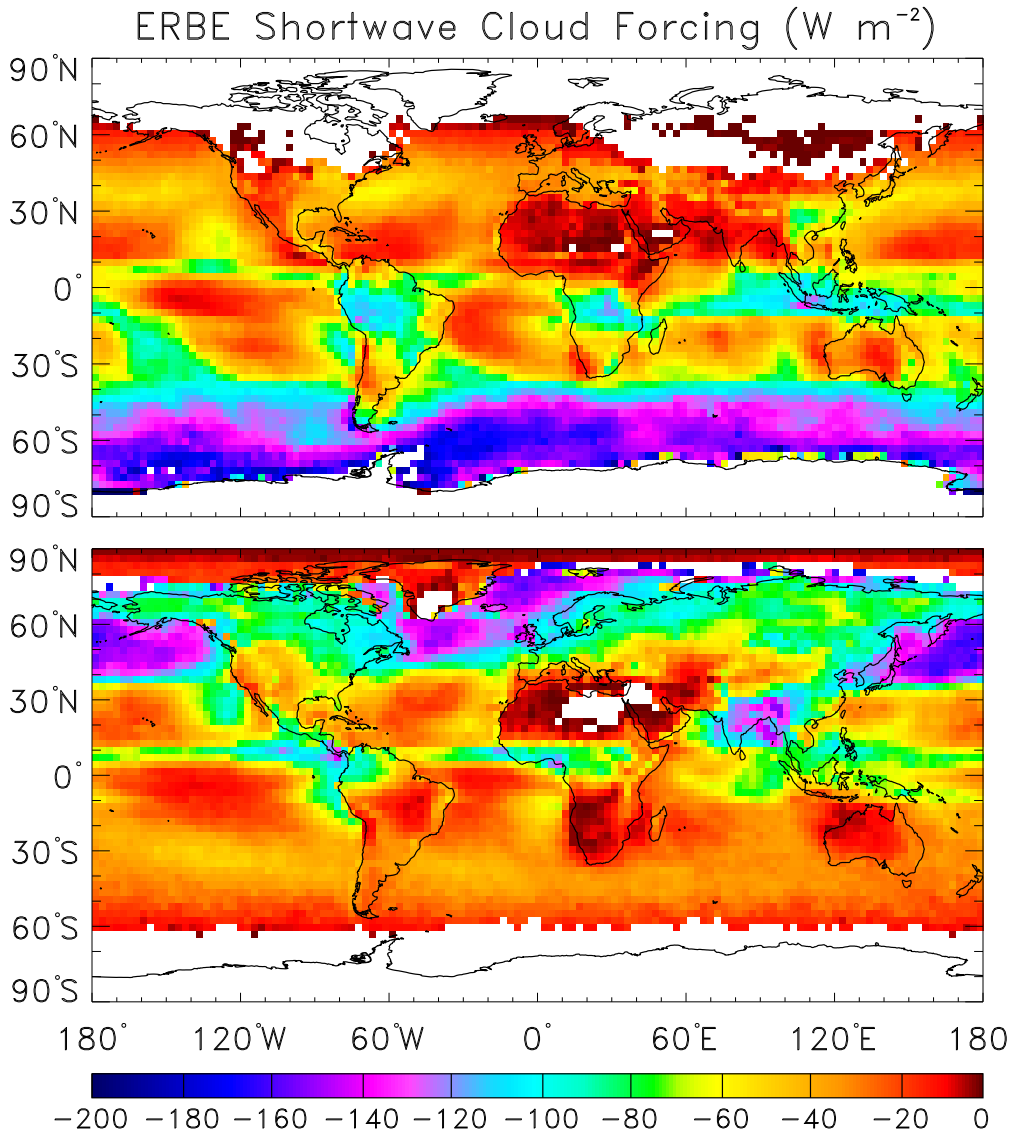

Figure 6: Geographic distribution of shortwave cloud forcing SWCF [W m^{-2}] for 1985–1989 from ERBE observations for (a) January and (b) July.

Figure 6 shows the shortwave cloud forcing (SWCF) observed by the ERBE satellite system from 1985–1989.

Figure 7 shows the zonal mean shortwave cloud forcing (SWCF) observed by the ERBE satellite system from 1985–1989.

Figure 8 shows the longwave cloud forcing (LWCF) observed by the ERBE satellite system from 1985–1989.

Figure 9 shows the zonal mean longwave cloud forcing (LWCF) observed by the ERBE satellite system from 1985–1989.

Figure 10 shows the balance between solar and terrestrial cloud forcing as observed by the ERBE satellite system from 1985–1989.

Figure 11 shows the interannual variability of the cloud forcing over the Pacific in terms of Hovmöller diagrams of cloud forcing.

9 Implementation in NCAR models

The discussion thus far has centered on the theoretical considerations of radiative transfer. In practice, these ideas must be implemented in computer codes which model, e.g., shortwave or longwave atmospheric fluxes and heating rates. This section describes how these ideas have been implemented in the NCAR narrow band models.

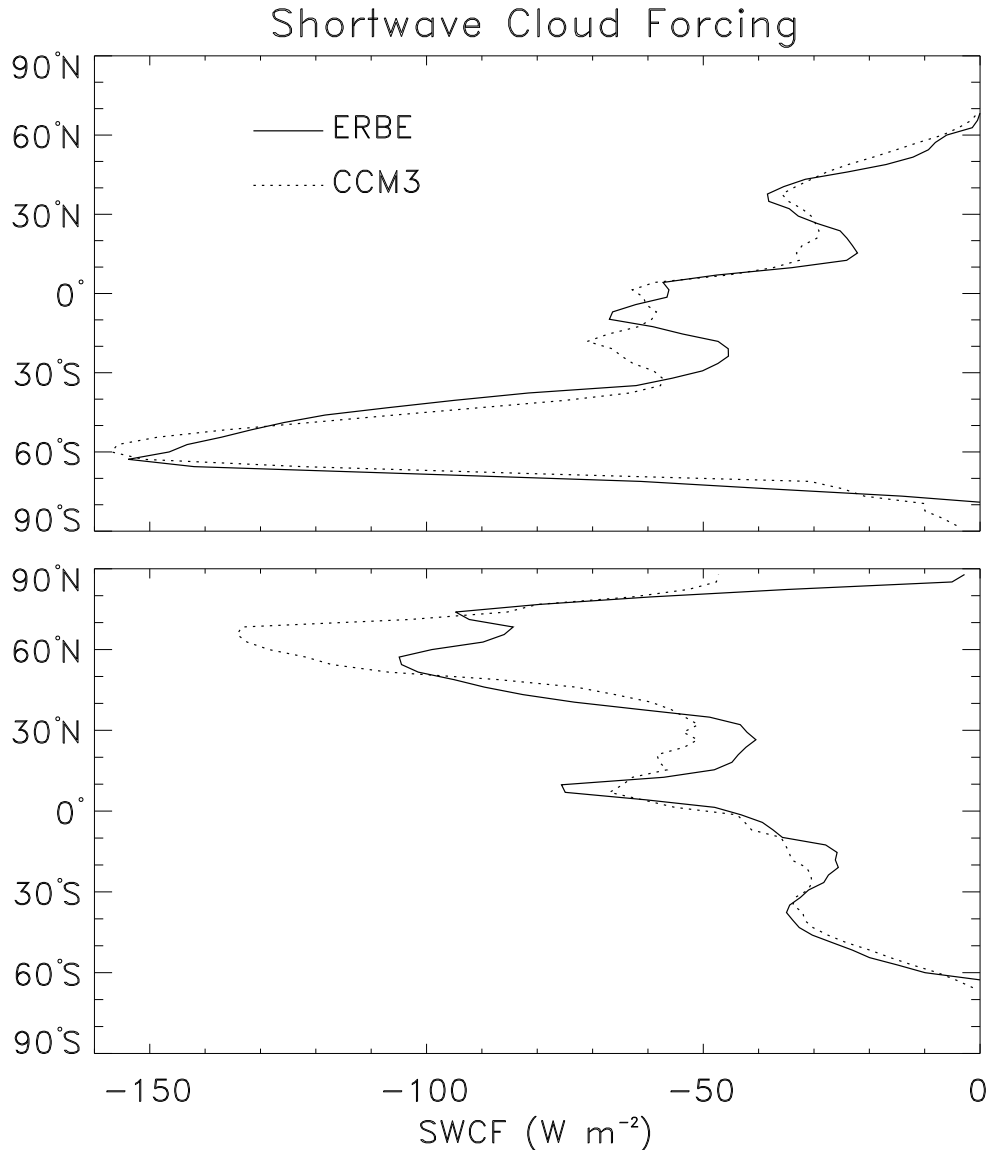

Figure 7: Zonal mean shortwave cloud forcing SWCF [$\mathrm{W\,m^{-2}}$] for 1985–1989 from ERBE observations and from CCM simulations for (a) January and (b) July.

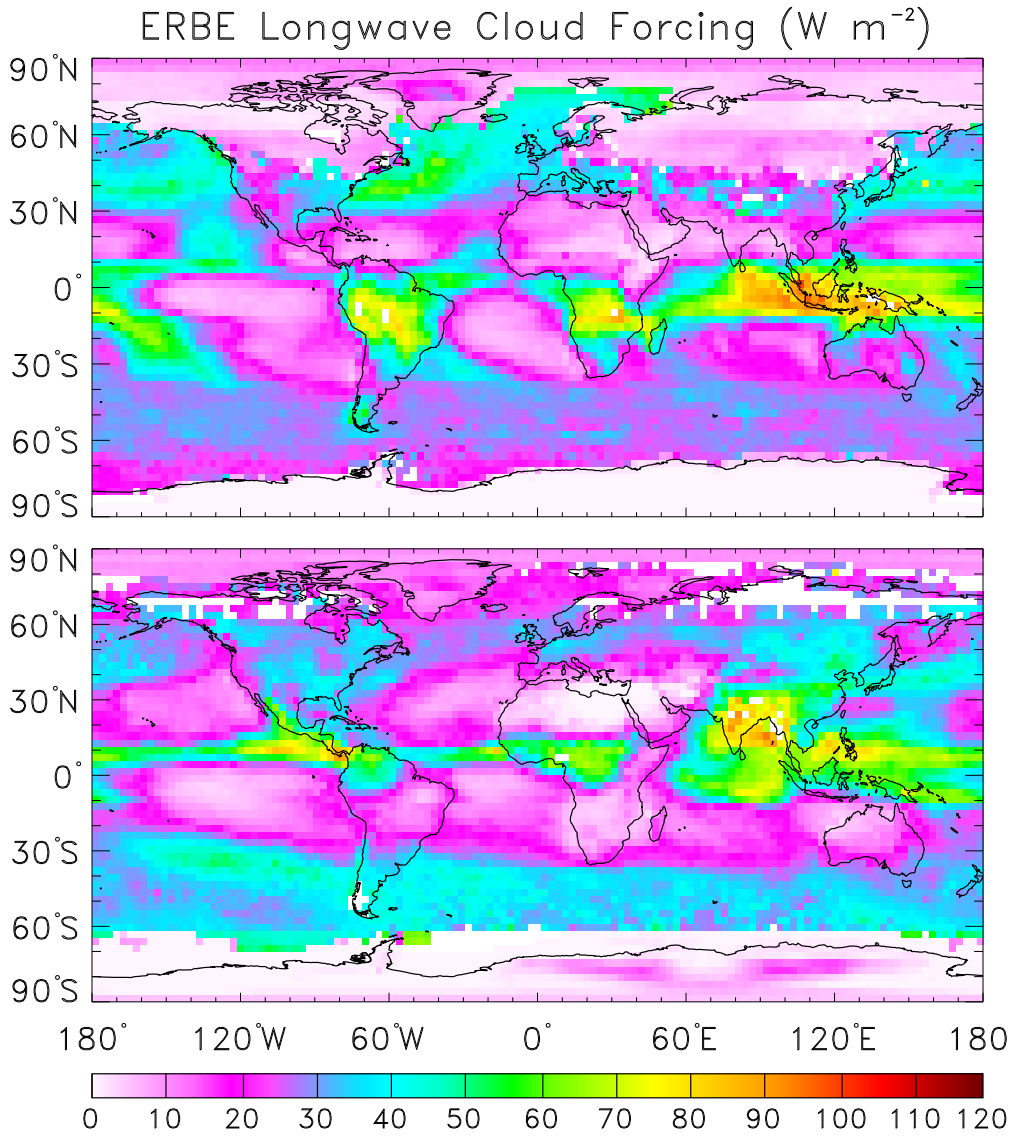

Figure 8: Geographic distribution of shortwave cloud forcing LWCF [W m^{-2}] for 1985–1989 from ERBE observations for (a) January and (b) July.

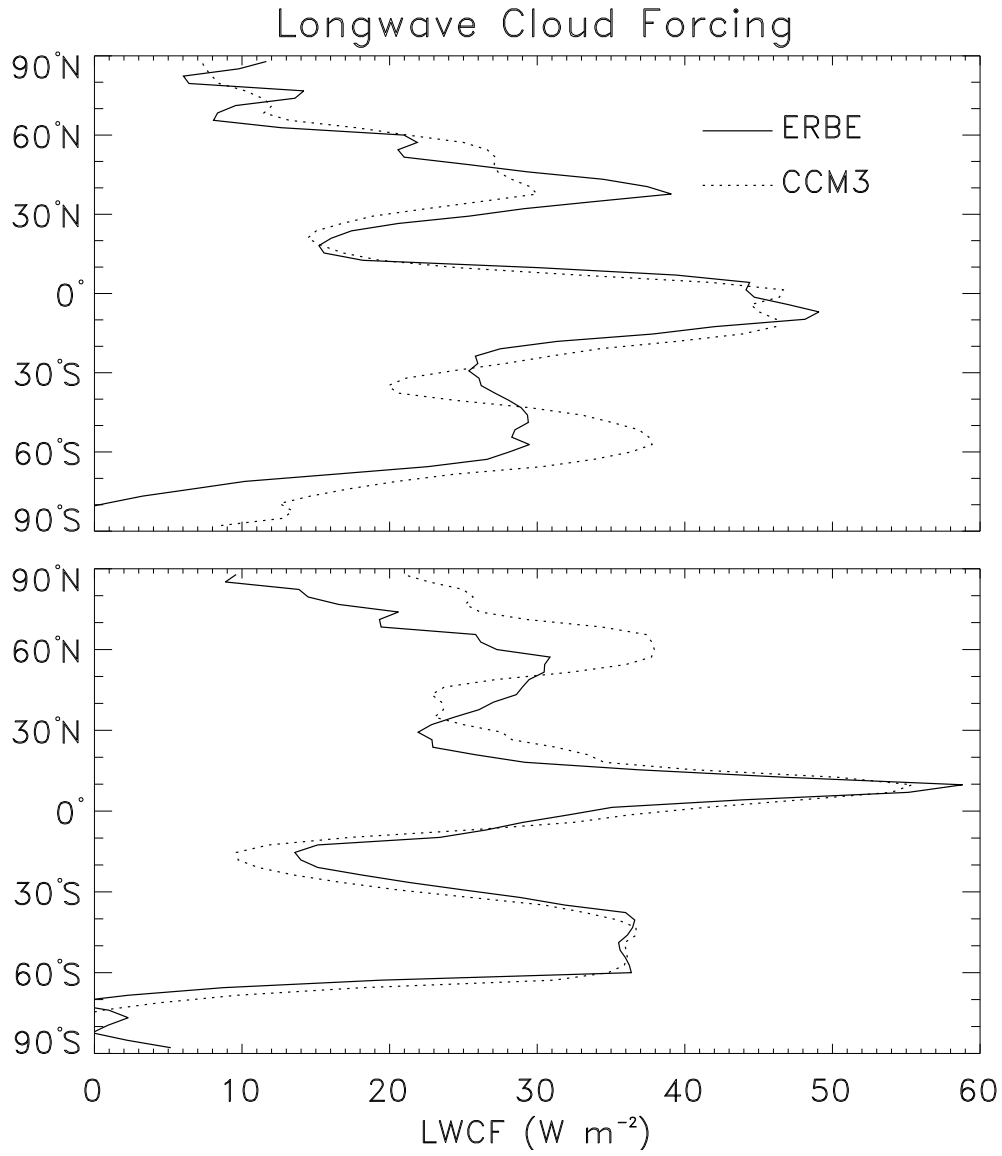

Figure 9: Zonal mean shortwave cloud forcing LWCF [$\mathrm{W\,m^{-2}}$] for 1985–1989 from ERBE observations and from CCM simulations for (a) January and (b) July.

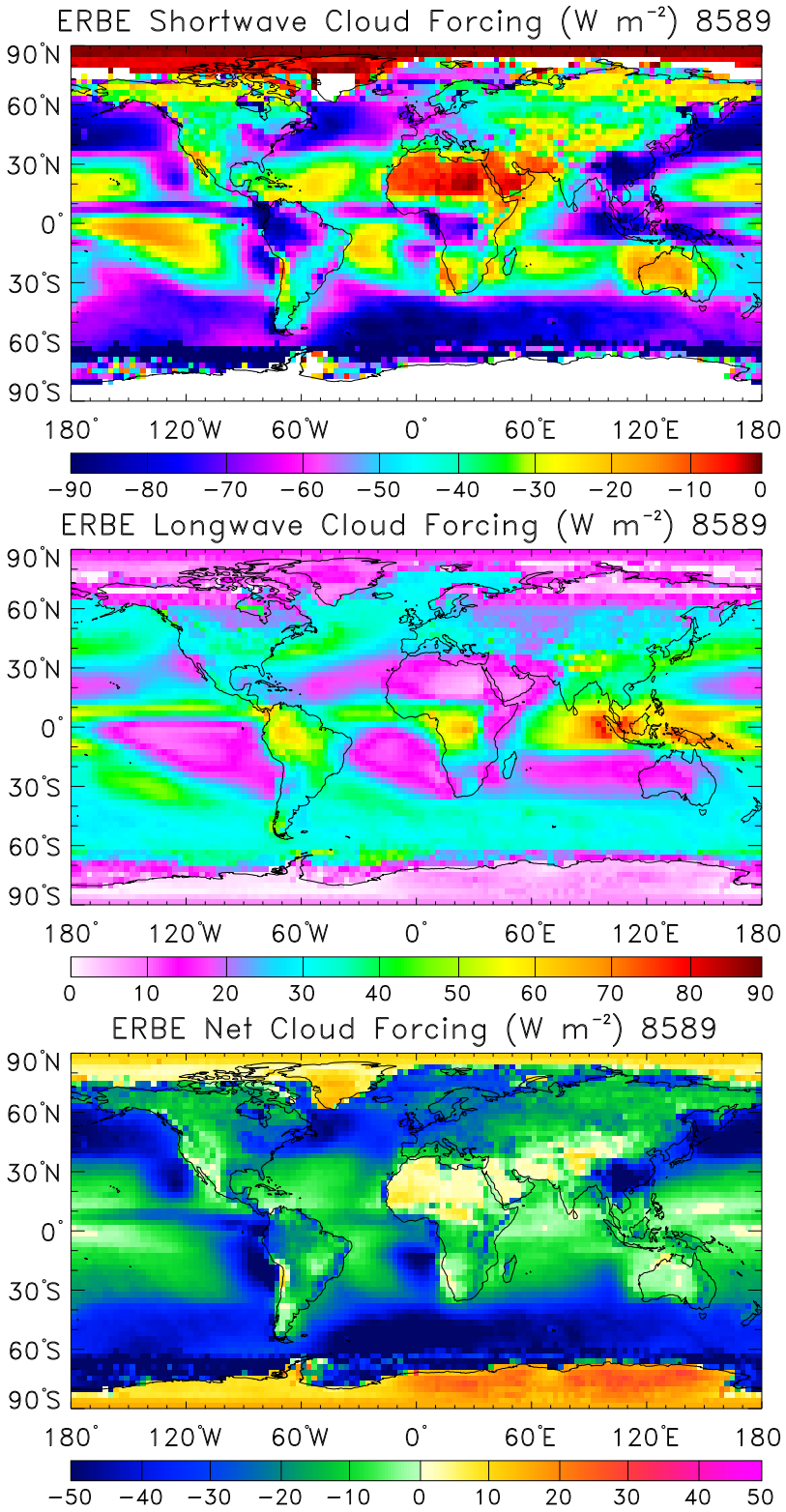

Figure 10: Geographic distribution of 1985–1989 climatological mean (a) shortwave cloud forcing SWCF, (b) longwave cloud forcing LWCF, and (c) net cloud forcing NCF [$\mathrm{W\,m^{-2}}$] from ERBE.

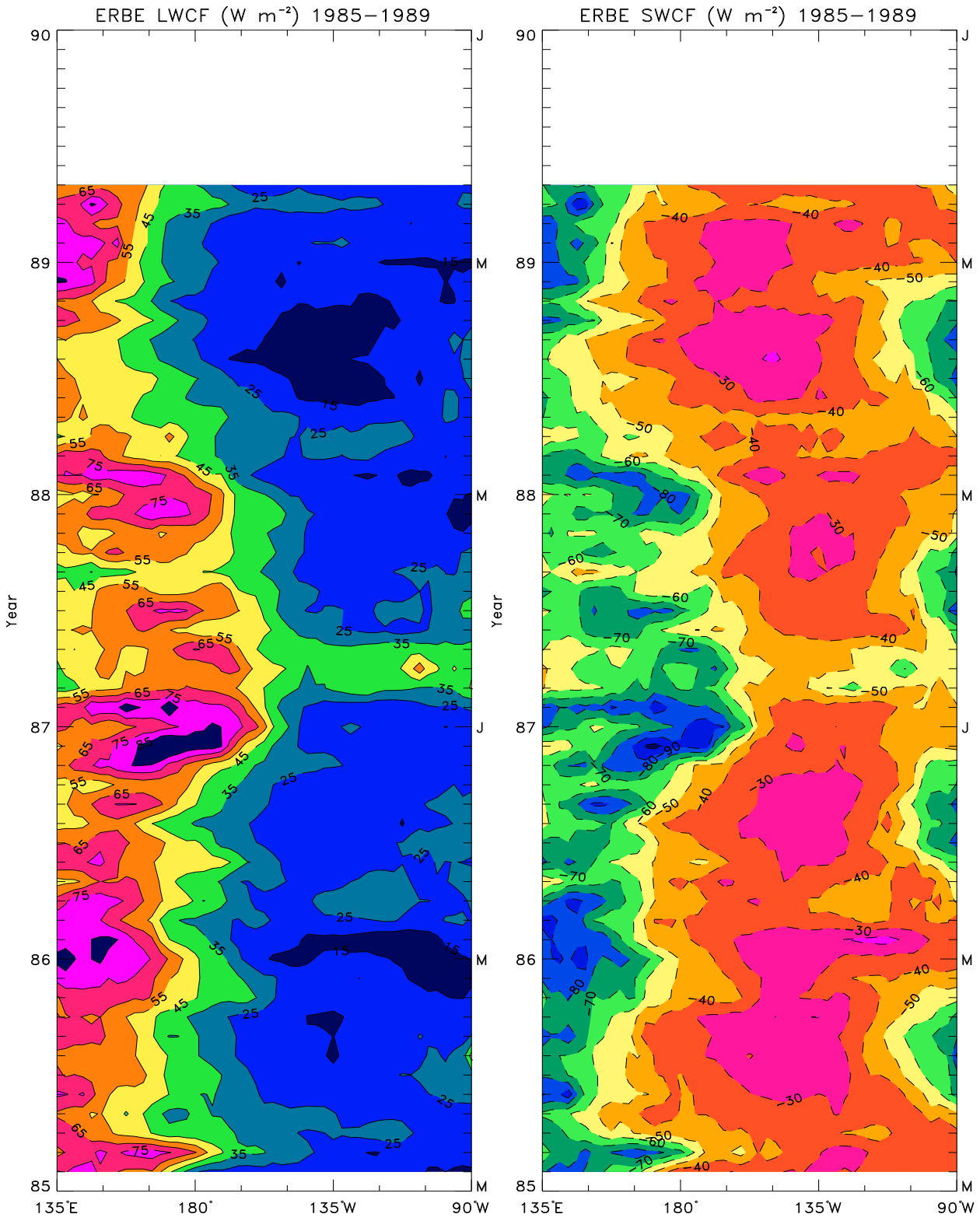

Figure 11: Hovmöller diagrams of cloud forcing [W m^{-2}] in the Equatorial Pacific (averaged 10 °S–10 °N). ERBE observations of (a) shortwave cloud forcing SWCF, and (b) longwave cloud forcing. Month 1 is January 1985. Contour interval is 10 W m^{-2}.

10 Appendix

10.1 Vector Identities

A number of vector identities are useful in the derivation of Mie theory. For arbitrary vectors $\mathbf{a}$, $\mathbf{b}$, and $\mathbf{c}$; arbitrary scalars α and β; and scalar fields $u = u(x, y, z)$ and $v = v(x, y, z)$, we have:

$$\text{Grad-linearity:} \quad \nabla(\alpha u + \beta v) = \alpha \nabla u + \beta \nabla v \tag{560a}$$

$$\text{Div-linearity:} \quad \nabla \cdot (\alpha \mathbf{a} + \beta \mathbf{b}) = \alpha \nabla \cdot \mathbf{a} + \beta \nabla \cdot \mathbf{b} \tag{560b}$$

$$\text{Curl-linearity:} \quad \nabla \times (\alpha \mathbf{a} + \beta \mathbf{b}) = \alpha \nabla \times \mathbf{a} + \beta \nabla \times \mathbf{b} \tag{560c}$$

$$\text{Dot-commutativity:} \quad \mathbf{a} \cdot \mathbf{b} = \mathbf{b} \cdot \mathbf{a} \tag{560d}$$

$$\text{Cross-(non)-commutativity:} \quad \mathbf{a} \times \mathbf{b} = -\mathbf{b} \times \mathbf{a} \tag{560e}$$

$$\text{Scalar Triple Product:} \quad \mathbf{a} \cdot \mathbf{b} \times \mathbf{c} = \mathbf{c} \cdot \mathbf{a} \times \mathbf{b} = \mathbf{b} \cdot \mathbf{c} \times \mathbf{a} \tag{560f}$$

$$\text{Cross-cross:} \quad \mathbf{a} \times (\mathbf{b} \times \mathbf{c}) = \mathbf{b}(\mathbf{a} \cdot \mathbf{c}) - \mathbf{c}(\mathbf{a} \cdot \mathbf{b}) \tag{560g}$$

$$(\mathbf{a} \times \mathbf{b}) \times \mathbf{c} = \mathbf{b}(\mathbf{a} \cdot \mathbf{c}) - \mathbf{a}(\mathbf{b} \cdot \mathbf{c}) \tag{560h}$$

$$\text{Curl-cross:} \quad \nabla \times (\mathbf{a} \times \mathbf{b}) = \mathbf{a}(\nabla \cdot \mathbf{b}) - \mathbf{b}(\nabla \cdot \mathbf{a}) + (\mathbf{b} \cdot \nabla)\mathbf{a} - (\mathbf{a} \cdot \nabla)\mathbf{b} \tag{560i}$$

$$\text{Curl-curl:} \quad \nabla \times (\nabla \times \mathbf{a}) = \nabla(\nabla \cdot \mathbf{a}) - \nabla \cdot (\nabla \mathbf{a})$$

$$= \nabla(\nabla \cdot \mathbf{a}) - \nabla^2 \mathbf{a} \tag{560j}$$

$$\text{Vector Laplacian:} \quad \nabla^2 \mathbf{a} \equiv (\nabla \cdot \nabla)\mathbf{a} \equiv \nabla \cdot (\nabla \mathbf{a}) \tag{560k}$$

$$= \nabla(\nabla \cdot \mathbf{a}) - \nabla \times (\nabla \times \mathbf{a}) \tag{560l}$$

$$\text{Grad-div:} \quad \nabla(\nabla \cdot \mathbf{a}) = \nabla^2 \mathbf{a} + \nabla \times (\nabla \times \mathbf{a}) \tag{560m}$$

$$\neq (\text{not equal}) \nabla^2 \mathbf{a}$$

$$\text{Grad-dot:} \quad \nabla(\mathbf{a} \cdot \mathbf{b}) = \mathbf{a} \times (\nabla \times \mathbf{b}) + \mathbf{b} \times (\nabla \times \mathbf{a}) + (\mathbf{b} \cdot \nabla)\mathbf{a} + (\mathbf{a} \cdot \nabla)\mathbf{b}$$

$$= (\mathbf{a} \cdot \nabla)\mathbf{b} + (\mathbf{b} \cdot \nabla)\mathbf{a} + \mathbf{a} \times (\nabla \times \mathbf{b}) + \mathbf{b} \times (\nabla \times \mathbf{a}) \tag{560n}$$

$$\text{Del-vector:} \quad \nabla \mathbf{a} \equiv \nabla_{ii} a_i \hat{\mathbf{x}}_i = \text{Dyadic} \tag{560o}$$

$$\text{Div-grad:} \quad \nabla \cdot (\nabla u) \equiv \nabla^2 u \tag{560p}$$

$$\text{Div-del:} \quad (\nabla \cdot \nabla)\mathbf{a} \equiv \nabla^2 \mathbf{a} \tag{560q}$$

$$\text{Dot-cross:} \quad \mathbf{a} \cdot (\mathbf{b} \times \mathbf{c}) = \mathbf{b} \cdot (\mathbf{c} \times \mathbf{a}) = \mathbf{c} \cdot (\mathbf{a} \times \mathbf{b}) \tag{560r}$$

$$\text{Div-curl:} \quad \nabla \cdot \nabla \times \mathbf{a} = 0 \tag{560s}$$

$$\text{Curl-grad:} \quad \nabla \times \nabla u = 0 \tag{560t}$$

$$\text{Div-product:} \quad \nabla \cdot (u\mathbf{a}) = u \nabla \cdot \mathbf{a} + \mathbf{a} \cdot \nabla u \tag{560u}$$

$$\text{Curl-product:} \quad \nabla \times (u\mathbf{a}) = \nabla u \times \mathbf{a} + u \nabla \times \mathbf{a} \tag{560v}$$

$$\text{Dot-del:} \quad (\mathbf{a} \cdot \nabla)\mathbf{a} = \frac{1}{2} \nabla |\mathbf{a}|^2 + (\nabla \times \mathbf{a}) \times \mathbf{a} \tag{560w}$$

The divergence of the curl vanishes (560s). The curl of the gradient vanishes (560t).

The Laplacian ∇^2 is shorthand for $(\nabla \cdot \nabla)$, and is usually read as "del-squared", though it is not the "square" of the del operator. The scalar Laplacian is the divergence of the gradient (560p). However, the vector Laplacian is not the gradient of the divergence (560m).

The vector Laplacian ∇^2 is defined by (??) which is obtained by simply re-arranging (560j). The vector Laplacian (??) is the gradient of the divergence (560m) minus the curl of the curl (560j).

10.2 Legendre Polynomials

The associated Legendre equation of degree n and order m is

$$\frac{\mathrm{d}}{\mathrm{d}\mu}\left[(1-\mu^2)\frac{\mathrm{d}\Theta}{\mathrm{d}\mu}\right]+\left[n(n+1)-\frac{m^2}{1-\mu^2}\right]\Theta \quad = \quad 0 \tag{561}$$

The solutions to (561) are associated Legendre polynomials, also called spherical harmonics. The associated Legendre polynomial of degree n, order m, and argument μ is denoted by $P_n^m(\mu)$. The $P_n^m(\mu)$ are orthogonal functions

$$\int_{-1}^{1} P_n^m(\mu)P_{n'}^m(\mu)\,\mathrm{d}\mu \quad = \quad \delta_{n,n'}\frac{2}{2n+1}\frac{(n+m)!}{(n-m)!} \tag{562}$$

When $m=0$, $P_n^m(\mu)$ reduces to the Legendre polynomial of order n, $P_n(\mu)$ whose orthogonality properties follow from (562) and are shown in (141). Applying suitable normalization to $P_n^m(\mu)$ yields the normalized associated Legendre polynomials $\Lambda_n^m(\mu)$

$$\Lambda_n^m(\mu) \quad \equiv \quad \sqrt{\frac{2n+1}{2}\frac{(n-m)!}{(n+m)!}}P_n^m(\mu) \tag{563}$$

The $\Lambda_n^m(\mu)$ are orthonormal and are the polar components of the spherical harmonics $Y_n^m(\theta,\phi)$ (566).

10.3 Spherical Harmonics

Spherical harmonics are the product of the normalized associated Legendre polynomials (563) and the orthonormal exponentials (564)

$$\Phi_m(\phi) \quad = \quad \frac{1}{\sqrt{2\pi}}\mathrm{e}^{\mathrm{i}m\phi} \tag{564}$$

The spherical harmonics $Y_n^m(\theta,\phi)$ of degree n and order m are

$$Y_n^m(\theta,\phi) \quad \equiv \quad (-1)^m\sqrt{\frac{2n+1}{4\pi}\frac{(n-m)!}{(n+m)!}}P_n^m(\cos\theta)\mathrm{e}^{\mathrm{i}m\phi} \tag{565}$$

The Condon-Shortley phase factor $(-1)^m$ is a convention which causes the sign alternation for the positive m spherical harmonics (Arfken, 1985, p. 682).

The spherical harmonics (566) are normalized such that

$$\int_{\phi=0}^{\phi=2\pi}\int_{\theta=0}^{\theta=\pi} Y_n^{m*}(\theta,\phi)Y_{n'}^{m'}(\theta,\phi) \quad \equiv \quad \delta_{n,n'}\delta_{m,m'} \tag{566}$$

where $*$ denotes the complex conjugate.

10.4 Bessel Functions

The definitive reference for properties of Bessel functions is Watson (1958). Other useful references are Abramowitz and Stegun (1964), p. 374 and Arfken (1985), p. 573. When the Helmholtz equation is solved by separation of variables in cylindrical or spherical coordinates (521), the radial component satisfies Bessel's equation (Watson, 1958, p. 19),

$$z^2 \frac{\mathrm{d}^2 w}{\mathrm{d}z^2} + z \frac{\mathrm{d}w}{\mathrm{d}z} + [z^2 - \nu^2] w \quad = \quad 0 \tag{567}$$

Bessel functions are solutions to (567). The order of the functions is indicated by the parameter ν (not to be confused with frequency). The functions take a single argument z. Both ν and z may be complex, e.g., $z = x + \mathrm{i}y$, although our particular applications depend only on real-valued ν. Indeed, we require only integer and half-integer ν.

Due to their power and range of applicability, a menagerie of inter-related solutions to (567) exist. Fortunately, the terminology to identify and describe them is standard. The standard Bessel functions of the first kind, second kind, and third kind, are denoted by $J_\nu(z)$, $Y_\nu(z)$, and $H_\nu^{(1)}(z)$ and $H_\nu^{(2)}(z)$, respectively. Bessel functions of the second kind are also called Neumann functions and notated with is $N_\nu(z)$ instead of $Y_\nu(z)$. Mathematical physics texts often use the Neumann function notation $N_\nu(z)$ to avoid confusion with spherical harmonics; whereas pure mathematical texts normally use the $Y_\nu(z)$ notation. Bessel functions of the third kind are also called Hankel functions. All of these satisfy (567) and so are properly called Bessel functions. Specialized versions of Bessel functions derive from the three basic kinds. These specializations include modified Bessel functions, and spherical Bessel functions.

General solutions to the Bessel equation (567) are formed from any two linearly independent Bessel functions. For non-integer ν, $J_\nu(z)$ and $J_{-\nu}(z)$ are linearly independent solutions and so form a complete basis. However, for integral ν

$$J_{-n}(z) \quad = \quad (-1)^n J_n(z) \quad \text{Integer } n \tag{568}$$

and these solutions are not linearly independent.

Bessel functions of the second kind $Y_\nu(z)$ are always linearly independent of $J_\nu(z)$. They may be defined as

$$Y_\nu(z) \quad = \quad N_\nu(z) = \frac{J_\nu(z)\cos(\nu\pi) - J_{-\nu}(z)}{\sin \nu\pi} \tag{569}$$

where the RHS limiting value used for integral ν. Bessel functions of the first and second kind, $J_\nu(z)$ and $Y_\nu(z)$ together form a complete basis. Series expansion (not shown) reveals that $Y_n(z)$ diverges logarithmically as $z \to 0$. Boundary conditions which require finite solutions at the origin ($z = 0$) therefore automatically exclude $Y_n(z)$. Conversely, $Y_n(z)$ may appear in any solution which does not require finite values at the origin.

Bessel functions of the third kind (Hankel functions), $H_\nu^{(1)}(z)$ and $H_\nu^{(2)}(z)$, are another set of linearly independent solutions to Bessel's equation. The relation between these complete bases is

$$H_\nu^{(1)}(z) = J_\nu(z) + \mathrm{i}Y_\nu(z) \tag{570a}$$

$$H_\nu^{(2)}(z) = J_\nu(z) - \mathrm{i}Y_\nu(z) \tag{570b}$$

10.4.1 Spherical Bessel Functions

The spherical Bessel functions of the first and second kind are

$$j_\nu(z) = \sqrt{\frac{\pi}{2z}} J_{\nu+1/2}(z) \tag{571a}$$

$$y_\nu(z) = \sqrt{\frac{\pi}{2z}} Y_{\nu+1/2}(z) \tag{571b}$$

In analogy to (570b) the spherical Bessel functions of the third kind, or spherical Hankel functions are

$$h_\nu^{(1)}(z) = j_\nu(z) + \mathrm{i} y_\nu(z) \tag{572a}$$

$$h_\nu^{(2)}(z) = j_\nu(z) - \mathrm{i} y_\nu(z) \tag{572b}$$

10.4.2 Recurrence Relations

Bessel functions (and thus spherical Bessel functions) satisfy the recurrence relations

$$Z_{\nu-1}(z) + Z_{\nu+1}(z) = \frac{2\nu}{z} Z_\nu(z) \tag{573a}$$

$$Z_{\nu-1}(z) - Z_{\nu+1}(z) = 2Z'_\nu(z) \tag{573b}$$

$$Z'_\nu(z) = Z_{\nu-1}(z) - \frac{\nu}{z} Z_\nu(z) \tag{573c}$$

$$Z'_\nu(z) = -Z_{\nu+1}(z) + \frac{\nu}{z} Z_\nu(z) \tag{573d}$$

Seed values for recurrence relations (573d) may be obtained from

$$J'_0(z) = -J_1(z) \tag{574a}$$

$$Y'_0(z) = -Y_1(z) \tag{574b}$$

10.4.3 Power Series Representation

The power series for regular Bessel functions of the first kind is

$$J_\nu(z) \quad = \quad (\tfrac{1}{2}z)^\nu \sum_{k=0}^{\infty} \frac{(-\frac{1}{4}z^2)^k}{k!\,\Gamma(\nu+k+1)} \tag{575}$$

Modified Bessel functions of the first kind are defined in terms ordinary Bessel functions as

$$I_\nu(z) \quad = \quad \mathrm{i}^{-\nu} J_\nu(\mathrm{i}z) \tag{576}$$

The power series for the modified Bessel function of the first kind, $I_\nu(z)$ differs from (575) due to the absence of the negative sign

$$I_\nu(z) \quad = \quad (\tfrac{1}{2}z)^\nu \sum_{k=0}^{\infty} \frac{(\frac{1}{4}z^2)^k}{k!\,\Gamma(\nu+k+1)} \tag{577}$$

Of particular interest to radiative transfer are $I_0(z)$ and $I_1(z)$ which appear in the solution to the mean beam absorptance (397) and equivalent width of an isolated Lorentz line.

$$I_0(z) = \sum_{k=0}^{\infty} \frac{(\frac{1}{2}z)^{2k}}{(k!)^2} \tag{578a}$$

$$I_1(z) = \sum_{k=0}^{\infty} \frac{(\frac{1}{2}z)^{2k+1}}{k!\,(k+1)!} \tag{578b}$$

For $z \ll 1$, (578) becomes

$$I_0(z \ll 1) \approx 1 \tag{579a}$$

$$I_1(z \ll 1) \approx z/2 \tag{579b}$$

10.4.4 Asymptotic Values

The asymptotic behavior of functions can often be ascertained from their power series representation. Bessel functions obey the following limits as $z \to 0$:

$$Z_\nu(z) \to (\tfrac{1}{2}z)^\nu/\Gamma(\nu+1) \quad (\nu \neq -1, -2, -3\ldots) \tag{580a}$$

$$Y_0(z) \to (2/\pi)\ln z \tag{580b}$$

$$Y_\nu(z) \to \frac{\Gamma(\nu)}{\pi(\frac{1}{2}z)^\nu} \tag{580c}$$

10.5 Gaussian Quadrature

The accuracy of automatic integration of analytic formulae by computers rests on three criteria:

1. Smoothness of function
2. Number of quadrature points
3. Placement of quadrature points

For many problems the functional form of the integrand is given. We are usually free to change, however, the number and placement of quadrature points. For many applications, the optimal number and location of quadrature points are related through Gaussian quadrature.

Gaussian quadrature points x_k have the property that

$$\int_a^b f(x)w(x)\,\mathrm{d}x \approx \sum_{k=1}^{n} A_k f(x_k) \tag{581}$$

is exact if $f(x)$ is any polynomial of degree $\leq 2n-1$. The values of the x_k are determined by the form of the weighting function $w(x)$ and the interval boundaries $[a,b]$. In fact the x_k are the roots of the orthogonal polynomial with weighting function $w(x)$ over the interval $[a,b]$ (see, e.g., Arfken, 1985, p. 969). A common case in radiative transfer has $w(x) = 1$, $[a,b] = [-1,1]$

$$\int_{-1}^{1} f(x)\,\mathrm{d}x \approx \sum_{k=1}^{n} A_k f(x_k) \tag{582}$$

For this case, the x_k are the n roots of the Legendre polynomial of degree n, $P_n(x)$, [18] and the Gaussian weights A_k are defined by the derivative of $P_n(x)$

$$x_k = x \in [0,1] \mid P_n(x_k) = 0 \tag{583}$$

$$A_k = \frac{2}{(1-x_k^2)[P_n'(x_k)]^2} \tag{584}$$

Radiative transfer problems often use Gaussian weights in the angular integration. Depending on whether we are concerned with net or hemispherical quantities the angular integration will have different intervals

$$\int_{-1}^{1} f(x)w(x)\,\mathrm{d}x \approx \sum_{k=1}^{n} A_k f(x_k) \tag{585}$$

$$\int_{0}^{1} f(y)w(y)\,\mathrm{d}y \approx \sum_{k=1}^{n} B_k f(y_k) \tag{586}$$

Equation (585) is known as full-range Gaussian quadrature and (586) as half-range Gaussian quadrature.

The half-range points and weights are intimately related to the full-range points and weights. The interval $y \in [0,1]$ is a simple linear transformation of $x \in [-1,1]$

$$y = \frac{x+1}{2} \tag{587}$$

$$x = 2y - 1 \tag{588}$$

The half-range points and weights may be obtained by applying the forward transformation (587) to (585). Thus

$$y_k = \frac{x_k + 1}{2} \tag{589}$$

The weights A_k depend only on n (fxm: I think) and are independent of $f(x)$ and $w(x)$. For Legendre polynomials, the A_k and B_k sum to the size of the interval

$$\sum_{k=1}^{n} A_k = 2 \tag{590}$$

$$\sum_{k=1}^{n} B_k = 1 \tag{591}$$

A common technique is to apply half of the full range quadrature points and weights to half of the full range interval, $[0,1]$. In this case the quadrature is no longer Gaussian (i.e., not exact for polynomials of degree $< 2n$), but the quadrature points are often quite optimal.

Table 9 lists the first five Legendre polynomials, their roots, the associated full Gaussian angles, and their Gaussian weights. Abramowitz and Stegun (1964), p. 917, list Gaussian quadrature points and weights for $n \leq 32$.

Table 10 summarizes the same information needed for half-range Gaussian quadrature.

[18] When $w(x) \neq 1$, the Gaussian quadrature points are the roots of other orthogonal polynomials, e.g., Chebyshev, Laguerre, Hermite.

Table 9: Full-range Gaussian quadrature[a]

n, k	Polynomial $P_n(\mu)$	Root μ_k	Decimal μ_k	Angle θ_k	Weight A_k
$1, 1$	μ	0	0.0	$90.0°$	2.0
$2, 1$	$\frac{1}{2}(3\mu^2 - 1)$	$1/\sqrt{3}$	0.577350	$54.7356°$	1.0
$3, 1$	$\frac{1}{2}(5\mu^3 - 3\mu)$	0	0.0	$90.0°$	0.888889
$3, 2$		$\sqrt{\frac{3}{5}}$	0.774597	$39.2321°$	0.555556
$4, 1$	$\frac{1}{8}(35\mu^4 - 30\mu^2 + 3)$	$\left(\frac{15-2\sqrt{30}}{35}\right)^{1/2}$	0.339981	$70.1243°$	0.652145
$4, 2$		$\left(\frac{15+2\sqrt{30}}{35}\right)^{1/2}$	0.861136	$30.5556°$	0.347855

[a]The μ_k and A_k are only supplied for $k \leq \frac{n+2}{2}$. The μ_k are antisymmetric, and the A_k are symmetric, about $k = n/2$. Thus $\mu_{n-k} = -\mu_k$ and $A_{n-k} = A_k$.

Table 10: Half-range Gaussian quadrature[a]

n, k	Polynomial $P_n(\mu)$	Root μ_k	Decimal μ_k	Angle θ_k	Weight A_k
$1, 1$	μ	0	0.0	$90.0°$	2.0
$2, 1$	$\frac{1}{2}(3\mu^2 - 1)$	$+1/\sqrt{3}$	$+0.57735$	$+54.7356°$	1.0
$3, 1$	$\frac{1}{2}(5\mu^3 - 3\mu)$				
$4, 1$	$\frac{1}{8}(35\mu^4 - 30\mu^2 + 3)$				

[a]The symmetries differ from Table 9. The polynomials, roots and weights need to be transformed from their full-range counterparts.

10.6 Gauss-Lobatto Quadrature

Lobatto quadrature, is a type of Gaussian quadrature that prescribes abscissae at the integration endpoints. The Lobatto quadrature rule of order L is

$$\int_{-1}^{+1} f(x)\,\mathrm{d}x = \sum_{l=1}^{l=L} H_l f(x_l) \tag{592}$$

$$= H_1 f(-1) + \sum_{l=1}^{l=L} H_l f(x_l) + H_L f(1) \tag{593}$$

Whereas Gaussian quadrature is exact for polynomials of degrees $\leq 2L-1$, Lobatto quadrature fixes two quadrature points and so is exact only for polynomials of degrees $\leq 2L-3$. Nevertheless, the placement of abscissae can give Lobatto quadrature a higher effective accuracy for certain classes of functions such as asymmetric phase functions (Wiscombe, 1977).

The free (non-prescribed) Lobatto abscissae x_l for $l = 2, \ldots, L-1$ are the $L-2$ zeros of the derivative of the Legendre polynomial of degree $L-1$

$$P'_{L-1}(x_l) = 0 \tag{594}$$

(By comparison, the abscissae in Gauss-Legendre quadrature are Legendre polynomial roots).

The interior Lobatto weights H_l satisfy

$$H_l = \frac{2}{L(L-1)[P_{L-1}(x_l)]^2} \tag{595}$$

while the endpoint weights are

$$H_1 = H_L = \frac{2}{L(L-1)} \tag{596}$$

Michels (1963) describes numerical approaches to determining Lobatto quadrature abscissae endpoints and weights. This procedure converges remarkably quickly and smoothly. However, the traditional quadrature variable $u = \cos(\theta)$ and range $[-1, 1]$ produce abscissae that a forward-clustered in $\cos(\theta)$ and thus angles that are relatively evenly distributed (rather than forward-clustered) in θ.

Wiscombe (1977) puts forward a solution to this problem. He changes the quadrature variable and domain to θ and $[0, \pi]$, respectively. Implementing this procedure is relatively straightforward. The Lobatto weights H_l must be normalized on the new integration domain

$$H_l = \frac{\pi}{L(L-1)[P_{L-1}(x_l)]^2} \tag{597}$$

while the endpoint weights are

$$H_1 = H_L = \frac{\pi}{L(L-1)} \tag{598}$$

10.7 Exponential Integrals

The exponential integrals $E_n(x)$ are defined by

$$E_n(x) = \int_1^\infty t^{-n} \mathrm{e}^{-tx}\,\mathrm{d}t \tag{599}$$

and by the behavior of $E_n(x)$ at $x = 0$

$$\begin{aligned} E_1(0) &= \infty \\ E_n(0) &= 1/(n-1) \end{aligned}$$

A definition equivalent to (599) is obtained by making the change of variable $w = t^{-1}$. This maps $t \in [1, \infty)$ into $w \in [1, 0]$

$$\begin{aligned} w &= t^{-1} \\ t &= w^{-1} \\ \mathrm{d}t &= -w^{-2}\,\mathrm{d}w \\ \mathrm{d}w &= -t^{-2}\,\mathrm{d}t \end{aligned} \tag{600}$$

Substituting (600) into (599) we obtain

$$\begin{aligned} E_n(x) &= \int_1^0 (w^{-1})^{-n} \mathrm{e}^{-x/w}(-w^{-2})\,\mathrm{d}w \\ &= \int_0^1 w^n w^{-2} \mathrm{e}^{-x/w}\,\mathrm{d}w \\ &= \int_0^1 w^{n-2} \mathrm{e}^{-x/w}\,\mathrm{d}w \end{aligned} \tag{601}$$

Exponential integrals satisfy two important recurrence relations

$$-E_n'(x) = -E_{n-1}(x) \tag{602a}$$

$$nE_{(n+1)}(x) = \mathrm{e}^{-x} - xE_n(x) \tag{602b}$$

The angular integral of many radiometric quantities may often be expressed in terms of the first few exponential integrals.

$$E_n(\tau) = \int_0^1 \mu^{n-2} \mathrm{e}^{-\tau/\mu}\,\mathrm{d}\mu \tag{603a}$$

$$E_1(\tau) = \int_0^1 \mu^{-1} \mathrm{e}^{-\tau/\mu}\,\mathrm{d}\mu \tag{603b}$$

$$E_2(\tau) = \int_0^1 \mathrm{e}^{-\tau/\mu}\,\mathrm{d}\mu \tag{603c}$$

$$E_3(\tau) = \int_0^1 \mu \mathrm{e}^{-\tau/\mu}\,\mathrm{d}\mu \tag{603d}$$

Bibliography

Abramowitz, M., and I. Stegun (1964), Handbook of Mathematical Functions, 1046 pp., Dover, New York. 10.4, 10.5

Arfken, G. (1985), Mathematical Methods for Physicists, third ed., Academic Press, San Diego, CA. 7.2, 10.3, 10.4, 10.5

Bennett, H. S., and G. J. Rosasco (1978), Resonances in the efficiency factors for absorption: Mie scattering theory, Appl. Opt., 17(4), 491–493. 7.2.7

Bohren, C. F., and D. R. Huffman (1983), Absorption and Scattering of Light by Small Particles, 530 pp., John Wiley & Sons, New York, NY. 1, 3.3, 7.1, 7.1.1, 7.1.1, 7.1.1, 7.2.1, 7.2.2, 7.2.6, 7.2.7

Boucher, O. (1998), On aerosol direct shortwave forcing and the Henyey-Greenstein phase function, J. Atmos. Sci., 55(1), 128–134. 2.2.7

Briegleb, B. P. (1992), Longwave band model for thermal radiation in climate studies, J. Geophys. Res., 97(D11), 11,475–11,485. 5.5.1, 6.1

Carrier, G. F., M. Krook, and C. E. Pearson (1983), Functions of a Complex Variable, Hod Books, Ithaca, NY. 2.1.11

Cess, R. D. (1985), Nuclear war: Illustrative effects of atmospheric smoke and dust upon solar radiation, Clim. Change, 7(2), 237–251, doi:10.1007/BF00140,508. 7.5.1

Chang, J. S., R. A. Brost, I. S. A. Isaksen, S. Madronich, P. Middleton, W. R. Stockwell, and C. J. Walcek (1987), A three-dimensional Eulerian acid deposition model: Physical concepts and formulation, J. Geophys. Res., 92, 14,681–14,700. 2.1.4

Chou, M. D., and A. Arking (1980), Computation of infrared cooling rates in the water vapor bands, J. Atmos. Sci., 37, 855–867. 6.3.2

Chýlek, P., J. T. Kiehl, and M. K. W. Ko (1978a), Narrow resonance structure in the Mie scattering characteristics, Appl. Opt., 17(19), 3019–3021. 7.2.7

Chýlek, P., J. T. Kiehl, and M. K. W. Ko (1978b), Optical levitation and partial-wave resonances, Phys. Rev. A, 18(5), 2229–2233. 7.2.7

Clough, S. A., F. X. Kneizys, and R. W. Davies (1989), Line shape and the water vapor continuum, Atmos. Res., 23, 229–241. 5.6.1

Colarco, P. R., O. B. Toon, O. Torres, and P. J. Rasch (2002), Determining the UV imaginary index of refraction of Saharan dust particles from Total Ozone Mapping Spectrometer data using a three-dimensional model of dust transport, J. Geophys. Res., 107(D16), doi:10.1029/2001JD000,903. 7.1

Crisp, D. (1997), Absorption of sunlight in clear and cloudy atmospheres: A solution to the cloud absorption anomaly?, Rejected by J. Geophys. Res. 5.6.1

Dahlback, A., and K. Stamnes (1991), A new spherical model for computing the radiation field available for photolysis and heating at twilight, Planet. Space Sci., 39(5), 671–683. 2.1.4

DeMore, W. B., S. P. Sander, D. M. Golden, R. F. Hampson, M. J. Kurylo, C. J. Howard, A. R. Ravishankara, C. E. Kolb, and M. J. Molina (1994), Chemical kinetics and photochemical data for use in stratospheric modeling, Evaluation Number 11 92-20, Jet Propulsion Laboratory, Pasadena Calif. 4.1.1

Ellingson, R. G., and W. J. Wiscombe (1996), The spectral radiance experiment (SPECTRE): Project description and sample results, Bull. Am. Meteorol. Soc., 77(9), 1967–1985. 5.6.1

Fu, Q., and K. N. Liou (1992), On the correlated k-distribution method for radiative transfer in nonhomogeneous atmospheres, J. Atmos. Sci., 49(22), 2139–2156. 5.6.1

Gamache, R. R., and L. S. Rothman (1992), Extension of the HITRAN database to non-LTE applications, J. Quant. Spectrosc. Radiat. Transfer, 48(5/6), 519–525. 5.5.1

Gamache, R. R., R. L. Hawkins, and L. S. Rothman (1990), Total internal partition sums in the temperature range 70–3000 k: atmospheric linear molecules, J. Mol. Spectrosc., 142, 205–219. 5.5.1

Gamache, R. R., S. Kennedy, R. L. Hawkins, and L. S. Rothman (2000), Total internal partition sums for molecules in the terrestrial atmosphere, Journal of Molecular Structure, 517/518, 413–431. 5.5.1

Godson, W. L. (1953), The evaluation of infra-red radiative fluxes due to atmospheric water vapour, Q. J. R. Meteorol. Soc., 79, 367–379. 6.2.1

Goody, R. M. (1952), A statistical model for water-vapour absorption, Q. J. R. Meteorol. Soc., 78, 165. 6.2.1

Goody, R. M., and Y. L. Yung (1989), Atmospheric Radiation Theoretical Basis, second ed., Oxford Univ. Press, New York. 1, 2.2.15, 13, 4.1.5, a, 6.2, 6.3.2

Gradshteyn, I. S., and I. M. Ryzhik (1965), Table of Integrals, Series, and Products, fourth ed., Academic Press, New York. 6.2.4

Guimarães, L. G., and H. M. Nussenzveig (1994), Uniform approximation to Mie resonances, J. Modern Optics, 41(3), 625–647. 7.2.7

Hansen, J. E., and L. D. Travis (1974), Light scattering in planetary atmospheres, Space Sci. Rev., 16, 527–610. 7.2.6

Hess, M., P. Koepke, and I. Schult (1998), Optical properties of aerosols and clouds: The software package OPAC, Bull. Am. Meteorol. Soc., 79(5), 831–844. 7.1

Hui, A. K., B. H. Armstrong, and A. A. Wray (1978), Rapid computation of the Voigt and complex error functions, J. Quant. Spectrosc. Radiat. Transfer, 19, 509–516. 4.1.5

Humlíček, J. (1982), Optimized computation of the Voigt and complex probability functions, J. Quant. Spectrosc. Radiat. Transfer, 27(4), 437–444. 4.1.5

Jackson, J. D. (1975), Classical Electrodynamics, 848 pp., John Wiley & Sons, New York. 7.1.1

Joseph, J. H., W. J. Wiscombe, and J. A. Weinman (1976), The delta-Eddington approximation for radiative flux transfer, J. Atmos. Sci., 33(12), 2452–2459. 2.2.7

Kiehl, J. T. (1997), Radiative transfer in troposphere-stratosphere global climate models, in The Stratosphere and its Role in the Climatic System, NATO ASI Series I, vol. 54, edited by G. P. Brasseur, chap. 4, pp. 102–131, Springer-Verlag, Berlin. 6.1

Kiehl, J. T., and V. Ramanathan (1983), CO_2 radiative parameterization used in climate models: Comparison with narrow band models and with laboratory data, J. Geophys. Res., 88(C9), 5191–5202. 6.1

Knyazikhin, Y., A. Marshak, W. J. Wiscombe, J. Martonchik, and R. B. Myneni (2002), A missing solution to the transport equation and its effect on estimation of cloud absorptive properties, J. Atmos. Sci., 59(23), 3572–3585. 7.5.1

Kuntz, M. (1997), A new implementation of the Humlicek algorithm for the calculation of the Voigt profile function, J. Quant. Spectrosc. Radiat. Transfer, 57(6), 819–824. 4.1.5

Ladenburg, R., and F. Reiche (1913), Unknown, Ann. Physik, 42, 181. 6.1.4

Landgraf, J., and P. J. Crutzen (1998), An efficient method for online calculations of photolysis and heating rates, J. Atmos. Sci., 55(5), 863–878. 2.1.4

Levin, Z., and E. Ganor (1996), The effects of desert particles on cloud and rain formation in the Eastern Mediterranean, in The Impact of Desert Dust Across the Mediterranean, edited by S. Guerzoni and R. Chester, pp. 77–86, Kluwer Academic Pub., Boston, MA. 3.6.2

Light, B., H. Eicken, G. A. Maykut, and T. C. Grenfell (1998), The effect of included particulates on the spectral albedo of sea ice, J. Geophys. Res., 103, 27,739–27,752. 3.6.3

Liou, K.-N. (1992), personal communication. a, 4.1.5, 6.3.2

Liou, K. N. (2002), An Introduction to Atmospheric Radiation, International Geophysics Series, vol. 84, second ed., Academic Press, Amsterdam. 3.2, 7.2.2, 7.2.3

Madronich, S. (1987), Photodissociation in the atmosphere 1. Actinic flux and the effects of ground reflections and clouds, J. Geophys. Res., 92(D8), 9740–9752. 2.1.3

Madronich, S. (1989), Numerical integration errors in calculated tropospheric photodissociation rate coefficients, J. Atmos. Chem., 10, 289–300. 2.1.4

Malkmus, W. (1967), Random Lorentz band model with exponential-tailed S^{-1} line-intensity distribution function, J. Opt. Soc. A, 57(3), 323–329. 6.2.1, 6.2.1, 6.2.1, 6.2.1

Markel, V. A. (2002), The effects of averaging on the enhancement factor for absorption of light by carbon particles in microdroplets of water, J. Quant. Spectrosc. Radiat. Transfer, 72(6), 765–774. 3.3, 7.2.7

Markel, V. A., and V. M. Shalaev (1999), Absorption of light by soot particles in microdroplets of water, J. Quant. Spectrosc. Radiat. Transfer, 63(2–6), 321–339, see erratum in JQSRT 66(6):591. 7.2.7

Melnikova, I. (2008), Range of application of the scattering theory within the multicomponent turbid media of the cloud atmosphere is the reason for anomalous absorption and incorrectness of climate prediction, Intl. J. Rem. Sens., 29(9), 2615–2628, doi:10.1080/01431160701767,443. 7.5.1

Michels, H. H. (1963), Abscissas and weight coefficients for Lobatto quadrature, Math. Comput., 17(83), 237–244. 10.6

Mitchell, D. L. (2000), Parameterization of the Mie extinction and absorption coefficients for water clouds, J. Atmos. Sci., 57(9), 1311–1326. 7.2.7

Mlawer, E. J., S. J. Taubman, P. D. Brown, M. J. Iacono, and S. A. Clough (1997), Radiative transfer for inhomogeneous atmospheres: RRTM, a validated correlated-k model for the longwave, J. Geophys. Res., 102(D14), 16,663–16,682. 5.6.1

Molotch, N. P., T. H. Painter, R. C. Bales, and J. Dozier (2004), Incorporating remotely-sensed snow albedo into a spatially-distributed snowmelt model, Geophys. Res. Lett., 31, L03,501, doi:10.1029/2003GL019,063. 2.3

Moncet, J. L., and S. A. Clough (1997), Accelerated monochromatic radiative transfer for scattering atmospheres: Application of a new model to spectral radiance observations, J. Geophys. Res., 102(D18), 21,853–21,866. 5.6.1

Nussenzveig, H. M. (1992), Diffraction Effects in Semiclassical Scattering, Montroll Memorial Lecture Series in Mathematical Physics, vol. 1, Cambridge Univ. Press, Cambridge, UK. 3.3

Nussenzveig, H. M. (2003), Light tunneling in clouds, Appl. Opt., 42(9), 1588–1593. 3.3, 3.3, 3.3, 3.3, 7.2.7

Partain, P. T., A. K. Heidinger, and G. L. Stephens (2000), High spectral resolution atmospheric radiative transfer: Application of the equivalence theorem, J. Geophys. Res., 105(D2), 2163–2178. 5.6.1

Patterson, E. M. (1981), Optical properties of the crustal aerosol: Relation to chemical and physical characteristics, J. Geophys. Res., 86(C4), 3236–3246. 7.1

Patterson, E. M., D. A. Gillette, and B. H. Stockton (1977), Complex index of refraction between 300 and 700 nm for Saharan aerosols, J. Geophys. Res., 82(21), 3153–3160. 7.1

Perovich, D. K., and J. W. Govoni (1991), Absorption coefficients of ice from 250 to 400 nm, Geophys. Res. Lett., 18(7), 1233–1235. 7.1

Petropavlovskikh, I. (1995), Evaluation of photodissociation coefficient calculations for use in atmospheric chemical models, Ph.D. thesis, Université Libre de Bruxellex and National Center for Atmospheric Research, Boulder, CO. 2.1.4

Quine, B. M., and J. R. Drummond (2001), GENSPECT: A line-by-line code with selectable interpolation error tolerance, sub judice, Q. J. R. Meteorol. Soc. 5.6.1

Rees, M. H. (1989), Physics and Chemistry of the Upper Atmosphere, Cambridge Univ. Press, Cambridge. 6.5.1

Rodgers, C. D., and C. D. Walshaw (1966), The computation of infra-red cooling rate in planetary atmospheres, Q. J. R. Meteorol. Soc., 92(391), 67–92. 6.4

Rogers, R. R., and M. K. Yau (1989), A Short Course in Cloud Physics, 293 pp., Pergamon Press, Elmsford, NY. 5.5.1

Rosenfeld, D., Y. Rudich, and R. Lahav (2001), Desert dust suppressing precipitation: A possible desertification feedback loop, Proc. Natl. Acad. Sci., 98, 5975–5980. 3.6.2

Rothman, L. S., et al. (1998), The HITRAN molecular spectroscopic database and HAWKS (HITRAN atmospheric workstations): 1996 edition, J. Quant. Spectrosc. Radiat. Transfer, 60(5), 665–710. 4.1.1, a, a, a, 5.3, 5.4, a, 5.5.1, 7.1

Rudich, Y., O. Khersonsky, and D. Rosenfeld (2002), Treating clouds with a grain of salt, Geophys. Res. Lett., 29, doi:10.1029/2002GL016,055. 3.6.2

Salby, M. L. (1996), Fundamentals of Atmospheric Physics, Academic Press, San Diego, CA. 2.2.5

Seinfeld, J. H., and S. N. Pandis (1997), Atmospheric Chemistry and Physics, 1326 pp., John Wiley & Sons, New York, NY. 4.1.3, 4.1.3

Shu, F. H. (1991), The Physics of Astrophysics Volume I: Radiation, University Science Books, Mill Valley, CA. 4.1.2

Sinyuk, A., O. Torres, and O. Dubovik (2003), Combined use of satellite and surface observations to infer the imaginary part of refractive index of Saharan dust, Geophys. Res. Lett., 30(2), 1081, doi:10.1029/2002GL016,189. 7.1

Sparks, L. (1997), Efficient line-by-line calculation of absorption coefficients to high numerical accuracy, J. Quant. Spectrosc. Radiat. Transfer, 57(5), 631–650. 5.6.1

Stamnes, K., and S.-C. Tsay (1990), Optimum spectral resolution for computing atmospheric heating and photodissociation rates, Planet. Space Sci., 38(6), 807–820. 2.1.4

Stamnes, K., S.-C. Tsay, W. Wiscombe, and K. Jayaweera (1988), Numerically stable algorithm for discrete-ordinate-method radiative transfer in multiple scattering and emitting layered media, Appl. Opt., 27(12), 2502–2509. 2.2.8

Tang, I. N. (1997), Thermodynamic and optical properties of mixed-salt aerosols of atmospheric importance, J. Geophys. Res., 102(D2), 1883–1893. 7.1

Thomas, G. E., and K. Stamnes (1999), Radiative Transfer in the Atmosphere and Ocean, Cambridge Atmospheric and Space Science Series, Cambridge Univ. Press, Cambridge. 1, 5.5.1

Toon, O. B., C. P. McKay, T. P. Ackerman, and K. Santhanam (1989), Rapid calculation or radiative heating rates and photodissociation rates in inhomogeneous multiple scattering atmospheres, J. Geophys. Res., 94(D13), 16,287–16,301. 2.1.4

Twomey, S. (1977), Atmospheric Aerosols, 302 pp., Elsevier Sci. Pub. Co., New York, NY. 3.6.2

van de Hulst, H. C. (1957), Light Scattering by Small Particles, Dover edition 1981, 470 pp., Dover, New York. 2.2.7, 3.2, 3.2, 3.3, 7.2.6

Vogelmann, A. M., V. Ramanathan, W. C. Conant, and W. E. Hunter (1998), Observational constraints on the non-lorentzian continuum effects in the near-infrared solar spectrum using ARM ARESE data, J. Quant. Spectrosc. Radiat. Transfer, 60(2), 231–246. 5.6.1

Volz, F. E. (1973), Infrared optical constants of ammonium sulfate, Sahara dust, volcanic pumice, and flyash, Appl. Opt., 12(3), 564–568. 7.1

Walden, V. P., S. G. Warren, F. J. Murcray, and R. G. Ellingson (1997), Infrared radiance spectra for testing radiative transfer models in cold and dry atmospheres: Test cases from the Antarctic plateau, Bull. Am. Meteorol. Soc., 78(10), 2246–2247. 5.6.1

Wang, Z., M. Barlage, X. Zeng, R. E. Dickinson, and C. B. Schaaf (2005), The solar zenith angle dependence of desert albedo, Geophys. Res. Lett., 32, L05,403, doi:10.1029/2004GL021,835. 2.3

Warren, S. G., and W. J. Wiscombe (1980), A model for the spectral albedo of snow. II: Snow containing atmospheric aerosols, J. Atmos. Sci., 37, 2734–2745. 3.6.3

Watson, G. N. (1958), A Treatise on the Theory of Bessel Functions, Cambridge Mathematical Library, Cambridge Univ. Press, Cambridge. 7.2.3, 10.4

Wild, O., X. Zhu, and M. Prather (2000), Fast-J: Accurate simulation of in- and below-cloud photolysis in tropospheric chemical models, J. Atmos. Chem., 37, 245–282. 2.1.4

Wiscombe, W. J. (1977), The delta-M method: Rapid yet accurate radiative flux calculations for strongly asymmetric phase functions, J. Atmos. Sci., 34, 1408–1422. 2.2.7, 2.2.8, 10.6, 10.6

Wiscombe, W. J. (1979, edited/revised 1996), Mie scattering calculations: Advances in technique and fast, vector-speed computer codes, Tech. Rep. NCAR/TN–140+STR, National Center for Atmospheric Research, Boulder, Colo. 2.2.7

Wiscombe, W. J., and G. W. Grams (1976), The backscattered fraction in two-stream approximations, J. Atmos. Sci., 33(12), 2440–2451. 2.2.7

Wiscombe, W. J., and S. G. Warren (1980), A model for the spectral albedo of snow. I: Pure snow, J. Atmos. Sci., 37, 2712–2733. 3.6.3

Wurzler, S., T. G. Reisin, and Z. Levin (2000), Modification of mineral dust particles by cloud processing and subsequent effects on drop size distributions, J. Geophys. Res., 105(D5), 4501–4512. 3.6.2

Zender, C. S., and J. Talamantes (2006), Solar absorption by Mie resonances in cloud droplets, J. Quant. Spectrosc. Radiat. Transfer, 98(1), 122–129, doi:10.1016/j.jqsrt.2005.05.084. 7.2.7

Zender, C. S., B. Bush, S. K. Pope, A. Bucholtz, W. D. Collins, J. T. Kiehl, F. P. J. Valero, and J. Vitko, Jr. (1997), Atmospheric absorption during the Atmospheric Radiation Measurement (ARM) Enhanced Shortwave Experiment (ARESE), J. Geophys. Res., 102(D25), 29,901–29,915. 6

Index